Appendix 6-D

Elk River Landslide Hazard Report (Stillwater, 2005)

Landslide Hazard in the Elk River Basin, Humboldt County, California

Prepared for
North Coast Regional Water Quality Control Board
Santa Rosa, California

Prepared by
Stillwater Sciences
Arcata, California

1 June 2007

Stillwater Sciences VESTRA Curry Group Inc.

Acknowledgements

The project benefited greatly from the following technical advisors who offered helpful discussion, guidance, and review of methods, model application, and model testing: Bill Dietrich (UC Berkeley, Department of Earth and Planetary Sciences), Bill Haneberg (Hanneberg Geoscience), Joshua Roering and Ben Mackey (University of Oregon, Department of Geological Sciences), Laura Vaugois (Washington Dept. of Natural Resources), and David Lamphear. Freshwater Creek Project Contractors Danny Hagens, Bill Weaver, and Eileen Weppner (Pacific Watershed Associates); and Drew Lewis (Sanborn Mapping) provided access to information and offered insightful discussion during the methodology workshop. Pacific Lumber Company graciously provided data and anecdotal information for the Elk River basin through coordination with Kate Sullivan, Amod Dhakal, John Ozwald, and Adrian Miller. Tom Hofweber and Chinmaya Lewis (Humboldt County Planning Department) and Sam Morrison (Bureau of Land Management) also provided access to essential data. The project would not have been possible without the interest and cooperation of these individuals and the organizations they represent.

Suggested citation:

Stillwater Sciences. 2007. Landslide Hazard in the Elk River Basin,
Humboldt County, California. Final report. Prepared by Stillwater Sciences, Arcata, California for the North Coast Regional Water Quality Control Board.

Table of Contents

Tables

Figures

Appendices

1 INTRODUCTION

The Elk River watershed is listed as an impaired water body under Section 303(d) of the Clean Water Act. Water quality problems cited under the listing include sedimentation, threat of sedimentation, impaired quality of irrigation water, impaired quality of domestic water supply, impaired spawning habitat, increased rate and depth of flooding due to sediment, and property damage. Erosion, sediment discharge, and sedimentation has significantly modified the channel conditions of Elk River and its tributaries such that a threat to public health, safety, and property is present from increased incidences and magnitude of routine flooding, constituting a nuisance condition according to the Porter-Cologne Water Quality Control Plan. A program has been developed to recover waterbodies listed under 303(d) of the Clean Water Act via the establishment of Total Maximum Daily Loads (TMDL). The North Coast Regional Water Quality Control Board (NCRWQCB) has begun the process of establishing a TMDL for sediment in the Elk River watershed, with the goal of restoring and maintaining the sediment impaired beneficial uses of water of Elk River and its tributaries. The North Coast Regional Water Quality Control Board retained the team of Stillwater Sciences, Vestra, and Curry Group to evaluate landslide hazards in the Elk River basin as one component of TMDL development.

Shallow landslides (both road-related and non-road-related) are acknowledged as the most common type of mass movement and dominant management-related sediment source impairing beneficial uses in Elk River (PWA 1998, PALCO 2004a, PALCO 2004b). Consequently, there is an immediate need for objective and repeatable methods that can be used in combination with existing terrain mapping, landslide inventories, and site-specific geotechnical slope stability assessments to reliably predict potential landslide hazards and identify land management activities compatible with recovery of sediment impaired beneficial uses. Such tools are ideally suited for use with additional information about sediment delivery and vulnerability of receptors to sediment impairment in assessing risk as part of the Elk River sediment TMDL analysis and implementation.

Landslide hazard assessment can be broadly grouped into three main approaches: inferential, statistical, and mechanistic or physically-based (Dietrich et al. 2001, National Research Council 2004, Sidle and Ochiai 2006). The inferential approach utilizes remote sensing imagery, topographic and geologic mapping, geomorphic information (e.g., surface materials and landforms), historical information, and field observations to generate maps of landslide features and their relative activity. The approach requires knowledge of local geomorphic processes and professional judgment. Consequently, the reliability of the results are dependent on a map-maker's skills and relevant experience. Although rooted in field observation, the process lacks objectivity and emphasizes where landslides have occurred rather than where there is potential for landslides to occur in the future. The statistical approach consists of inventorying all parameters related to landslide occurrence and subsequently conducting bivariate or multivariate statistical analyses to determine their relative importance. The process is more objective, but weighting of factors based on local experience introduces subjectivity and results are difficult to extrapolate beyond specific areas of study (Sidle and Ochiai 2006). Mechanistic or physically-based approaches use quantitative, process-based slope stability and shallow subsurface flow theories to predict the spatial distribution of relative slope stability (e.g., Hammond et al. 1992, Wu and Sidle 1995, Dietrich et al. 1995, Pack and Tarboton 1997, Dietrich and Montgomery 1998, Dhakal and Sidle 2003, Haneberg 2004). These approaches are more objective and have evolved rapidly with improved technologies for characterizing fine scale topography over large areas (e.g., LiDAR).

These models, however, typically require spatially and temporally distributed model parameters (e.g., soil cohesion, root cohesion, soil bulk density, water table level, friction angle, soil depth, and hillslope gradient) and are highly simplified due to difficulty in characterizing parameter variability over large areas.

Distributed, physically-based modeling approaches that predict the spatial distribution of relative slope stability from process-based models of slope stability and shallow subsurface flow using high-resolution digital topography take two general forms: probabilistic and deterministic (Haneberg 2000). Probabilistic approaches allow for uncertainty by assigning probability distributions to model parameters, while deterministic approaches establish invariant or spatially explicit parameter values and lack an element of uncertainty.

1.1 Goals and objectives

Both deterministic and probabilistic physically-based modeling approaches are used in this study to predict potential landslide hazards in the Elk River basin. The specific objectives of the work include the following:

1. Develop a database of observed shallow and deep-seated landslides,
2. Predict potentially unstable areas using grid-based deterministic and probabilistic hillslope stability models, and
3. Objectively test model predictions of potential instability by relating predicted instability to observed landslide occurrence.

1.2 Project Area

The Elk River basin (151 km^2) is located south and east of the city of Eureka in Humboldt County, California (Figure 1-1, Table 1-1). The Elk River basin originates from the seaward slope of the outer Coast Range and flows westward across the coastal plain into Humboldt Bay. The basin can be divided into four main areas: (1) North Fork Elk River (58.2 km^2), (2) South Fork (50.4 km^2), (3) the lower Elk River downstream of the North Fork and South Fork confluence (26.9 km^2), and (4) Martin Slough (15.3 km^2). The majority of the North Fork Elk River basin is privately managed for industrial timber harvest, with private residential properties occupying only the lower 2%. The majority of the South Fork Elk River basin is also privately managed for industrial timber operations (65%), but 30% of the basin occurs within the Headwaters Forest Reserve (transferred to and managed by Bureau of Land Management since the 1999 Headwaters Deal) and the remaining 5% is private residential property in the lower South Fork Elk River valley. Lower Elk River is comprised of mixed private ownership, with approximately 24% zoned for timber production. Martin Slough is in mixed private ownership and includes urban development in the southeast portion of the City of Eureka.

Table 1-1. Subwatersheds in the Elk River basin.

Subwatershed		Area, km²	Area by Hillslope Gradient, km²						Length by Channel Gradient, km						Area by Geology, km²					Area by Stand Age, km²					
			<5%	5-15%	15-35%	35-50%	50-65%	>65%	0-1%	1-2%	2-4%	4-8%	8-12%	>12%	Qh-Qmts-Qrt	Q-Qds	Qtwu	Ty	Kjfs	unknown	0-13 yr	116-500 yr	14-30 yr	31-50 yr	51-115 yr
7	Upper North Fork Elk River	11.3	0.2	1.1	3.1	2.3	1.9	2.7	1.4	3.4	6.8	9.3	6.9	28.5	0.0	0.0	5.7	0.9	4.5	0.20	3.23	0.86	4.45	2.35	0.21
10	North Branch North Fork Elk River	10.4	0.1	0.7	2.8	2.6	2.1	2.2	0.5	1.3	3.3	6.9	7.1	33.5	0.0	0.0	5.9	1.8	2.6	0.03	0.62	0.00	1.86	5.74	2.15
18	South Branch North Fork Elk River	5.0	0.1	0.5	1.6	1.1	0.8	0.9	0.1	0.8	2.1	3.3	4.8	15.8	0.0	0.0	4.0	0.9	0.0	0.07	0.76	0.06	2.58	1.32	0.17
8	McWhinney Creek	3.3	0.0	0.2	0.8	0.9	0.8	0.6	0.4	2.0	1.1	1.6	1.5	7.3	0.0	0.0	3.3	0.0	0.0	0.01	0.99	0.00	0.13	1.35	0.80
4	Bridge Creek	5.7	0.0	0.2	1.0	1.5	1.6	1.4	1.7	1.8	3.1	4.2	3.3	12.6	0.0	0.0	5.7	0.0	0.0	0.01	1.65	0.00	0.01	0.01	4.07
15	Lake Creek	5.5	0.1	0.5	1.6	1.3	1.0	1.0	0.7	1.9	1.6	3.1	3.4	16.4	0.0	0.0	5.5	0.1	0.0	0.00	1.57	0.00	0.47	2.59	0.88
6	Browns Gulch	2.3	0.0	0.2	0.7	0.6	0.4	0.3	0.5	1.0	2.3	1.3	1.1	4.0	0.0	0.0	2.3	0.0	0.0	0.02	0.64	0.00	0.00	0.00	1.69
5	Dunlap Gulch	1.7	0.0	0.2	0.5	0.5	0.3	0.2	0.2	0.9	1.2	1.0	0.8	4.6	0.0	0.0	1.7	0.0	0.0	0.07	0.57	0.00	0.00	0.00	1.08
9	Lower North Fork Elk River	13.0	0.5	1.8	4.0	2.9	2.0	1.8	16.5	3.2	4.2	7.5	8.0	28.4	0.8	0.4	10.9	1.0	0.0	1.08	2.41	0.00	0.81	4.30	4.41
20	Corrigan Creek	4.3	0.1	0.4	1.4	1.1	0.7	0.7	0.4	1.5	2.4	4.7	3.4	9.1	0.0	0.0	3.2	1.1	0.0	0.02	0.08	0.05	2.35	1.72	0.11
17	Upper South Fork Elk River	16.7	0.2	2.0	6.0	3.8	2.4	2.2	1.3	5.2	6.5	13.2	16.9	59.5	0.0	0.0	5.4	11.2	0.0	6.37	3.10	0.33	2.39	3.80	0.68
19	Little South Fork Elk River	9.3	0.0	0.6	2.6	2.5	1.9	1.7	0.5	1.0	4.0	10.1	8.4	23.0	0.0	0.0	7.3	1.9	0.0	9.27	0.02	0.00	0.00	0.04	0.00
16	McCloud Creek	6.1	0.1	0.6	2.3	1.5	0.9	0.8	0.8	1.1	1.5	5.5	5.6	22.4	0.0	0.0	6.1	0.0	0.0	5.26	0.00	0.00	0.21	0.51	0.16
14	Tom Gulch	6.5	0.1	0.9	2.6	1.4	0.8	0.7	1.7	1.4	2.2	5.5	6.6	17.8	0.6	0.0	5.9	0.0	0.0	1.66	0.00	0.00	0.59	4.26	0.00
11	Lower South Fork Elk River	7.5	0.3	1.0	2.5	1.6	1.1	1.0	9.6	1.5	1.9	5.1	4.0	19.1	0.1	0.4	7.0	0.0	0.0	2.79	0.13	0.00	0.20	3.81	0.57
12	Railroad Gulch	3.1	0.1	0.4	1.0	0.6	0.5	0.5	1.3	1.2	1.6	2.2	1.4	6.6	1.7	0.2	1.1	0.0	0.0	0.10	0.87	0.00	0.32	1.00	0.81
13	Clapp Gulch	2.6	0.1	0.3	0.7	0.5	0.4	0.6	0.3	1.2	1.4	2.4	2.4	4.2	1.7	0.2	0.7	0.0	0.0	0.08	0.12	0.00	0.41	1.86	0.16
1	Martin Slough	15.3	4.8	3.9	2.9	1.6	1.1	0.9	15.9	11.1	13.3	9.3	4.5	6.7	11.2	1.9	2.1	0.0	0.0	15.27	0.00	0.00	0.00	0.00	0.00
3	Lower Elk River	15.1	4.9	2.7	3.2	1.8	1.3	1.2	21.0	3.7	6.8	11.5	9.2	12.4	6.1	6.0	2.9	0.0	0.0	13.17	0.15	0.00	0.42	1.22	0.12
2	Lower Elk River West	6.1	1.7	1.9	1.2	0.3	0.1	0.1	6.6	1.3	3.0	5.4	3.0	2.3	4.1	1.9	0.0	0.0	0.0	5.34	0.00	0.00	0.00	0.00	0.00
Total		**151**	**13**	**20**	**42**	**31**	**22**	**22**	**81.4**	**46.3**	**70.6**	**113.2**	**102.2**	**334.4**	**26.3**	**11.0**	**86.7**	**18.9**	**7.1**	**60.80**	**16.94**	**1.30**	**17.21**	**35.88**	**18.05**

1.2.1 Geologic setting

The Elk River basin is located along the southeastern margin of the actively uplifting and deforming southern Cascadia forearc basin at the leading edge of the northward migrating Mendocino triple junction. Northwest-trending faults and folds bound the dominant mountain ranges. The two basement units in the Project Area include the Franciscan Complex Central Belt – a Mesozoic to early Cenozoic age accretionary mélange enclosing blocks of more coherent sandstone, greenstone, and chert; and the Yager terrane – a Paleogene trench-slope deposit of thin-bedded argillite and sandstone turbidites with minor pebbly conglomerate (Ogle, 1953; McLaughlin et al., 2000, Marshall and Mendes 2005). The Wildcat Group, a thick transgressive-regressive sequence of marine siltstone and fine-grained sandstone of late Miocene to Pliocene age, rests unconformably on these basement units. Undifferentiated shallow water marine and fluvial deposits of middle to late Pleistocene age (Hookton Formation and related deposits) cap broad, accordant ridges across the western portions of the Elk River basin. These geologic terrains and the dominant hillslope geomorphic processes occurring within them are discussed in more detail in Section 2.1.1.

1.2.2 Climate

The Mediterranean climate of the Elk River basin is characterized by mild, wet winters and a prolonged summer dry season. Mean surface air temperature at the coast ranges from 9°C in January to 13°C in June, with summer temperature moderated by fog. Roughly 90% of the annual precipitation occurs as rainfall between October and April. Mean annual precipitation ranges from 99 cm at Eureka to 152 cm near Kneeland, located 20 km inland (elevation 810 m).

Winter rainfall intensity and storm runoff are highly variable due to orographic lifting of moisture-laden, frontal air masses as they intersect the outer Coast Range. Storm events with rainfall intensity exceeding 3–4 inches a day are considered capable of initiating landslides (PALCO 2004b). A 24-hour rainfall total of 4–5 inches in the Eureka area (up to approximately 2000 ft) has an estimated return interval of 5 years (NOAA Atlas Vol XI Northern California cited in PALCO 2004b). Rainfall intensities exceeding 5 inches per day are rare and have only occurred 3 times between 1941 and 1998 (water years 1950, 1959, and 1997). The 24-hour rainfall total of 6.8 inches on December 27, 2002 set many records and caused widespread landslide damage and flooding. Annual peak discharges recorded at an Elk River gauge, located 0.3 km downstream of the North Fork Elk River and South Fork Elk River confluence, range from 23.4 m^3s^{-1} to 112.2 m^3s^{-1} for the period 1957–1967, 1997–1998. Estimated peak discharge for the 1.5-year flood at the Elk River gauge is 44.8 m^3s^{-1} (Klein and Anderson, 1999).

1.2.3 Forest management history

The maritime coastal climate supports a coniferous lowland forest community dominated by redwood (Sequoia sempervirens), western hemlock (Tsuga heterophylla), Sitka spruce (Picea sitchensis), grand fir (Abies grandis), and Douglas-fir (Pseudotsuga menziesii). While large-scale harvest of these species has occurred in the Elk River watershed since the late 1800s, there has been a marked increase in harvest using clearcut silviculture in North Fork Elk River (Figures 1-2, 1-3, and 1-4) and South Fork Elk River (Figures 1-5 and 1-6) since 1994 (White, 2007). Harvest data for Lower Elk River and Martin Slough were not available at the time of this report.

1.2.4 Sediment sources

This landslide hazard assessment utilized landslide mapping and other related data collected during several prior studies focused on characterizing the rate and causes of sediment production and delivery in the Elk River basin. Pacific Watershed Associates (PWA) conducted a sediment source inventory in the North Fork Elk River basin in 1998 that identified sources of erosion and sediment delivery to stream channels, distinguished between natural and management-related sediment sources, and assessed opportunities for preventing and controlling future sediment sources (PWA 1998). The 1998 study involved extensive aerial photographic analysis and field inventory of erosion processes in the North Fork Elk River basin. PWA has conducted similar unpublished inventories for South Fork Elk River. A draft watershed analysis for the Elk River and Salmon Creek areas (PALCO 2004a), completed as a provision of PALCO's Habitat Conservation Plan (PALCO 1999), included further analysis of mass wasting and surface erosion processes. Additional sediment source studies are ongoing in the watershed as part of the HCP agreement and cooperative projects with NCRWQCB (PALCO 2004b).

Sediment budgets have been compiled by the Pacific Lumber Company for both North Fork and South Fork Elk rivers (Table 1-2). The majority of sediment delivered to the North Fork Elk River system originates from landslides. The main factors contributing to landslides and other management-related sediment supply in the Elk River basin are (PWA 1998, PALCO 1999, PALCO 2004a, PALCO 2004b):

- poorly located, constructed, or maintained roads;
- logging with ground-based systems on steep slopes;
- harvesting on inherently unstable slopes;
- temporary reduction in root strength from clearcutting; and
- legacy problems associated with old skid trails and abandoned roads.

Table 1-2. Sediment Budgets developed for North Fork and South Fork Elk rivers.

	North Fork		North Fork		North Fork and South Fork		North Fork and South Fork	
Time Period	**1955–1997 [1] (42 year average)**		**1995-1997 [1] (3 year average)**		**1988–2000 [2] (12 year average)**		**1988–2000 [3] (12 year average)**	
units	**$yd^3mi^{-2}\ yr^{-1}$**	**% of total**	**$yd^3mi^{-2}\ yr^{-1}$**	**% of total**	**$yd^3mi^{-2}\ yr^{-1}$**	**% of total**	**$yd^3mi^{-2}\ yr^{-1}$**	**% of total**
Non-road related landslides	316	51	741	51	183	23	153	23
Torrent track scour	21	3	207	14	–	–	–	–
Bank erosion & streambank slides	37	6	40	3	243	30	222	33
Scour of filled channels	103	17	112	8	–	–	–	–
Low order valley fill incision	–	–	–	–	–	–	–	–
Surface erosion from disturbed areas	43	7	102	7	6	1	5	1
Soil creep	–	–	–	–	76	9	63	9
Road-related erosion[4]	96	16	263	18	298	37	225	34
Total	**617**	**100**	**1,466**	**100**	**806**	**100**	**668**	**100**

[1] Data from Table 9 in PWA 1998.
[2] Data from Table B-17 (medium estimates) in PALCO 2004a.
[3] Data estimated from Figure 3.2 in PALCO 2004b.
[4] Road-related erosion is a combination of landslides, surface erosion, gullying and stream crossing failure.

1.3 Overview of Approach and Products

This landslide hazard assessment involved preliminary modeling and model testing in pilot basins, review of preliminary results in pilot basins by a technical advisory panel, and subsequent application of a refined modeling and model testing approach to the entire Elk River basin. Analysts first compiled and verified existing information related to landsliding in the Project Area (e.g., geology, soil properties, land cover and vegetation characteristics, hillslope and channel gradient, existing sediment source inventories, climate, land use, and harvest history). A technical advisory panel comprised of the model authors, staff from the NCRWQCB, and other consulting scientists provided initial guidance during selection and development of modeling and model testing approaches in pilot subwatersheds within the Project area. The modeling and model testing approaches were refined based on the collective feedback from the advisory panel during a workshop convened on 24 April 2006 to discuss preliminary methods and results in pilot areas. The revised modeling and model testing approaches were applied to the entire Elk River basin, and the validity of the results were objectively tested using available landslide mapping in the Elk River basin.

The products of the landslide hazard assessment include the following:

- A data base of available terrain and landslide information for the Elk River basin;
- 4-m digital elevation model (DEM) derived from LiDAR data and used as input for hillslope stability modeling;
- Grid-based results from individual models that predict potential shallow and deep-seated instability; and
- Results of validation tests used to evaluate and compare model performance.

2 METHODS

2.1 Geomorphic Terrains

Evaluation of sediment production and transport potential at the watershed scale can be effectively organized by stratifying the watershed into geomorphic terrains. Four attributes were used to define geomorphic terrains in the Elk River Project Area based on their dominant role in determining and/or regulating erosion and transport processes: geology, hillslope gradient, channel gradient, and vegetation cover type (Table 2-1). Stand age classes were also defined for the Project area where records of forest management history were available. Other characteristics, such as local facies changes and strike and dip of geologic strata, yarding and silvicultural methods, and road construction and use are also important factors influencing slope instability, but are more difficult to characterize at the watershed scale.

Geologic and stand age attributes were used in this study to (1) assign unique parameter values for hillslope stability modeling using PISA; (2) test the validity of model results for potential shallow instability; and (3) assess appropriate breaks in potential instability classes. Combining all four geomorphic terrain attributes provides the basis for conducting spatial analyses, extrapolating geomorphic processes and rates, and developing load management strategies during subsequent steps in the sediment TMDL process.

2.1.1 Geology

The Franciscan Complex Central Belt (Kjsf) comprises 4.7% of the Project Area, located exclusively in the Upper North Fork and North Branch North Fork subwatersheds, where it is in contact with the Yager terrane along the Freshwater fault (Figure 2-1). The Central belt Franciscan Complex is a late Jurassic to Cretaceous age accretionary mélange of meta-sandstone and meta-argillite enclosing blocks of more competent sandstone, greenstone, and chert. Large, deep-seated landslides and earthflows enclosing competent blocks are common in the Central belt Franciscan complex (Marshall and Mendes 2005). Blocks of competent sandstone commonly support steep slopes and weather to soils with low cohesion that are susceptible to debris slides and debris flows (Marshall and Mendes 2005).

Table 2-1. Terrain attributes in the Elk River Basin.

Geology		Hillslope Gradient, %	Channel Gradient, %	Cover Type	Stand Age, yr
Q-Qds	Quaternary alluvium, dune sand deposits	0−5	<1	barren/urban	0−13
Qh-Qrt-Qmts	Hookton Formation and related Quaternary terrace deposits	5−15	0−1	agricultural	13−30
Qtwu	Wildcat Group	15−35	1−2	herbaceous	31−50
Ty	Yager terrain	35−50	2−4	shrub	>51
Kjfs	Franciscan Complex Central Belt	50−65	4−8	conifer, hardwood, and mixed conifer-hardwood	
		>65	8−12		
			>12		

Geology modified from McLaughlin et al. 2000 and Marshall and Mendes 2005. Hillslope and channel gradient derived from 1-m DEM from LiDAR data. Channel network created using 2.5 ha for channel initiation. Cover type modified from CDF-LCMMP, Stand age from unpublished data provided by PALCO.

Yager terrane (Ty) of the Franciscan Complex Coastal Belt comprises 12.5% of the Project Area, located predominantly in the Upper South Fork, Upper North Fork, and North Branch North Fork watersheds (Figure 2-1). Yager terrane is a Paleogene trench-slope deposit that typically consists of highly folded and often sheared, dark gray argillite, sandstone, and conglomerate. In the North Fork Elk River, argillite (mudstones, siltstones, and shales) comprise 70% of the area; sandstones 25 %, and conglomerate less than 5% (PWA 1998). The sandstone facies is commonly a cliff-forming unit and exerts local base level control where streams have incised through younger, less resistant overlap deposits. The argillite facies is typically deeply weathered and sheared, promoting deep-seated flow failures on moderate slopes (Marshall and Mendes 2005). The Elk River Watershed analysis reports 2.5 shallow landslides per square kilometer in the Yager terrain over the period 1954–2000 (PALCO 2004a).

The dominant geologic unit in the Elk River Basin is the Wildcat Group (Qtwu) (57.4% of the Project Area), a thick transgressive-regressive sequence of late Miocene to middle Quaternary marine and nonmarine overlap deposits that thins to the east (Ogle 1953, McCrory 1989, Clarke 1992). The Wildcat Group typically consists of poorly to moderately indurated siltstone and fine-grained silty sandstone that weathers to granular, non-cohesive, non-plastic clayey silts and clayey sands (Marshall and Mendes 2005). Wildcat Group terrain is characterized by steep and dissected topography sculpted by debris sliding, and is known for high historical erosion rates by shallow landsliding and debris flow. Shallow landslides in the Wildcat Group are commonly associated with headwall swales, inner gorges, and hollows where weathered soil and colluvium accumulate over relatively resistant, partially indurated, slowly permeable bedrock with bedding planes subparallel to the hillslope (PWA 1998). The Watershed Sensitivity Factor for bedrock geology (PALCO 1999) identifies the Wildcat Group as the most sensitive geology factor, and PWA (1998) reports that debris landslides from Wildcat terrain contribute 51% of the total sediment delivered to watercourses in the North Fork Elk River watershed. In the adjacent Freshwater Creek Watershed, 83% of all debris landslides are associated with siltstones comprising the Wildcat Group. The Elk River Watershed analysis reports 4.9 shallow landslides per square kilometer in Wildcat terrain over the period 1954–2000 (PALCO 2004a).

Undifferentiated shallow water marine and fluvial deposits (gravel, sand, and silt) of the Hookton formation (Qh) cap broad, accordant ridge crests in the western part of the Elk River basin. These deposits and similar Quaternary marine terrace (Qmts) and Quaternary river terrace (Qrt) deposits comprised of poorly consolidated sand and gravel are prone to shallow landsliding on steep slopes and terrace risers. These deposits comprise 17.4% of the Project Area. The Elk River Watershed Analysis reports 9.9 shallow landslides per square kilometer in Hookton terrain over a 46-year period (1954–2000) (PALCO 2004a). Shallow landsliding and deep-seated bedding plane failures are common in Hookton terrain (Marshall and Mendes 2005).

2.1.2 Hillslope and channel gradient

Hillslope gradient is perhaps the most important factor controlling hillslope stability. For the purpose of stratifying the Project Areas into hillslope terrains meaningful to identification and management of landslide hazards, slope gradient was classified in 6 categories (0−5%, 5−15%, 15−35%, 35−50%, 50−65%, and >65%) based on values that have either been mandated in regulation or have emerged as practical thresholds (Table 2-1, Figure 2-2) (California Forest Practice Rules 2005, NMFS 2000, CGS 1997, Planwest Partners et al. 2005, PALCO 1999, PWA 1998). At a site scale, threshold slopes for instability may be strongly influenced by the

geotechnical properties of the soil mantle and parent material; local surface and subsurface hydrology; and the type, age, and density of vegetation. Hillslope gradients in the Elk River basin were derived from a 1-m DEM generated from LiDAR data.

Six channel gradient classes (<1%, 1–2%, 2–4%, 4–8%, 8–12, and >12%) were defined using 2-m DEM data from LiDAR and a 2.5 ha threshold for channel initiation (Table 2-1) (Buffleben, pers. comm., 19 December 2005). Gradient classes reflect characteristic channel morphologies, capacity for sediment transport, and potential for sediment storage (Montgomery and Buffington 1997, 1998). Channel gradient classes to do not integrate directly into analyses of landslide hazard, but are classified to inform subsequent TMDL analyses regarding potential for sediment delivery and transport.

2.1.3 Cover type and stand age

Vegetation cover reflects the relative potential for erosion due to differences in canopy cover, rainfall interception, and the effects of root distribution and strength on slope stability. Five vegetation cover types were defined in the Elk River Project Area: (1) mixed conifer-hardwood, (2) shrub, (3) herbaceous, (4) agricultural, and (5) urban and barren ground (Figure 2-3). These five categories were aggregated from vegetation data compiled as part of the Land Cover Mapping and Monitoring (LCMMP) program conducted by the USDA Forest Service Region 5 Remote Sensing Lab and the California Department of Forestry and Fire Protection's Fire and Resource Assessment Program (FRAP). Approximately 85% of the Elk River basin is mixed-conifer hardwood; the remainder is distributed evenly among herbaceous, agricultural, and urban cover types located predominantly in the lower watershed.

Five stand age classes were defined using PALCO stand age data: <13 yr, 13−30 yr, 31−50 yr, and >51 yr (Figure 2-4, Table 1-1). At the time of this study, stand age data was available only for Pacific Lumber Company ownership (PALCO unpublished data). Stand age is used here to assign cohesive root strength parameters for modeling shallow landslide hazards using SHALSTAB.V, PISA, and PISA.V.

2.2 Pilot Basins

Four pilot subwatersheds were selected to conduct preliminary tests on optimal DEM grid size for modeling landslide hazards and to experiment with model parameters: Bridge Creek, Railroad Gulch, North Branch North Fork Elk, and Upper South Fork Elk (Figure 2-5, Table 2-2). Bridge Creek is comprised predominantly of relatively homogeneous bedrock of the Wildcat Group (Qtwu) that forms steep ridge and valley topography indicative of shallow debris slide and debris flow processes. Railroad Gulch is comprised of poorly consolidated gravel, sand, and silt deposits of the Hookton formation. North Branch North Fork Elk is one of only two basins where Franciscan Complex Central Belt (Kjfs) occurs over a large area. Topography is highly variable due to structural control by the Freshwater fault, the presence of highly sheared mélange units with a propensity for large deep-seated flow failure, and the occurrence of more resistant siltstone and sandstone units that form steep, ridge-and-valley topography. Upper South Fork Elk is comprised of eastward thinning Wildcat Group overlying Yager terrane. Planar, northeast-facing slopes parallel to bedding planes in Yager terrain exhibit deep-seated flow failure, while steeper south-facing slopes exhibit predominantly shallow landsliding.

Each of the six hillslope stability models (SHALSTAB, SHALSTAB.V, PISA, PISA.V, DSLED-Rough, and DSLED-Drain) were applied in the pilot watersheds; mass wasting features were verified from existing landslide inventories using 2003 aerial photographs (scale 1:12,000) and DEM hillshade images; and preliminary tests were developed to validate and compare model results.

Table 2-2. Summary of terrain characteristics in pilot subwatersheds.[1]

Subwatershed	% conifer−hardwood in subwatershed	Stand age, yr	Area (ha) by hillslope gradient class						Total area, ha
			0–5%	5–15%	15–35%	35–50%	50–65%	> 65%	
Bridge Creek	98%	unknown	0.10	0.25	0.42	0.13	0.04	0.03	1.0
		0–13	2.5	12	37	43	41	30	165
		14–30	0.04	0.26	0.28	0.11	0.05	0.02	0.77
		31–50	0.07	0.23	0.33	0.23	0.12	0.03	1.0
		>51	2.2	13	60	102	120	110	407
North Branch North Fork Elk River	100%	unknown	0.04	0.40	1.2	0.72	0.41	0.25	3.0
		0–13	0.72	4.4	17	18	14	8.3	62
		14–30	1.4	13	53	44	32	42	186
		31–50	5.3	40	157	143	114	115	574
		>51	1.6	12	49	53	49	50	215
Railroad Gulch	99%	unknown	0.53	1.3	3.6	2.0	1.3	1.6	10
		0–13	7.8	16	27	16	11	9.9	87
		14–30	0.39	4.3	12	7.0	4.3	4.0	32
		31–50	1.3	12	32	21	16	18	100
		>51	0.38	5.6	23	18	15	19	81
Upper South Fork Elk River	92%	unknown	10	90	247	136	79	75	637
		0–13	4.0	36	108	70	47	45	310
		116–500	0.31	2.3	9.4	8.2	6.2	6.8	33
		14–30	3.8	26	86	59	36	29	239
		31–50	4.7	42	136	91	58	49	380
		>51	0.74	3.7	16	18	15	14	68
Total			**48**	**334**	**1,074**	**852**	**657**	**627**	**3,592**

[1] Reference year for stand age is 2005.

2.3 Modeling Landslide Hazards

The following sections describe methods used in modeling landslide hazards in the Elk River basin, including development of DEM topography from LiDAR data and application of models for predicting the location of shallow and deep-seated instability.

2.3.1 DEM development

2.3.1.1 LiDAR data

Topographic data (i.e. digital elevation model) for modeling landslide hazards in the Elk River basin was derived from LiDAR (Light Detection and Ranging) data collected during March 2005 by Space Imaging under contract to the North Coast Regional Water Quality Control Board (Sanborn 2005). LiDAR data capture in the Elk River and Freshwater Creek watersheds occurred using an OPTEC ALTM (Airborne Laser Terrain Mapping) LiDAR system referencing two airborne GPS base stations. Table 2-3 shows the planned LIDAR acquisition parameters.

Table 2-3. LIDAR acquisition parameters.

Average altitude	1,000 meters above ground level
Airspeed	~100 knots
Scan frequency	40 hertz
Scan width half angle	16 degrees
Pulse rate	50000 hertz

A GPS survey network comprised of four points was used to make observations and adjustments on the GRS80 ellipsoid, and final airborne GPS data were post-processed using Waypoint's GravNAV^{TM} software (version 6.03). The GPS trajectory was combined with the raw IMU data and post-processed using Applanix Inc.'s POSPROC Kalman Filtering software. The best estimated trajectory and refined attitude data were then re-introduced into the Optech REALM software to compute the laser point-positions. The trajectory was combined with the attitude data and laser range measurements to produce 3-dimensional coordinates of the mass points.

The LiDAR survey effort was designed to collect masspoints at approximately 4.5 points per m^2 over an approximately 300 km^2 area. First and last returns were produced within REALM software, and last return data was filtered using TerraScan software. Filtered last return data representing the bare earth surface (average 2.2 points per m^2) was used to interpolate a regularly spaced grid of elevation values. The filtered bare earth (last return) data were compiled in 1291 separate text files, each containing x and y coordinates and elevation values for filtered points in a 2.5 km^2 tile unit of the project area.

2.3.1.2 DEM generation

Several methods for interpolating a regular spaced grid of elevation data from the irregulary spaced bare earth point data were tested. Both inverse distance weighted and spline interpolators were discarded after tests indicated a propensity to create circular or rounded artifacts near points, especially if the distance and the elevation between points changed significantly. Two preferrred interpolation methods were selected: a Traingulated Irregular Network (TIN) and kriging. Two 1-m DEM grids were intially generated for a single test tile (2.5 km^2) by TINing and kriging. TINing, although much faster, produced faceted trianglular planes that overgeneralized the surface in areas with sparse bare earth points, steep slopes, and/or thick canopy (Figure 2-6, Figure 2-7). The TINing process had a significant effect on SHALSTAB prediction of potential hillslope instability by reducing the number of cells representing highly unstable area (Table 2-4).

Table 2-4. Comparison of SHALSTAB potential instability in pilot area based on TIN vs krig grids.

Instability	Cumulative % of area TIN	Cumulative % of area Krig	Difference (Krig - TIN)
Chronic Instability	4.15	6.27	2.12
<-3.1	5.44	7.54	2.10
-3.1–-2.8	6.42	8.50	2.08
-2.8–-2.5	8.45	10.35	1.90
-2.5–-2.2	12.14	13.82	1.68
>-2.2	44.80	42.86	-1.94
Stable	100.00	100.00	0.00

Based on these tests, the kriging method was chosen to create a DEM grid from LiDAR bare earth ploints. Kriging assumes that points are spatially autocorrelated (points closest to the interpolating cell will have more influence on the cell's value). Weights are based on the distance between measured points and their spatial arrangement. The kriging algorithm (available in the Spatial Analyst or 3D Analyst extentions of ArcGIS, as well as in Surfer) requires the following input parameters:

Search radius: the maximum search distance (from the interpolated cell) used to include points in the interpolation.

Number of points: minimum and maximum number of points included in the interpolation.

Lag size: lag is the vector separating any 2 points. To describe a variogram's structure, similar lags are grouped (i.e., pairs of points aligned in roughly the same direction and roughly the same distance from each other) into bins. Lag size is the width (distance) of the bins into which these vectors are grouped.

Variogram model: The variogram defines the degree of spatial dependence of a dataset and shows the expected difference in the values being measured (e.g., elevation) as they become further apart. These differences eventually flatten out (become spatially

independent), and the distance to where the curve first flattens out is known as the range. The linear model defines a straight line from 0 until the range.

In creating a DEM surface from bare earth points, slope angles and roughness should faithfully represent the actual landscape in order to accurately characterize potential instability. Specifiying a small number of points and small search radius minimizes computation time and generates a rougher surface over small length scales; whereas specifying a large number of points and a wide radius substantially increases computation time and leads to a smoother surface. A 1-m grid from kriging was initially created for the Project Area from bare earth LiDAR points using a spherical semivariogram, search radius of 20 m, and maximum of 16 points (Sanborn 2005). Hillslope stability models were run in four pilot areas using this 1-m grid. Elevation anomolies over small length scales (e.g., ground artifacts such as stumps, fallen logs, and vegetative piles) created topographic "noise" (small scale roughness) in the 1-m grid that led to a wide distribution of high potential instability in isolated grid cells. In addition, tiling artifacts were apparent in shaded relief, flow accumulation, hillslope gradient, and curvature plots (Figure 2-8).

Several approaches were tested in pilot areas to objectively smooth topographic noise from the 1-m grid, including a second order local polynomial interpolator and a soil production model (refer to Section 2.3.2.1 for description of the model). The second order local polynomial interpolator resulted in significant artifacts. The soil production and transport model, an approach to estimating spatially distributed soil depth as part of the SHALSTAB.V model (refer to Section 2.3.2.2), effectively removed most elevation anomolies but excessively smoothed the landscape to the point that high potential instability was concentrated exclusively in steep swales and low order channels.

After testing various smoothing techniques, kriging was used on LiDAR bare earth points in a pilot area to create different size DEM grids (2m, 3m, 4m and 5m). Comparison of curvature and elevation differences with respect to the 1m grid (Figure 2-9) and contour patterns from the various grid sizes (Figure 2-10) suggested that the 4-m grid was optimal for modeling hillslope stability in the Project Area because it (1) substantially reduced variance in curvature over short length scales while minimizing elevation change relative to the 1-m grid, (2) maintained the definition of unchanneled valleys apparent in 5-m contours, and (3) reduced computation time required for model application and other spatial analyses.

To create the final 4-m DEM used in modeling hillslope stability in the Project Area, grids were recreated from the 1291 tiles using the kriging algorithm (linear variogram, radius of 200 m, and maximum of 64 points). To minimize tiling artifacts, tile boundaries were first buffered by 100 m, and points within buffers on adjacent tiles were combined. Point shapefiles were exported to text files and read into Surfer (the kriging algorithm ran faster in Surfer than in ArcGIS). Output grids from Surfer were then mosaiced in ArcGIS. To further minimize tiling artifacts, each buffered grid was first clipped to the coordinates of the corners of each tile, and the clipped grid tiles were mosaiced together into a single 4m grid for the Elk River basin. Minor tiling artifacts were still apparent in the 4-m DEM after creating the final 4-m DEM mosaic.

2.3.2 Shallow landslide models

Two distributed, physically-based models were initially selected for predicting potential shallow landslide hazards based on their common usage and past performance in forested mountainous terrain: the deterministic model SHALSTAB (Montgomery and Dietrich 1994, Dietrich et al. 2001) and the probabilistic model PISA (Haneberg 2004, 2005). Two variations of these models were subsequently included in the analyses to allow more parameterization, most notably, spatially variation in soil depth. These include SHALSTAB.V (Dietrich et al. 1995), and what we refer to here as PISA.V. All four approaches are objective, mechanistic models based on high resolution (4-m) DEM topography developed from LiDAR data.

2.3.2.1 SHALSTAB

SHALSTAB is a physically-based, deterministic model that combines an infinite slope stability model and a steady-state hydrologic model to predict the potential for shallow landsliding controlled by topography and pore water pressure (Montgomery and Dietrich 1994, Dietrich et al. 2001). SHALSTAB utilizes a coupled hydrologic-slope stability equation that relates the pattern of soil saturation to a hydrologic ratio (q/T) and a topographic ratio (a/b sinθ). Solving for the hydrologic ratio provides the basis for SHALSTAB:

$$\frac{q}{T} = \frac{\rho_s}{\rho_w}\left(1 - \frac{\tan\theta}{\tan\phi}\right)\frac{b}{a}\sin\theta \qquad (1)$$

where

$\sin\theta$	=	head gradient
$\tan\phi$	=	angle of internal friction of the soil mass at the failure plane,
ρ_s	=	soil bulk density
ρ_w	=	water bulk density
q	=	effective precipitation
T	=	vertical integral of saturated conductivity
a	=	drainage area
b	=	width of the outflow boundary.

Refer to Montgomery and Dietrich (1994), Dietrich and Montgomery (1998), and Dietrich et al (2001) for the derivation and theory behind the equation. The hydrologic ratio q/T captures the magnitude of effective precipitation (represented by q) relative to the subsurface downslope transmissivity (represented by T). The larger q is relative to T, the more likely the ground is to saturate and the greater the potential instability. The topographic ratio a/b sinθ captures the effects of convergent topography on concentrating runoff and elevating pore water pressure. Topographic parameters, such as hillslope angle (θ), drainage area (a), and width of the outflow boundary (b) are determined from a 4-m DEM.

Assumptions of the basic SHALSTAB model:

- The failure plane and shallow subsurface flow are parallel to the hillslope,
- Subsurface flow is driven by head gradient equal to the topographic slope,

- Soils are cohesionless,
- Root strength is neglected (although root strength strongly effects slope stability, it is highly variable over small spatial and termporal scales and difficult to quantify), and
- Unit weights of saturated and unsaturated soil are equal.

Soil bulk density and the angle of internal friction are treated as spatially constant. Soil bulk density is set at 1,700 kg m^{-3} (saturated bulk density typically lies between about 1,700 and 2,000 kg m^{-3}). The angle of internal friction is set at a relatively high value of 45 degrees, in part, to compensate for the absence of root strength.

This basic version of SHALSTAB has been shown to reliably delineate areas prone to shallow landsliding in parts of the Coast Ranges of northern California, Oregon, and Washington (Montgomery et al. 1998, Shaw and Vaugeois 1999, Dietrich et al. 2001). The model does not predict the location of deep-seated instability nor instability associated with steep, planar slopes typical of inner gorges. The model and documentation for use with ArcView is available from the University of California Berkeley at http://socrates.berkeley.edu/~geomorph/shalstab/index.htm.

2.3.2.2 SHALSTAB.V

Soil thickness strongly affects relative slope stability by supporting vegetation that increases root strength and by influencing the role of subsurface to overland flow. Soils are typically thinnest on ridges and side slopes and thickest in unchanneled valleys, but the spatial variation in soil thickness is rarely incorporated into deterministic hillslope stability models because it is highly variable and impractical to measure over large areas. Dietrich et al. (1995) developed a variation of the basic SHALSTAB model that incorporates greater parameterization, especially the spatial variability in soil depth:

$$\frac{q}{k_1} = \frac{b \sin\theta}{a n_1}\left(e^{-n_1 \beta \cos\theta} - e^{-n_1 h_0 \cos\theta} + \frac{k_2 n_1}{n_2 k_1} e^{-n_2 h_0 \cos\theta} \right) \quad (2)$$

where

$$\beta = 1 - \frac{\rho_s}{\rho_w}\left[1 - \frac{1}{\tan\phi}\left(\tan\theta - \frac{C_r + C_{sw}}{h \rho_s g \cos^2\theta} \right) \right] \quad (3)$$

where

g = gravity,
k_1 = saturated hydraulic conductivity at the ground surface,
k_2 = saturated hydraulic conductivity at the ground surface when bedrock is projected to the ground surface,
e = elevation of the bedrock-soil interface,
h = soil thickness,
h_o = depth,
C_r = cohesive strength contributed by roots,

C_{sw} = cohesive strength of soil when wet.

n_1 and n_2 are exponents describing the decrease in hydraulic conductivity normal to the ground surface,

Refer to Dietrich et al (1995) for the derivation and theory behind these equations. The hydrologic ratio q/k_1 in SHALSTAB.V is conceptually equivalent to the hydrologic ratio q/T in SHALSTAB. Hillslope angle (θ), drainage area (a), and width of the outflow boundary (b) are determined from a 4-m DEM. Nine parameters must be specified to use SHASTAB.V (equation 2) once the topography and soil depth are defined: h_0, n_1, n_2, k_1, k_2, ϕ, p_s, C_s, and C_r. These parameters vary systematically in space and time over a watershed, but are difficult to define and are treated here as constants for simplicity (Table 2-5).

Table 2-5. Summary of parameter values used in SHALSTAB.V (equations 2 and 3).

Parameter	Value	Reference
h_0	1.5	Dietrich et al. 1995
n_1	0.5 m^{-1}	Dietrich et al. 1995
n_2	1.4 m^{-1}	Dietrich et al. 1995
k_1	2x10-4 m s^{-1}	Dietrich et al. 1995
k_2	4x10-5 m s^{-1}	Dietrich et al. 1995
ϕ	32 degrees	Prellwitz et al. 2001, Hammond et al. 1992, NAVFEC 1986
p_s	1,656 kg m^{-3}	Prellwitz et al. 2001, Hammond et al. 1992, NAVFEC 1986
C_s	0	Prellwitz et al. 2001, Hammond et al. 1992, NAVFEC 1986
C_r	2,000 N m^{-2}	Hammond et al. 1992, Schmidt et al. 2001

A continuous soil production and transport model was used to predict soil depths as input to SHALSTAB.V (Dietrich, et al. 1995). Field observations and cosmogenic radionuclide dating (Heimsath et al. 2001) confirm that the rate of conversion of intact bedrock to mobile soil declines exponentially with soil depth, and can be expressed as:

$$\frac{\partial z_b}{\partial t} = \varepsilon e^{-ah} \tag{4}$$

where

z_b = height of the soil-bedrock boundary above datum (m)
t = time
ε = soil production rate (m y^{-1}) at zero soil thickness
a = rate constant (m^{-1})
h = soil thickness normal to the bedrock boundary (m)

This expression is coupled to a nonlinear soil transport equation describing soil flux (q_s) across a hillslope (Roering et al. 1999):

$$q_s = \frac{k\nabla z}{1 - \left(\frac{|\nabla z|}{s_c} \right)^2} \quad (5)$$

where

K = nonlinear diffusion coefficient

S_c = critical gradient at which flux becomes infinite for the nonlinear transport law

∇z = topographic gradient derived from DEM

Soil is produced and diffused downslope at each time step based on the non-linear diffusivity coefficient (Roering et al. 1999). An initial soil depth (h) of approximately 33 cm was solved for by setting the production rate equal to a lowering rate of 0.01 cm y^{-1} (Stallman 2003), assuming a steady state where soil production is equal to the lowering rate. The run time is intended to approximate the time to steady-state equilibrium when flux rate converges to the lowering rate. A run time of approximately 7,000 years gave a distribution of soils depths similar to that observed in the Bridge Creek pilot basin (Prellwitz et al. 2001; J. Berman, Arcata Soil Survey Office, pers. comm., 7 April 2006). Refer to Table 2-6 for a summary of parameter constants used in predicting soil depth.

Table 2-6. Summary of parameter constants used in predicting soil depth (equations 4 and 5).

	Parameter	Value	Reference
ε	Soil production rate	0.000268 m y^{-1}	Heimsath et al. 2001
a	Rate constant	0.0003 m^{-1}	Heimsath et al. 2001
k	Nonlinear diffusion coefficient	0.0032 m^2 y^{-1}	Roering 1999; Roering, pers. comm., 6 April 2006
Sc	Critical gradient	1.25 m m^{-1}	Roering 1999
	Lowering rate	0.01 cm y^{-1}	Stallman 2003

Assumptions of the SHALSTAB.V model:

- Subsurface flow is driven by head gradient equal to the topographic slope,
- Saturated conductivity does not vary with depth
- Soils are cohesionless
- Root strength treated as constant,
- Vertical surcharge of vegetation neglected,
- Unit weights of saturated and unsaturated soil are equal and treated as constants,
- Bulk density of wet and saturated soil are equal and treated as constants,
- Angle of internal friction is treated as constant,
- The lower the ratio of effective precipitation to transmissivity (q/k_1), the more unstable.

2.3.2.3 PISA

PISA is a physically based, probabilistic model that predicts spatially distributed static and seismic shallow slope stability for topography obtained from a digital elevation model and

geotechnical information (Haneberg 2004, 2005). Geotechnical information include shear strength parameters c and ϕ, phreatic surface height, and root strength and surcharge. PISA is based on a first-order, second moment (FOSM) formulation of the infinite slope equation used by the USFS slope stability program LISA and DLISA (Hammond et al. 1992):

$$FS = \frac{C_r + C_s + \left[q_t + \gamma_m D + \left(\gamma_{sat} - \gamma_w - \lambda_m\right) H_w D\right] \cos^2 \beta \tan \phi}{\left[q_t + \gamma_m D + \left(\gamma_{sat} - \gamma_m\right) H_w D\right] \sin \beta \cos \beta} \quad (6)$$

where

C_r = cohesive strength contributed by roots
C_s = cohesive strength of soil
Q_t = uniform surcharge due to weight of vegetation
γ_m = unit weight of moist soil above phreatic surface
γ_{sat} = unit weight of moist soil below phreatic surface
γ_w = unit weight of water (9810 N m^{-3})
D = thickness of soil above the slip surface
H_w = height of phreatic surface above slip surface normalized relative to soil thickness
β = slope angle (degrees)
ϕ = angle of internal friction of the soil mass at the failure plane (degrees)

Refer to Haneberg 2004, 2005 for the derivation and theory behind the PISA model. Model documentation is available from Haneberg Geoscience at http://www.haneberg.com/Haneberg%20Geoscience/PISA.html.

PISA incorporates parameter uncertainty and variability using first-order, second-moment (FOSM) approximations. The mean value of FS is first calculated using mean values of each of the independent variables. For the uncorrelated independent variables, variance (second moment about the mean) is estimated by the first-order truncated Taylor series. One mean and variance for each geotechnical variable is specified for a specific geotechnical map unit (e.g. geologic or geomorphic terrain). PISA takes the parameters for each distribution as input and converts them to an equivalent mean and variance if the distribution is not normal. Four kinds of non-normal distributions are allowed: uniform, triangular, β-pert, and extreme value (Hanegerg 2004, 2005).

Unique geotechnical parameters were defined for the four dominant geologic terrain units forming hillslopes in the Elk River basin (
Table 2-7). Parameter values were estimated based on inventory data from 17 non-road-related landslides (Prellwitz et al. 2001) that occurred in the four dominant geologic terrains on PALCO property. These estimates were supplemented and corroborated by published values for similar geologic and soil materials and vegetation cover types (Hammond et al. 1992, Schmidt et al. 2001, NAVFEC 1986). β–PERT distributions were chosen as the best-fit models for all parameters except H_w because they allow flexibly shaped distributions to be specified in terms of three parameters: minimum, mode, and maximum (sometimes referred to as the optimistic, most likely, and pessimistic estimates). The β-PERT gives more weight to the modal, or most likely value and less weight to the tails of the distribution.

Table 2-7. Summary of parameter values used in PISA.

Parameter		Unit	Values for defining β-PERT distributions in PISA[1]		
			Minimum	Maximum	Likely
Franciscan Complex Central Belt (Kjfs)					
γ_m	unit weight of soil, dry	kg m^3	1,201	1,602	1,361
γ_{sat}	unit weight of soil, saturated	kg m^3	1,762	2,002	1,842
ϕ	angle of internal friction	degrees	18	32	25
C_s	soil cohesion	N m^2	4,762	21,905	9,524
Yager terrane (Ty)					
γ_m	unit weight of soil, dry	kg m^3	1,361	2,082	1,602
γ_{sat}	unit weight of soil, saturated	kg m^3	1,842	2,322	2,002
ϕ	angle of internal friction	degrees	28	35	31
C_s	soil cohesion	N m^2	0	13,333	6,667
Wildcat Group (Qtwu)					
γ_m	unit weight of soil, dry	kg m^3	1,361	2,002	1,602
γ_{sat}	unit weight of soil, saturated	kg m^3	1,842	2,274	2,002
ϕ	angle of internal friction	degrees	30	34	32
C_s	soil cohesion	N m^2	4,762	14,286	7,619
Hookton Formation and related Quaternary terrace deposits (Qh-Qt-Qrt)					
γ_m	unit weight of soil, dry	kg m^3	1,602	2,082	1,842
γ_{sat}	unit weight of soil, saturated	kg m^3	2,002	2,322	2,162
ϕ	angle of internal friction	degrees	31	35	33
C_s	soil cohesion	N m^2	0	10,952	2,381
All terrains					
C_r	root cohesion, <13 yr stands	N m^2	0	4,762	2,381
C_r	root cohesion, >13 yr stands	N m^2	4,762	25,000	4,762
Q_t	surcharge, <13 yr stands	N m^2	0	476	238
Q_t	surcharge, >13 yr stands	N m^2	238	1905	1190
γ_w	unit weight of water	N m^2	na	na	9,810
d	soil mantle depth	m	1	13	5

[1] β-PERT distributions are used for all parameters except H_w, which follows an extreme value distribution. Parameter values estimated from Prellwitz et al. 2001 (based on data from 17 non-road-related landslides on PALCO property), Hammond et al. 1992, Schmidt et al. 2001, and NAVFEC 1986.

An extreme value distribution was used to describe H_w, where the phreatic surface height ranges over $0 < h < 1$. The extreme value distribution includes the parameter μ as a measure of location (similar to a mean value) and the term σ as a measure of dispersion (similar to a standard deviation). μ was set at 0.5 to represent slopes that have moderate peak annual pore pressures (h) in most years, but have the potential to become fully saturated on rare occasions and never have peak annual pore pressures below about 0.25. The term σ was set at 0.1 to scale the probability density function so that it tapers off to nearly zero at h= 1, thereby prohibiting significant artesian pore water pressure (Haneberg pers. comm., 2 May 2007).

PISA results are expressed in terms of the time-independent probability that the factor of safety is less than unity given all possible values of the variable used in the analysis. It is used to make stability comparisons between different areas or map units, delineate critical areas in need of further investigation, and determine appropriate management alternatives for achieving recovery objectives.

Assumptions of the PISA model:

- The model predicts the probability of shallow landsliding with translational movement and a low ratio of thickness to length.
- The influence of groundwater is incorporated using slope-parallel phreatic surface, so pore water pressure is equal to the pressure exerted by a column of water equal in height to that of the phreatic surface above a potential slip surface.
- Parameter distributions appropriately describe the spatial variability in parameter values.

Probability distributions for input parameters are often poorly understood, difficult to quantify, and may not be independent if parameters vary systematically. It is widely acknowledged that soil depth exerts an important control on shallow landsliding, yet varies systematically from ridge crests to slopes to hollows. The primary distinction between SHALSTAB and SHALSTAB.V is incorporation of spatially variable soil depth predicted using a soil production and transport model. A second version of PISA (hereafter referred to as PISA.V) was therefore developed using the 4-m grid of variable soil depth predicted by the soil production and transport model (see Section 2.3.2.2 for description of the model). The 4-m grid of variable soil depths used in PISA.V is identical to that used in SHALSTAB.V. All other parameters and probability distributions used for PISA.V are identical to that described for PISA.

2.3.3 Deep-seated landslide models

Large storm events can activate debris slides and rotational landslides associated with pre-existing deep-seated landslide features (De La Fuente et al. 2002). Despite the potential importance of deep-seated landslides to sediment delivery, the physical factors controlling deep-seated mass movement are poorly understood and few physical models have been developed to assess deep-seated landslide hazards (Miller 1995). Deep-seated landslide morphology is typically characterized by crescent-shaped major and minor scarps; flat-lying and backtilted blocks; benched topography; and lobate accumulation zones with hummocky topography, seepage lines and springs, ponding, and deflected or irregular drainage patterns. Deep-seated landslides and their corresponding level of activity are typically identified based on interpretation of these topographic signatures and patterns of drainage development in maps and aerial photographs supplemented by field observations. These approaches, however, require substantial effort, are limited by vegetation that obscures relevant features, and require

professional judgment based on experience with the local geology and topography; resulting in hazard mapping that is subjective.

A suite of tools for objective delineation of terrain prone to deep-seated landslides and earthflows using high-resolution digital topographic data is currently being developed (McKean and Roering 2004, Roering et al. 2005, Mackey et al. 2005, Mackey et al. 2006, Roering et al. 2006). These deep-seated landslide and earthflow detection (DSLED) algorithms identify terrain that has already experienced deep-seated slope instability, and thus has a higher potential for reactivation (Roering et al. 2006). The methods provide predictive power in identifying slide-prone terrain, and are best utilized as reconnaissance tools in combination with aerial photographic interpretation and field mapping. The models are being developed and tested at sites in the northern California Coast Range, Western Cascade Range of Oregon, and elsewhere (Roering et al. 2006); and have been used to successfully identify deep-seated mass movement associated with the Franciscan melange in the nearby Eel River basin (Mackey et al. 2005, Mackey et al. 2006). Two of the three DSLED algorithms, DSLED Rough and DSLED Drain, are used to identify surface roughness and drainage patterns associated with potential deep-seated mass movement in the Elk River basin.

2.3.3.1 DSLED-Rough

DLSED-Rough uses the eigenvalue ratio of cell-normal vector dispersion to identify local terrain roughness from airborne LiDAR topographic data (McKean and Roering 2004, Roering et al. 2006). The approach is based on observations that landslide surfaces are commonly rougher (on a local scale of a few meters) than adjacent unfailed slopes. DSLED Rough is used to construct unit vectors perpendicular to each cell in the DEM, and the statistical method of eigenvalue ratios (ln[S1/S2]) is used to describe the clustering of vector orientations (refer to McKean and Roering 2004 for the methods and theory behind eigenvalue ratios). The rougher the surface, the more divergent and less clustered the vector orientations. Mass movement and internal deformation of a deep-seated slide mass leads to rougher terrain with low ln (S1/S2) values relative to surrounding unfailed terrain.

Eigenvalue ratios (ln [S1/S2]) in the Elk River basin were calculated in a 15x15 m circular sampling window that moves over the 1-m DEM. Ln (S1/S2) values were then spatially averaged using a circular moving window with a 50-m radius. The DSLED-Rough algorithm identifies terrace and floodplain areas as "rough" due to small-scale variations in aspect on relatively flat surfaces. To objectively remove these types of false positives and isolate signatures of potential deep-seated instability between ridges and valleys, the following portions of the watershed were filtered from the spatially averaged DSLED-Rough results:

1. Polygons mapped at a coarse scale as alluvium (Qal of McLaughlin et al. 2000, Q and Qds of Marshall and Mendes 2005) were adjusted to fit terrain slope (7–9%) and curvature signatures extracted from alluviated valley bottoms in the Project Area using a 1-m DEM grid;
2. In the NW section of Elk River basin only (Martin Slough, Lower Elk River, Lower Elk River West), a slope threshold of 9% was used to identify low gradient valley bottoms (not mapped as alluvium) and broad-crested ridges,
3. Watershed divides were buffered 20 m on each side, and
4. Channels were buffered on each side using the square of the Strahler order (e.g., 1-m buffer for Strahler order 1 and 36-m buffer for Strahler order 6).

2.3.3.2 DSLED-drain

DSLED-Drain uses spatially-averaged values of drainage area per unit contour width (a/b) calculated using high-resolution topographic data from airborne LiDAR to identify large, poorly-drained landforms commonly associated with deep-seated slope instability (Mackey et al. 2005, Mackey et al. 2006). Deep-seated mass movement typically affects hillslope hydrology by impeding channel incision and slowing drainage network development, leading to large areas with lower a/b values than surrounding unfailed terrain (Mackey et al. 2005, Mackey e l. 2006).

DSLED-Drain calculates a/b values using the multiple-directional flow algorithm FD8 (Quinn et al. 1995, Costa-Cabral and Burgess 1994, Tarboton 1997). FD8 divides flow into each downstream neighboring cell based on the slope to that neighbor, while increasing the degree of flow convergence from the watershed divide to the channel head. The approach explicitly recognizes divergent flow on convex slopes and convergent flow on concave slopes and along valley bottoms. The catchment area, FD a/b, is the total drainage area for each cell divided by the cell width. FD a/b values were spatially averaged using a circular moving window with a 50-m radius. False positives associated with ridge crests and valley bottoms were filtered using the steps described above for DSLED-Rough.

2.4 Model Testing

2.4.1 Shallow landslide model testing

Hypothesis tests were developed to objectively validate model results and to evaluate the relative performance of the various modeling approaches. Validation tests and analyses of test results had the following primary objectives:

1. Evaluate the success of each model at correctly classifying potential instability at mapped shallow landslides in the Project Area,
2. Evaluate the aerial extent to which each model may over predict potential shallow instability in the Project Area;
3. Compare the relative performance of various modeling approaches; and
4. Determine appropriate thresholds for breaks in potential instability classes that balance the goals of maximizing correct landslide prediction and minimizing over prediction of unstable area.

Different geologic terrains in the Elk River basin (refer Section 2.1 above for descriptions of geologic terrains) are dominated by different hillslope geomorphic processes and rates due to different parent materials, weathering processes and rates, slope angles, surface and subsurface hydrologic interactions, and drainage density. Validation tests were therefore, independently conducted in the four dominant geologic terrains in the Elk River basin: Hookton and similar Quaternary terrace deposits (Qh-Qt-Qrt), Wildcat group (Qtwu), Yager terrain (Ty), and Franciscan Complex Central Belt (Kjfs). Tests in difference geologic terrains were conducted with the goal of evaluating the extent to which model performance and model threshold values vary in different geologic terrains.

2.4.1.1 Hypothesis testing

An objective and repeatable method of hypothesis testing was developed to address two basic questions:

1. Do shallow landslide models predict greater potential instability at known slide locations than at random positions in the landscape?
2. Are the models better predictors of instability than predictions based solely on hillslope gradient?

Two statistical tests were developed to address these questions, one based on randomly selected points (irrespective of slope), and the other accounting for the covariate hillslope gradient during the point selection process. For both tests, the null hypothesis states that model predictions of potential instability at randomly selected points in the Elk River basin will be greater than or equal to model predictions at a landslide point. For both tests, the alternative hypothesis states that model predictions of potential instability will be greater at slide points than at random points. A p-test value, indicating the extent to which models predict greater instability at random points than at a landslide point, was estimated as:

$$p_j = \frac{\sum_{i=1}^{B} (Z_i \geq Z_j)}{B},$$

where Z_i is the model value at the ith randomly selected point, Z_j is the model value at the jth slide, and B is the number of randomly selected points (B=5,000); ($Z_i \geq Z_j$) is 1 if true and 0 if false ($\geq$ defined here as greater instability). P-values vary from 0 to 1; with a value of 0 indicating a test where predicted instability is always greater at a slide than at random points, and a value of 1 indicating a test where predicted instability is always greater at random points than at a slide. A p-value <0.5 indicates that the model predicts greater instability at a landslide than at more than half of the 5,000 random points. The percentage of p-values <0.5 were summarized for each model validation test. Different threshold p-values can be selected to change the rigor of the test.

To address the first question, model values for potential instability at mapped landslide points were tested against model values of potential instability at a set of random points (sampled with replacement) within the Elk River basin. Random sampling with replacement (i.e., the same point can be selected more than once) is used here because comparisons using model values for all 4-m grid cells in the Project Area were computationally unfeasible (e.g., the 4-m grid of model results includes over 9 million cells in the 151 km^2 Project Area). The large number of randomly selected points (B=5,000) ensures that the sample is representative of the population of all points in the Project Area. Random sampling occurred using the "sample" function in the "R" statistical package (R Development Core Team 2006).

To address the second question, model values for potential instability at mapped landslide points were tested against model values for potential instability at a set of random points sampled (with replacement) from a probability distribution of potentially unstable slopes defined by hillslope gradient at landslide points. By incorporating hillslope gradient as a covariate, the second test specifically evaluates whether the models are better predictors of

instability than predictions based solely on hillslope gradient. Probability density functions for hillslope gradient were constructed for each geologic terrain using the mean and standard deviation of gradient values at all non-road-related landslide points mapped in that geologic terrain. Probability densities were calculated for all points in the landscape, assuming a normal distribution for hillslope gradient (a reasonable assumption based on graphical analyses of hillslope gradient values at landslide points). The probability densities were calculated using the "dnorm" function in the "R" statistical package. Unique probability distributions for gradient were developed for each terrain type (Appendix A). Probability densities for hillslope gradient at landslide points were then used to weight random sampling of points using the "sample" function in the "R" statistical package.

The performance of landslide models in validation tests may be significantly influenced by uncertainties in the location of landslide initiation points due to inaccuracies in the original mapping of landslides on aerial photos (approximately 1:18000 scale) and on coarse-scale topographic maps (1:24,000 USGS quadrangles) during field observations. Due to uncertainty in the location of landslide initiation relative to mapped shallow landslide points, statistical tests were conducted at two spatial resolutions: (1) model values for potential instability *at a landslide point*, and (2) model values for the highest potential instability *within a specified neighborhood* of a landslide point. The first resolution assumes that shallow landslide points in the existing landslide database are indeed initiation points, landslide initiation points are accurately and precisely mapped within 4 meters (grid cell size), and that model predicted values at slide initiation points accurately reflect the limiting instability associated with failure. The second resolution allows for uncertainty in the spatial location of landslide initiation relative to the mapped landslide point by determining the model value with the highest (most limiting) potential instability within an 8-meter radius around a mapped landslide point. An 8-m radius considers the model results in all 4-m grid cells adjacent to the mapped landslide initiation point.

2.4.1.2 Correct landslide prediction versus area predicted to be unstable

The fraction of slides and random points within each geologic terrain was used to evaluate relationships between (1) the fraction of slides correctly classified and (2) the fraction of the Elk River basin predicted to be unstable. The analysis was intended to guide selection of model thresholds that consider both the extent to which a model correctly classifies mapped landslides as unstable and the potential over prediction of unstable areas. Cumulative relative frequency distributions were graphed by fitting smoothed logistic regression curves to the data (i.e., model predictions of potential instability, fraction of slides correctly classified, and fraction of area predicted to be unstable) using the "sm" library (Bowman and Azzalini 1997, 2005) within the "R" statistical package. A kernel smoothing technique was used to generate the curves representing the cumulative relative frequency functions using the "sm.binomial" function in the "R" statistical package. For each model type, two cumulative relative frequency functions were generated, one for the most unstable value within an 8 m radius of slide points (*RS*), and the other for the most unstable value within an 8 m radius of randomly selected points (*RL*). We defined *RL(x)* as the *fraction of the Project Area* within a particular terrain type for which the model predicted potential instability is greater than *x*, and *RS(x)* as the *fraction of the slides* within a particular terrain type for which model predicted potential instability is greater than *x*. *RL(x)* is estimated based on the large sample (5,000) of random points, and the random selection process ensures that this large sample is representative of the population of all points in the Project Area.

2.4.1.3 Determination of potential instability thresholds

In selecting appropriate threshold model values for potential instability classes, there is a fundamental tradeoff between (1) the cost of incorrectly classifying landslides and (2) the cost of over predicting potentially unstable area. An instability threshold that incorrectly classifies a landslide location as stable may not adequately protect similar areas prone to landsliding. Conversely, overprediction of unstable area may result in unnecessary restrictions and associated site evaluation costs in stable and economically productive areas. A particularly useful threshold for managing landslide hazards can be defined as the potential instability value that simultaneously minimizes the total costs associated with incorrect slide classification and over prediction of potential instability.

The total cost of incorrectly predicting slides as stable (more stable than threshold x) can be expressed as: $A*(1-RS(x))$, where A is the total cost associated with incorrectly classifying slides as stable in the Project Area. The total cost associated with over predicting unstable areas can be expressed as: $B*(RL(x)-c)$, where B is the total cost due to over prediction in the Project Area, and c is the fraction of the landscape that is unstable (estimated by the number of slides over the number of cells in the landscape). The value of x that minimizes the total cost [$A*(1-RS(x))+B*(RL(x)-c)$] is the same value that maximizes $A*RS(x)-B*RL(x)$. If the total cost associated with incorrectly classifying slides as stable is equal to the total cost due to over prediction (i.e., $A=B$), then the problem reduces to maximizing $RS(x)-RL(x)$. In practice, the maximum value for $RS(x)-RL(x)$ is found by calculating the difference between the two cumulative relative frequency functions for model predicted instability.

To obtain an expected value and confidence interval for the threshold value based on this approach, the following steps were taken:

1. Bootstrap samples of model predicted potential instability within an 8 m radius of slides and model predicted instability within an 8 m radius of randomly selected points were generated;
2. Logistic regression curves were fit to data from both bootstrap samples by kernel smoothing (refer to methods described above);
3. A threshold value was calculated based on the method described above;
4. Steps 1−3 were repeated 5,000 times;
5. The expected value (i.e., calculated as the mean of all samples) and 95% confidence interval for the threshold value (based on the 2.5 percentile and 97.5 percentile), along with the expected value and 95% confidence interval for the cumulative relative frequencies $RS(x)$ and $RL(x)$ associated with the threshold model value, were calculated.

2.4.1.4 Landslide density graphs

A second, independent method of evaluating model performance is to compare the landslide density (i.e., number of landslides counted in an instability class divided by the total area in that instability class) to the random point density in each instability class (Dietrich et al. 2001). Model performance can be objectively determined by significantly greater landslide density in increasingly unstable classes compared to the nearly constant density of random points across instability classes. If a model performs poorly, there would be little difference between the densities of landslides and random points. If model predicted instability strongly covaries with

slope, the random point distribution may reflect the distribution of hillslope gradient in the basin.

Classes of model values were defined for Shalstab and Shalstab V and for PISA and PISA V; and three values were calculated for each class: 1) number of random points, 2) number of slide points, and 3) watershed area. For each class, point densities were calculated by dividing either the number of random points or the number of slide points by the watershed area. Densities are based on maximum instability within an 8 m radius of points. The number of random points in a given terrain was scaled to match the total number of landslide points by calculating the proportion of random points within each defined class and then multiplying these proportions by the total number of slide points. Relative densities in different instability classes are therefore, more important than the absolute density values.

2.4.1.5 Existing landslide inventories

Several independent sets of landslide data exist for the Elk River basin. These include:

- a sediment source inventory initially prepared by Pacific Watershed Associates in 1998 for Pacific Lumber Company and subsequently updated by Pacific Watershed Associates in 2001 as part of Watershed Analysis;
- a forensic landslide investigation prepared by Pacific Lumber Company in 2003;
- compilation of landslide mapping by Pacific Lumber Company in 2006; and
- compilation of landslide mapping from review of timber harvest plans by the California Geologic Survey in 2005.

Table 2-8 summarizes the important attributes of existing landslide inventories relevant to testing the validity of shallow landslide model results in the Elk River basin.

The 2001 inventory of landslides in the ElK River basin conducted by Pacific Watershed Associates for Pacific Lumber Company was undertaken as part of a sediment source inventory for Watershed Analysis (PALCO 2004a). The landslide inventory involved mapping landslide features and attributes from an historical aerial photographic time series (1954, 1966, 1974, 1987, 1994, 1997, and 2000). Over 850 shallow landslide initiation points were mapped from air photos and transferred onto base maps at a scale of 1:18,000. A sample of landslide features mapped from aerial photography were field verified during Watershed Analysis and during sediment source inventories on Pacific Lumber Company land prior to 1998 (PWA 1998). The landslide forensic investigation conducted by Pacific Lumber Company in 2003 supplemented the sediment source inventory by mapping 64 shallow landslides in the Elk River basin that were triggered by an intense rainfall event in December 2002 (PALCO unpublished data). The study also identified causal mechanisms for landslide initiation and estimated associated sediment delivery. Accepted field methods were used in the 2003 forensic study to document landslide type, morphology, and dimensions; geologic, geomorphologic, and hydrologic controls; soil shear strength parameters; volume of sediment production and delivery; vegetation characteristics; forest management and timber harvest associations; and road and stream crossing associations. The methods used in the 2003 forensic study were generally consistent and compatible with those used in the 2001 landslide inventory by PWA.

Pacific Lumber Company provided Stillwater Sciences with a coverage and associated database of attributes that included landslide initiation points identified in the 2001 landslide inventory and 2003 forensic study, as well as landslide initiation points and polygons identified during

more recent geologic investigations associated with THP development in pilot subwatersheds. The data base contained 1,144 shallow landslide initiation points in the Elk River basin. Mapping of erosion and depositional areas for individual shallow landslides was not available for the Project Area at the time of this study. These data are the most comprehensive and extensively ground-verified landslide data available for the Project Area. All shallow landslide initiation points from this compilation that were characterized as debris slides, translational slides, or translational debris slides and occurred on open slopes with no apparent road association were used in model validation tests (Figure 2-11).

The California Geological Survey mapped landslides and their attributes from aerial photographs (1940 to 2000), compiled existing landslide mapping, and interpreted relative landslide potential in the Elk River basin during preparation of the Watershed Mapping Series for the Elk River Watershed (Marshall and Mendes 2005). Nearly 550 shallow landslide features were mapped from aerial photographs and classified following DMG (1997) and Cruden and Varnes (1996). Landslide data compiled by Marshall and Mendes (2005) were not used in model validation tests for the following reasons: (1) landslides were mapped and compiled at a coarse scale (1:24,000), (2) no landslide mapping was available for the period after 2000, (3) field verification of the mapping was limited, (4) the work included no assessment of positional accuracy, and (5) the data do not include an attribute for road association. CGS interpreted relative landslide potential in the Elk River basin based on a matrix of values assigned to various classes of (1) landslide feature type and activity level, (2) hillslope and channel gradient derived from 10-m DEM data, (3) potential instability predicted by SHALSTAB, and (4) geologic terrain type. Individual coverages were converted to grids, assigned values according to the matrix, and merged into final grid.

The performance of landslide models in validation tests may be significantly influenced by uncertainties in the location of landslide initiation points related to inaccuracies in the original mapping of landslides on aerial photos (approximately 1:18000 scale) and on coarse-scale topographic maps (1:24,000 USGS quadrangles) during field observations. Stillwater Sciences verified mass wasting features in pilot areas using 2003 aerial photographs (scale 1:12,000) and hillshade images from a 1-m DEM derived from LiDAR. A standardized data sheet was used to characterize specific attributes of mass wasting features, based on landform identification and mapping standards outlined in Bedrossian (1983), Selby (1993), and Cruden and Varnes (1996). These attributes were consistent with landslide mapping by PWA (2001, unpublished data), PALCO (unpublished data), and Marshall and Mendes (2005). Where feasible, the slide scar was distinguished from the runout track. Some older mass wasting features were not visible in the 2003 aerial photos. Despite verification of the positional accuracy of mapped landslides in pilot areas, uncertainty associated with existing shallow landslide initiation points throughout the Elk River basin could not be directly assessed as part of this effort.

Table 2-8. Existing landslide data in the Elk River basin.

	2001 landslide inventory	2003 landslide investigation	2005 landslide mapping
Source	PWA	SCOPAC	CGS
Objective	sediment source inventory	investigation of slides triggered by 2002 storm event	regional landform and landslide mapping
Methods	aerial photo inventory, field survey	field survey	aerial photo inventory, review of geologic field surveys from THP reports, limited field observation
Base data	historical aerial photography 1954-2000	2003 color air photos	historical aerial photography 1940-2000
Scale	1:12,000 to 1:21,120	1:12,000	1:12,000 to 1:36,000; compiled on orthophotoquads at 1:24,000
Data	feature type, certainty, photo year, erosion dimensions (L, W, D, V), depositional dimensions, delivery, management association (road, harvest, landuse), geomorphic association (landform, hillslope gradient, horizontal curvature), veg cover	feature type, activity, dimensions (L, W, D), runout length, delivery, management association (road type, stand type)	initiation type and confidence, activity, source year and approximate age, area, delivery, thickness, harvest history, THP number
Format	initiation points	initiation points	initiation points (shallow landslides), polygons (deep-seated landslides), and lines (debris flows)

2.4.2 Deep-seated landslide modeling

DSLED-Rough and DSLED-Drain modeling approaches are in development and have not been extensively or systematically tested using independent deep-seated landslide data sources. Testing of model results for potential deep-seated hillslope instability were limited by available deep-seated landslide mapping in the Project Area. After comparison of modeling results with mapped deep-seated features mapped by CGS (Marshall and Mendes 2005) and discussion of alternative approaches, it was determined that there is currently insufficient information to objectively test the modeling results using existing landslide mapping. This is largely due to uncertainties in the types, boundaries, and activity level of existing deep-seated landslide mapping. Evaluation of deep-seated model performance in later sections of this report are therefore qualitative.

3 RESULTS

3.1 Shallow Landslide Modeling Results

Four distributed, physically-based models were employed to predict potential shallow landslide hazards in the Elk River basin: the deterministic models SHALSTAB and SHALSTAB.V, and the probabilistic models PISA and PISA.V. Results are based on topographic data obtained from a 4-m DEM constructed from LiDAR data and the parameter values discussed above.

The spatial distribution and magnitude of log (q/T) results for SHALSTAB and SHALSTAB.V are shown in Figure 3-1 Figure 3-2, respectively. High, moderately high, and moderate potential instability are represented by areas where log q/T is less than or equal to -3.1, -2.8, and -2.5, respectively. These preliminary classes are based on suggested log(q/T) thresholds reported for SHALSTAB applications in other areas (Dietrich et al 2001, Montgomery et al. 1998). The pattern of potential instability predicted by SHASTAB and SHALSTAB.V is similar, where areas with relatively high potential for shallow instability generally occur on steep convergent slopes. SHALSTAB V focuses instability in steep, convergent areas with thicker soil mantle and predicts greater stability in divergent areas and less steep convergent areas with thinner soil mantle.

The spatial distribution and magnitude of probability of failure predicted by PISA and PISA.V are shown in Figure 3-3 and Figure 3-4, respectively. Probability of failure classes shown for PISA and PISA.V were classified in order to best illustrate the range of potential instability. PISA.V results in notably lower probabilities of failure.

The magnitude and distribution of the modeling results are further discussed and compared in the following sections on model testing.

3.2 Shallow Landslide Model Testing

3.2.1 Model performance based on p-tests

Statistical p-tests were used within a hypothesis testing framework to address two basic questions:

1. Do shallow landslide models predict greater potential instability at known slide locations than at random positions in the landscape?
2. Are the models better predictors of instability than predictions based solely on hillslope gradient?

To address the first question, model values for potential instability at mapped landslide points were tested against model values of potential instability at a set of random points sampled within the Elk River Project Area. To address the second question, model values for potential instability at mapped landslide points were tested against model values for potential instability at a set of random points sampled from a probability distribution of potentially unstable slopes defined by hillslope gradient at landslide points (Appendix A). A p-test value of less than 0.5 ($p<0.5$) means

that the model value at a landslide point predicted higher potential instability than model values at more than half of the 5,000 random points. P-test results for individual landslides are shown in Appendix B for tests conducted based on randomly sampled points, and in Appendix c for tests conducted based on points randomly sampled from a distribution of potentially unstable slopes. Reliable model validation based on p-testing was not possible in Franciscan Complex Central Belt due to the small sample size (n=6) for non-road-related shallow landslide initiation points in that terrain.

Table 3-1 summarizes the percent of shallow landslides in each geologic terrain where $p<0.5$. The percent of shallow landslides where $p<0.5$ was significantly higher when p-tests were based on the highest potential instability (most limiting) *within an 8-meter radius* of a point rather than instability *at a point*, and we assume hereafter that maximum instability within a radius is more representation of model performance. A second percentage (reported in parentheses in Table 3-1) was calculated after removing landslides where $p>0.5$ for all four models, indicating poor performance for all models. In removing these landslide points, we assume they are not located accurately enough to encompass the landslide initiation area (limiting instability) within an 8-m radius and are therefore less useful in evaluating model performance.

For three of the four models (SHALSTAB, SHALSTAB.V, and PISA), p-values based on random sampling were less than 0.5 for 73% or more of the landslide points. In other words, for 73% or more of the landslides in a given terrain, all three models predicted greater potential instability at the slide point than at more than half of the random points. This percentage increased to 82% or more when considering only landslides where $p<0.5$ for at least one model. When P-tests were conducted by randomly sampling points from a distribution of potentially unstable slopes (defined by hillslope gradient at landslide points), p values were still <0.5 for 64% or more landslide points, and 75% or more landslide points where $p<0.5$ for at least one model. These p-test results statistically demonstrate that (1) shallow landslide models do predict greater potential instability at known slide locations than at random locations, and (2) the models are significantly better predictors of potential instability than predictions based solely on hillslope gradient. The performance of shallow landslide models relative to each other was determined for each geologic terrain based on comparison of p-test values, where the relative performance is defined as the percent of shallow landslides with $p<0.5$.(Tables 3-2 , 3-3, and 3-4). The following results are apparent when comparing p-test results based on the highest (most limiting) instability within an 8-meter radius of a point and using only landslide points where $p<0.5$ for at least one model:

- **Qh-Qmts-Qrt terrain:** SHALSTAB.V and PISA.V both performed better than other models. Differences between SHALSTAB.V and PISA.V, however, were small (within 3%). Differences between PISA and PISA.V were also small (within 3%).
- **Qtwu terrain:** SHALSTAB.V and PISA both performed better than other models. Differences between SHALSTAB.V and PISA, however, were small (within 3%).
- **Ty terrain:** SHALSTAB.V performed significantly better than PISA. Differences in all other model comparisons were small (within 3%).

In summary, comparisons of model performance based on p-values indicate that SHALSTAB.V is the best-performing deterministic model and PISA is typically the best-performing probabilistic model. Differences between SHALSTAB.V and PISA are typically small (within 3%).

Table 3-1. Percent of shallow landslides where P-test results were less than 0.5.

Test	Percent based on potential instability at point				Percent based on max instability within 8-m radius[1]			
	SHALSTAB	SHALSTAB.V	PISA	PISA.V	SHALSTAB	SHALSTAB.V	PISA	PISA.V
Qh Terrain (n=78 landslides, n=68 landslides where p<0.5 for at least one model)								
Random points	58	55	67	50	76 (87)	78 (90)	76 (87)	71 (81)
Random points sampled from slope distribution at landslides	58	55	62	50	68 (79)	71 (82)	71 (82)	71 (82)
Qtwu Terrain (n=397 landslides, n=355 landslides where p<0.5 for at least one model)								
Random points	66	57	70	22	73 (82)	73 (82)	75 (84)	64 (72)
Random points sampled from slope distribution at landslides	60	57	60	22	66 (75)	66 (76)	71 (81)	64 (73)
Ty Terrain (n=88 landslides, n=77 landslides where p<0.5 for at least one model)								
Random points	68	59	73	40	78 (87)	73 (83)	75 (86)	67 (77)
Random points sampled from slope distribution at landslides	66	59	64	40	69 (84)	64 (77)	70 (85)	65 (78)

1 Number in parentheses is the percentage of shallow landslides where P-test results were <0.5 when including only those landslides points where p<0.5 for at least one model.

Table 3-2. Comparative model performance in Qh-Qmts-Qrt terrain based on p-values relating potential instability at landslide points to potential instability at random points. Values are percent of shallow landslides for which model in column is a better (lower p-value), equal (equal p-value), or worse (higher p-value) predictor of potential instability than model in row.

	Based on potential instability at points (78 landslides)								
	SHALSTAB V			**PISA**			**PISA V**		
	better	**equal**	**worse**	**better**	**equal**	**worse**	**better**	**equal**	**worse**
SHALSTAB	32%	35%	33%	69%	3%	28%	27%	37%	36%
SHALSTAB V				58%	3%	40%	22%	41%	37%
PISA							33%	3%	64%
	Based on maximum instability within 8-m radius of points								
	SHALSTAB V			**PISA**			**PISA V**		
	better	**equal**	**worse**	**better**	**equal**	**worse**	**better**	**equal**	**worse**
SHALSTAB	53%	14%	33%	59%	0%	41%	58%	5%	37%
SHALSTAB V				54%	1%	45%	53%	8%	40%
PISA							53%	0%	47%
	Based on maximum instability within 8-m radius and only slide points where P<0.5 for at least one model (68 landslides)								
	SHALSTAB V			**PISA**			**PISA V**		
	better	**equal**	**worse**	**better**	**equal**	**worse**	**better**	**equal**	**worse**
SHALSTAB	60%	3%	37%	53%	0%	47%	59%	0%	41%
SHALSTAB V				47%	1%	51%	53%	1%	46%
PISA							53%	0%	47%

Table 3-3. Comparative model performance in Qtwu terrain based on p-values relating potential instability at landslide points to potential instability at random points. Values are percent of shallow landslides for which model in column is a better (lower p-value), equal (equal p-value), or worse (higher p-value) predictor of potential instability than model in row.

	Based on potential instability at points (397 landslides)								
	SHALSTAB V			**PISA**			**PISA V**		
	better	**equal**	**worse**	**better**	**equal**	**worse**	**better**	**equal**	**worse**
SHALSTAB	30%	27%	43%	66%	3%	30%	16%	31%	52%
SHALSTAB V				65%	3%	32%	16%	41%	44%
PISA							17%	3%	81%
	Based on maximum instability within 8-m radius of points								
	SHALSTAB V			**PISA**			**PISA V**		
	better	**equal**	**worse**	**better**	**equal**	**worse**	**better**	**equal**	**worse**
SHALSTAB	55%	11%	34%	57%	0%	43%	40%	8%	52%
SHALSTAB V				57%	0%	43%	38%	12%	51%
PISA							40%	0%	60%
	Based on maximum instability within 8-m radius and only slide points where P<0.5 for at least one model (359 landslides)								
	SHALSTAB V			**PISA**			**PISA V**		
	better	**equal**	**worse**	**better**	**equal**	**worse**	**better**	**equal**	**worse**
SHALSTAB	60%	4%	36%	56%	0%	44%	45%	1%	54%
SHALSTAB V				53%	0%	46%	42%	3%	55%
PISA							45%	0%	55%

Table 3-4. Comparative model performance in Ty terrain based on p-values relating potential instability at landslide points to potential instability at random points. Values are percent of shallow landslides for which model in column is a better (lower p-value), equal (equal p-value), or worse (higher p-value) predictor of potential instability than model in row.

	Based on potential instability at points (88 landslides)								
	SHALSTAB V			**PISA**			**PISA V**		
	better	**equal**	**worse**	**better**	**equal**	**worse**	**better**	**equal**	**worse**
SHALSTAB	34%	31%	35%	75%	2%	23%	28%	28%	43%
SHALSTAB V				70%	2%	27%	20%	39%	41%
PISA							22%	3%	75%
	Based on maximum instability within 8-m radius of points								
	SHALSTAB V			**PISA**			**PISA V**		
	better	**equal**	**worse**	**better**	**equal**	**worse**	**better**	**equal**	**worse**
SHALSTAB	42%	14%	44%	51%	0%	49%	41%	9%	50%
SHALSTAB V				48%	0%	52%	43%	15%	42%
PISA							43%	0%	57%
	Based on maximum instability within 8-m radius and only slide points where P<0.5 for at least one model (77 landslides)								
	SHALSTAB V			**PISA**			**PISA V**		
	better	**equal**	**worse**	**better**	**equal**	**worse**	**better**	**equal**	**worse**
SHALSTAB	48%	5%	47%	48%	0%	52%	47%	0%	53%
SHALSTAB V				40%	0%	60%	49%	3%	48%
PISA							49%	0%	51%

3.2.2 Model performance based on landslide density

As an alternative approach to evaluating model performance, landslide density graphs were generated using methods similar to Dietrich et al. (2001). Model performance can be objectively determined by an increase in landslide density in increasingly unstable classes compared to the nearly constant density of random points across instability classes. Plots showing the density of landslide points versus the density of random points in the three dominant geologic terrains are shown in Figure 3-5 for SHALSTAB and Figure 3-6 for SHALSTAB.V. The SHALSTAB and SHALSTAB.V results demonstrate significant and increasing divergence between landslide density and random point density at log [q/T] values less than -2.2 in Qh-Qmts-Qrt and less than -2.5 to -2.8 in Qtwu terrain. SHALSTAB results in Ty terrain indicate a significant divergence between landslide density and random point density at log [q/T] values less than about -2.8.

Plots showing the density of landslide points versus the density of random points in the three dominant geologic terrains are shown in Figure 3-7 for PISA and Figure 3-8 for PISA.V. The PISA and PISA.V results also demonstrate increases in landslide density at the higher instability classes relative to random point density. In the case of PISA, landslide and random point densities diverge at failure probabilities of about 0.15 in Qh-Qmts-Qrt terrain, gradually above about 0.1 then abruptly at 0.3 in Qtwu terrain, and above about 0.15 in Ty terrain. In the case of PISA.V, divergence occurs at failure probabilities of 0.25 in Qh-Qmts-Qrt terrain and abruptly

from the origin in Qtwu terrain. Landslide densities area not reported for Ty terrain due to the small number of landslides mapped in different probability classes within that terrain

3.2.3 Correct landslide prediction versus area predicted to be unstable

The fraction of watershed area encompassed by a model-predicted potential instability value (log (q/T) or probability of failure) relative to the number of mapped landslides correctly predicted by that instability value is a useful measure for determining relevant landslide hazard classes (Dietrich et al. 2001). The approach considers both (1) the extent to which a model threshold correctly classifies mapped landslides as unstable and (2) the potential over prediction of unstable area. Figure 3-9 and Figure 3-10 show the cumulative percent area and cumulative percent of mapped landslides in the Elk River watershed for potential instability predicted by SHALSTAB, SHALSTAB V, PISA, and PISA V (Table 3-5). Figure 3-11 shows cumulative percent of watershed area plotted as a function of the cumulative percent of landslides correctly predicted by a given potential instability value. SHALSTAB and SHALSTAB V values are plotted for classes used in validation tests in the Coast Ranges of California and Oregon (Dietrich et al. 2001). PISA and PISA V classes are plotted at intervals within the range of probability of sliding values encompassing the majority of landslides in the Elk River basin (0–0.5).

SHALSTAB V results in the Elk River basin, when compared to previous SHALSTAB validation studies in similar terrain, correctly predict fewer landslides and classify less of the watershed area as unstable for a given log (q/T) threshold. Dietrich et al. (2001) found that for 7 watersheds in the northern California Coast Range, the cumulative percentage of mapped in-unit landslides for the less than -3.1, -2.8, and –2.5 categories was 46, 58, and 73 percent, respectively. The cumulative area covered by the less than -3.1, -2.8, and –2.5 categories was 11.4, 16, and 25.7 percent, respectively. A study of 629 landslides in Washington Coast Range found that 86% of the slides occurred within log (q/T) less than -2.5 using 30-m data (K. Sullivan, pers. com., 1994 as cited in Dietrich et al. 2001). Montgomery et al. (1998), found that when SHALSTAB was tested against 3,224 landslides in 14 watersheds of the Oregon and Washington Coast Ranges, about 66% of the landslides occurred within log (q/T) less than -2.5 using 30-m grid data. In comparison, the cumulative percentage of landslides in the less than -3.1, -2.8, and –2.5 categories in the Elk River basin was 10, 19, and 29 percent, respectively; and the area covered by the less than -3.1, -2.8, and –2.5 categories was 3, 6, and 13 percent, respectively (Table 3-5). Discrepancies between validation results reported for the Elk River basin and those reported for other areas are likely due to (1) uncertainties in the actual location of shallow landslide initiation relative to the mapped landslide points used to test model results; (2) differences in the resolution of topography used in mapping, modeling, and model testing; and (3) differences between the processes controlling model-predicted potential instability (shallow failure in areas with steep, convergent topography and thick soil accumulation) and the processes controlling shallow landsliding in the Elk River basin.

Table 3-5. Summary of validation results: cumulative percent of area and cumulative percent of landslides by instability class.

SHALSTAB

	-3.1 to -9.9		-2.8 to -3.1		-2.5 to -2.8		-2.2 to -2.5	
Geologic Terrain	**area**	**slides**	**area**	**slides**	**area**	**slides**	**area**	**slides**
Kjfs	5%	17%	8%	33%	15%	50%	26%	67%
Ty	4%	13%	8%	19%	13%	31%	22%	48%
Qtwu	2%	5%	4%	9%	8%	19%	16%	31%
Qh-Qmts-Qrt	2%	9%	4%	11%	8%	16%	15%	34%
Total	**3%**	**7%**	**5%**	**11%**	**9%**	**20%**	**17%**	**34%**

SHALSTAB V

	-3.1 to -9.9		-2.8 to -3.1		-2.5 to -2.8		-2.2 to -2.5	
Geologic Terrain	**area**	**slides**	**area**	**slides**	**area**	**slides**	**area**	**slides**
Kjfs	6%	33%	10%	50%	19%	67%	29%	83%
Ty	5%	19%	9%	30%	16%	35%	24%	46%
Qtwu	3%	8%	6%	18%	12%	26%	21%	42%
Qh-Qmts-Qrt	3%	8%	6%	14%	11%	32%	20%	39%
Total	**3%**	**10%**	**6%**	**19%**	**13%**	**29%**	**22%**	**43%**

PISA

	0.2 to 0.3		0.1 to 0.2		0.05 to 0.1		0.01 to 0.05		0.001 to 0.01	
Geologic Terrain	**area**	**slides**	**area**	**slides**	**area**	**slides**	**area**	**slides**	**area**	**slides**
Kjfs	1%	17%	4%	17%	11%	33%	29%	83%	50%	83%
Ty	2%	5%	7%	24%	13%	41%	27%	57%	45%	72%
Qtwu	1%	2%	2%	7%	6%	17%	18%	37%	36%	59%
Qh-Qmts-Qrt	6%	14%	12%	22%	17%	32%	29%	50%	43%	68%
Total	**1%**	**5%**	**4%**	**12%**	**8%**	**22%**	**20%**	**42%**	**39%**	**63%**

PISA V

	0.2 to 0.3		0.1 to 0.2		0.05 to 0.1		0.01 to 0.05		0.001 to 0.01	
Geologic Terrain	**area**	**slides**	**area**	**slides**	**area**	**slides**	**area**	**slides**	**area**	**slides**
Kjfs	0%	0%	0%	0%	0%	0%	1%	0%	2%	17%
Ty	0%	1%	0%	4%	1%	5%	1%	6%	3%	10%
Qtwu	0%	0%	0%	1%	0%	1%	0%	2%	1%	4%
Qh-Qmts-Qrt	1%	1%	1%	1%	2%	5%	4%	14%	9%	16%
Total	**0%**	**1%**	**0%**	**1%**	**0%**	**2%**	**1%**	**5%**	**2%**	**7%**

The sampling approach outlined in Section 2.4.1.3 was independently used to determine a threshold for managing landslide hazard that minimizes the total cost associated with incorrect slide classification and over prediction of potentially unstable area. Table 3-6 summarizes confidence intervals for threshold values and the associated cumulative fraction of slides or random points classified by the threshold value (refer also to Appendix E). The 95% confidence intervals are based on the 2.5 percentile and 97.5 percentile from 5000 bootstrap iterations.

Log(q/T) thresholds for SHALSTAB and SHALSTAB.V based on the sampling approach are similar for a given geologic terrain, ranging from -2.1 in Qh-Qmts-Qrt terrain to -2.5 in Ty terrain (Table 3-5). *RS(x)* and *RL(x)* for the inferred SHALSTAB and SHALSTAB.V thresholds were also similar for a given geologic terrain (Table 3-6). Threshold values determined by the *RS(x)-RL(x)* method, however, were lower, and therefore more conservative than suggested log(q/T) thresholds reported for SHALSTAB applications in other areas (Dietrich et al 2001, Shaw and Vaugeois 1999, Montgomery et al. 1998). Dietrich et al. (2001), for example, recommend using a log (q/T) threshold of -2.5 or lower (more unstable).

Probability of failure thresholds for PISA and PISA.V based on the sampling approach varied for a given geologic terrain (Table 3-6). PISA thresholds ranged from 0.06 in Qtwu terrain to 0.10 in Ty terrain and 0.17 in Qh-Qmts-Qrt terrain. PISA.V thresholds were lower, ranging from 0.02 in Qtwu terrain to 0.14 in Qh-Qmts-Qrt terrain. *RS(x)* and *RL(x)* for the inferred PISA.V thresholds were lower than for inferred PISA thresholds (Table 3-6). Threshold values for PISA determined by the sampling approach were lower than probability of failure thresholds reported for PISA applications in other areas. Haneberg (2004) found that in the Wheeling area of West Virginia, the correspondence between active landslide area and probabilities of sliding at the 0.5, 0.3, and 0.1 thresholds was approximately 64, 89, and 99 percent respectively. These results, however, report the distribution of calculated probability of sliding values for each hazard unit, and may not be directly comparable to *RS(x)* and *RL(x)* reported here for the Elk River basin.

Table 3-6. Confidence intervals for threshold values and associated cumulative fraction of slides or area classified by the threshold value.

Model	Geologic terrain	Threshold potential instability[2]			Cumulative fraction of slides (*RS(x)*)[3]			Cumulative fraction of area (*RL(x)*)[4]		
		Upper limit	Expected value	Lower limit	Upper limit	Expected value	Lower limit	Upper limit	Expected value	Lower limit
Shalstab	Qh-Qmts-Qrt	-2.33	-2.06	-1.80	0.85	0.74	0.58	0.57	0.45	0.33
Shalstab	Qtwu	-2.47	-2.32	-2.18	0.66	0.59	0.52	0.43	0.36	0.30
Shalstab	Ty	-3.79	-2.51	-2.04	0.83	0.65	0.35	0.54	0.37	0.07
Shalstab V	Qh-Qmts-Qrt	-2.42	-2.12	-1.80	0.84	0.72	0.57	0.52	0.40	0.29
Shalstab V	Qtwu	-2.51	-2.35	-2.20	0.66	0.59	0.52	0.42	0.35	0.29
Shalstab V	Ty	-2.97	-2.48	-1.93	0.80	0.62	0.43	0.55	0.35	0.19
PISA	Qh-Qmts-Qrt	0.237	0.174	0.134	0.70	0.57	0.44	0.31	0.24	0.17
PISA	Qtwu	0.060	0.055	0.050	0.55	0.49	0.41	0.27	0.22	0.17
PISA	Ty	0.145	0.092	0.073	0.68	0.57	0.42	0.31	0.25	0.14
PISA V	Qh-Qmts-Qrt	0.268	0.143	0.062	0.75	0.31	0.18	0.16	0.04	0.00
PISA V	Qtwu	0.030	0.021	0.020	0.53	0.46	0.33	0.14	0.09	0.02

[1] Determined by maximizing *RS(x)-RL(x)*. Confidence intervals calculated from bootstrap sampling with more than 5000 iterations.
[2] Upper limits reflect greater potential instability. Upper and lower limits are 95% confidence interval.
[3] Cumulative fraction of slides located within areas classified as equal to or more unstable than the threshold potential instability value.
[4] Based on cumulative fraction of random points located within areas classified as equal to or more unstable than the threshold potential instability value.

3.3 Deep-Seated Landslide Modeling Results

The spatial distribution of DSED-Rough and DSLED-Drain results are shown in Figure 3-12 and Figure 3-13, respectively. Although model performance was not objectively tested, deep-seated modeling results were qualitatively evaluated by comparing model predictions of potential deep-seated instability in select areas with clearly defined deep-seated landslide morphology visible in aerial photography and hillshade plots developed from 1-m LiDAR DEM data. One potential approach to testing the deep-seated modeling results is to overlay the boundaries of mapped deep-seated landslides of varying activity class onto a grid of model results and look for statistical differences in typical signatures for unfailed terrain (e.g., ridge-and-valley terrain sculpted by shallow landslide and debris flow processes) and deep-seated landslides of different activity class (active, dormant-young, dormant mature, and dormant old). Figures 3-14 and 3-15 illustrate several mapped deep-seated landslide features of varying activity class in Railroad Gulch. Figure 3-16 illustrates a typical signature of ridge-and-valley terrain in Bridge Creek, where topography has been sculpted by shallow landslide and debris flow processes and where deep-seated landsliding is conspicuously absent. The median ln(S1/S2) values from the DSLED-Rough results in Railroad Gulch and Bridge Creek were significantly different for signature 1 (active and dormant-young deep-seated landslides), signature 2 (dormant mature and dormant old deep-seated landslides), and signature 3 (ridge and valley terrain) (Table 3-7). Active and dormant young features had significantly lower ln(S1/S2) values (less clustered vector orientations indicating rougher topography indicative of more active mass movement) than dormant mature and dormant old features, and both deep-seated landslides signatures had lower ln(S1/S2) values than ridge-and-valley topography. These preliminary results suggest that the deep-seated modeling approaches are an objective and effective means of delineating terrain prone to deep-seated landsliding and earthflow. DSLED-Rough and DSLED-Drain results warrant a more objective and rigorous validation test when more detailed mapping and inventory of the type, boundaries, and activity level of deep-seated mass movement features in the Elk River basin become available.

Table 3-7. Descriptive statistics for deep-seated landslide and ridge-and-valley signatures.

Signature		DSLED-Rough values (ln[S1/S2])[1]		
		Median	Lower Limit	Upper Limit
1	Active and dormant young deep-seated landslides	0.643	0.640	0.646
2	Dormant mature and dormant old deep-seated landslides	0.670	0.669	0.672
3	ridge and valley terrain	0.976	0.974	0.978

[1] Upper and lower limits are for the 95% confidence interval.

4 LANDSLIDE HAZARDS IN THE ELK RIVER BASIN

This report summarizes spatially distributed modeling of potential instability conducted in the Elk River Basin to assist in assigning a set of landslide hazard classes that will be used in developing a sediment TMDL and related strategy for recovery of sediment impaired beneficial uses in the Elk River basin. Mechanistic/physically-based modeling was conducted using the best available topographic data (4-m grid from LiDAR data), and model results were tested using the best available landslide data. Modeling and model testing results from this report will be integrated by NRWQCB to define landslide hazards that can be combined with information about sediment delivery and vulnerability of receptors to sediment impairment in assessing risk as part of TMDL analysis and implementation in Elk River. Landslide hazard, in this context, refers to the potential for occurrence of a damaging landslide within a given area; such damage could include loss of life or injury, property damage, social and economic disruption, or environmental degradation (National Research Council 2004). Landslide hazard classes will be integrated by normalizing results from the best-performing deterministic (SHALSTAB and SHALSTAB.V) and probabilistic (PISA and PISA.V) model approaches.

P-tests and comparisons of landslide density to random point density in each instability class statistically demonstrate that (1) shallow landslide models predict greater instability at landslide initiation sites than at randomly selected points, and (2) the models are significantly better predictors of potential shallow instability than predictions based solely on hillslope gradient. P-tests indicated that three of the four models (SHALSTAB, SHALSTAB.V, and PISA) predicted greater instability at 82% or more of the landslide initiation sites than at randomly selected points (Table 3-1).[1] When p-tests were conducted by randomly sampling points from a distribution of potentially unstable slopes (defined by hillslope gradient at landslide points), these models predicted greater instability at 75% or more of the landslide initiation sites (Table 3-1).[1] Landslide densities significantly increased above random point densities at the log [q/T] values of about -2.5 to -2.8 using SHALSTAB and SHALSTAB.V (Figures 3-5 and 3-6), and at failure probabilities of about 0.15 to 0.3 using PISA (Figures 3-7and 3-8). Comparisons of model performance based on p-tests indicated that SHALSTAB.V was the best performing deterministic model and PISA was the best performing probabilistic model (Tables 3-2 through 3-4).

Previous SHALSTAB validation studies have suggested potential log q/T thresholds from -2.2 to -3.1. In terms of correct landslide prediction and cumulative area encompassed by potential instability in the Elk River watershed, PISA probabilities of 0.01 to 0.10 are comparable to SHALSTAB V log (q/T) –2.2 to –3.1 (Table 3-5, Figure 3-11). SHALSTAB V results in the Elk River basin, however, correctly classified fewer landslides and less of the watershed area as unstable for a given log (q/T) threshold compared to previous SHALSTAB validation studies in similar terrain.

Bootstrap samples of model predicted instability in the vicinity of slides and randomly selected points were used to assess thresholds for managing landslide hazard that minimize the total costs associated with incorrect slide classification and over prediction of potentially unstable area.

[1] Results summarized here are based on $p<0.5$, maximum instability within 8-m radius, and include only landslides where $p<0.5$ for at least one model. Refer to Section 2.4.1 for a description of p-test methods and Section 3.2.1 for p-test results.

Log(q/T) thresholds for SHALSTAB.V based on the bootstrap sampling approach ranged from -2.12 in Qh-Qmts-Qrt terrain to -2.48 in Ty terrain to -2.51 in Qtwu terrain (Table 3-5). PISA thresholds ranged from 0.06 in Qtwu terrain to 0.10 in Ty terrain to 0.17 in Qh-Qmts-Qrt terrain. Threshold values determined by the bootstrap sampling method were lower than suggested thresholds reported for SHALSTAB applications in other areas (Dietrich et al 2001, Montgomery et al. 1998).

4.1 Uses and Limitations

Although modeling of potential hillslope instability and assessment of potential landslide hazard thresholds is intended to inform resource agencies, land managers, and the public about hillslopes that are most sensitivity to management activities; the landslide hazard assessment does not assess how slopes will specifically respond to management-related slope alterations (drainage and excavation) or large seismic triggering events, both of which can increase hazard. Landslide hazard mapping is intended to show where further field investigation is necessary and prudent. Specific sites with higher and lower hazard may exist within any of the hazard classes, and hazard mapping should be used in combination with field geomorphic mapping and geotechnical investigations at specific locations. Hazard mapping is most applicable at the scale and resolution of the input data. This scale allows project level planning and review, but site-specific determination of landslide hazard and risk should be based on site-specific data and evaluation by qualified professionals. Lastly, landslide hazard mapping does not directly address potential sediment delivery from landslide-prone areas to a watercourse and/or other important receptors. Landslide hazard mapping, however, may be used in combination with information about hillslope and channel gradient and empirical data on sediment delivery to assess sediment delivery potential.

4.2 Future Analyses

Analysis of potential instability and delineation of landslide hazard is dependent on the precision, accuracy, and resolution of available information. Analyses in this report were conducted with best available information. However, many input parameters are poorly constrained and landslide data available for model testing are limited by spatial precision and accuracy. Analyses of landslide hazard can be improved in the future as the accuracy, precision, and resolution of input information improve over time. Specific areas for future improvement and research include the following:

- Root strength and the rate of root strength decay following disturbance is a large source of uncertainty in predictions of potential hillslope instability. More research is needed to better constrain root strength parameters for different vegetation cover types and root strength decay with time since disturbance (e.g., fire or timber harvest)
- This landslide hazard assessment evaluated potential instability of open slopes controlled primarily by topography and pore water pressure. More work is needed to assess how management-related slope alterations (road excavation and drainage) influence potential hillslope instability within different landslide hazard classes and geologic terrains.
- Correlation of the factors influencing hillslope instability to landslide occurrence on a watershed scale has historically been limited by the resolution of the topographic data available for mapping observed landslide initiation areas. High-resolution topographic data from LiDAR is now available to more accurately and precisely map the location of landslide initiation, erosional, and depositional areas in the Elk River basin. Landslide

field and aerial photo inventories consisting of erosional and depositional map polygons registered to the same LiDAR topographic data used here to model potential instability would provide a better means of testing the modeling results and determining thresholds of instability for landslide hazard classes.

- More work is needed to develop methods of estimating sediment production and delivery under different management scenarios using the landslide hazard assessment in combination with other data sources.
- More work is needed to characterize the type, boundaries, timing, and activity level of deep-seated landslides in the basin in order to better validate the deep-seated model results and develop appropriate hazard classes.

5 LITERATURE CITED

Bachman, S. B., M. B. Underwood, and J. S. Menack. 1984. Cenozoic evolution of coastal northern California. Pages 55-66 *in* J. K. Crouch and S. B. Bachman, editors. Tectonics and sedimentation along the California margin. Pacific Section Book Series, Volume 38. Society of Economic Paleontologists and Mineralogists, Los Angeles, California.

Bedrossian, T. L. 1983. Watersheds mapping in northern California. California Geology 36: 140-147.

Blake, M. C., Jr., A. S. Jayko, and R. J. McLaughlin. 1985. Tectonostratigraphic terranes of the northern coast ranges, California. Pages 159-171 *in* D. G. Howell, editor. Tectonostratigraphic terranes of the circum-Pacific region. Earth Sciences Series 1. Circum-Pacific Council for Energy and Mineral Resources.

Bowman, A. W., and A. Azzalini. 1997. Applied smoothing techniques for data analysis: the kernel approach with S-Plus illustrations. Oxford Statistical Science Series No. 18. Clarendon Press, Oxford, England.

Bowman, A. W., and A. Azzalini. 2005. Smoothing methods for nonparametric regression and density estimation. R package Version 2.1-0. Ported to R by B. D. Ripley up to Version 2.0.

California Department of Conservation. 1999. Factors affecting landslides in forested terrain, Note 50. California Department of Conservation, Division of Mines and Geology, Sacramento, California.

California Department of Forestry and Fire Protection. 2005. California Forest Practice Rules. Title 14, California Code of Regulations: Chapters 4, 4.5, and 10. Prepared by California Department of Forestry and Fire Protection Resource Management, Forest Practice Program, Sacramento, California, for California Licensed Timber Operators and California Registered Professional Foresters.

Clarke, S. H., Jr., and G. A. Carver. 1992. Late Holocene tectonics and paleoseismicity, southern Cascadia subduction zone. Science 255: 188-192.

Cruden, D. M., and D. J. Varnes. 1996. Landslide types and processes. Pages 36-75 *in* Landslides investigation and mitigation. Special Report 247. Transportation Research Board, Washington, D. C.

De la Fuente, J., D. Elder, and A. Miller. 2002. Does deforestation influence the activity of deep-seated landslides? Observations from the flood of 1997 in the central Klamath Mountains, northern California. Abstracts with Programs - Geological Society of America 34: 88.

Dhakal, A. S., and R. C. Sidle. 2003. Long-term modeling of landslides for different forest management practices. Earth Surface Processes and Landforms 28: 853-868.

Dietrich, W. E., D. Bellugi, and R. Real de Asua. 2001. Validation of the shallow landslide model, SHALSTAB, for forest management. Pages 195-227 *in* Land use and watersheds: human influence on hydrology and geomorphology in urban and forest areas. American Geophysical Union.

Dietrich, W. E., and D. R. Montgomery. 1998. SHALSTAB: a digital terrain model for mapping shallow landslide potential. Prepared for publication as a technical report by NCASI.

Dietrich, W. E., R. Reiss, M.-L. Hsu, and D. R. Montgomery. 1995. A process-based model for colluvial soil depth and shallow landsliding using digital elevation data. Hydrological Processes 9: 383-400.

Earth Science Associates. 1975. Geology of the Humboldt Bay region. Prepared for Pacific Gas & Electric Company

Hammond, C., D. Hall, S. Miller, and P. Swetik. 1992. Level I stability analysis (LISA) documentation for Version 2.0. General Technical Report INT-285. USDA Forest Service, Intermountain Research Station, Ogden, Utah.

Haneberg, W. C. 2000. Deterministic and probabilistic approaches to geologic hazard assessment. Environmental and Engineering Geoscience VI: 209-226.

Haneberg, W. C. 2004. A rational probabilistic method for spatially distributed landslide hazard assessment. Environmental and Engineering Geoscience X: 27-43.

Haneberg, W. C. 2005. PISA: probabilistic infinite slope analysis, user manual. Version 1.0. Haneberg Geoscience.

Heimsath, A. M., W. E. Dietrich, K. Nishiizumi, and R. C. Finkel. 1997. The soil production function and landscape equilibrium. Nature 388: 358-361.

Heimsath, A. M., W. E. Dietrich, K. Nishiizumi, and R. C. Finkel. 2001. Stochastic processes of soil production and transport: erosion rates, topographic variation and cosmogenic nuclides in the Oregon Coast Range. Earth Surface Processes and Landforms 26: 531-552.

Heimsath, A. M., W. E. Dietrich, and L. Nishiizumi. 1999. Cosmogenic nuclides, topography, and the spatial variation of soil depth. Geomorphology 27: 151-172.

Ingle, J. C., Jr. 1987. The depositional, tectonic, and paleoceanography history of the Eel River (Humboldt), Point Arena, and Bodega (Point Reyes) basins of northern California; a summary of stratigraphic evidence. H. Schymiczek and R. Suchsland, editors. Tectonics, sedimentation and evolution of the Eel River and associated coastal basins of northern California. San Joaquin Geological Society, Bakersfield, California.

Jayco, A. S., and Jr. M. C. Blake. 1987. Geologic terranes of coastal northern California and southern Oregon. H. Schymiczek and R. Suchsland, editors. Tectonics, sedimentation and evolution of the Eel River and associated coastal basins of northern California. San Joaquin Geological Society, Bakersfield, California.

Klein, R. D., and J. K. Anderson. 1999. Channel migration zone delineation pilot study on North Fork Eel River. Review draft. Prepared for Scotia Pacific Company, LLC.

Mackey, B. H., J. J. Roering, and W. E. Dietrich. 2005. Determining the topographic manifestation of widespread landsliding with high resolution airborne laser swath mapping (ALSM) data, South Fork Eel River, northern California. American Geophysical Union Fall Meeting 2005: abstract #H34B-04.

Mackey, B. H., J. J. Roering, J. McKean, and W. E. Dietrich. 2006. Analyzing the spatial pattern of deep-seated landsliding - evidence for base level control, South Fork Eel River, California. American Geophysical Union Fall Meeting 2006: abstract #H53B-0619.

Marshall, G. J., and E. Mendes. 2005. Geologic and geomorphic features related to landsliding and landslide potential in the Eel River watershed. State of California, Department of Conservation, California Geological Survey, Sacramento, California.

McCrory, P. A. 1989. Late Neogene geohistory analysis of the Humboldt basin and its relationships to convergence of the Jaun de Fuca plate. Journal of Geophysical Research 94: 3126-3138.

McKean, J., and J. Roering. 2004. Objective landslide detection and surface morphology mapping using high-resolution airborne laser altimetry. Geomorphology 57: 331-351.

McLaughlin, J. W., M. R. Gale, and C. C. Trettin. 2000. Soil organic matter and nitrogen cycling in response to harvesting, mechanical site preparation, and fertilization in a wetland with a mineral substrate. Forest Ecology and Management 129: 7-24.

Miller, A. J. 1995. Valley morphology and boundary conditions influencing spatial patterns of flood flow. Pages 57-81 *in* J. E. Costa, A. J. Miller, K. W. Potter and P. R. Wilcock, editors. Natural and anthropogenic influences in fluvial geomorphology: the Wolman volume. Geophysical Monograph 89. American Geophysical Union, Washington, D. C.

Miller, D. J. 1995. Coupling GIS with physical models to assess deep-seated landslide hazards. Environmental and Engineering Geoscience 1: 263-276.

Miller, D. R., J. G. Williams, and C. W. Sims. 1983. Distribution, abundance, and growth of juvenile salmonids off the coast of Oregon and Washington, summer 1980. Fisheries Research 2: 1-17.

Montgomery, D. R., and W. E. Dietrich. 1994. A physically based model for the topographic control on shallow landsliding. Water Resources Research 30: 1153-1171.

Montgomery, D. R., K. Sullivan, and H. M. Greenberg. 1998. Regional test of a model for shallow landsliding. Hydrological Processes 12: 943-955.

Naval Facilities Engineering Command (NAVFEC). 1986. Design manual 7.02. Soils and foundations design manuals. Alexandria, Virginia.

NMFS (National Marine Fisheries Service). 2000. Salmonid guidelines for forestry practices in California. Presented by NMFS to the State Board of Forestry, Sacramento, California.

North Coast Regional Water Quality Control Board. 2005. Empirical harvest-related landslide sediment delivery reduction model, Attachment C. Landslide reduction model for WWDRs in Elk River and Freshwater Creek.

NRC (National Research Council). 2004. Partnerships for reducing landslide risk, assessment of the national landslide hazards mitigation strategy. Committee on the review of the National Landslide Hazards Mitigation Strategy Board on Earth Sciences and Resources, Division on Earth and Life Studies, National Research Council. The National Academies Press, Washington, D. C.

Ogle, B. A. 1953. Geology of Eel River Valley area. Bulletin No. 164. California Division of Mines, San Francisco.

Ogle, B. A. 1953. Geology of the Eel River valley area. Division of Mines, Bulletin 164:

Orange, D. L. 1999. Tectonics, sedimentation, and erosion in northern California: submarine geomorphology and sediment preservation potential as a result of three competing processes. Marine Geology 154: 369-382.

Pack, R. T., and D. G. Tarboton. 1997. New developments in terrain stability mapping in B. C. Pages 1-15 *in* Proceedings of the 11th Vancouver Geotechnical Society Symposium on forestry geotechnique and resource engineering.

PALCO (Pacific Lumber Company). 1999. Habitat Conservation Plan. Prepared by Pacific Lumber Company, Scotia Pacific Holding Company, and Salmon Creek Corporation.

PALCO (Pacific Lumber Company). 2003. Reconnaissance level forensic landslide investigation. Geology SOP-08 (Standard operating procedure 08), Version 1.0.

PALCO (Pacific Lumber Company). 2004a. Elk River/Salmon Creek watershed analysis Scotia, California. SRT review draft, 1602000. Prepared for PALCO, Scotia, California by Hart Crowser, Oregon.

PALCO (Pacific Lumber Company). 2004b. Report of waste discharge Elk River. Prepared by PALCO, Scotia, California.

Planwest Partners Inc., Schatz Energy Research Center, Net Gain, Center for Environmental Economic Development, and Winzler & Kelly. 2005. Humboldt County general plan 2025.

Prellwitz, R. W., J. Oswald, and W. Adams. 2001. Management-related landslides on Pacific Lumber lands, Humboldt County, California: a geotechnical perspective. Prepared for Scotia Pacific Company, LLC, Scotia, California.

PWA (Pacific Watershed Associates). 1998. Sediment source investigation and sediment reduction plan for the North Fork Elk River Watershed, Humboldt County, California. Prepared by PWA, Arcata, California for The Pacific Lumber Company, Scotia, California.

PWA. 2001, unpublished data. Landslide database. Provided by PALCO, Scotia, California

R Development Core Team. 2006. R: a language and environment for statistical computing. R Foundation for Statistical Computing, Vienna, Austria. http://www.R-project.org.

Roering, J. J., J. W. Kirchner, and W. E. Dietrich. 1999. Evidence for nonlinear, diffusive sediment transport on hillslopes and implications for landscape morphology. Water Resources Research 35: 853-870.

Roering, J. J., J. W. Kirchner, and W. E. Dietrich. 2005. Characterizing structural and lithologic controls on deep-seated landsliding: implications for topographic relief and landscape evolution in the Oregon Coast Range, USA. GSA Bulletin 117: 1-15.

Roering, J. J., B. Mackey, and J. McKean. 2006. Deep-seated landslide and earthflow detection (DSLED): a suite of automated algorithms for mapping landslide-prone terrain with digital topographic data. American Geophysical Union Fall Meeting 2006: abstract #H53B-0620.

Sanborn. 2005. Freshwater Creek watershed and Elk River watershed tributaries of Humboldt Bay, California. LIDAR Campaign, Final report.

Schmidt, K. M., J. J. Roering, J. D. Stock, W. E. Dietrich, D. R. Montgomery, and T. Schaub. 2001. The variability of root cohesion as an influence on shallow landslide susceptibility in the Oregon Coast Range. Canadian Geotechnical Journal 38: 995-1024.

Selby, M. J. 1993. Hillslope materials and processes. Second edition. Oxford University Press, New York.

Shaw, S. C., and L. M. Vaugeois. 1999. Comparison of GIS-based models of shallow landsliding for application to watershed management. TFW-PR10-99-001. Timber, Fish and Wildlife.

Sidle, R. C., and H. Ochiai. 2006. Landslides: processes, prediction, and land use. American Geophysical Union, Washington, D.C.

White, A. 2007. Data summary of harvest histories for Elk River. North Coast Regional Water Quality Control Board, Santa Rosa, CA.

Figures

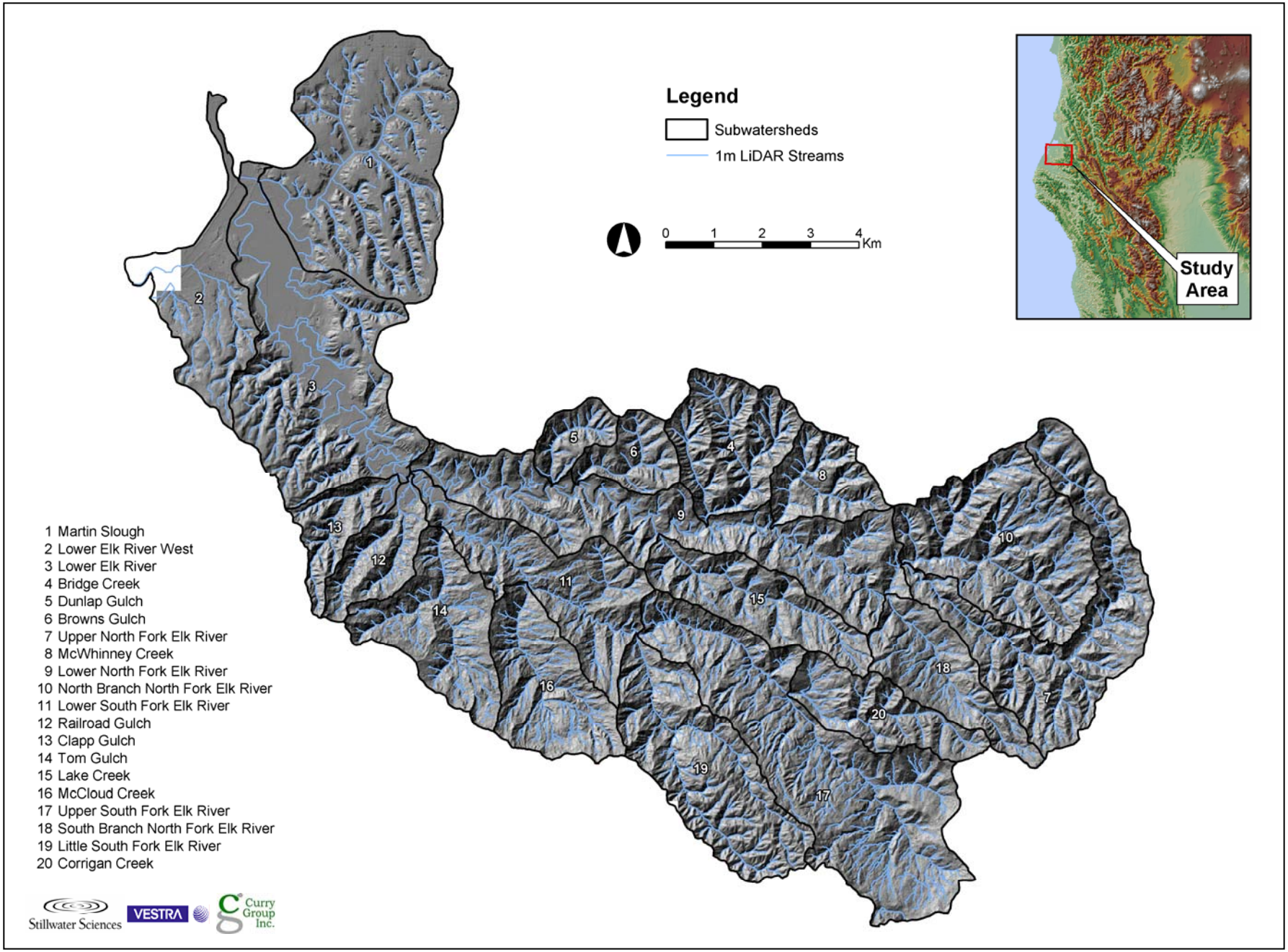

Figure 1-1. Elk River basin and subwatesheds.

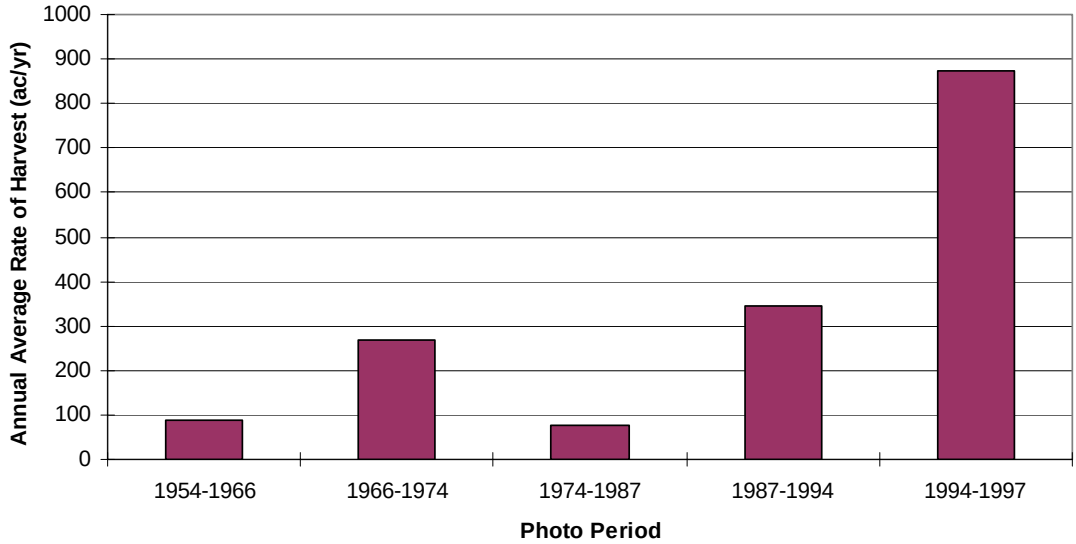

Figure 1-2. Annual average harvest rate for available photo periods in North Fork Elk River.

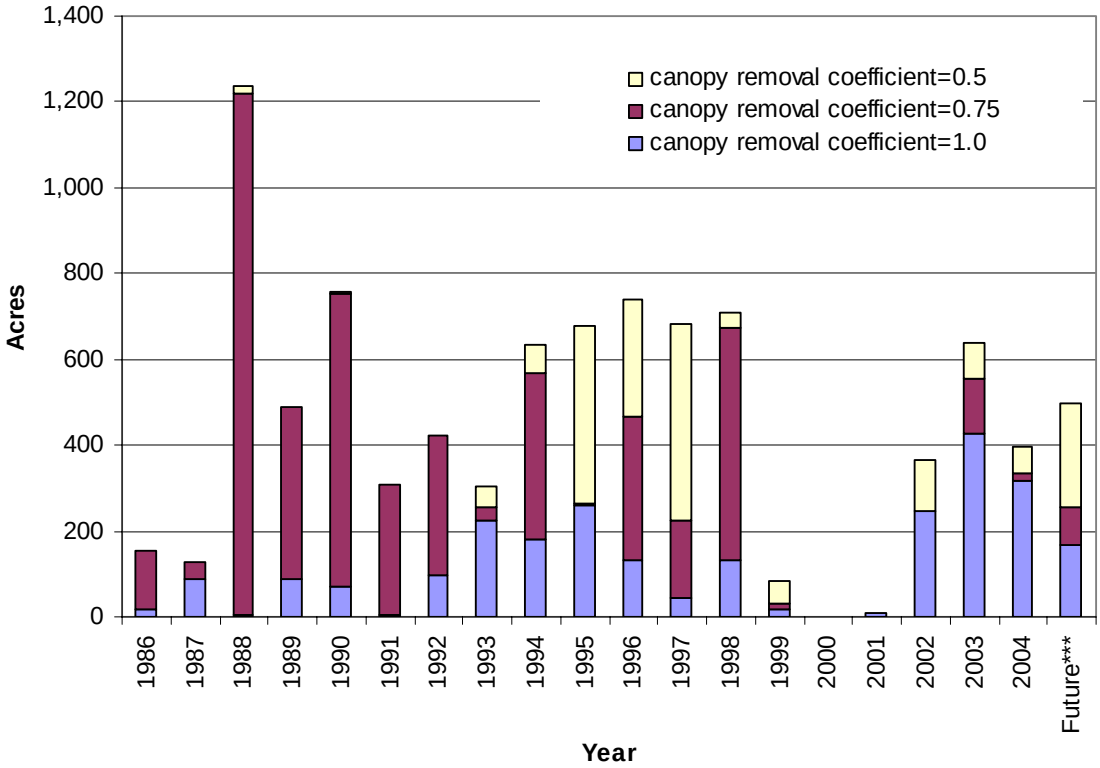

Figure 1-3. Annual harvest acreage for North Fork Elk River (all ownerships) as expressed in clear-cut equivalent acres (canopy removal coefficient of 1.0 for clear cutting, 0.75 for intermediate steps, and 0.5 for selection and commercial thin).

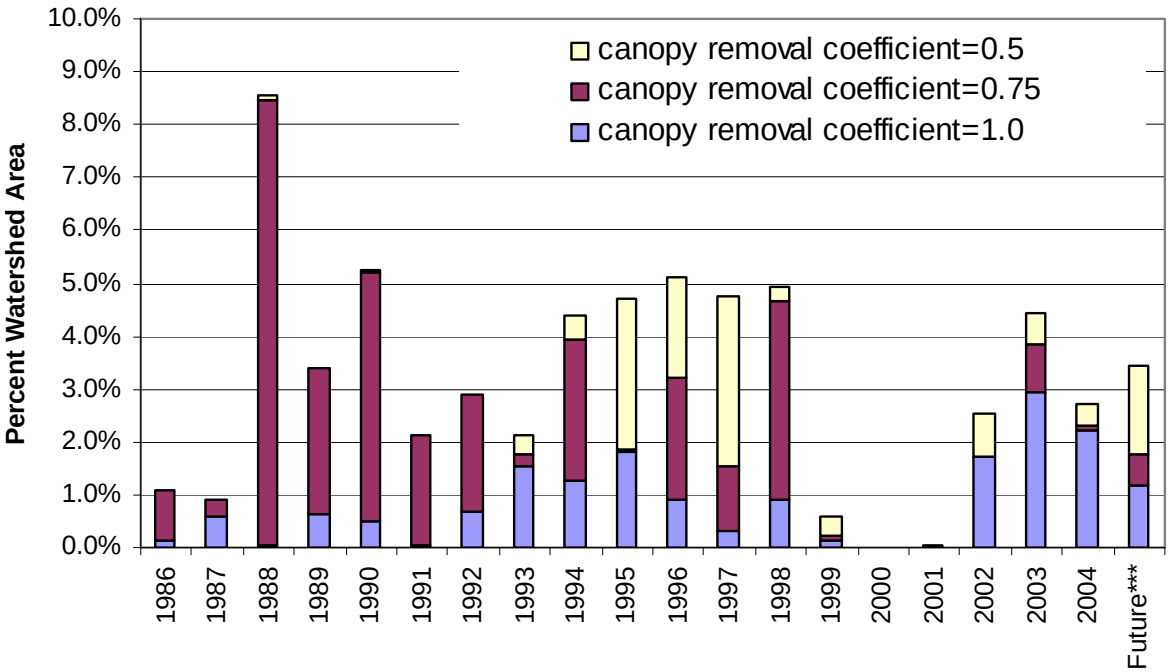

Figure 1-4. Percent of watershed harvest annually for North Fork Elk River (all ownerships) as expressed in clear-cut equivalent acres (canopy removal coefficient of 1.0 for clear cutting, 0.75 for intermediate steps, and 0.5 for selection and commercial thin).

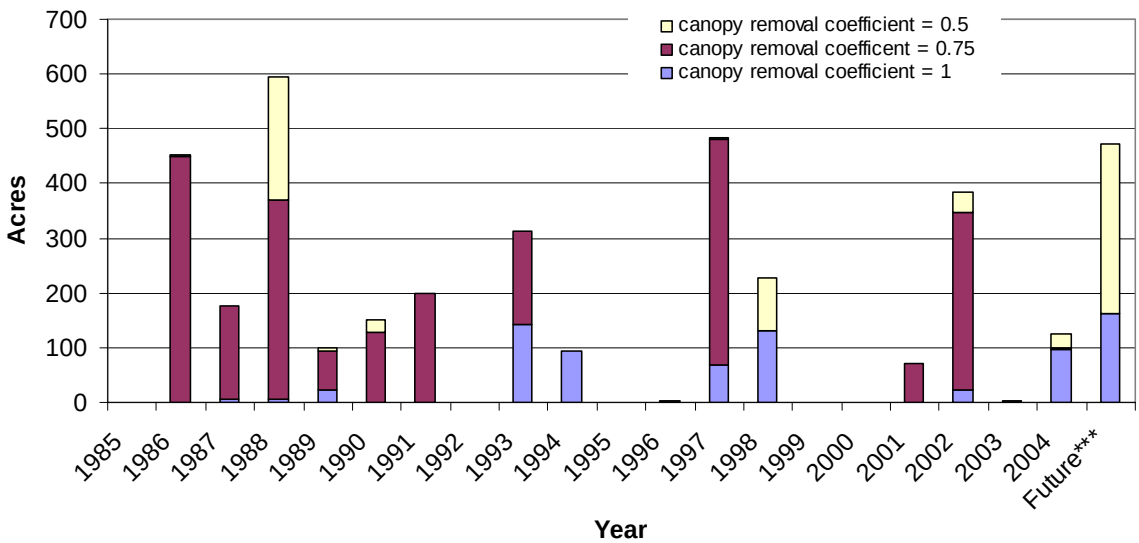

Figure 1-5. Annual harvest acreage for South Fork Elk River (all ownerships) as expressed in clear-cut equivalent acres (canopy removal coefficient of 1.0 for clear cutting, 0.75 for intermediate steps, and 0.5 for selection and commercial thin).

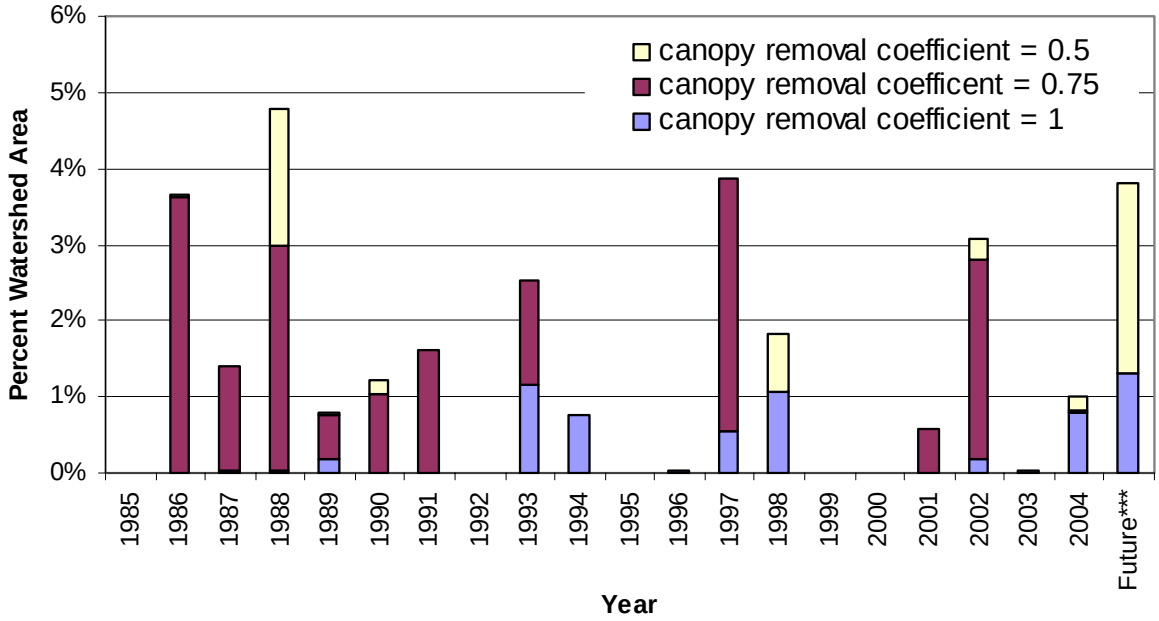

Figure 1-6. Percent of watershed harvest annually for South Fork Elk River (all ownerships) as expressed in clear-cut equivalent acres (canopy removal coefficient of 1.0 for clear cutting, 0.75 for intermediate steps, and 0.5 for selection and commercial thin).

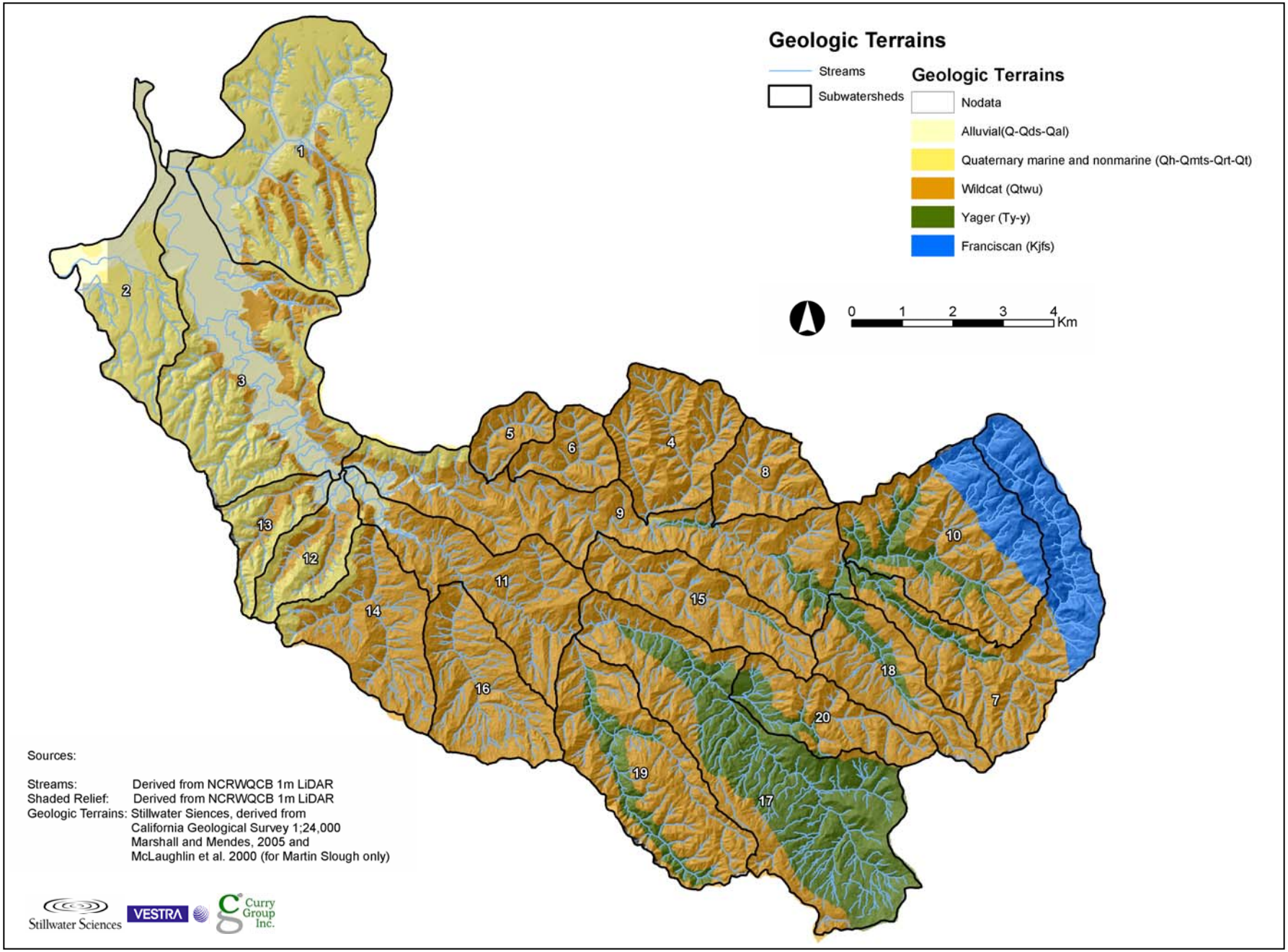

Figure 2-1. Geology in the Elk River basin (modified from McLaughlin et al. 2000, Marshall and Mendes 2005).

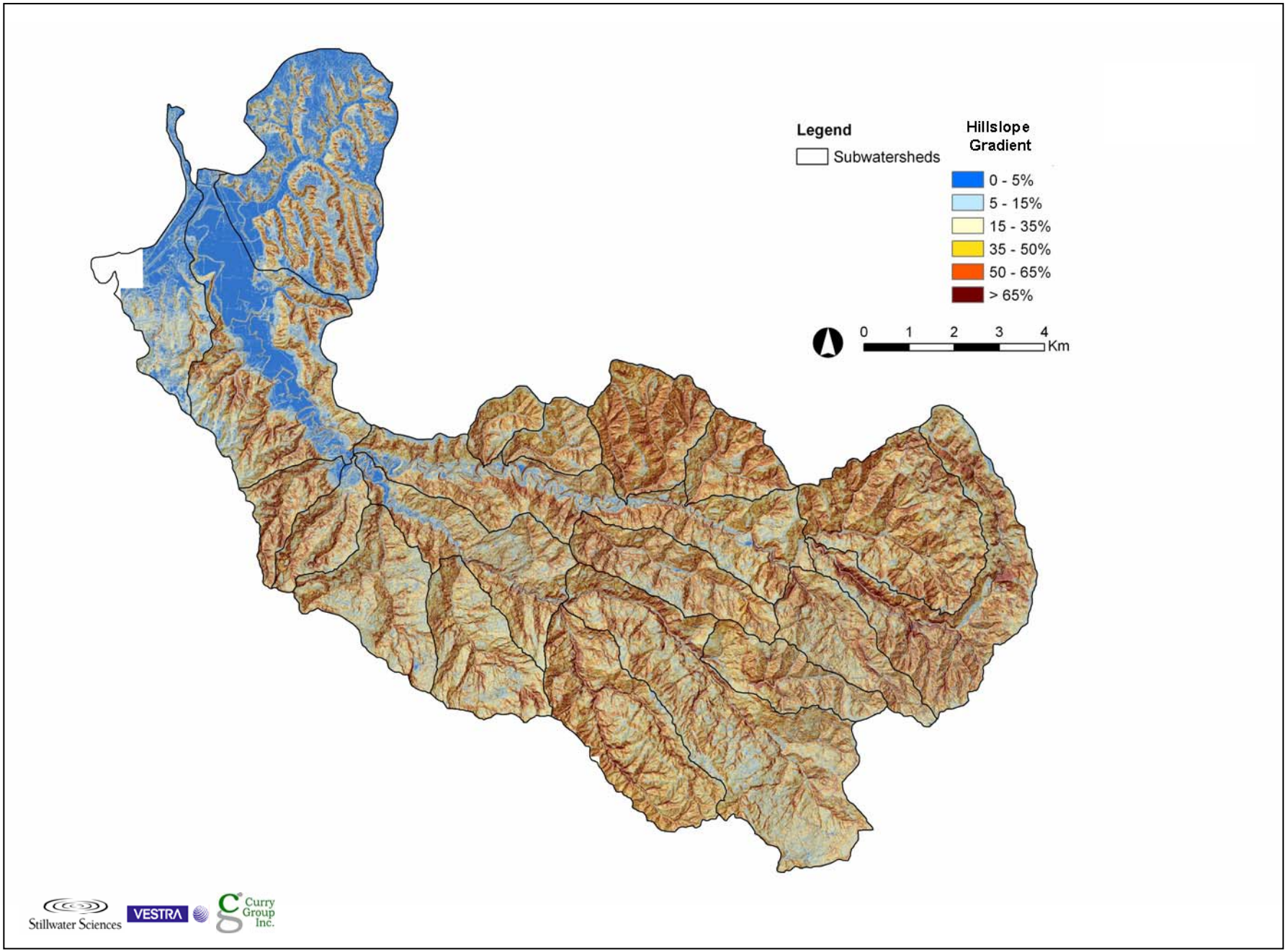

Figure 2-2. Hillslope gradient in the Elk River basin (derived from 1-m LiDAR DEM).

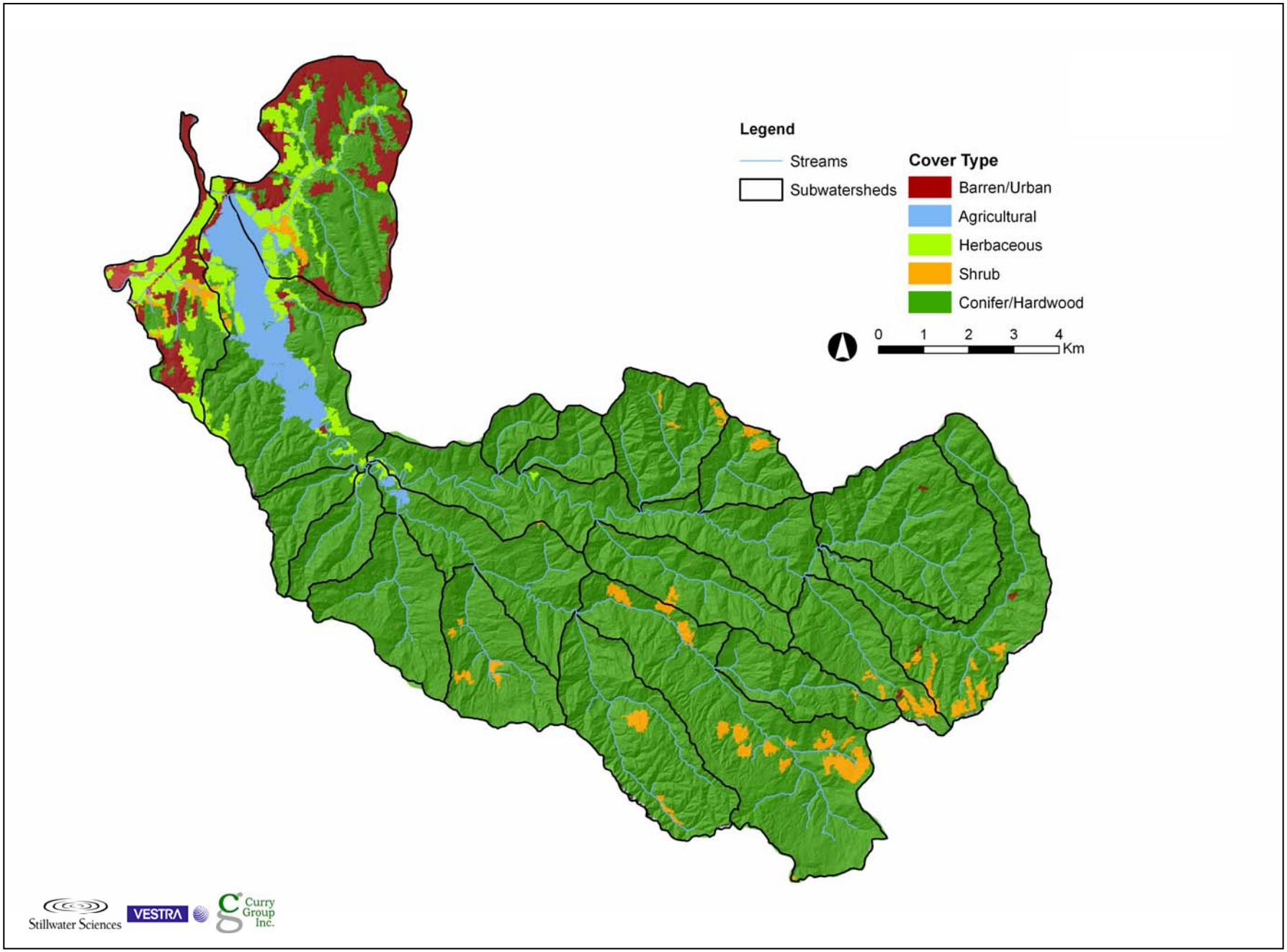

Figure 2-3. Cover type in the Elk River basin (modified from CDF-LCMMP vegetation mapping).

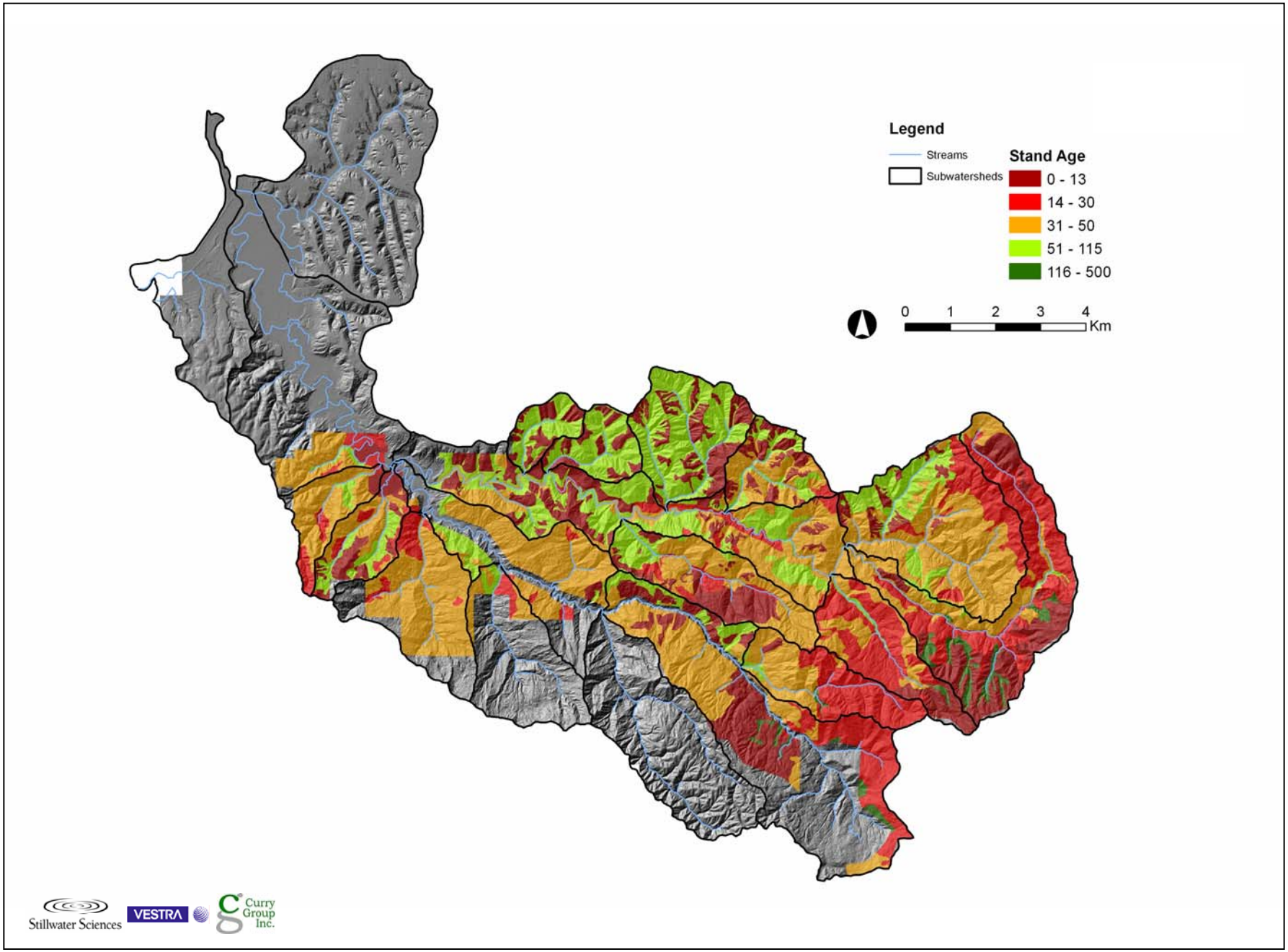

Figure 2-4. Stand age in portions of the Elk River basin (derived from PALCO stand age coverage).

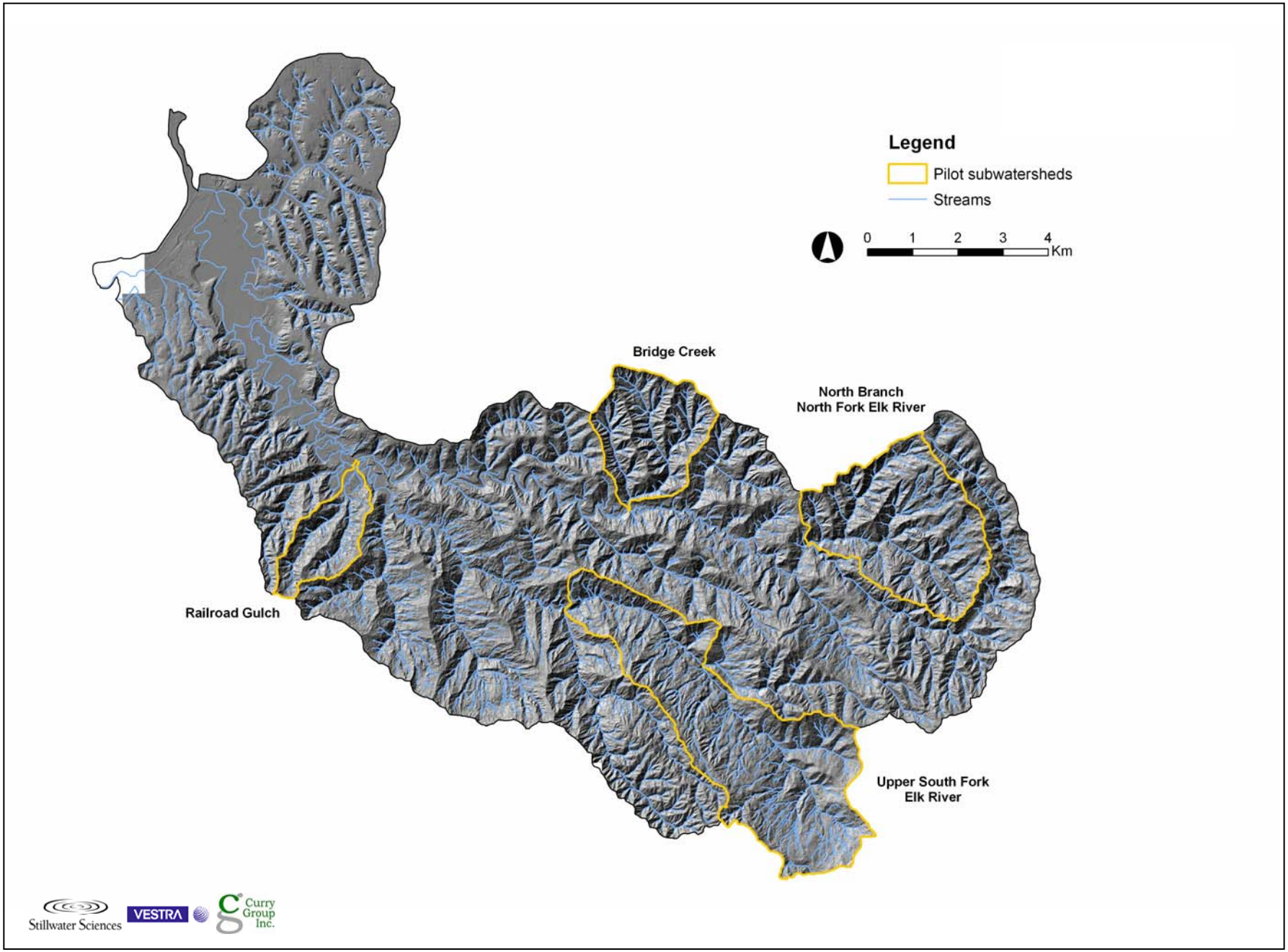

Figure 2-5. Pilot subwatersheds in the Elk River basin.

kriged 1-m DEM
Spherical semivariogram model, 8 points, 20-m radius

TIN-lattice 1-m DEM
Bilinear interpolation among 4 cells

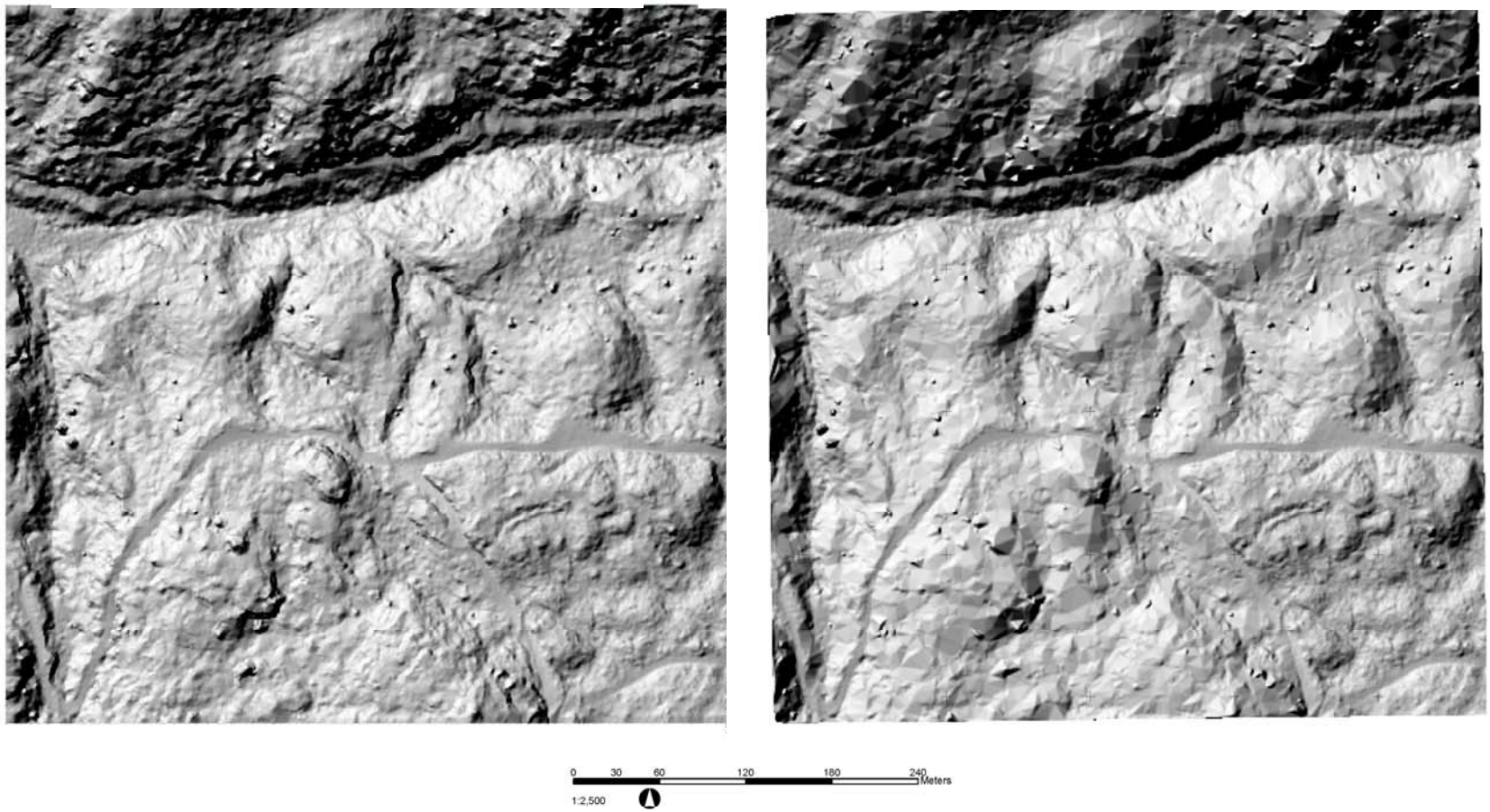

Figure 2-6. Comparison of hillshade images from 1-m grids created from TINing and Kriging methods.

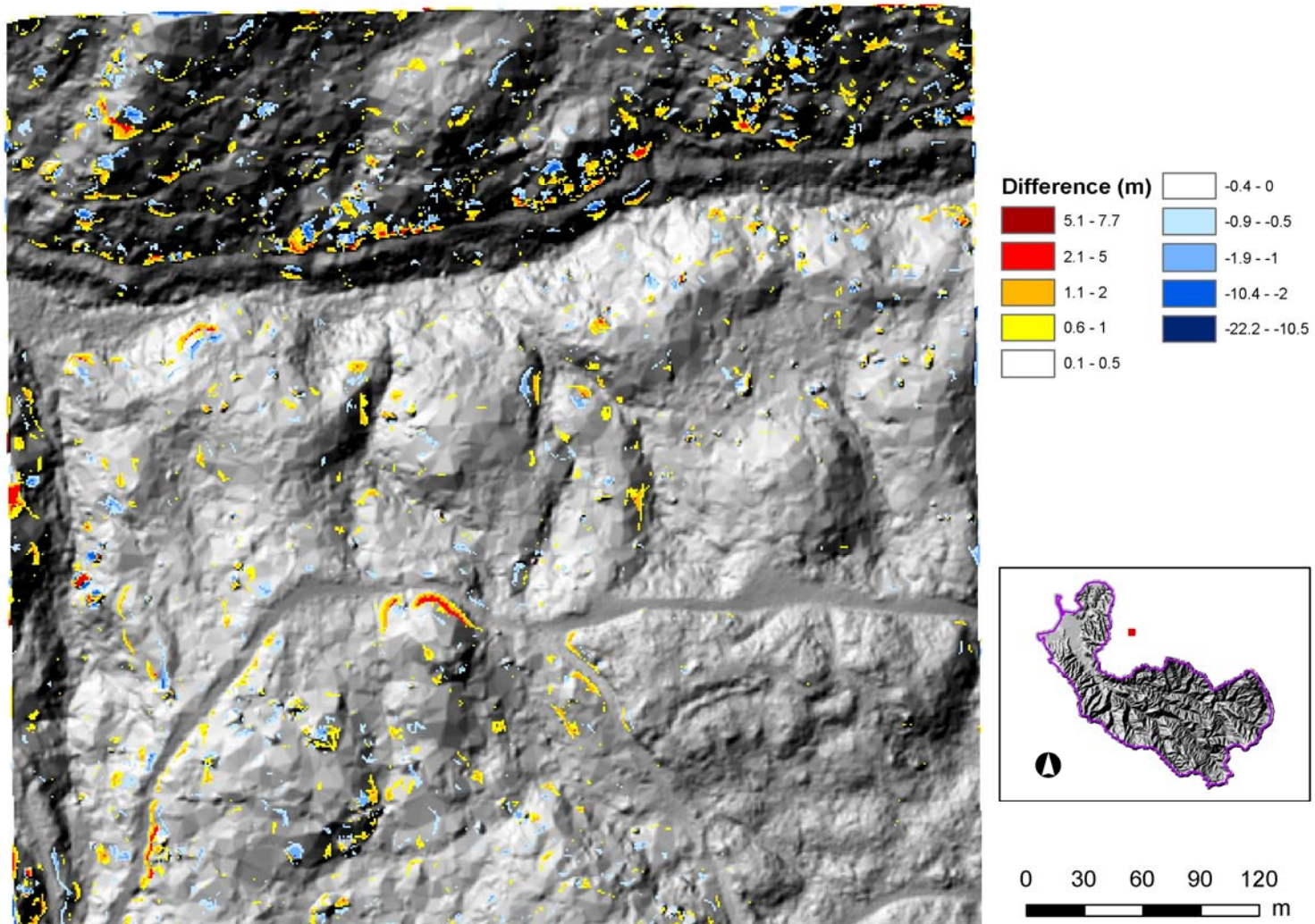

Figure 2-7. Elevation differences between 1-m grids created by TINing and Kriging methods.

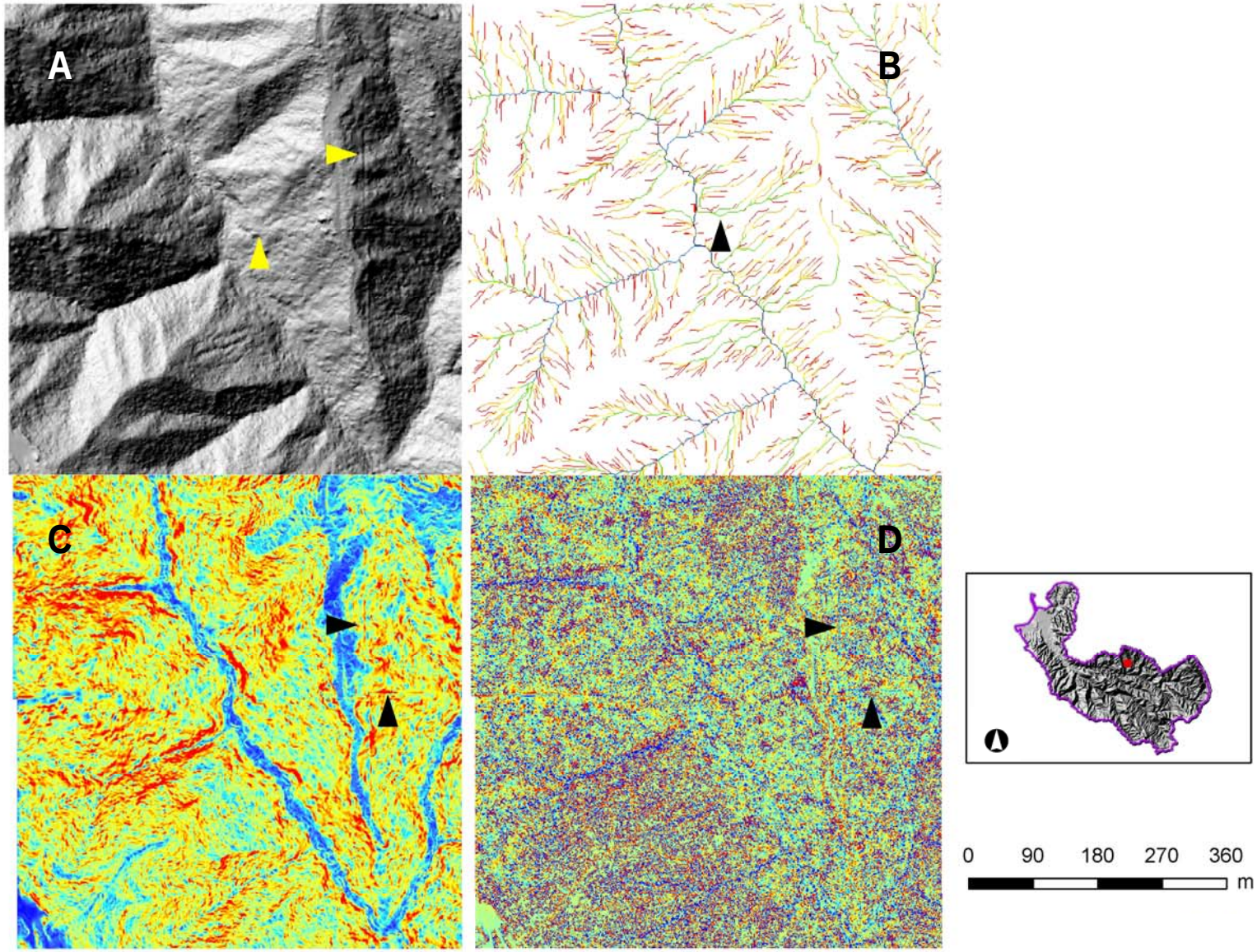

Figure 2-8. Tiling artifacts from the initial 1-m grid created by kriging (spherical semivariogram, search raddius 20, maximum of 16 points)(Sanborn 2005). A) shaded relief, B) flow accumulation, C) hillslope gradient, D) curvature.

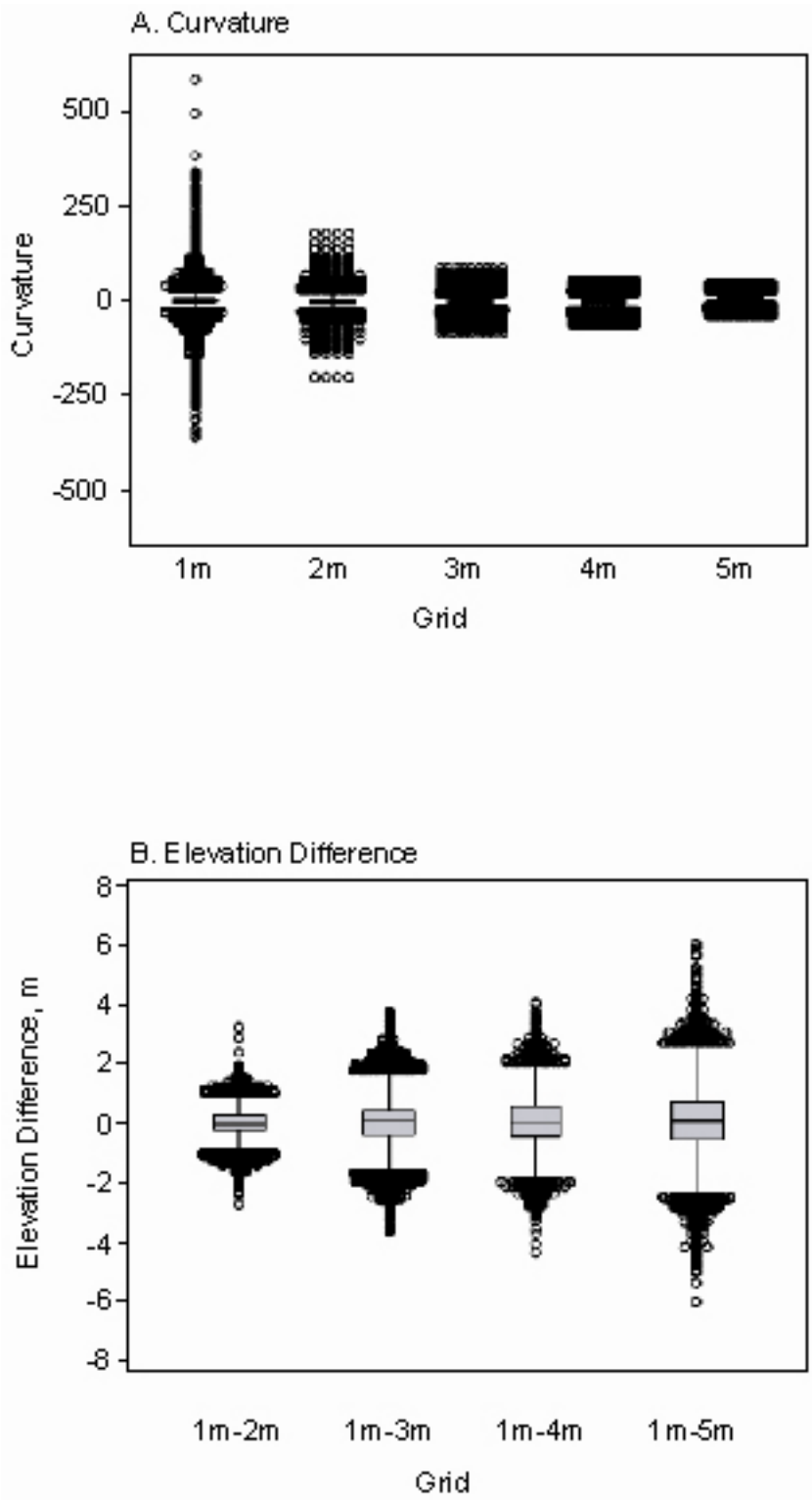

Figure 2-9. Comparison of curvature and elevation changes for different DEM grid sizes.

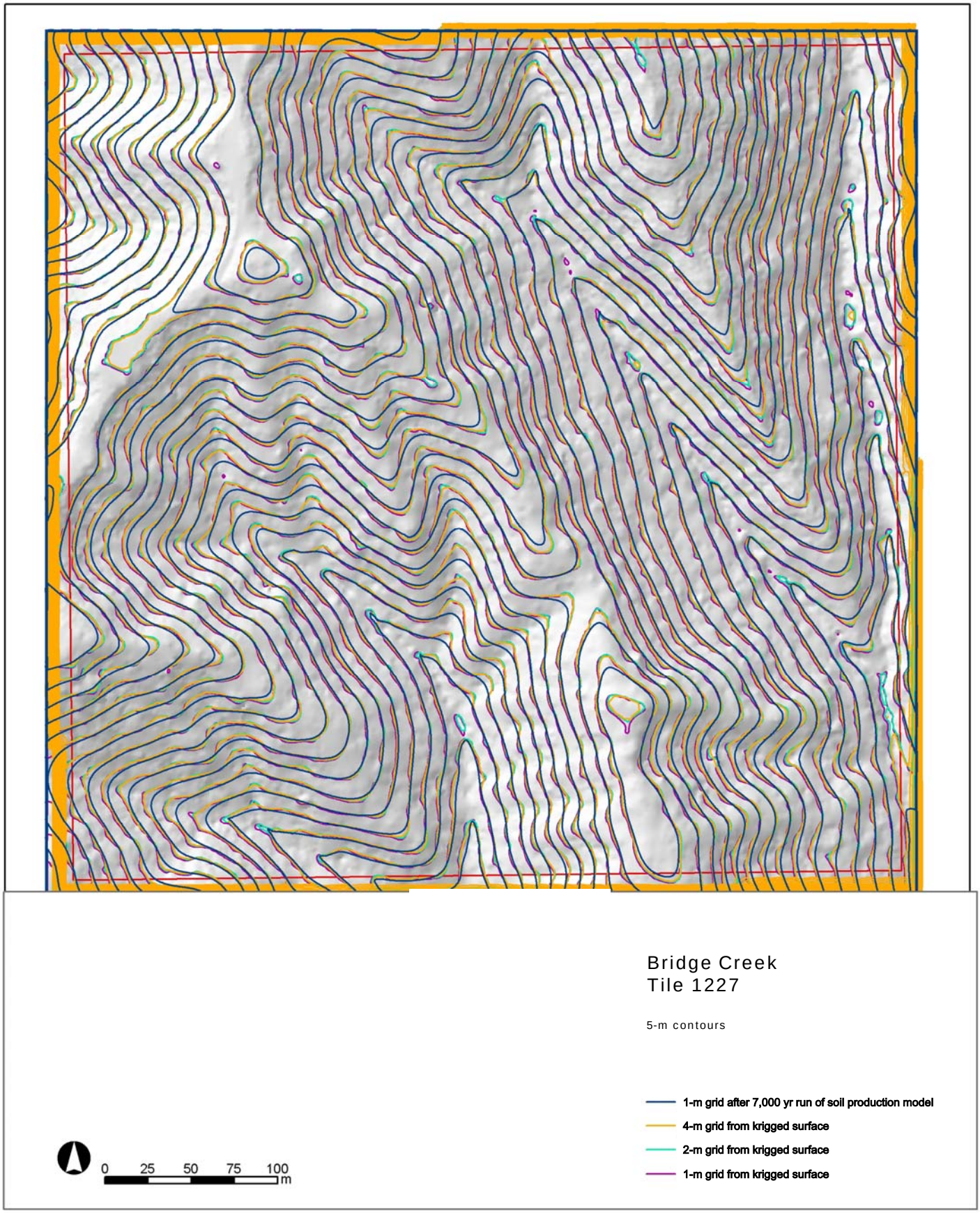

Figure 2-10. Comparison of contours generated from different DEM grid sizes and methods.

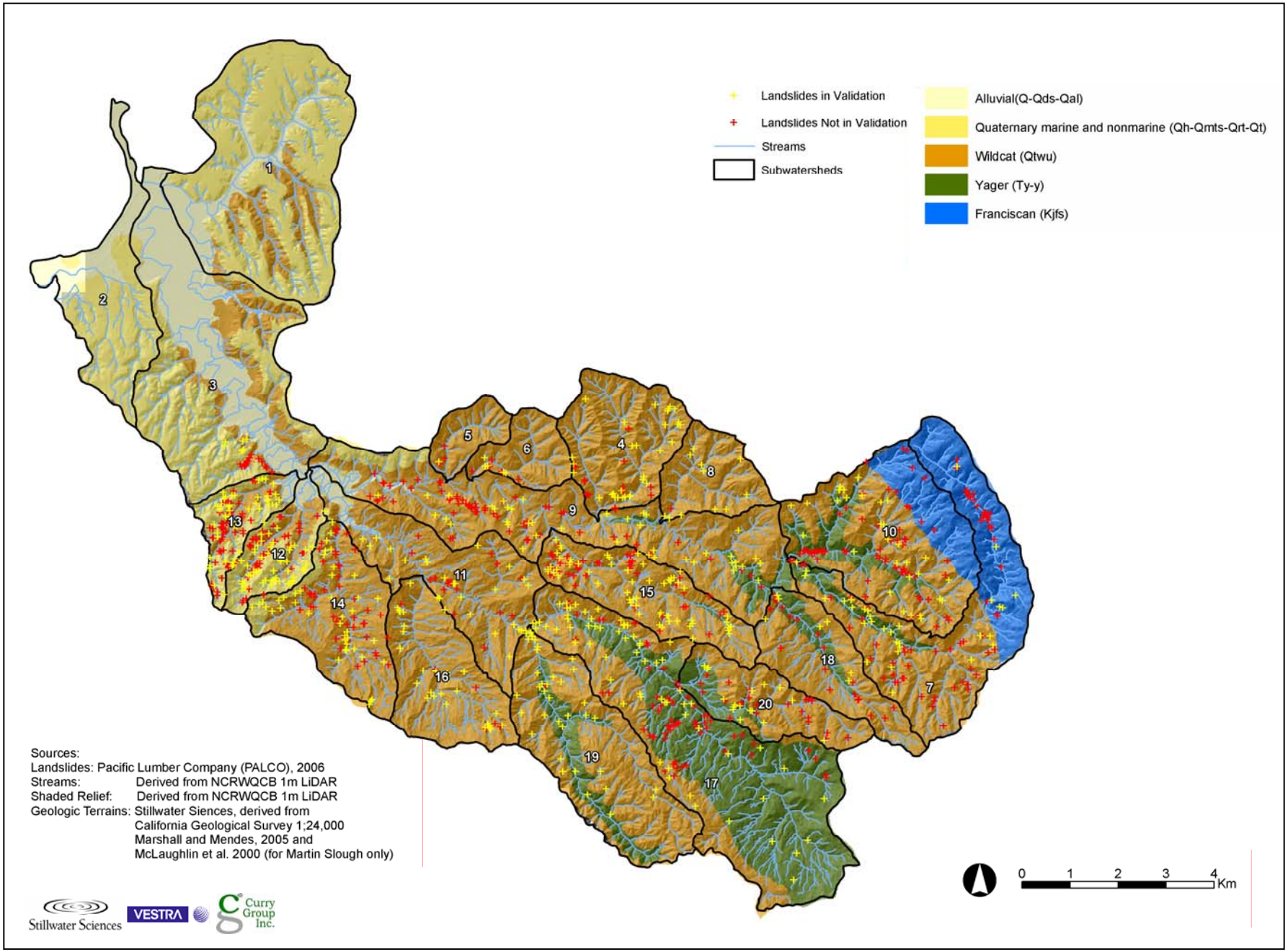

Figure 2-11. Composite shallow landslide data for model testing in the Elk River basin.

Figure 3-1. SHALSTAB results in the Elk River basin.

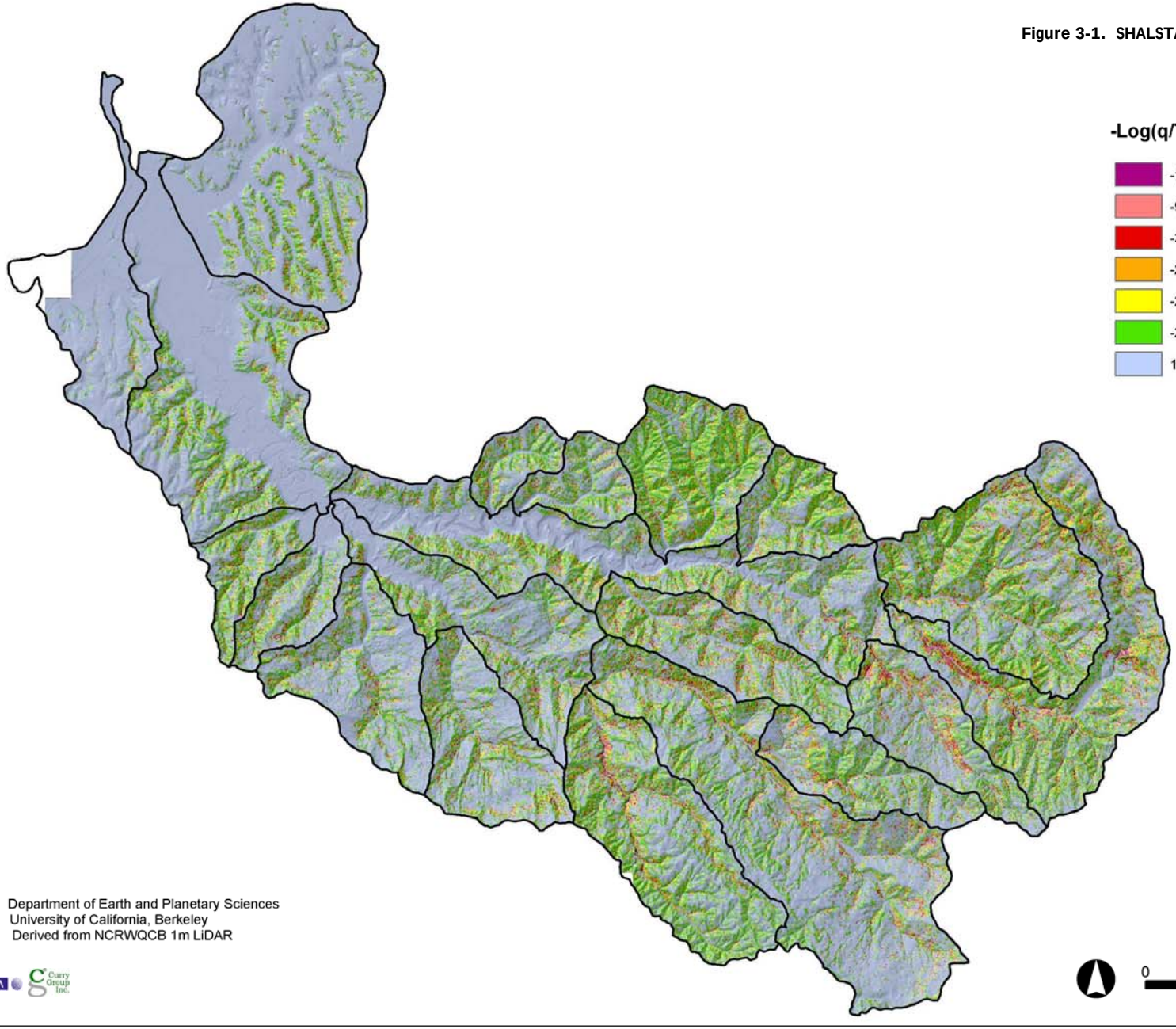

Figure 3-2. SHALSTAB V results in the Elk River basin.

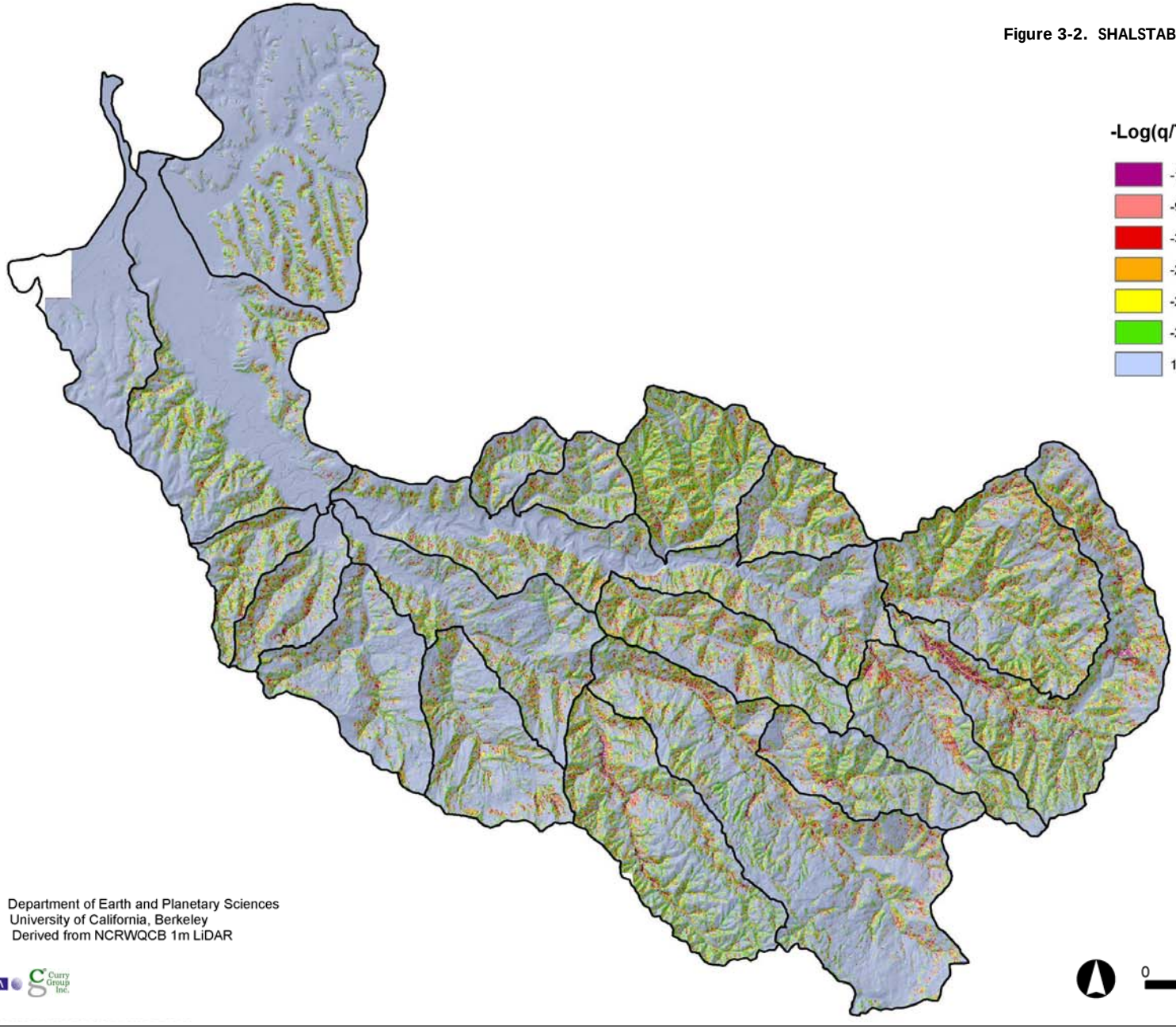

Figure 3-3. PISA results in the Elk River basin.

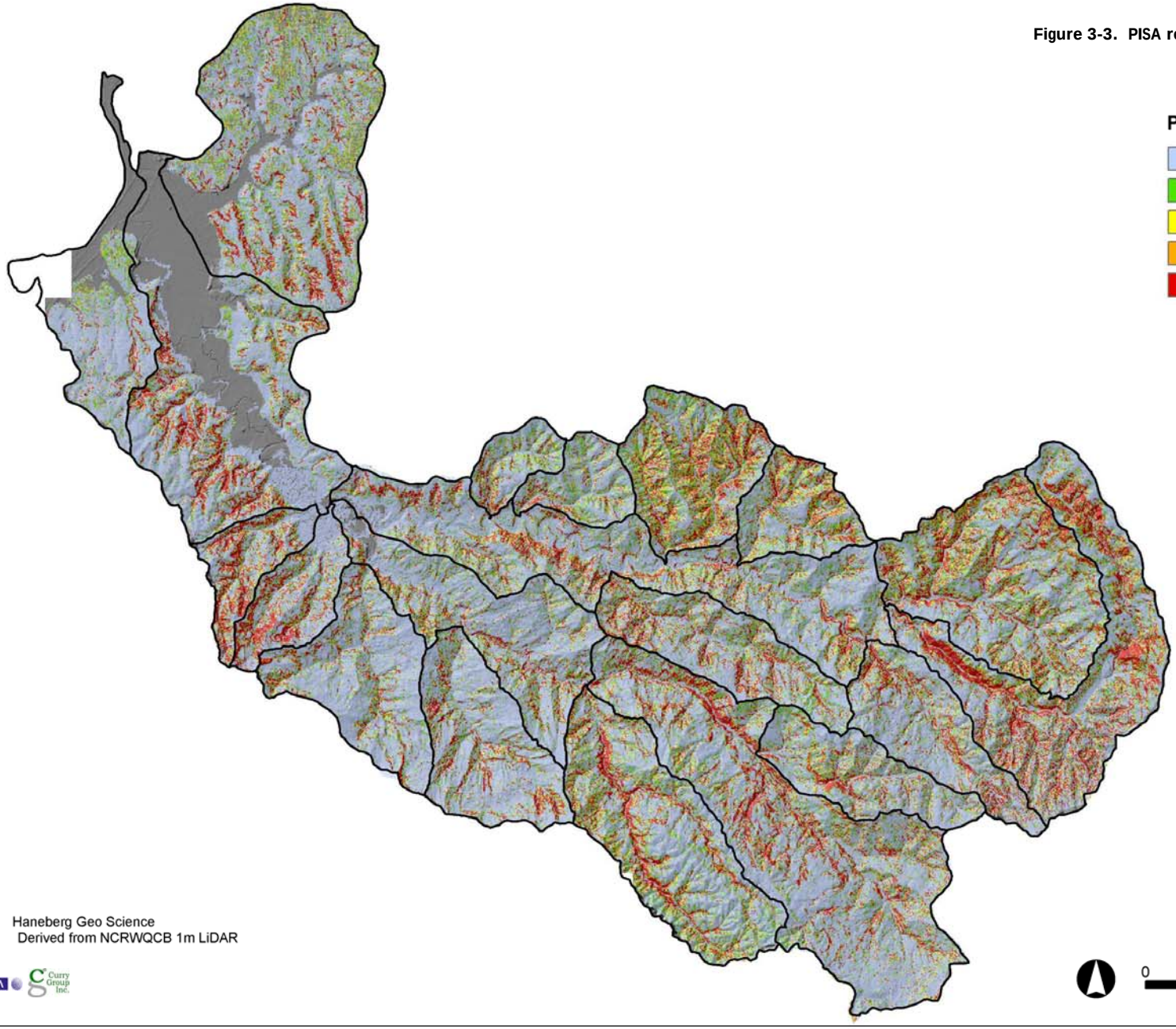

Figure 3-4. PISA.V results in the Elk River basin.

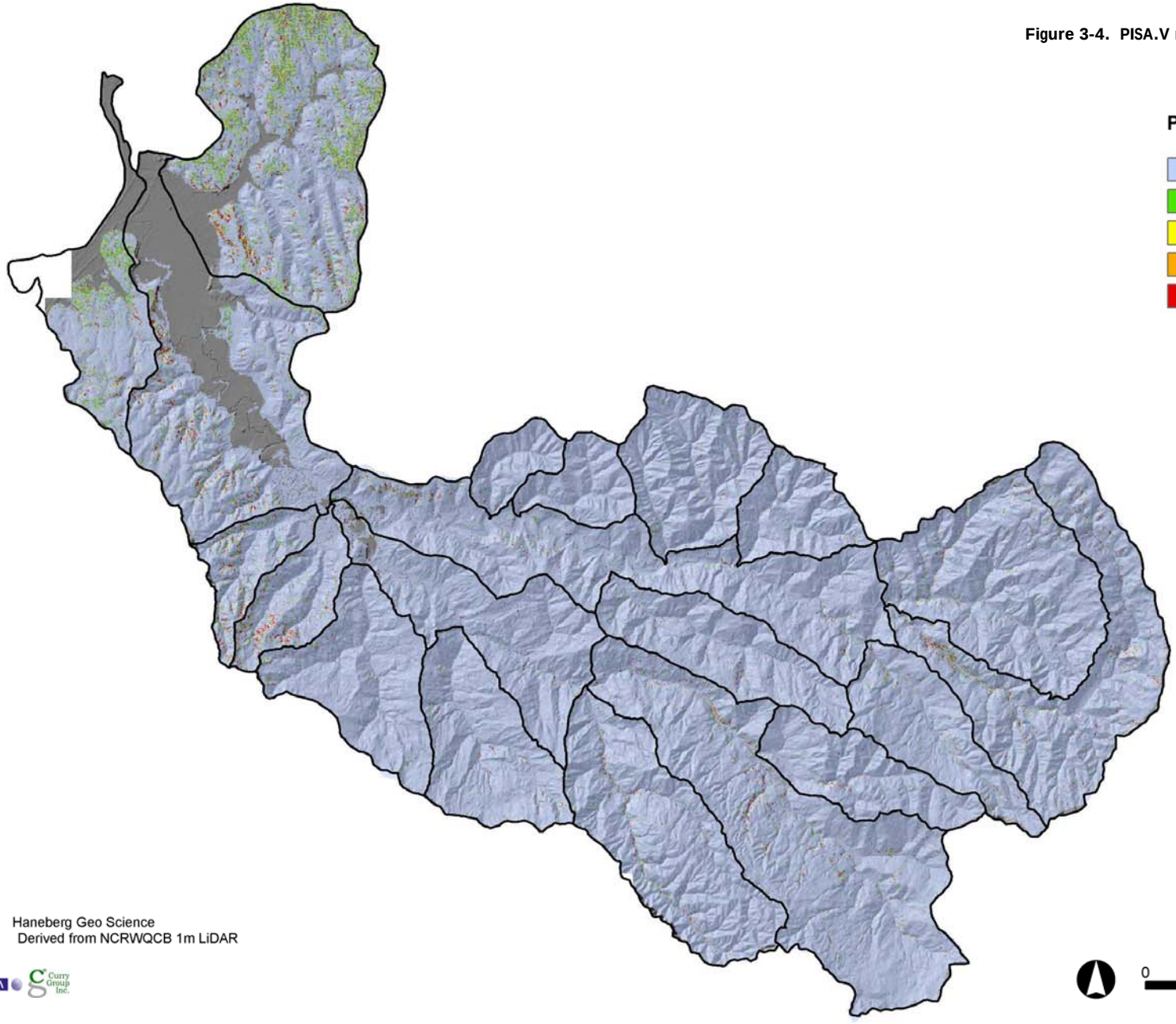

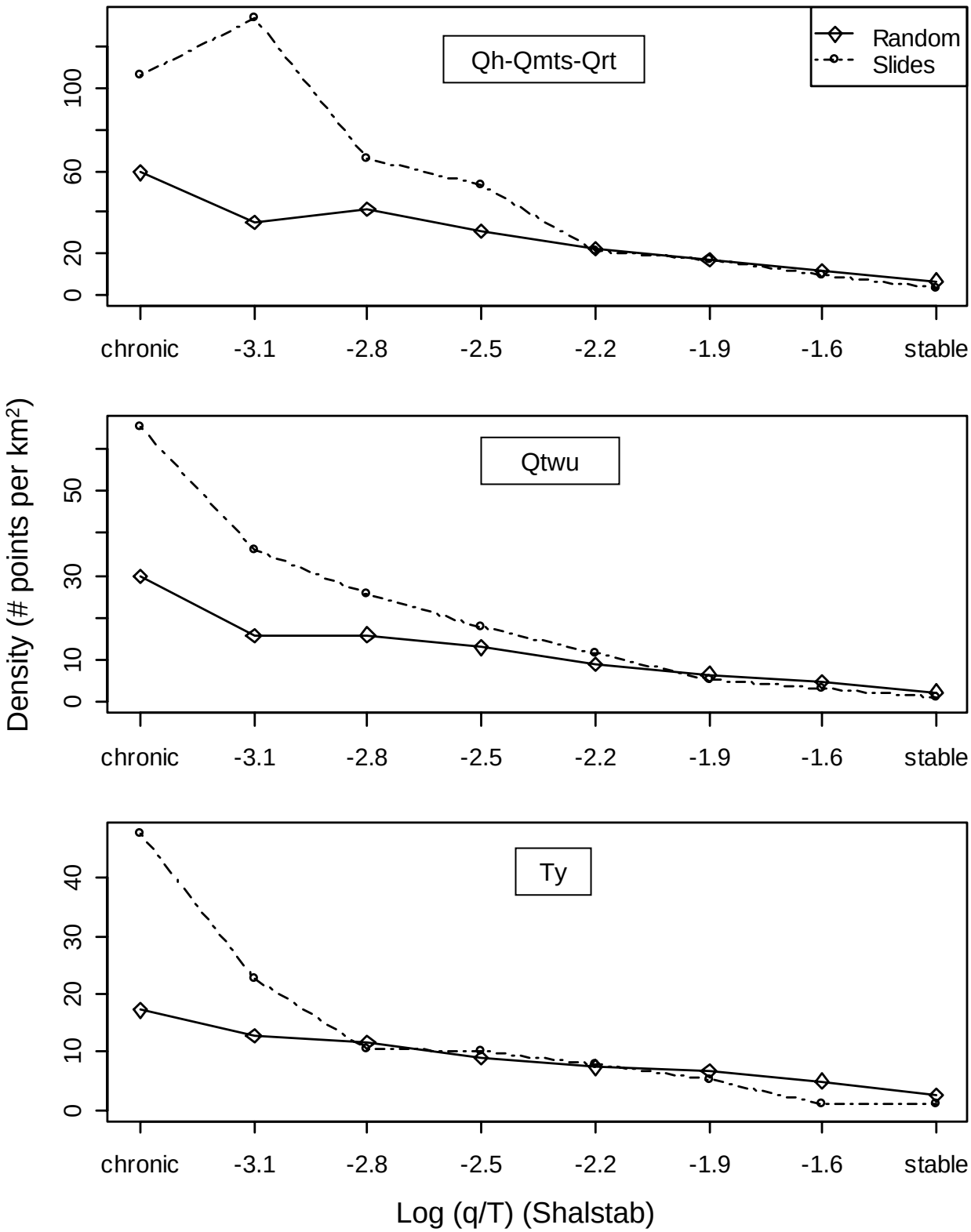

Figure 3-5. Density of landslides and random points by log (q/T) class from SHALSTAB.

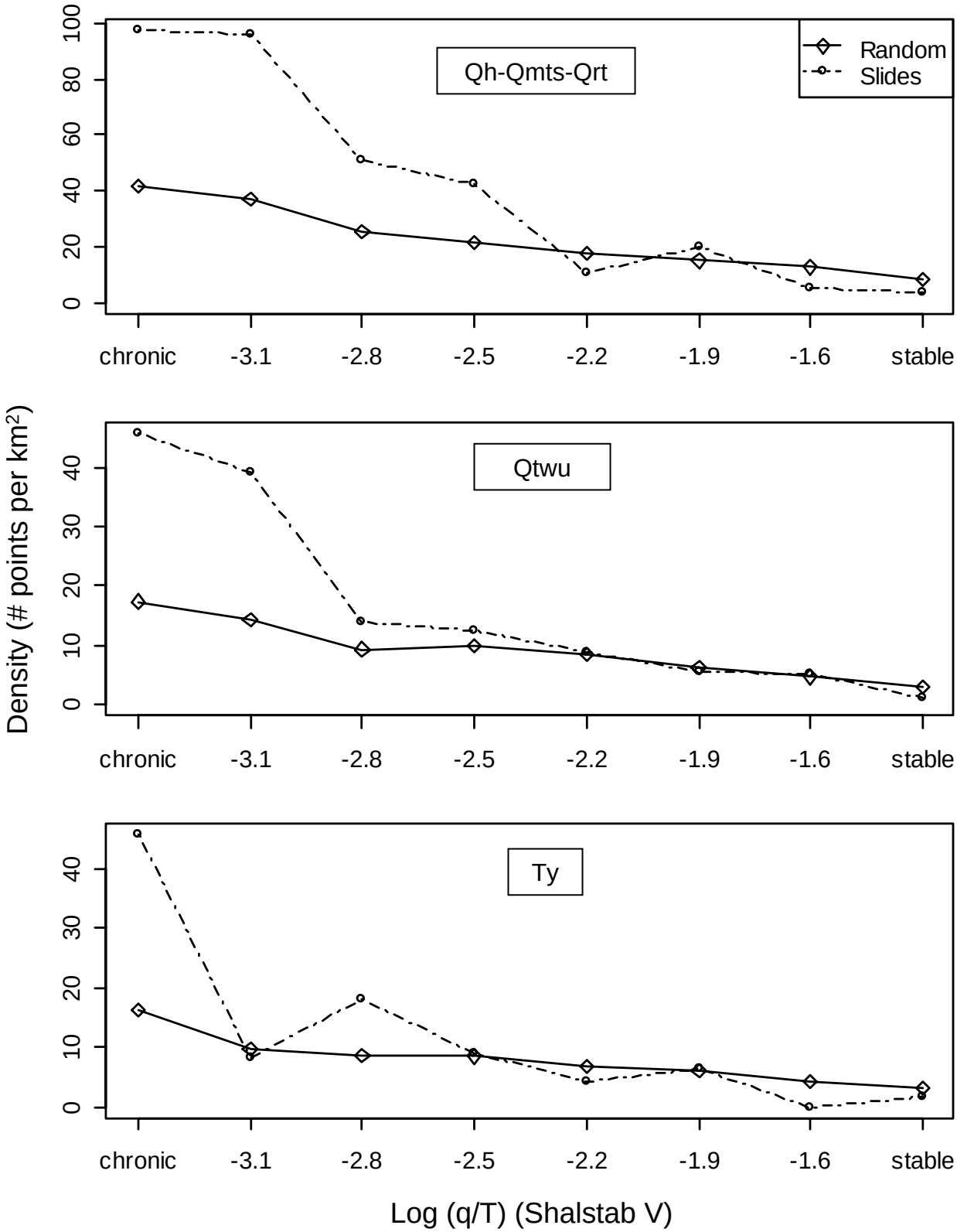

Figure 3-6. Density of landslides and random points by log (q/T) class from SHALSTAB.V.

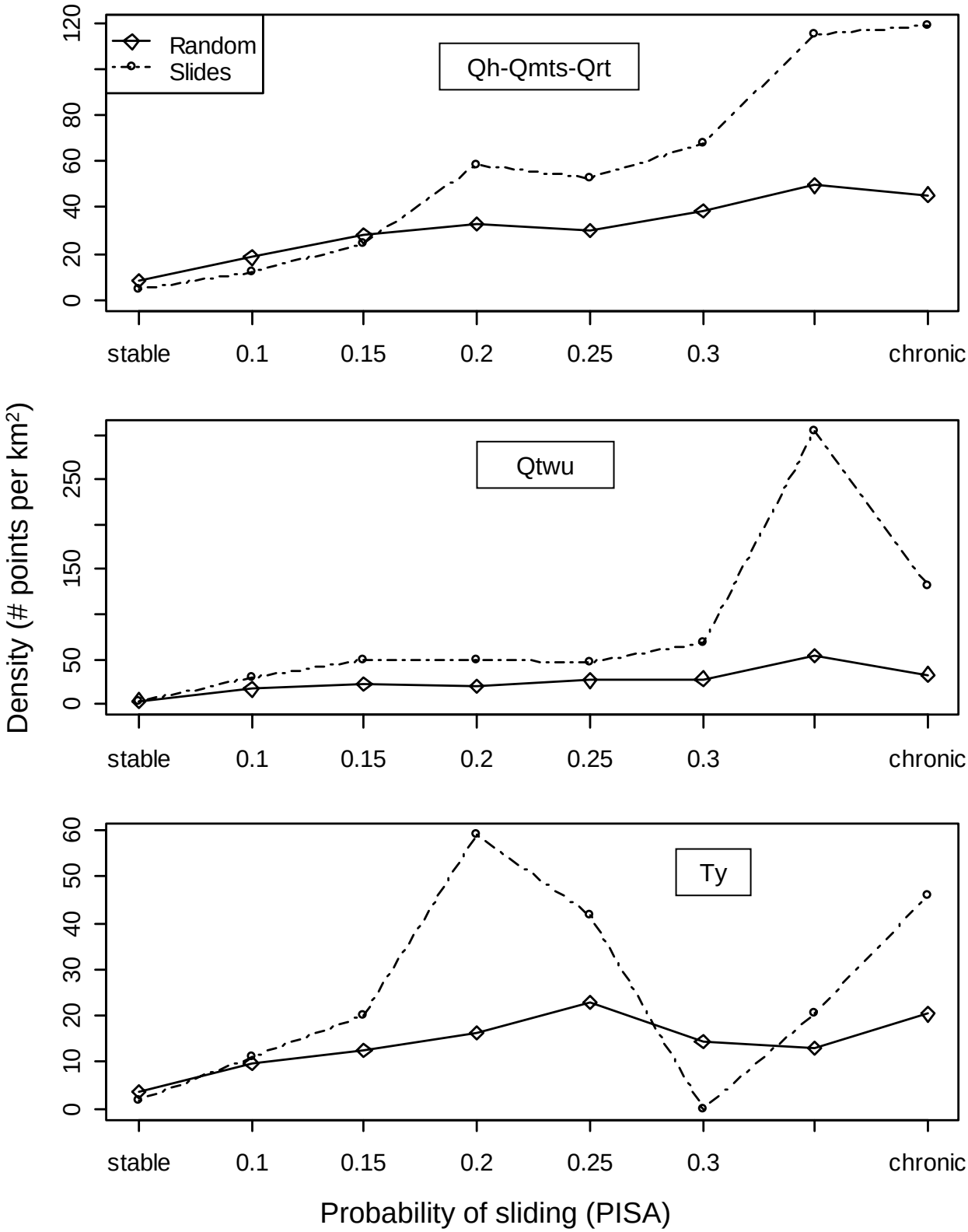

Figure 3-7. Density of landslides and random points by probability of sliding from PISA.

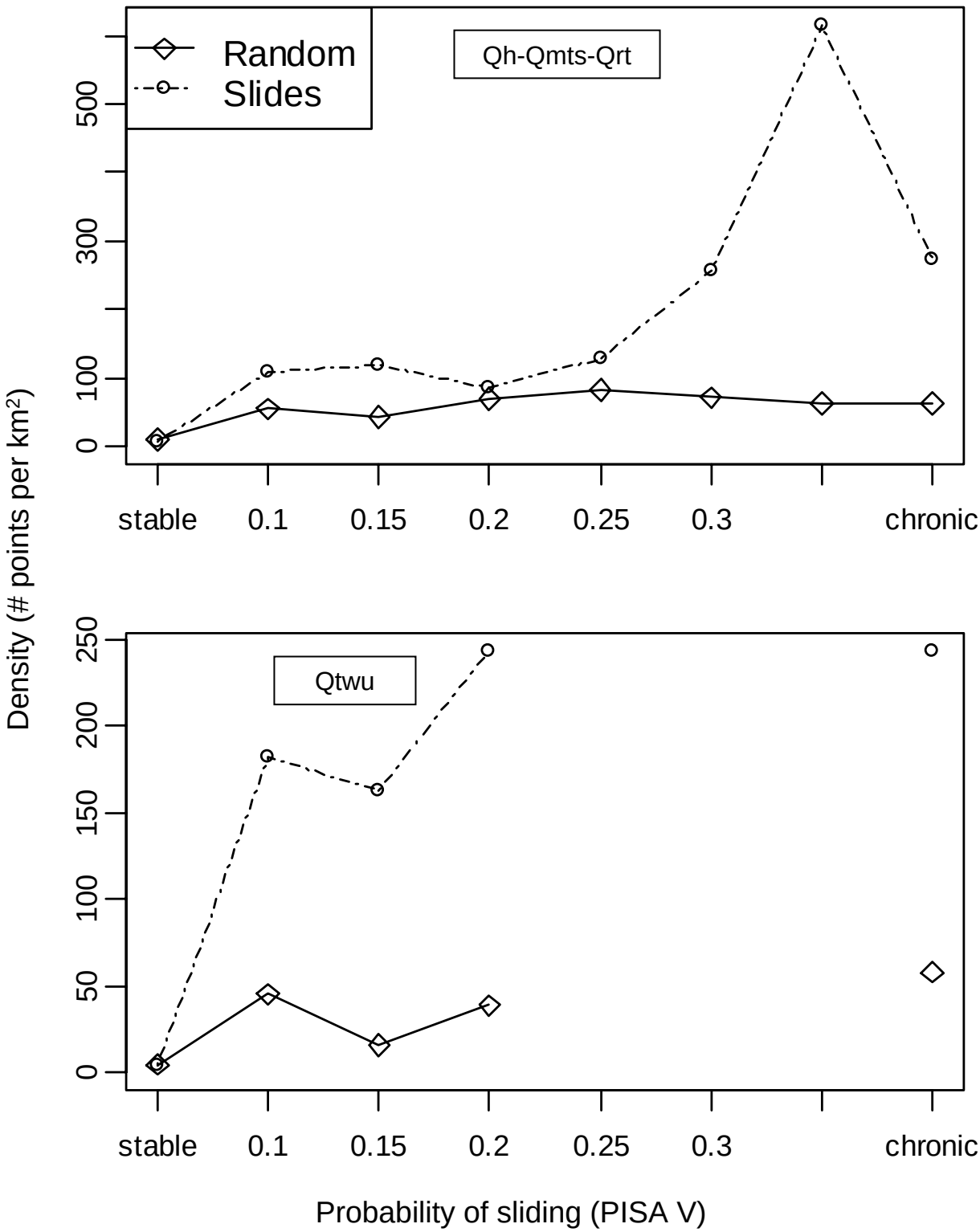

Figure 3-8. Density of landslides and random points by probability of sliding from PISA.V.

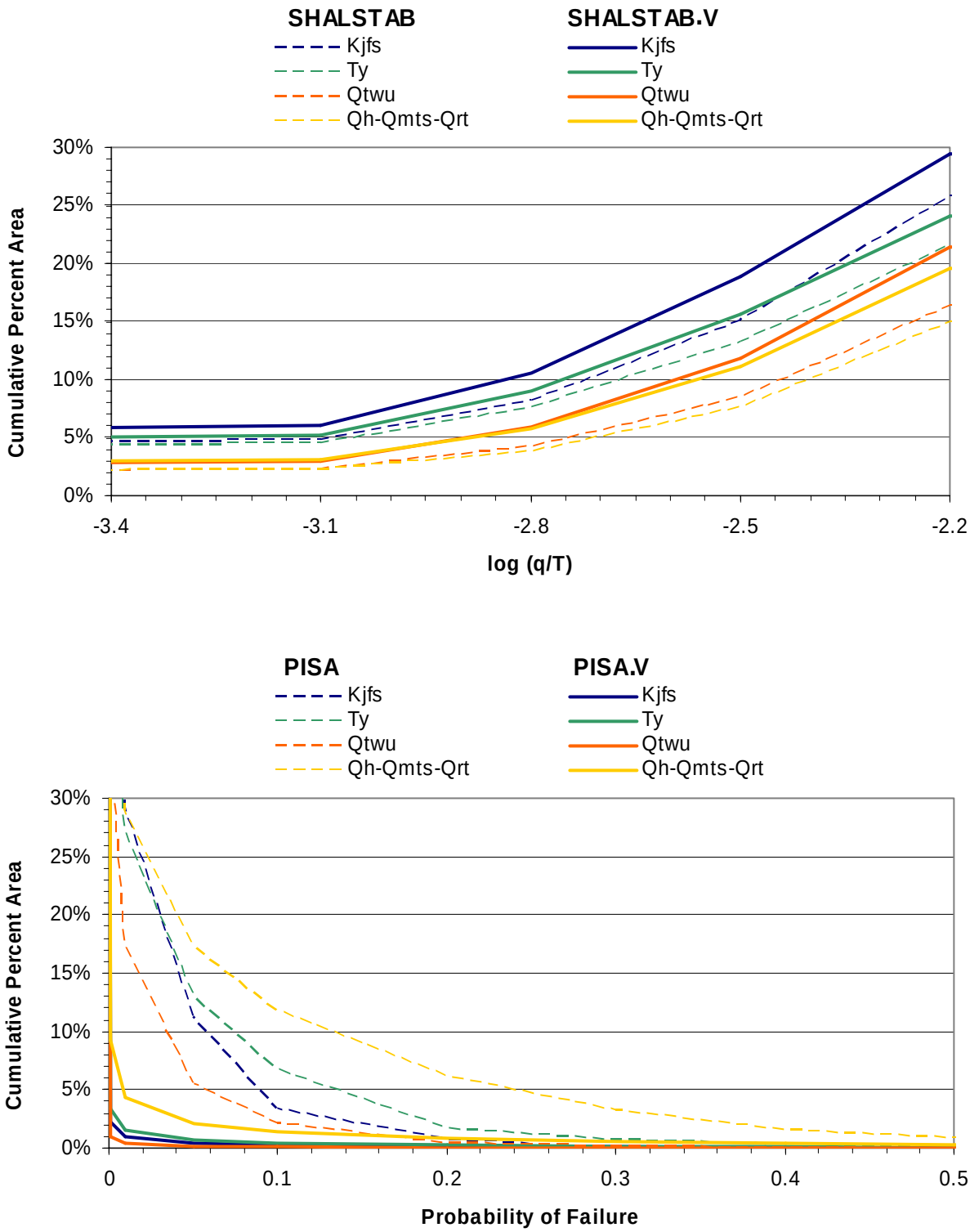

Figure 3-9. Cumulative percent of watershed area in instability classes: a) SHALSTAB and SHALSTAB.V, b) PISA and PISA.V.

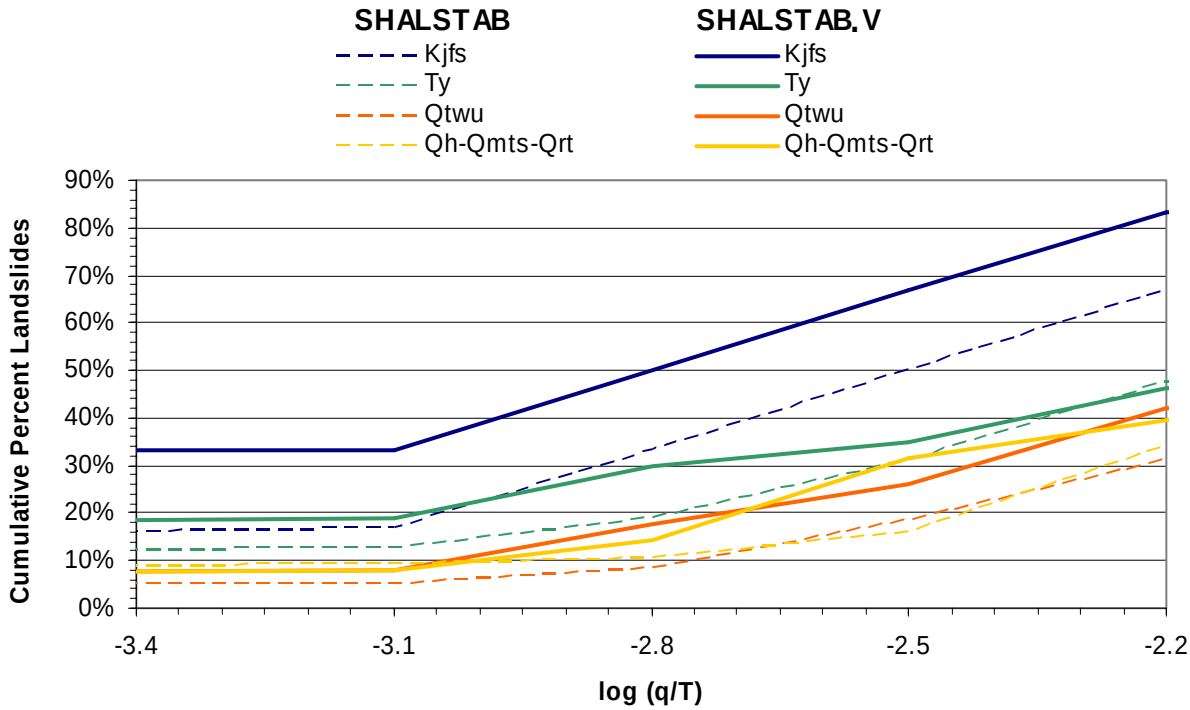

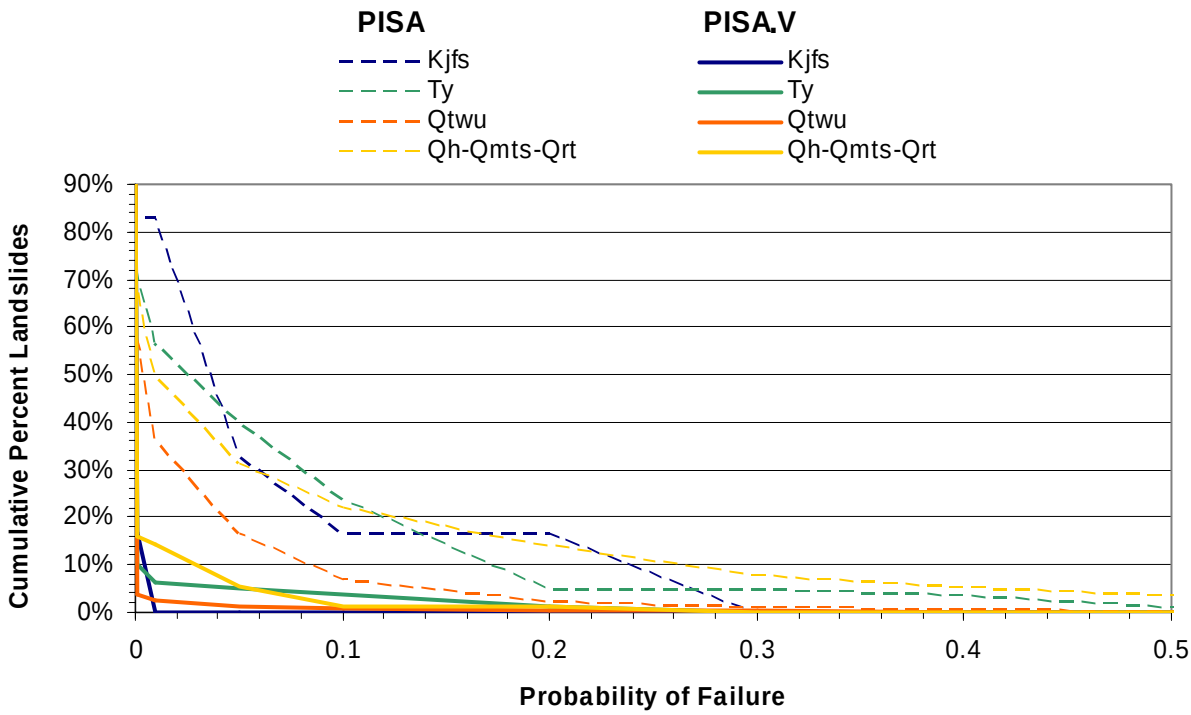

Figure 3-10. Cumulative percent of landslides in instability classes: a) SHALSTAB and SHALSTAB.V, b) PISA and PISA.V.

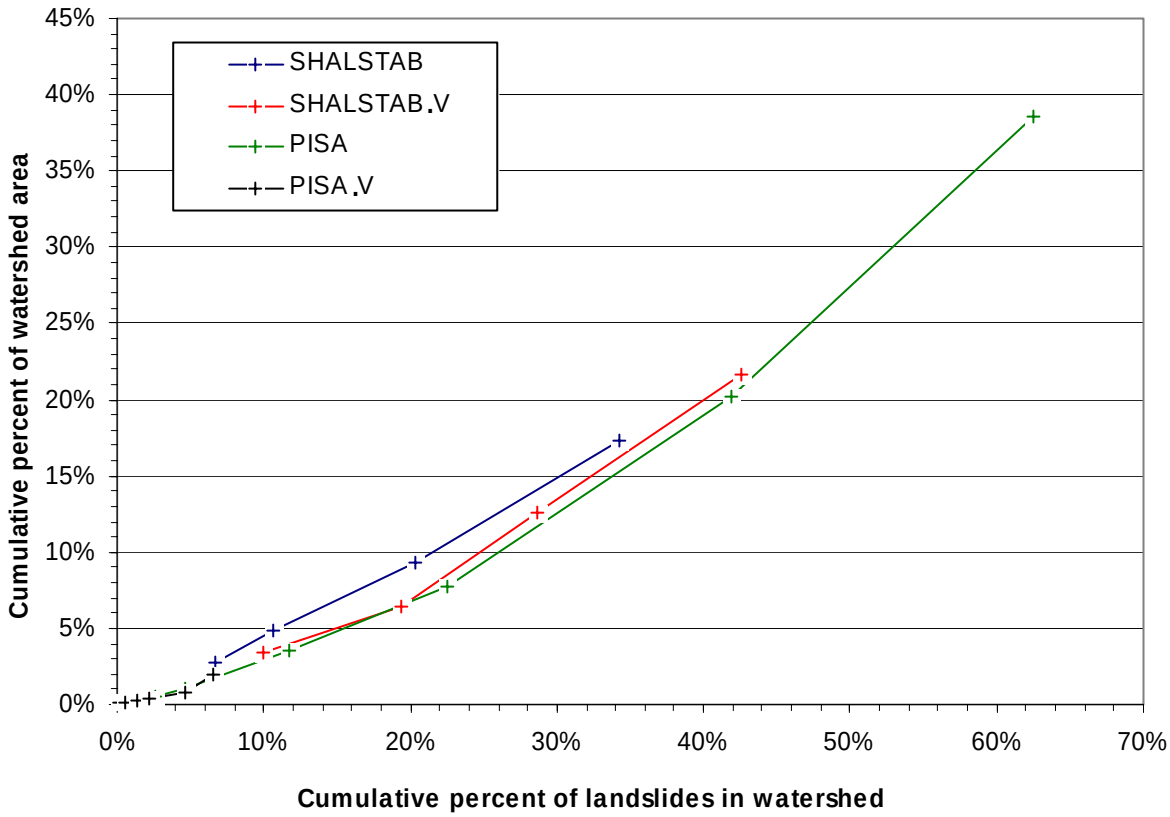

Figure 3-11. Cumulative percent of watershed area as a function of the cumulative percent of the number of landslides.

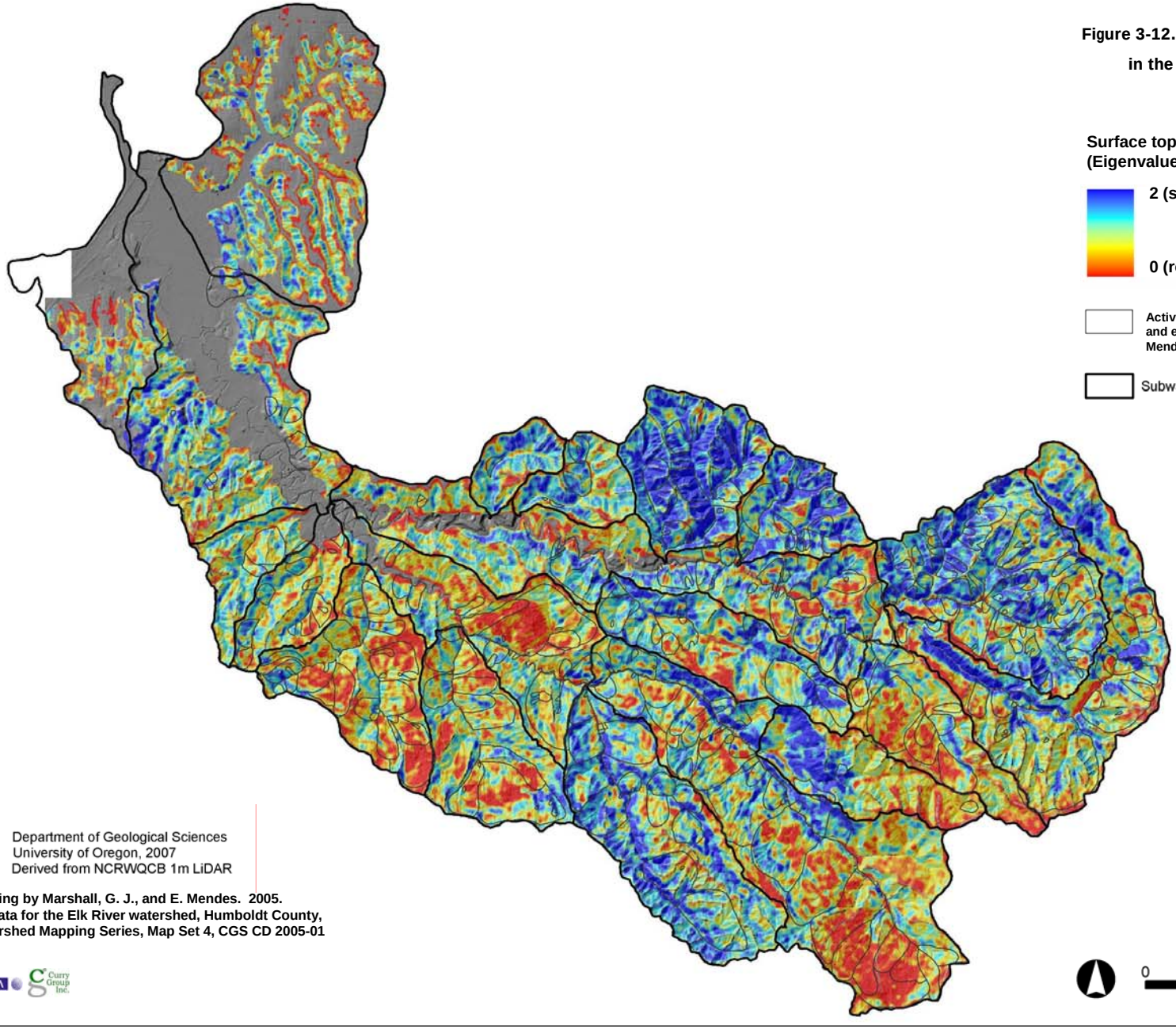

Figure 3-12. DSLED-Rough results in the Elk River basin.

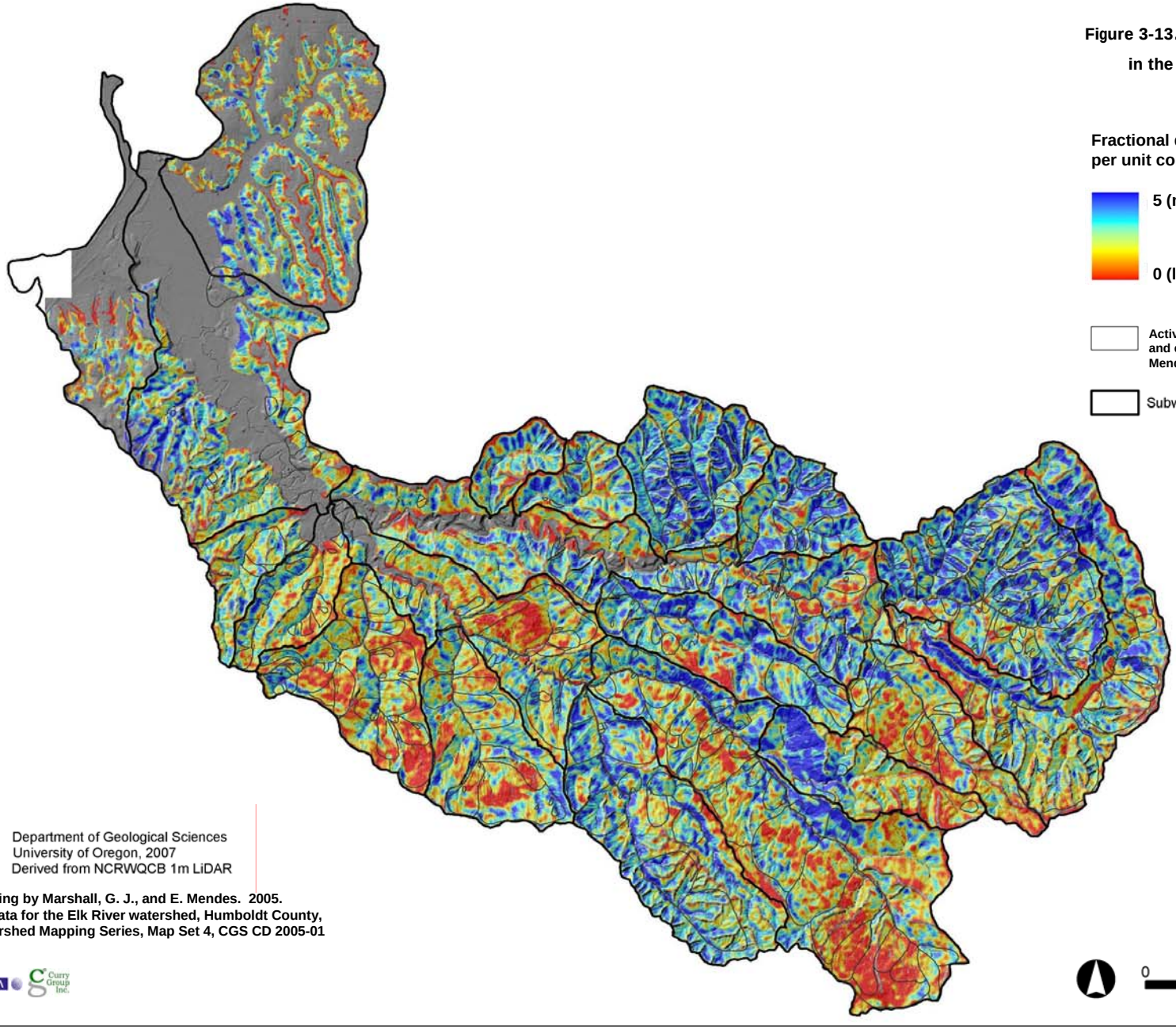

Figure 3-13. DSLED-Drain results in the Elk River basin.

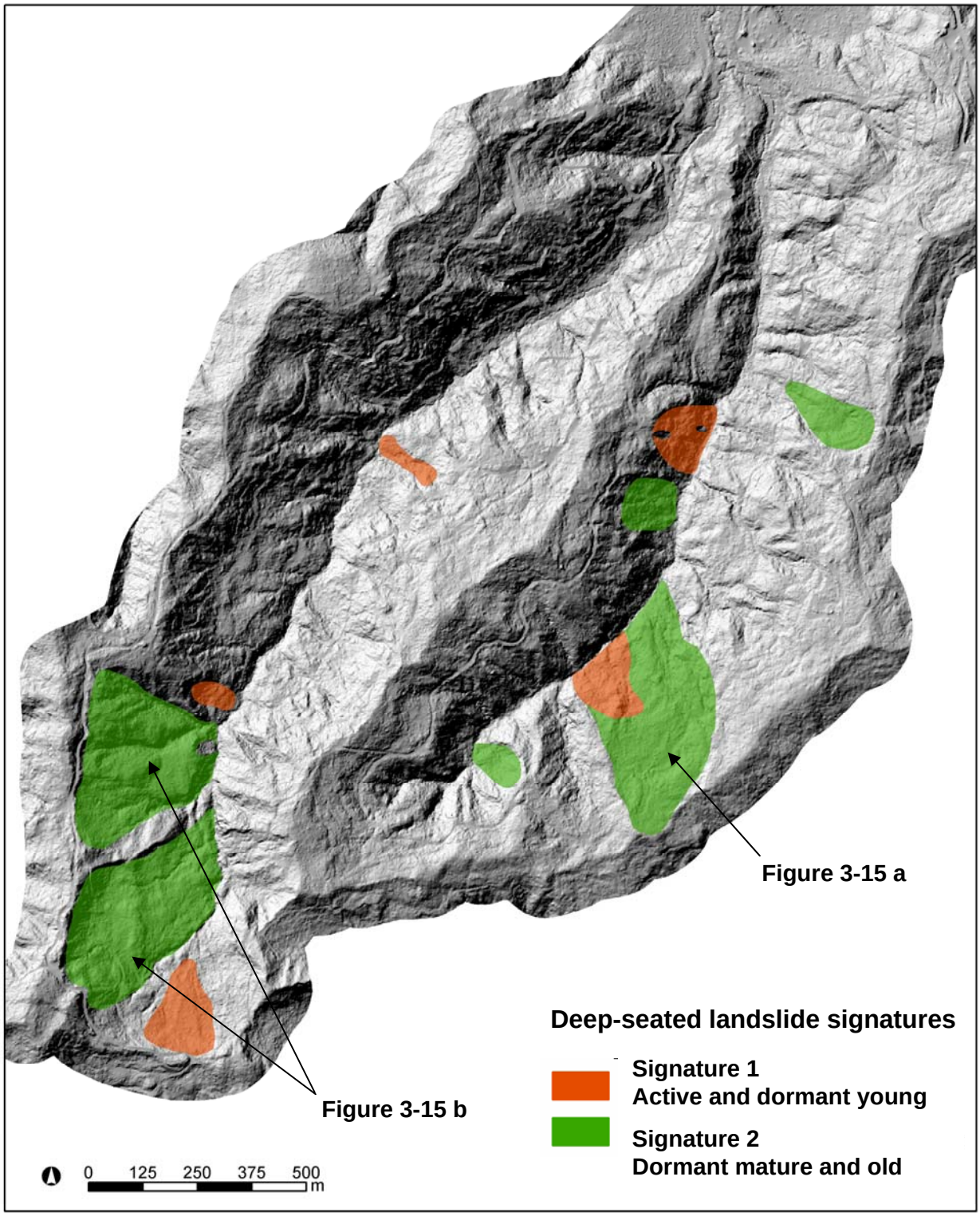

Figure 3-14. Deep-seated landslide signatures in Railroad Gulch.

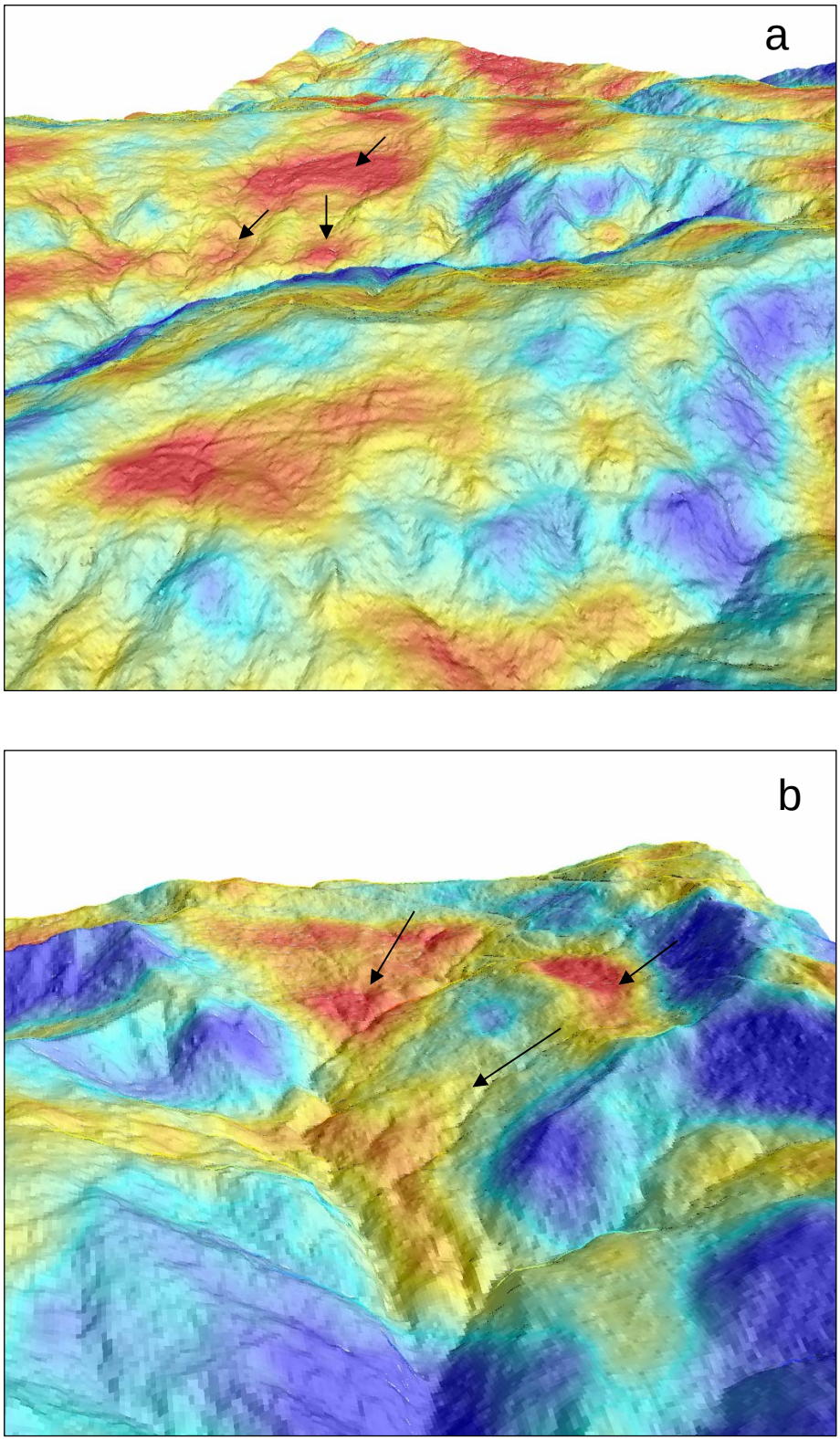

Figure 3-15. DSLED-Rough results in the vicinity of mapped deep-seated landslides in Railroad Gulch.

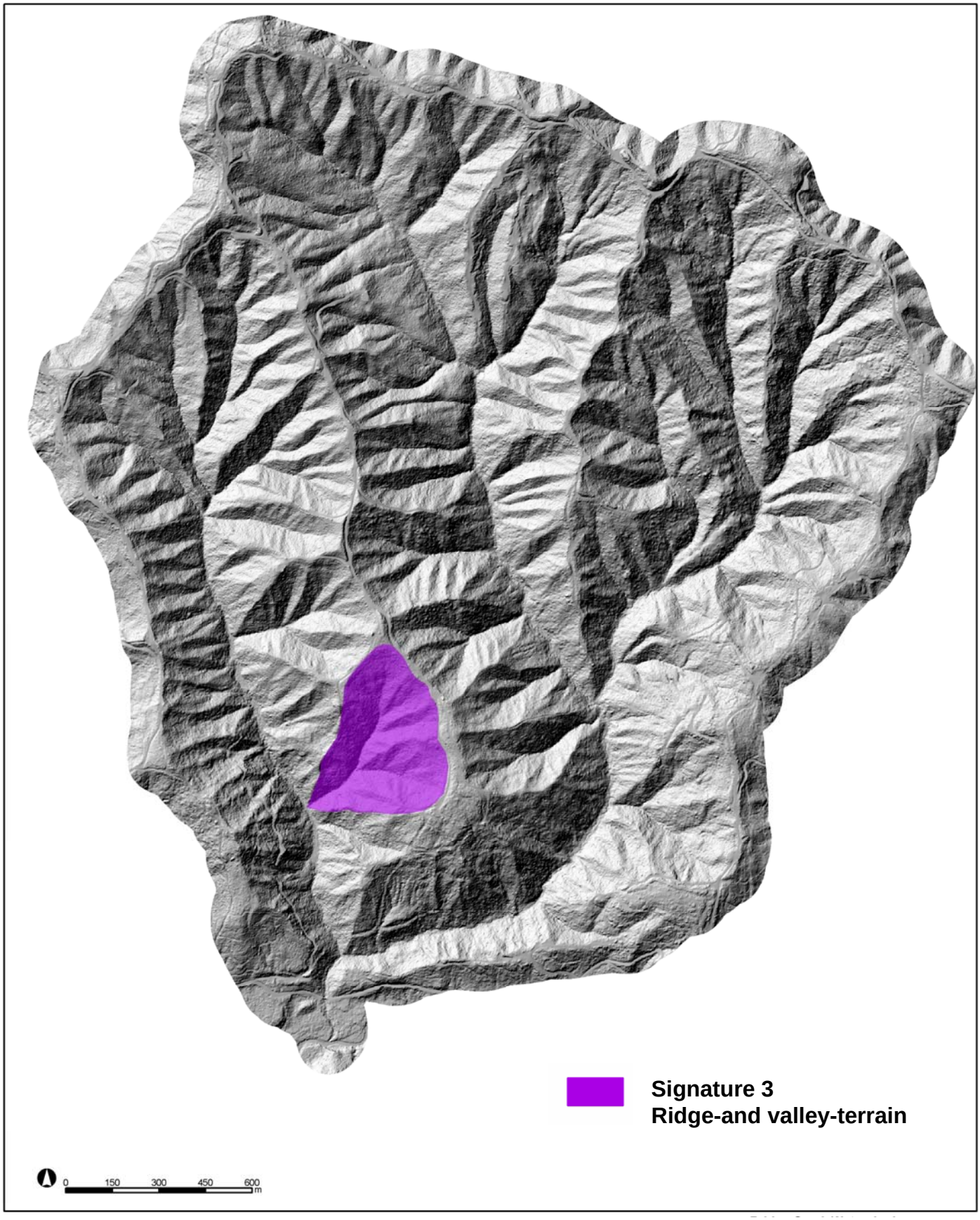

Figure 3-16. Signature of ridge-and-valley topography in Bridge Creek.

Appendix A

Probabilility Density Functions for Hillslope Gradient at Landslide Points in Different Geologic Terrains

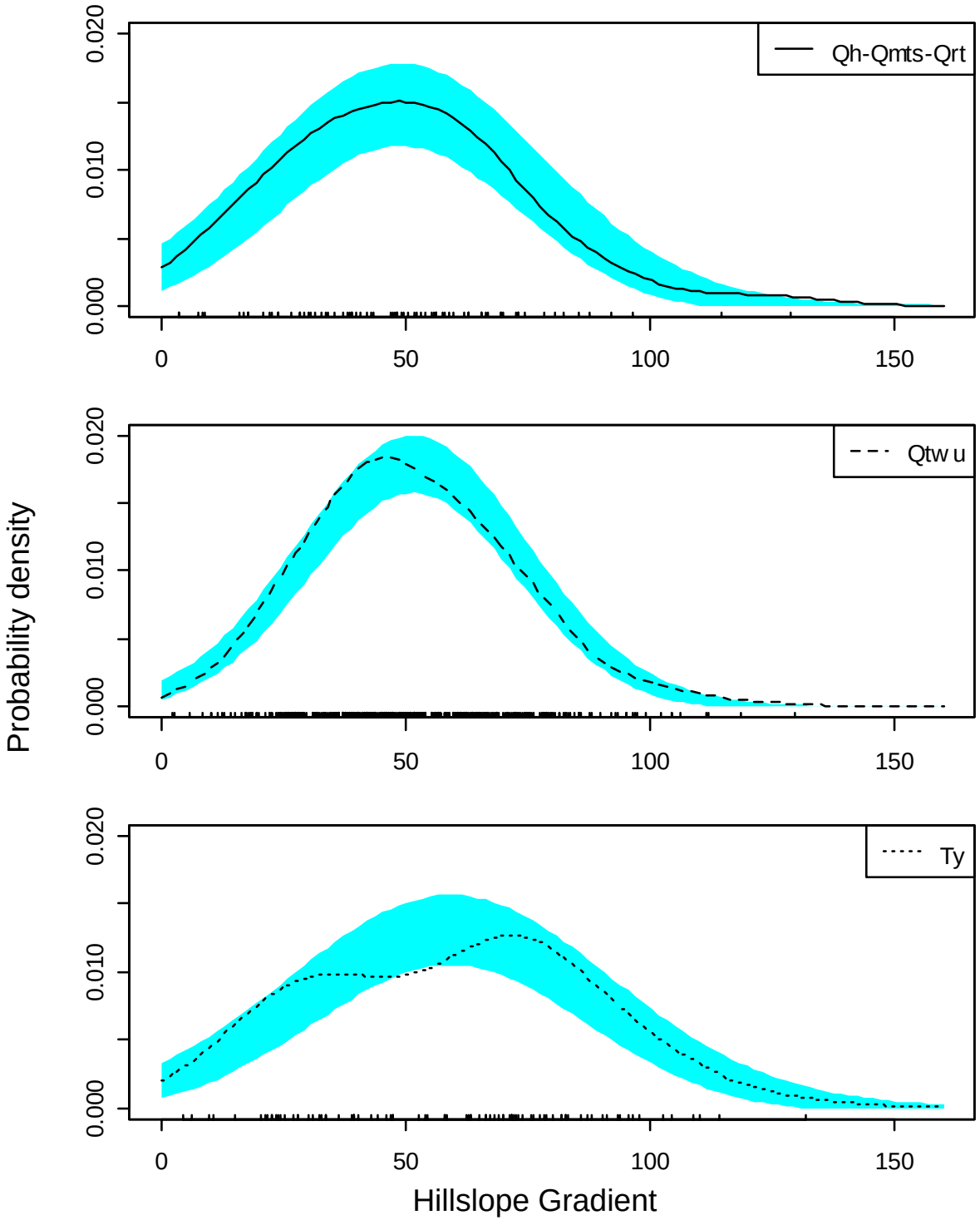

Figure A-1. Probability density for hillslope gradient at landslide points; a) in Hookton formation and Quaternary terrace deposits (Qh-Qmts-Qrt), b) in undifferentiated Wildcat Groiup (Qtw), and c) in Yager terrain (Ty). Rug plots along the x-axis indicate hillslope gradient values at landslides points.

Appendix B

Model Values at Landslide Initiation Points

Model values at landslide points in Qh-Qmts-Qrt terrain

	values of model at points				values in 8m radius			
SLIDE.ID	SHAL	SHALV	PISA	PISAS	SHAL	SHALV	PISA	PISAS
872	-2.16	-2.44	0.0594	0.0015	-10.00	-10.00	0.8549	0.6599
873	-2.16	-2.44	0.0594	0.0015	-10.00	-10.00	0.8549	0.6599
886	10.00	10.00	0.0000	0.0000	10.00	10.00	0.0003	0.0000
906	10.00	10.00	0.0000	0.0000	10.00	10.00	0.0000	0.0000
907	10.00	10.00	0.0007	0.0000	-2.11	-2.09	0.0076	0.0000
908	-2.65	-2.91	0.0156	0.0002	-3.25	-3.27	0.3270	0.1430
917	-2.46	-2.38	0.2871	0.1666	-3.11	-2.79	0.2871	0.2836
918	10.00	-3.26	0.0000	0.0000	-4.08	-3.26	0.2477	0.0006
926	-2.75	-3.05	0.0698	0.0069	-3.15	-3.24	0.4050	0.3051
934	-1.40	10.00	0.0090	0.0000	-2.09	-2.16	0.6803	0.0214
936	-1.97	-2.47	0.3051	0.0024	-3.52	-3.92	0.8077	0.3175
938	-1.71	10.00	0.0143	0.0000	-3.33	-3.20	0.2169	0.2111
942	10.00	-2.44	0.0001	0.0000	-2.64	-2.93	0.1437	0.0005
943	-3.13	-10.00	0.3582	0.9640	-10.00	-10.00	0.5403	0.9640
944	10.00	-2.61	0.0004	0.0000	-2.52	-2.79	0.1219	0.0769
954	10.00	-2.54	0.0000	0.0000	-2.27	-2.55	0.1860	0.0524
957	-2.54	-2.60	0.2107	0.0072	-2.60	-2.61	0.4221	0.0402
958	-2.75	-10.00	0.0779	0.0343	-10.00	-10.00	0.4305	0.7159
959	-1.95	-2.17	0.1103	0.0005	-2.03	-2.32	0.3858	0.0051
960	10.00	10.00	0.0091	0.0000	-1.80	-2.29	0.0406	0.0000
964	-1.36	10.00	0.1625	0.0000	-1.89	-1.96	0.6985	0.0010
970	10.00	10.00	0.0050	0.0027	10.00	10.00	0.0050	0.0027
982	-3.35	-3.30	0.0191	0.0103	-3.35	-3.30	0.6110	0.6644
983	10.00	10.00	0.0000	0.0000	10.00	10.00	0.0042	0.0005
990	10.00	10.00	0.0000	0.0000	-2.16	10.00	0.0477	0.0029
991	-1.96	-2.29	0.3745	0.0234	-2.55	-2.63	0.6388	0.4455
997	10.00	10.00	0.0000	0.0000	-3.22	10.00	0.0030	0.0000
998	-2.85	-3.66	0.3953	0.4978	-2.91	-10.00	0.7408	0.5119
1001	10.00	10.00	0.0000	0.0000	-1.98	-2.12	0.0081	0.0000
1003	10.00	10.00	0.0017	0.0000	-3.02	-3.05	0.0276	0.0006
1011	-1.91	-1.81	0.1209	0.0000	-2.39	-2.54	0.2724	0.1075
1014	-2.59	-10.00	0.3009	0.0636	-2.86	-10.00	0.3914	0.0636
1025	-2.35	-2.32	0.1175	0.0000	-2.54	-2.96	0.2424	0.0001
1030	-10.00	-10.00	0.4982	0.0000	-10.00	-10.00	0.5380	0.5358
1031	10.00	10.00	0.0000	0.0000	10.00	10.00	0.0000	0.0000
1032	10.00	10.00	0.0000	0.0000	10.00	10.00	0.0000	0.0000
1033	-2.42	-2.90	0.1301	0.0813	-2.57	-2.97	0.2551	0.1018
1040	-2.26	-3.11	0.1238	0.0024	-10.00	-10.00	0.4891	0.1069
1044	10.00	10.00	0.0000	0.0000	-1.68	-1.80	0.0530	0.0000
1048	10.00	10.00	0.0000	0.0000	10.00	10.00	0.0000	0.0000
1050	-3.19	-2.92	0.0068	0.0005	-3.25	-3.01	0.1883	0.0131
1061	-1.81	10.00	0.0442	0.0000	-2.15	-2.03	0.3264	0.0000
1068	-2.14	-2.21	0.0103	0.0000	-2.32	-2.69	0.2345	0.0752
1078	10.00	10.00	0.0044	0.0000	-2.48	-2.61	0.1032	0.0017
1081	-2.29	10.00	0.0051	0.0000	-2.61	-2.58	0.0085	0.0000
1090	-2.64	-2.48	0.0475	0.0000	-2.70	-2.73	0.1674	0.0519
1096	10.00	10.00	0.0000	0.0000	10.00	10.00	0.0002	0.0000
1097	10.00	10.00	0.0000	0.0000	10.00	10.00	0.0002	0.0000
1143	-2.38	10.00	0.3575	0.0000	-2.57	-2.66	0.3902	0.0063
1173	10.00	10.00	0.0000	0.0000	-2.96	-3.05	0.0883	0.0000
1179	10.00	10.00	0.0000	0.0000	-1.87	10.00	0.1669	0.0000
1200	-2.14	-2.13	0.0316	0.0000	-2.40	-2.63	0.1818	0.0427
1210	-2.19	-2.21	0.0840	0.0325	-2.19	-2.22	0.1293	0.0325

1215	-10.00	-10.00	0.4633	0.1904	-10.00	-10.00	0.5115	0.3735
1222	10.00	10.00	0.0000	0.0000	-2.48	10.00	0.0196	0.0000
1225	-3.08	-3.25	0.1564	0.3346	-3.09	-3.25	0.3530	0.3346
1229	-1.51	10.00	0.1086	0.0000	-2.21	-2.29	0.2449	0.0002
1232	-1.67	-1.68	0.0603	0.0000	-1.95	-2.18	0.2744	0.0006
1233	-1.83	-2.46	0.0077	0.0000	-3.09	-3.09	0.2572	0.0028
1234	10.00	-2.54	0.0000	0.0000	-2.52	-3.29	0.0685	0.0175
1236	10.00	10.00	0.0002	0.0000	-2.08	-2.07	0.0315	0.0002
1237	10.00	10.00	0.0002	0.0000	-2.08	-2.07	0.0315	0.0002
1238	-2.62	10.00	0.0582	0.0000	-2.79	-2.77	0.1077	0.0013
1242	10.00	10.00	0.0001	0.0000	-2.18	-1.91	0.2408	0.0000
1243	-2.40	-2.29	0.0084	0.0002	-2.48	-2.45	0.0524	0.0007
1263	10.00	10.00	0.0000	0.0000	-1.71	10.00	0.0143	0.0000
1272	10.00	10.00	0.0000	0.0000	10.00	10.00	0.0000	0.0000
1279	-2.31	-2.46	0.1082	0.0000	-2.84	-2.96	0.1847	0.0089
1282	-2.63	-3.35	0.1855	0.2579	-2.63	-10.00	0.3058	0.2579
1283	-2.01	-2.10	0.0013	0.0000	-2.41	-2.66	0.3071	0.3065
1289	-1.96	-1.96	0.0082	0.0000	-2.10	-2.14	0.0635	0.0002
1300	10.00	-2.22	0.0006	0.0000	-2.49	-2.57	0.0156	0.0000
1302	10.00	10.00	0.0000	0.0000	-1.77	-2.15	0.1909	0.0000
1330	-1.75	-1.92	0.2071	0.0000	-2.24	-2.35	0.3520	0.0016
1335	-2.14	-2.24	0.0280	0.0000	-2.62	-2.80	0.3054	0.0253
1336	-3.11	-3.10	0.0152	0.0152	-3.11	-3.16	0.1829	0.1720
1945	10.00	10.00	0.0001	0.0000	10.00	10.00	0.0002	0.0000
2498	-2.35	-2.65	0.2431	0.0002	-3.50	-4.32	0.3372	0.4347

Model values at landslide points in Qtw terrain

	values of model at points				values in 8m radius			
SLIDE.ID	SHAL	SHALV	PISA	PISAS	SHAL	SHALV	PISA	PISAS
507	10.00	10.00	0.0000	0.0000	-1.88	-1.87	0.0117	0.0000
510	10.00	10.00	0.0000	0.0000	10.00	10.00	0.0000	0.0000
511	10.00	10.00	0.0001	0.0000	-1.90	10.00	0.0013	0.0000
513	-3.34	-10.00	0.1236	0.0023	-10.00	-10.00	0.1663	0.0028
514	10.00	10.00	0.0000	0.0000	-2.07	10.00	0.0023	0.0000
516	10.00	10.00	0.0000	0.0000	10.00	10.00	0.0001	0.0000
519	10.00	10.00	0.0001	0.0000	-1.76	10.00	0.0011	0.0000
521	-2.00	10.00	0.0007	0.0000	-2.32	-2.29	0.0046	0.0000
525	10.00	10.00	0.0001	0.0000	-5.01	-2.26	0.3410	0.0000
530	10.00	10.00	0.0000	0.0000	-2.12	10.00	0.0235	0.0003
532	-1.56	10.00	0.0025	0.0000	-1.57	10.00	0.0052	0.0000
538	-2.60	-2.25	0.0054	0.0000	-2.64	-2.59	0.0363	0.0003
545	-2.77	-2.87	0.0044	0.0000	-2.85	-2.96	0.0208	0.0000
550	-2.27	-2.27	0.0785	0.0000	-2.36	-2.67	0.1010	0.0000
554	-2.29	-2.73	0.0024	0.0000	-3.12	-3.36	0.0304	0.0002
557	-2.23	-2.47	0.1067	0.0000	-3.06	-10.00	0.1247	0.0299
560	-2.61	10.00	0.0970	0.0000	-10.00	-10.00	0.1778	0.0025
563	-2.10	-2.59	0.0247	0.0000	-2.47	-2.64	0.1344	0.0003
564	10.00	-2.67	0.0000	0.0000	-3.48	-3.01	0.0244	0.0000
567	-1.85	-1.91	0.0259	0.0000	-10.00	-10.00	0.1490	0.0000
586	-1.70	-1.94	0.0007	0.0000	-2.00	-2.07	0.1066	0.0000
590	-1.95	-1.94	0.0026	0.0000	-2.09	-2.09	0.0181	0.0000
591	-1.95	-1.94	0.0026	0.0000	-2.09	-2.09	0.0181	0.0000
592	10.00	10.00	0.0000	0.0000	-2.19	-2.16	0.0214	0.0000
602	-2.28	-2.39	0.0013	0.0000	-2.44	-2.49	0.0033	0.0000
608	10.00	10.00	0.0000	0.0000	10.00	10.00	0.0000	0.0000
614	-2.65	-2.76	0.0032	0.0000	-3.15	-3.11	0.0108	0.0000
616	10.00	10.00	0.0000	0.0000	-2.01	-2.06	0.0042	0.0000
617	-2.48	-2.88	0.2306	0.0001	-10.00	-3.64	0.6429	0.0665
619	-2.41	-10.00	0.2960	0.1354	-10.00	-10.00	0.4899	0.1436
626	-3.35	-3.37	0.0107	0.0000	-3.98	-3.37	0.0485	0.0000
633	10.00	10.00	0.0001	0.0000	10.00	-2.59	0.0003	0.0000
635	-2.27	-3.14	0.0434	0.0000	-10.00	-10.00	0.1509	0.2182
639	10.00	10.00	0.0000	0.0000	10.00	10.00	0.0001	0.0000
640	-2.03	-1.64	0.0820	0.0000	-2.75	-10.00	0.1227	0.0000
642	10.00	-1.99	0.0001	0.0000	-1.99	-2.08	0.0022	0.0000
643	-1.42	10.00	0.0013	0.0000	-1.78	-2.02	0.0155	0.0000
644	10.00	10.00	0.0000	0.0000	-4.09	-2.63	0.0783	0.0000
647	-1.90	-1.85	0.0012	0.0000	-2.00	-2.05	0.0145	0.0000
648	10.00	10.00	0.0000	0.0000	-2.08	-2.38	0.0192	0.0000
653	-1.88	10.00	0.0034	0.0000	-2.32	-2.35	0.0881	0.0006
654	-1.63	-1.71	0.0007	0.0000	-2.08	-2.05	0.0317	0.0001
655	-2.04	10.00	0.0010	0.0000	-2.19	-2.19	0.0191	0.0000
659	10.00	10.00	0.0004	0.0000	-2.30	-2.12	0.0376	0.0000
668	-10.00	-10.00	0.1533	0.0000	-10.00	-10.00	0.1608	0.0051
672	10.00	10.00	0.0008	0.0002	10.00	10.00	0.0025	0.0009
674	10.00	-2.82	0.0000	0.0000	-3.75	-3.08	0.3237	0.1536
675	-2.30	-2.33	0.0013	0.0000	-2.61	-2.52	0.0196	0.0000
676	10.00	10.00	0.0000	0.0000	10.00	10.00	0.0005	0.0000
679	10.00	10.00	0.0000	0.0000	-2.16	-2.15	0.0042	0.0000
680	-2.03	-1.80	0.0823	0.0000	-2.03	-2.08	0.0861	0.0005
682	10.00	10.00	0.0000	0.0000	10.00	10.00	0.0001	0.0000
683	10.00	10.00	0.0000	0.0000	10.00	10.00	0.0000	0.0000

686	-2.18	-2.31	0.0003	0.0000	-2.30	-2.54	0.0025	0.0000
687	-2.18	-2.31	0.0003	0.0000	-2.30	-2.54	0.0025	0.0000
688	-2.18	-2.31	0.0003	0.0000	-2.30	-2.54	0.0025	0.0000
689	-1.53	10.00	0.0004	0.0000	-2.15	-2.02	0.0672	0.0000
690	-2.62	-10.00	0.1074	0.0000	-10.00	-10.00	0.1741	0.0011
692	-1.41	10.00	0.0005	0.0000	-1.94	-2.20	0.0782	0.0000
694	-2.15	-2.31	0.0012	0.0000	-2.41	-2.49	0.0122	0.0000
699	-1.67	10.00	0.0002	0.0000	-2.00	-2.00	0.0390	0.0000
700	-2.31	-2.46	0.0477	0.0000	-2.49	-3.35	0.0817	0.0056
706	10.00	10.00	0.0001	0.0000	10.00	10.00	0.0001	0.0000
708	10.00	-2.36	0.0000	0.0000	-2.31	-2.77	0.0243	0.0002
709	-10.00	-10.00	0.1438	0.2740	-10.00	-10.00	0.1438	0.2740
710	-2.30	-2.40	0.0295	0.0000	-2.42	-2.47	0.0295	0.0000
712	-2.48	10.00	0.0012	0.0000	-2.99	-3.00	0.0113	0.0000
713	-10.00	-10.00	0.1875	0.1884	-10.00	-10.00	0.1923	0.1884
714	10.00	10.00	0.0000	0.0000	10.00	10.00	0.0000	0.0000
720	-2.68	-2.88	0.0243	0.0000	-2.96	-3.14	0.0243	0.0000
722	-2.35	-2.42	0.0497	0.0000	-2.61	-2.54	0.0645	0.0016
723	-2.45	-2.69	0.0676	0.0000	-10.00	-10.00	0.1502	0.0005
725	10.00	-2.55	0.0000	0.0000	-2.71	-2.80	0.0801	0.0086
728	10.00	-2.12	0.0000	0.0000	-2.30	-2.18	0.0150	0.0000
729	-10.00	-2.27	0.6022	0.0000	-10.00	-10.00	0.6828	0.0000
730	10.00	-2.57	0.0000	0.0000	-2.48	-2.77	0.0255	0.0000
736	-2.58	-2.42	0.0005	0.0000	-2.62	-2.60	0.0083	0.0000
738	10.00	10.00	0.0001	0.0000	-2.09	-2.41	0.0006	0.0000
739	10	10	2E-05	0	-2.897	-2.625	0.1002	3E-08
740	-2.271	-2.336	0.0176	0	-2.485	-2.728	0.0664	0
741	-2.271	-2.336	0.0176	0	-2.485	-2.728	0.0664	0
742	10	10	1E-06	0	-1.955	10	0.0169	0
743	-1.304	10	0.0451	0	-10	-3.032	0.4838	5E-05
744	-1.704	10	0.0052	0	-2.088	10	0.0052	0
746	-2.707	-3.275	0.0216	2E-06	-3.577	-3.528	0.0216	0.0002
747	-2.707	-3.275	0.0216	2E-06	-3.577	-3.528	0.0216	0.0002
750	-1.551	10	0.0473	0	-1.982	-1.95	0.082	0
751	10	10	2E-07	0	10	10	0.0002	0
752	10	10	7E-05	0	-1.943	-2.08	0.0017	0
753	-2.891	-3.302	0.05	0	-3.463	-10	0.0781	0.018
757	-1.931	-2.006	0.0437	0	-10	-10	0.1643	0.0001
758	-1.694	-1.569	0.0134	0	-3.381	-1.569	0.0252	0
759	-1.694	-1.569	0.0134	0	-3.381	-1.569	0.0252	0
760	10	10	7E-06	0	-1.945	-2.419	0.0054	4E-07
761	-2.681	-2.717	0.0061	2E-07	-4.144	-3.782	0.0119	2E-06
762	10	10	4E-05	0	10	10	0.0001	0
763	-1.913	-1.989	0.0036	0	-2.473	-2.395	0.0222	2E-06
764	-1.599	10	0.0163	0	-2.053	-1.713	0.0644	0
765	-1.599	10	0.0163	0	-2.053	-1.713	0.0644	0
767	-2.408	-2.405	0.0012	0	-2.686	-2.528	0.0141	3E-08
769	-1.656	-1.825	0.0284	0	-2.468	-1.889	0.1296	0
770	-1.962	10	0.0005	0	-2.232	-2.298	0.0428	0
771	-1.903	-1.779	0.0022	0	-2.04	-1.818	0.0511	0
772	-1.903	-1.779	0.0022	0	-2.04	-1.818	0.0511	0
773	10	10	4E-05	0	-2.262	-2.45	0.0701	1E-06
774	10	10	1E-05	0	-2.213	-2.184	0.0162	0
775	-2.228	-2.251	0.0025	2E-07	-2.522	-2.526	0.0254	2E-06
776	-2.556	10	0.0001	0	-2.595	-2.282	0.0046	0
777	10	10	2E-05	0	10	10	0.0002	0
778	10	10	0.0001	0	-2.575	-2.806	0.002	0
779	-1.561	10	0.0003	0	-1.786	-1.98	0.0017	0

782	-2.047	-2.464	0.0635	3E-08	-10	-2.926	0.1453	2E-07
783	-2.418	-2.688	0.1793	0	-3.261	-3.121	0.2117	0.0382
784	10	10	0	0	-2.644	10	0.0017	0
787	-2.384	-2.583	0.1065	0	-3.416	-3.386	0.184	0.0166
788	10	10	0.0001	0	-3.219	-3.33	0.0005	5E-06
789	-3.56	-3.929	0.0673	0.216	-3.56	-3.929	0.2837	0.216
790	-1.87	10	0.0581	0	-2.854	-2.633	0.3461	0
791	-2.233	-2.135	0.0505	0	-2.546	-2.659	0.2539	0
794	-10	-2.889	0.4477	0.0012	-10	-3.682	0.4547	0.4588
795	-2.239	-2.265	0.0026	0	-2.42	-2.372	0.0047	0
797	10	10	9E-07	0	10	10	7E-05	0
798	10	10	9E-07	0	10	10	7E-05	0
799	-1.872	10	0.0661	0	-2.208	-2.268	0.0947	6E-08
800	-2.543	10	0.0007	0	-4.128	-4.155	0.0461	6E-06
802	-1.592	10	0.0016	0	-1.641	10	0.0144	0
804	-1.927	-2.118	0.0148	6E-08	-2.205	-2.176	0.027	1E-06
805	-2.631	-2.478	0.111	2E-06	-2.991	-3.054	0.1269	0.0489
806	-2.631	-2.478	0.111	2E-06	-2.991	-3.054	0.1269	0.0489
808	-2.423	-2.762	0.1937	0.0239	-3.123	-3.167	0.2753	0.0548
809	-2.472	-2.57	0.0027	0	-2.579	-2.616	0.085	1E-06
810	-2.239	-2.184	0.1399	0	-2.983	-2.987	0.3409	0.0282
812	-2.159	-2.492	0.0879	0	-2.605	-3.195	0.1102	0.007
814	-1.956	-1.734	0.0933	0	-10	-2.256	0.1427	3E-08
817	-10	-2.644	0.5077	0	-10	-10	0.5077	0.1034
818	-2.408	-2.508	0.0009	0	-2.727	-2.698	0.0047	5E-07
825	-1.986	-2.2	0.0179	0	-2.317	-10	0.0892	0.0006
826	10	-2.379	6E-05	0	-2.521	-2.503	0.0105	0.0001
827	10	-3.353	0.0002	3E-08	-3.24	-3.411	0.0354	0.0007
830	-2.601	-2.82	0.0439	0.0008	-2.891	-3.195	0.0439	0.0008
831	-2.347	-2.346	0.0005	3E-08	-2.41	-2.462	0.0248	4E-06
832	10	10	8E-06	0	-2.294	-2.608	0.007	0
834	-10	-10	0.4481	0.056	-10	-10	0.4481	0.8837
835	-2.066	-2.933	0.0119	0	-2.632	-10	0.1192	0.065
837	-2.266	-2.415	0.0029	8E-07	-2.296	-2.564	0.0179	0.0011
838	10	10	4E-05	0	-3.339	10	0.0305	0
840	10	-2.789	8E-06	0	-3.047	-2.882	0.0009	6E-08
841	-2.208	-2.243	0.0013	0	-2.286	-2.247	0.0119	2E-07
842	-2.644	-10	0.2178	0.0997	-3.224	-10	0.3684	0.0997
844	-1.454	10	0.0083	0	-1.811	-1.751	0.0804	0
847	10	10	3E-05	0	-2.295	-2.171	0.0116	3E-08
849	-1.149	10	0.0018	0	-1.469	10	0.063	2E-05
850	-1.149	10	0.0018	0	-1.469	10	0.063	2E-05
854	10	10	2E-07	0	10	10	5E-05	0
855	-1.355	10	0.0138	0	-2.031	-1.745	0.2661	0
856	-2.642	-2.747	0.0064	2E-07	-3.215	-3.164	0.2043	0.1419
857	10	10	2E-06	0	10	10	0.0003	0
858	10	10	0.0002	0	10	10	0.0002	0
859	10	10	0.0002	0	10	10	0.0002	0
860	10	10	3E-08	0	10	10	1E-05	0
861	10	10	3E-06	0	-2.615	-3.161	0.0016	0
862	-2.814	-2.81	0.0263	0	-2.856	-3.271	0.3111	0
863	10	10	3E-08	0	-1.573	10	0.0013	0
864	-1.926	-1.944	0.0343	0	-2.088	-2.059	0.0693	0
865	-2.342	10	0.0038	0	-2.697	-3.93	0.0178	9E-08
866	10	10	3E-06	0	-1.642	10	0.0003	0
867	-1.891	-2.125	0.0046	2E-07	-2.227	-2.215	0.111	2E-07
868	-3.387	10	0.065	0	-10	-10	0.1888	2E-05
869	10	10	5E-05	0	-3.124	-3.07	0.0307	0

871	-1.689	-1.809	0.0042	0	-2.2	-2.069	0.0607	0
874	-2.122	-2.137	0.0311	0	-4.015	-3.65	0.1464	9E-06
876	10	10	9E-08	0	10	10	2E-06	0
877	-2.186	10	0.0008	0	-2.374	-2.585	0.0755	0
878	10	-2.387	0.0003	0	-2.603	-2.581	0.0162	0
880	10	10	4E-07	0	-1.861	-2.041	0.0927	7E-05
881	10	10	4E-07	0	-1.861	-2.041	0.0927	7E-05
884	-2.669	10	0.0163	0	-2.926	-2.546	0.0486	3E-08
888	-1.831	10	0.0112	0	-2.486	-2.858	0.0766	0.0002
889	-1.831	10	0.0112	0	-2.486	-2.858	0.0766	0.0002
890	10	10	3E-07	0	10	-2.175	0.0002	0
891	-2.01	-2.22	0.0254	6E-07	-2.27	-2.372	0.0894	0.0001
893	10	10	9E-08	0	-2.355	-2.407	0.1452	0.0003
896	-2.343	-2.261	0.07	6E-08	-2.343	-2.399	0.07	3E-05
897	10	10	3E-05	0	-1.678	10	0.0035	0
899	-1.708	10	0.0003	0	-1.734	-2.358	0.0153	0
900	10	10	5E-07	0	10	-2.207	0.0003	0
901	10	10	5E-05	0	-1.654	10	0.0006	0
903	-2.222	10	0.0128	0	-2.533	-2.47	0.0998	0
911	10	-2.158	0.0002	0	-2.218	-2.247	0.0453	5E-07
913	-1.806	10	0.0046	0	-1.955	-1.977	0.0144	0
923	-3.898	10	0.0042	0	-3.898	-2.867	0.0276	0
924	10	10	1E-05	0	-3.089	-3.155	0.0037	0.0001
925	10	-2.181	1E-05	0	-2.407	-2.718	0.0082	0
927	-2.32	-2.682	0.0009	0	-2.339	-2.806	0.0131	0
928	10	10	2E-06	0	10	10	0.0001	0
930	-2.561	10	0.0008	0	-2.692	-2.668	0.0059	0
931	10	10	0	0	-1.601	10	0.0003	0
932	-1.974	-2.403	0.0047	0	-2.539	-2.613	0.011	0.0009
933	10	10	0	0	10	10	0.0001	0.0001
935	10	-3.114	0.0001	0	-3.16	-3.182	0.013	1E-06
937	10	10	3E-08	0	-2.164	10	0.0033	0
940	-1.986	10	0.0002	0	-2.068	-2.103	0.0172	3E-08
945	10	10	6E-06	0	-3.165	-3.198	0.0043	0
946	10	10	6E-06	0	-3.165	-3.198	0.0043	0
949	-2.453	-2.77	0.032	1E-07	-3.594	-3.345	0.0872	0.0008
950	-1.956	-1.828	0.0658	0	-2.15	-2.354	0.0705	0.0002
955	-1.771	-1.902	0.0011	0	-2.306	-2.35	0.0088	1E-06
962	-1.981	-1.894	0.037	0	-2.106	-2.241	0.0745	3E-06
963	-2.408	-2.935	0.0036	0	-3.217	-3.63	0.0193	7E-07
968	-2.155	-2.528	0.0004	1E-07	-2.202	-2.589	0.0558	0.0022
969	-1.895	-2.39	0.1406	0	-3.156	-3.393	0.2459	0.0542
974	-2.033	-2.049	0.0007	0	-2.067	-2.063	0.0052	3E-08
976	-1.819	10	0.009	0	-10	-3.218	0.1564	2E-06
977	10	10	4E-07	0	-1.401	10	0.0027	6E-06
978	10	10	1E-07	0	10	10	2E-07	0
980	10	10	1E-05	0	-2.713	-2.783	0.0728	3E-07
984	-2.835	-3.389	0.0062	0	-3.619	-3.543	0.1137	2E-05
985	-2.453	-2.623	0.0012	0	-3.396	-3.344	0.0025	6E-07
986	-2.697	-2.811	0.0253	6E-06	-2.903	-3.12	0.0785	0.0025
988	-1.627	-1.651	0.0913	0	-2.349	-2.484	0.3746	6E-06
995	-2.388	-2.283	0.0057	8E-05	-2.739	-2.594	0.0466	8E-05
996	10	10	0	0	-2.739	-2.744	0.0466	8E-05
999	10	10	0	0	-1.893	10	0.0158	0
1000	-1.698	10	0.0292	0	-3.567	-2.089	0.149	5E-06
1002	-2.574	-2.368	0.0401	3E-08	-2.7	-2.641	0.0604	0.0037
1004	10	10	0.0001	0	10	10	0.0004	0
1006	10	10	9E-08	0	-2.15	10	0.0017	0

1007	10	10	1E-05	0	-1.821	-1.877	8E-05	0
1008	10	-2.419	1E-07	0	-2.838	-2.667	0.0869	0.0155
1013	-1.59	10	0.0004	0	-2.567	-2.018	0.0248	0
1017	10	-3.618	0.0002	0	-3.772	-3.812	0.0707	6E-05
1026	10	10	2E-07	0	-3.789	-3.07	0.0067	7E-07
1027	10	10	2E-07	0	-2.709	10	0.0011	0
1029	-2.11	-2.189	0.0228	0	-2.962	-2.94	0.0391	4E-07
1035	10	-2.806	7E-05	0	-2.638	-2.806	0.0051	6E-08
1036	-2.221	-2.544	0.0026	0	-2.699	-2.856	0.0631	0.0003
1037	10	-2.545	0.0002	3E-08	-2.666	-2.783	0.1153	0.0023
1042	10	10	4E-05	0	-2.16	-2.23	0.102	0
1043	10	10	5E-07	0	-2.465	10	0.0008	0
1046	-2.869	-2.867	0.0005	0	-3.408	-3.111	0.0514	0.0008
1047	10	10	1E-07	0	10	10	0.0002	0
1049	10	10	2E-05	0	-1.888	-2.252	0.0623	3E-08
1055	10	10	3E-07	0	10	-2.334	0.0002	0
1057	-3.029	-3.119	0.0072	8E-06	-3.029	-3.119	0.02	9E-05
1062	-3.088	-3.383	0.0004	0	-3.37	-3.389	0.0978	0.0229
1066	-1.83	10	0.0008	0	-2.053	-2.495	0.0008	0
1067	10	-3.236	7E-05	0	-3.459	-3.463	0.0043	2E-05
1072	-2.512	-2.81	0.0106	9E-06	-2.667	-3.856	0.085	0.0123
1074	-1.986	-2.121	0.0303	0	-2.897	-3.338	0.0894	0.0011
1080	-2.246	10	0.0004	0	-3.465	-3.388	0.0104	9E-07
1082	-1.577	10	0.0281	0	-3.29	-3.378	0.0693	8E-05
1084	-2.011	-2.081	0.0098	0	-2.268	-2.353	0.041	0.0001
1085	10	-1.755	1E-05	0	-2.052	-2.05	0.0072	0
1086	-1.864	-2.047	0.0052	5E-06	-1.9	-2.238	0.0163	5E-06
1087	-1.615	-1.489	0.0621	0	-1.876	-1.877	0.1157	0
1088	-3.169	-3.146	0.0009	0	-3.255	-3.29	0.0426	5E-05
1089	-2.14	10	0.0013	0	-2.388	-2.438	0.0307	6E-08
1092	-2.625	-3.396	0.0605	0.0006	-2.655	-3.6	0.0808	0.0007
1094	10	10	3E-08	0	-1.644	-3.04	0.0558	3E-08
1095	10	10	2E-06	0	10	10	1E-05	0
1098	-2.601	-2.84	0.0609	3E-08	-3.428	-3.57	0.061	0.0016
1100	-1.177	10	0.0004	0	-10	-1.834	0.1754	0
1101	-1.177	10	0.0004	0	-10	-1.834	0.1754	0
1102	10	10	0	0	10	10	1E-07	0
1104	10	10	0.0001	0	-2.757	-2.534	0.056	0
1105	10	10	0.0001	0	-2.757	-2.534	0.056	0
1106	10	10	2E-07	0	10	10	0.0004	3E-08
1107	-2.766	-2.82	0.0472	0	-3.005	-3.131	0.1039	0.0055
1109	-2.988	-10	0.0821	2E-05	-10	-10	0.1622	0.0173
1110	-2.08	-2.132	0.0215	2E-06	-2.171	-2.249	0.0279	4E-06
1112	-1.709	10	0.0002	0	-4.023	-4	0.006	0
1114	10	-2.429	2E-06	0	-2.662	-2.629	0.0092	8E-07
1115	-1.69	10	0.0141	0	-2.845	-2.401	0.112	0
1121	-2.077	-1.913	0.0277	0	-2.217	-2.313	0.0371	1E-06
1123	10	10	1E-06	0	10	10	0.0003	0
1126	-2.091	-2.159	0.0051	0	-2.607	-3.017	0.0513	0
1127	-1.984	-2.426	0.0289	1E-06	-2.534	-2.904	0.1215	0.0039
1128	-1.984	-2.426	0.0289	1E-06	-2.534	-2.904	0.1215	0.0039
1135	-2.431	-2.967	0.0702	0.0002	-2.516	-10	0.0963	0.094
1137	10	10	9E-07	0	-1.888	-1.793	0.0575	0
1140	-3.925	-10	0.1454	0.8143	-10	-10	0.1908	0.8143
1141	-10	-10	0.156	0	-10	-10	0.1873	0.344
1145	-2.627	-2.256	0.0608	0	-3.146	-10	0.1181	0.0005
1146	10	10	6E-08	0	10	10	0.0064	2E-06
1149	-1.698	10	0.0435	0	-2.122	-2.105	0.0684	0

1150	-1.698	10	0.0435	0	-2.122	-2.105	0.0684	0
1157	-2.43	-2.519	0.0874	0	-3.732	-10	0.1119	0.0005
1158	-2.872	-2.932	0.198	0	-2.913	-3.118	0.2357	0.0001
1159	-1.97	-2.785	0.0076	2E-07	-2.587	-2.785	0.1499	2E-07
1160	-1.572	10	0.0032	0	-1.896	-1.898	0.061	0
1166	-2.939	-2.951	0.002	0	-2.96	-3.144	0.0162	5E-05
1167	-2.939	-2.951	0.002	0	-2.96	-3.144	0.0162	5E-05
1168	-1.959	-2.062	0.0004	0	-2.051	-2.206	0.023	7E-07
1169	-1.745	10	0.0004	0	-2.957	-3.173	0.1013	0.0023
1170	10	10	6E-06	0	-2.874	-2.996	0.0343	0.0074
1177	-2.462	-2.89	0.0444	0.0004	-3.354	-10	0.1175	0.1104
1182	10	10	3E-05	0	-2.407	-2.527	0.0051	0
1183	10	10	0.0041	2E-05	10	10	0.0178	0.0002
1186	10	10	4E-06	0	10	10	0.0002	0
1189	-2.536	10	0.0225	0	-2.604	-2.643	0.0417	6E-06
1190	10	10	0.0018	0	-2.171	-2.136	0.0109	0
1192	-2.028	-2.224	0.017	3E-08	-3.885	-2.902	0.0597	8E-05
1193	10	10	0.0076	6E-08	10	10	0.0579	0.0002
1194	-2.753	-3.221	0.0071	3E-06	-3.217	-3.319	0.0516	0.0049
1196	-2.353	-2.697	0.0085	6E-06	-2.679	-2.71	0.0609	4E-05
1199	-2.512	-2.571	0.018	0	-2.895	-3.226	0.0974	3E-07
1203	10	10	6E-08	0	-3.305	-3.099	0.0022	0
1205	10	10	5E-05	0	-2.416	-2.53	0.0083	1E-05
1209	10	10	0.3159	0.1513	10	10	0.3921	0.1513
1211	-2.029	10	0.0022	0	-2.435	-2.367	0.0034	0
1212	-1.79	-2.073	0.1209	0	-2.606	-2.876	0.346	0.001
1217	10	10	0.0013	2E-05	10	10	0.0563	0.0007
1219	10	-3.315	2E-05	0	-3.363	-3.376	0.0055	5E-05
1220	10	10	0	0	10	10	2E-05	0
1221	-1.99	-1.989	0.0074	3E-08	-2.815	-2.155	0.0369	2E-07
1223	-1.937	-2.383	0.0163	0	-2.532	-10	0.1045	0.1222
1224	-1.937	-2.383	0.0163	0	-2.532	-10	0.1045	0.1222
1226	-10	-1.935	0.1499	0	-10	-10	0.1798	0
1241	10	10	0.0004	0	10	10	0.0037	6E-08
1245	10	10	0.0004	5E-05	10	10	0.0004	0.0001
1246	-2.101	-2.298	0.0167	0	-2.276	-2.668	0.0517	0.0002
1250	-2.272	-2.275	0.0701	0	-2.903	-10	0.1053	0.0767
1251	-2.055	-2.249	0.036	4E-07	-2.304	-2.4	0.0465	0.0004
1254	-2.282	-2.855	0.0078	0	-3.393	-3.551	0.037	0
1255	-2.548	-2.383	0.0001	0	-2.548	-2.383	0.0168	4E-07
1257	-1.997	-2.158	0.0027	0	-2.433	-2.344	0.0843	0
1259	-2.716	-2.942	0.0072	0	-2.83	-3.105	0.0198	3E-06
1262	-2.455	-2.718	0.0127	2E-07	-2.744	-2.792	0.0282	6E-07
1265	-2.178	-2.202	0.0131	0	-2.403	-2.35	0.0386	6E-06
1266	-2.25	-2.538	0.0081	3E-08	-2.6	-2.712	0.0558	6E-06
1273	-2.029	-2.33	0.0659	3E-08	-2.397	-2.675	0.13	6E-05
1275	-1.372	10	0.0009	0	-2.161	-2.457	0.0259	0
1276	-2.629	-2.993	0.051	0.0013	-3.013	-3.502	0.094	0.1696
1277	10	10	0.0025	3E-08	10	10	0.0153	6E-08
1278	-1.888	-1.961	0.0114	0	-2.004	-2.209	0.0547	4E-05
1280	-3.115	-3.022	0.0005	0	-3.136	-3.101	0.0319	2E-06
1281	-1.589	10	0.0071	0	-2.539	-2.815	0.0222	1E-05
1284	-2.119	-2.253	0.0135	0	-2.431	-2.446	0.0549	2E-05
1285	10	-2.187	2E-07	0	-2.353	-2.582	0.0111	4E-06
1287	-1.554	-1.692	0.0046	0	-1.764	-2.113	0.0902	0
1288	-1.554	-1.692	0.0046	0	-1.764	-2.113	0.0902	0
1291	-2.177	-2.259	0.0018	0	-2.479	-2.473	0.0324	6E-05
1293	-1.814	-1.797	0.0104	0	-2.158	-2.276	0.0545	0

1298	-2.605	-2.494	0.0002	0	-2.744	-2.614	0.0247	3E-08
1301	-1.9	-1.987	0.022	0	-2.071	-2.216	0.0656	6E-07
1303	-2.66	-2.589	0.0002	3E-08	-2.715	-2.711	0.0318	0.0001
1304	10	-2.27	2E-06	0	-2.48	-2.368	0.0017	0
1305	-2.464	-2.533	0.0004	0	-2.568	-2.608	0.0354	3E-06
1306	-2.58	-2.706	0.0234	0.0002	-2.622	-2.706	0.1327	0.0002
1309	-1.748	10	0.004	0	-2.231	-2.323	0.0297	0
1310	-2.811	-2.979	0.0494	8E-05	-2.834	-2.979	0.2331	0.1054
1311	10	-2.679	9E-08	0	-2.141	-2.964	0.3273	0.0211
1312	-2.192	-2.448	0.1296	1E-05	-2.342	-2.646	0.3344	0.0068
1313	10	10	3E-06	0	-2.556	-2.677	0.0107	0
1316	-1.467	10	0.0239	0	-1.807	-1.862	0.1771	0
1318	-2.466	-2.55	0.0569	6E-07	-2.577	-2.705	0.2279	0.008
1320	-2.471	-2.653	0.0016	0	-2.788	-2.871	0.036	0.0003
1322	-2.791	-2.75	0.0047	8E-06	-2.813	-2.75	0.0268	8E-06
1323	-2.126	10	0.0009	0	-2.419	-2.401	0.1737	3E-08
1327	-2.01	-1.905	0.0672	0	-2.257	-10	0.0914	5E-06
1329	-2.126	-2.242	0.005	0	-2.35	-2.371	0.0351	0
1331	-2	-2.402	0.0038	0	-2.705	-2.939	0.0569	1E-05
1332	-1.992	-2.108	0.0064	0	-2.282	-2.414	0.0291	3E-07
1333	-1.868	-1.793	0.0622	0	-1.868	-1.963	0.0622	3E-08
1334	-2.194	-2.127	0.0126	0	-2.474	-2.458	0.0273	0
1337	-2.838	-4.763	0.0587	0.0044	-3.085	-10	0.1221	0.069
1338	-2.149	-2.257	0.0034	0	-2.327	-2.408	0.0195	4E-06
1340	-1.911	-2.208	0.018	0	-2.162	-3.007	0.249	0.0003
1341	10	-2.185	0.0002	0	-1.938	-2.885	0.2734	0.0003
1342	10	10	3E-08	0	-3.035	-3.049	0.0639	0.0018
1343	-1.884	-1.995	0.0005	0	-2.277	-2.271	0.0571	1E-07
1344	-1.774	10	0.0114	0	-2.37	-2.356	0.0114	0
1345	-2.011	-2.054	0.0099	0	-2.219	-2.195	0.0594	0
1346	-2.128	-2.322	0.1122	3E-05	-3.305	-2.488	0.2502	9E-05
1347	-1.376	10	0.0892	0	-1.774	-2.012	0.1953	0
1348	-2.124	-2.656	0.0456	7E-07	-2.55	-3.003	0.0987	0.0002
1349	-2.371	-2.686	0.0312	0.0001	-3.033	-3.131	0.0675	0.0008
1415	-3.043	-3.246	0.0491	0.0001	-3.753	-3.575	0.3256	0.0004
1425	-2.965	-2.858	0.0018	0	-3.016	-2.908	0.111	2E-05
1432	-3.192	-3.113	0.0162	7E-06	-3.253	-3.13	0.0328	5E-05
1435	-1.974	-2.089	0.0144	0	-2.373	-2.371	0.0348	4E-07
1436	-2.086	-2.468	0.0719	0	-2.689	-10	0.0729	0.0403
1443	-2.923	-3.272	0.0016	3E-05	-10	-10	0.1705	0.0032
1447	-2.275	-2.59	0.0011	0	-2.466	-3.019	0.0448	0.0007
1451	10	-1.977	9E-06	0	-10	-2.452	0.1523	1E-06
1452	-2.401	-2.568	0.007	0	-3.079	-2.922	0.147	2E-06
1455	-2.247	-2.455	0.0692	0.1102	-2.412	-2.455	0.3723	0.1102
1459	10	10	4E-06	7E-07	-3.006	10	0.0141	7E-07
1468	-2.441	-2.929	0.0985	2E-06	-2.515	-3.804	0.2554	0.0532
1471	-3.358	-3.641	0.2656	0.6047	-3.414	-3.789	0.3429	0.6047
1472	-2.387	-3.018	0.1347	0.0214	-2.973	-3.474	0.3619	0.3019
1478	-1.756	10	0.0133	0	-2.367	-1.783	0.3525	0
1486	-2.253	-2.319	0.103	0	-3.924	-3.577	0.2649	0.0001
2083	10	10	0	0	10	10	3E-05	0
2158	-1.802	-1.832	0.0052	0	-1.915	-1.965	0.0736	2E-07
2303	-2.408	-2.953	0.0002	0	-3.719	-3.355	0.1183	0.012
2588	10	10	1E-06	0	10	10	2E-06	1E-07

Model values at landslide points in Ty terrain

	values of model at points				values in 8m radius			
SLIDE.ID	SHAL	SHALV	PISA	PISAS	SHAL	SHALV	PISA	PISAS
494	10.00	10.00	0.0001	0.0000	10.00	10.00	0.0015	0.0001
495	10.00	10.00	0.0000	0.0000	10.00	10.00	0.0001	0.0000
499	10.00	10.00	0.0000	0.0000	10.00	10.00	0.0002	0.0000
500	-2.65	-2.84	0.2825	0.0221	-3.27	-2.97	0.3509	0.4109
502	-1.90	-1.98	0.0207	0.0000	-2.43	-2.61	0.0870	0.0000
504	-2.00	-2.19	0.0526	0.0000	-2.42	-2.51	0.0598	0.0000
508	10.00	10.00	0.0002	0.0000	10.00	10.00	0.0002	0.0000
509	-1.98	10.00	0.0442	0.0000	-2.42	-2.56	0.0528	0.0026
512	-3.20	-10.00	0.1763	0.0000	-10.00	-10.00	0.2257	0.1981
520	-3.23	-2.92	0.0544	0.0000	-3.39	-3.40	0.0777	0.0000
522	10.00	-2.25	0.0001	0.0000	-2.18	-2.27	0.3030	0.0516
534	-2.13	-1.99	0.1039	0.0000	-2.36	-2.34	0.1039	0.0002
536	-2.30	10.00	0.0065	0.0000	-2.59	-2.28	0.0120	0.0000
549	10.00	10.00	0.0000	0.0000	10.00	10.00	0.0000	0.0000
556	-10.00	-10.00	0.1784	0.0000	-10.00	-10.00	0.1921	0.0041
570	10.00	10.00	0.0006	0.0000	-2.18	-2.15	0.0083	0.0000
571	-1.78	-1.85	0.0310	0.0000	-2.07	-2.07	0.1104	0.0000
577	10.00	10.00	0.0000	0.0000	-2.79	-2.31	0.0140	0.0000
580	10.00	10.00	0.0001	0.0000	-2.54	-2.25	0.1808	0.0000
581	10.00	10.00	0.0000	0.0000	-1.91	10.00	0.0014	0.0000
582	10.00	10.00	0.0000	0.0000	-1.91	10.00	0.0014	0.0000
583	-2.12	-2.81	0.0619	0.0000	-3.13	-3.05	0.1010	0.0000
587	-1.72	10.00	0.0368	0.0000	-10.00	-2.08	0.1935	0.0000
588	-1.72	10.00	0.0368	0.0000	-10.00	-2.08	0.1935	0.0000
589	-10.00	-10.00	0.1746	0.0000	-10.00	-10.00	0.1746	0.0000
594	-2.69	-10.00	0.0887	0.0008	-10.00	-10.00	0.1839	0.0826
595	10.00	-2.70	0.0004	0.0000	-2.82	-2.90	0.0405	0.0047
596	10.00	10.00	0.0007	0.0000	-2.65	-2.67	0.0953	0.0000
604	10.00	10.00	0.0000	0.0000	-1.92	-2.15	0.0077	0.0000
606	-2.65	-2.59	0.0874	0.0000	-3.36	-10.00	0.1430	0.0001
611	10.00	10.00	0.0009	0.0000	-1.59	-2.67	0.0139	0.0000
613	-10.00	-10.00	0.4815	0.0064	-10.00	-10.00	0.5175	0.1309
627	10.00	10.00	0.0000	0.0000	10.00	10.00	0.0033	0.0001
628	10.00	10.00	0.0000	0.0000	10.00	10.00	0.0033	0.0001
637	-2.58	-2.68	0.0663	0.0000	-2.77	-2.98	0.0996	0.0091
638	-2.58	-2.68	0.0663	0.0000	-2.77	-2.98	0.0996	0.0091
651	-10.00	-10.00	0.2127	0.0000	-10.00	-10.00	0.2127	0.0306
652	-2.92	-2.99	0.1578	0.0009	-10.00	-3.73	0.1818	0.2623
660	-3.02	-3.53	0.0254	0.0002	-3.78	-3.98	0.1207	0.0304
661	-3.02	-3.53	0.0254	0.0002	-3.78	-3.98	0.1207	0.0304
669	-2.71	-10.00	0.1192	0.0090	-4.17	-10.00	0.1690	0.0090
670	-1.10	10.00	0.0001	0.0000	-10.00	10.00	0.2168	0.0000
684	10.00	10.00	0.0000	0.0000	-1.96	10.00	0.0069	0.0000
693	-2.06	10.00	0.0152	0.0000	-2.16	-2.18	0.0223	0.0000
698	10.00	10.00	0.0004	0.0000	-2.99	-2.80	0.1575	0.0001
701	-2.89	-3.26	0.1563	0.0000	-3.00	-10.00	0.1576	0.0829
703	-3.20	-2.71	0.6823	0.0001	-3.66	-3.48	0.7196	0.4988
705	10.00	10.00	0.0000	0.0000	10.00	10.00	0.0033	0.0000
718	-2.18	10.00	0.0506	0.0000	-2.78	-2.86	0.0773	0.0024
726	-2.48	-2.72	0.0052	0.0000	-3.23	-3.45	0.1573	0.4342
733	-1.65	10.00	0.0491	0.0000	-2.54	-1.93	0.1541	0.0000
734	-2.58	-2.67	0.5627	0.0114	-2.83	-3.74	0.6565	0.2206
748	10.00	10.00	0.0000	0.0000	10.00	10.00	0.0003	0.0000

749	10.00	10.00	0.0000	0.0000	10.00	10.00	0.0003	0.0000
756	-2.62	-2.57	0.1610	0.0000	-10.00	-3.38	0.1843	0.0000
766	-2.52	-2.73	0.0935	0.0000	-2.74	-3.25	0.0935	0.0014
780	-2.60	-2.52	0.0375	0.0000	-2.96	-2.79	0.0526	0.0000
781	-2.60	-2.52	0.0375	0.0000	-2.96	-2.79	0.0526	0.0000
785	-2.26	-2.52	0.0571	0.0000	-2.31	-2.71	0.0844	0.0000
786	10.00	10.00	0.0001	0.0000	-1.73	10.00	0.0265	0.0000
792	10.00	10.00	0.0005	0.0000	-2.33	10.00	0.0042	0.0000
793	-2.73	-10.00	0.1013	0.0006	-10.00	-10.00	0.1948	0.0241
824	-2.55	-3.04	0.0821	0.0000	-3.19	-10.00	0.1549	0.0011
853	-4.01	-3.91	0.0892	0.0000	-4.91	-10.00	0.1832	0.0009
870	-3.31	-10.00	0.3309	0.0277	-3.64	-10.00	0.4158	0.2727
885	-2.78	-2.47	0.0020	0.0000	-3.24	-3.07	0.1100	0.0169
895	-2.65	-2.30	0.0623	0.0000	-10.00	-10.00	0.1943	0.0003
898	-2.43	-2.25	0.0030	0.0000	-3.47	-2.27	0.0544	0.0000
929	-2.50	-2.51	0.0022	0.0000	-2.50	-2.52	0.0197	0.0000
941	10.00	10.00	0.0001	0.0000	-2.36	-2.06	0.1316	0.0000
951	-3.99	10.00	0.0083	0.0000	-4.58	-4.45	0.0400	0.0000
973	-10.00	-10.00	0.2230	0.0004	-10.00	-10.00	0.2252	0.4820
979	-2.08	-2.27	0.0835	0.0000	-10.00	-2.67	0.1771	0.0002
989	10.00	10.00	0.0000	0.0000	10.00	10.00	0.0015	0.0000
992	-2.33	-2.57	0.1021	0.0004	-2.35	-3.06	0.1182	0.0160
993	-2.33	-2.57	0.1021	0.0004	-2.35	-3.06	0.1182	0.0160
994	-2.33	-2.57	0.1021	0.0004	-2.35	-3.06	0.1182	0.0160
1009	-10.00	-10.00	0.1882	0.0010	-10.00	-10.00	0.2205	0.0301
1012	-2.619	-1.981	0.156	0	-10	-10	0.1973	0.0039
1015	-2.764	-2.593	0.1588	0.0082	-2.785	-2.913	0.159	0.0316
1045	-2.307	-2.214	0.1353	0	-10	-2.829	0.1934	0.0081
1063	-2.013	-2.117	0.0143	0	-2.569	-2.598	0.0271	6E-05
1113	-2.283	-2.555	0.1166	0.003	-3.595	-3.199	0.1278	0.0077
1174	10	10	2E-06	0	10	10	0.0005	6E-06
1228	-2.158	-2.204	0.0454	3E-05	-2.278	-3.052	0.0454	3E-05
1239	-1.727	10	0.0041	0	-2.206	-2.284	0.035	4E-05
1470	-2.765	-2.898	0.0171	0.0027	-6.507	-3.083	0.0621	0.0027
1480	10	10	0.0006	0	-2.171	10	0.1031	0

Appendix C

P-test Results at Landslide Initiation Points Based on Random Points

Terrain-based landslide model validation test in Qh-Qmts-Qrt terrain
Based on random points

Performance of landslide models at landslides
(p-tests for slide locations vs random points)

	using values of model at points				using values in 8m radius			
SLIDE.ID	SHAL	SHALV	PISA	PISAS	SHAL	SHALV	PISA	PISAS
872	0.17	0.13	0.1632	0.0862	0.02	0.03	0.0042	0.0108
873	0.17	0.13	0.1632	0.0862	0.02	0.03	0.0042	0.0108
886	1.00	1.00	1.0000	1.0000	1.00	1.00	0.8468	0.8158
906	1.00	1.00	1.0000	1.0000	1.00	1.00	0.9518	1
907	1.00	1.00	0.4562	1.0000	0.44	0.43	0.631	0.6262
908	0.05	0.05	0.2690	0.1384	0.08	0.08	0.1152	0.0618
917	0.09	0.14	0.0370	0.0098	0.10	0.16	0.1422	0.037
918	1.00	0.02	0.6104	1.0000	0.03	0.08	0.1698	0.3904
926	0.04	0.04	0.1508	0.0542	0.09	0.08	0.071	0.0342
934	0.39	1.00	0.3018	1.0000	0.46	0.40	0.0184	0.1604
936	0.24	0.12	0.0336	0.0762	0.06	0.03	0.0066	0.0336
938	0.33	1.00	0.2748	1.0000	0.08	0.09	0.1956	0.0486
942	1.00	0.13	0.5758	1.0000	0.20	0.14	0.2774	0.401
943	0.02	0.01	0.0248	0.0006	0.02	0.03	0.029	0.0034
944	1.00	0.09	0.4902	0.2582	0.24	0.17	0.304	0.092
954	1.00	0.10	0.6230	0.3580	0.36	0.24	0.2254	0.11
957	0.07	0.09	0.0590	0.0526	0.21	0.22	0.0642	0.1226
958	0.04	0.01	0.1388	0.0270	0.02	0.03	0.061	0.0092
959	0.25	0.21	0.1074	0.1142	0.49	0.33	0.0802	0.2386
960	1.00	1.00	0.3016	1.0000	0.59	0.35	0.4636	1
964	0.39	1.00	0.0780	1.0000	0.55	0.47	0.0154	0.3578
970	1.00	1.00	0.3316	0.0730	1.00	1.00	0.6714	0.2838
982	0.02	0.02	0.2554	0.0466	0.07	0.08	0.024	0.0108
983	1.00	1.00	0.8986	1.0000	1.00	1.00	0.6846	0.4026
990	1.00	1.00	0.6616	1.0000	0.41	1.00	0.4418	0.2786
991	0.24	0.17	0.0224	0.0332	0.23	0.22	0.0218	0.0204
997	1.00	1.00	0.6336	1.0000	0.09	1.00	0.7112	0.7954
998	0.04	0.01	0.0194	0.0030	0.14	0.03	0.012	0.0164
1001	1.00	1.00	0.8486	1.0000	0.51	0.41	0.6234	0.7248
1003	1.00	1.00	0.4010	0.1948	0.11	0.11	0.505	0.3924
1011	0.26	0.30	0.1006	0.3818	0.30	0.25	0.1546	0.0756
1014	0.06	0.01	0.0340	0.0206	0.14	0.03	0.0774	0.101
1025	0.11	0.16	0.1020	0.3280	0.23	0.13	0.1742	0.4788
1030	0.00	0.01	0.0110	1.0000	0.02	0.03	0.0304	0.0148
1031	1.00	1.00	0.8244	1.0000	1.00	1.00	0.9776	0.8714
1032	1.00	1.00	0.8244	1.0000	1.00	1.00	0.9776	0.8714
1033	0.09	0.05	0.0952	0.0184	0.22	0.13	0.1654	0.0782
1040	0.14	0.03	0.0982	0.0754	0.02	0.03	0.041	0.076
1044	1.00	1.00	0.5976	1.0000	0.62	0.51	0.4302	0.6336
1048	1.00	1.00	0.7512	1.0000	1.00	1.00	0.9636	1
1050	0.02	0.05	0.3166	0.1156	0.08	0.12	0.2236	0.185
1061	0.30	1.00	0.1874	1.0000	0.42	0.45	0.1156	0.6442
1068	0.18	0.20	0.2946	0.3040	0.33	0.19	0.18	0.0926
1078	1.00	1.00	0.3408	1.0000	0.26	0.22	0.3336	0.3162
1081	0.13	1.00	0.3310	0.3386	0.20	0.23	0.6192	0.6376
1090	0.06	0.12	0.1816	0.2250	0.18	0.18	0.2452	0.1106
1096	1.00	1.00	0.7262	1.0000	1.00	1.00	0.8774	0.8434
1097	1.00	1.00	0.7262	1.0000	1.00	1.00	0.8774	0.8434
1143	0.11	1.00	0.0248	1.0000	0.22	0.21	0.0774	0.223

1173	1.00	1.00	0.5892	1.0000	0.12	0.11	0.3616	0.7016
1179	1.00	1.00	0.8176	1.0000	0.56	1.00	0.2458	1
1200	0.18	0.22	0.2168	0.2440	0.30	0.21	0.2324	0.1198
1210	0.16	0.20	0.1334	0.0278	0.40	0.38	0.2944	0.1356
1215	0.00	0.01	0.0136	0.0094	0.02	0.03	0.0356	0.0278
1222	1.00	1.00	0.6622	1.0000	0.26	1.00	0.5426	0.8714
1225	0.02	0.03	0.0802	0.0060	0.10	0.08	0.0962	0.0318
1229	0.38	1.00	0.1084	1.0000	0.39	0.35	0.172	0.4664
1232	0.34	0.31	0.1616	1.0000	0.53	0.39	0.1528	0.3922
1233	0.29	0.12	0.3086	0.2730	0.10	0.11	0.1638	0.2808
1234	1.00	0.10	0.9378	1.0000	0.24	0.08	0.3938	0.1682
1236	1.00	1.00	0.5264	1.0000	0.46	0.44	0.491	0.4634
1237	1.00	1.00	0.5264	1.0000	0.46	0.44	0.491	0.4634
1238	0.06	1.00	0.1648	1.0000	0.16	0.17	0.325	0.3366
1242	1.00	1.00	0.5474	1.0000	0.40	0.49	0.175	0.699
1243	0.10	0.17	0.3042	0.1456	0.26	0.28	0.4324	0.38
1263	1.00	1.00	0.6432	1.0000	0.62	1.00	0.5692	1
1272	1.00	1.00	0.9378	1.0000	1.00	1.00	0.9944	1
1279	0.13	0.12	0.1088	0.2884	0.15	0.13	0.2272	0.2058
1282	0.06	0.02	0.0676	0.0072	0.20	0.03	0.1278	0.0412
1283	0.23	0.23	0.4196	1.0000	0.29	0.20	0.1266	0.0342
1289	0.24	0.26	0.3054	0.2770	0.45	0.41	0.4058	0.458
1300	1.00	0.19	0.4620	1.0000	0.25	0.23	0.5598	0.5596
1302	1.00	1.00	0.7608	1.0000	0.60	0.40	0.221	0.8714
1330	0.32	0.28	0.0592	0.4524	0.37	0.32	0.0978	0.3242
1335	0.18	0.18	0.2278	0.2666	0.20	0.16	0.128	0.1514
1336	0.02	0.03	0.2712	0.0406	0.10	0.09	0.231	0.0564
1945	1.00	1.00	0.5702	1.0000	1.00	1.00	0.8728	1
2498	0.11	0.08	0.0472	0.1378	0.06	0.03	0.107	0.0222
% < 0.5	58%	55%	67%	50%	76%	78%	76%	71%

Terrain-based landslide model validation test in Qh-Qmts-Qrt Based on random points, where p<0.5 for at least one model

Performance of landslide models at landslides (p-tests for slide locations vs random points)

	using values in 8m radius			
SLIDE.ID	SHAL	SHALV	PISA	PISAS
872	0.02	0.03	0.0042	0.0108
873	0.02	0.03	0.0042	0.0108
907	0.44	0.43	0.6310	0.6262
908	0.08	0.08	0.1152	0.0618
917	0.10	0.16	0.1422	0.0370
918	0.03	0.08	0.1698	0.3904
926	0.09	0.08	0.0710	0.0342
934	0.46	0.40	0.0184	0.1604
936	0.06	0.03	0.0066	0.0336
938	0.08	0.09	0.1956	0.0486
942	0.20	0.14	0.2774	0.4010
943	0.02	0.03	0.0290	0.0034
944	0.24	0.17	0.3040	0.0920
954	0.36	0.24	0.2254	0.1100
957	0.21	0.22	0.0642	0.1226
958	0.02	0.03	0.0610	0.0092
959	0.49	0.33	0.0802	0.2386
960	0.59	0.35	0.4636	1.0000
964	0.55	0.47	0.0154	0.3578
970	1.00	1.00	0.6714	0.2838
982	0.07	0.08	0.0240	0.0108
983	1.00	1.00	0.6846	0.4026
990	0.41	1.00	0.4418	0.2786
991	0.23	0.22	0.0218	0.0204
997	0.09	1.00	0.7112	0.7954
998	0.14	0.03	0.0120	0.0164
1001	0.51	0.41	0.6234	0.7248
1003	0.11	0.11	0.5050	0.3924
1011	0.30	0.25	0.1546	0.0756
1014	0.14	0.03	0.0774	0.1010
1025	0.23	0.13	0.1742	0.4788
1030	0.02	0.03	0.0304	0.0148
1033	0.22	0.13	0.1654	0.0782
1040	0.02	0.03	0.0410	0.0760
1044	0.62	0.51	0.4302	0.6336
1050	0.08	0.12	0.2236	0.1850
1061	0.42	0.45	0.1156	0.6442
1068	0.33	0.19	0.1800	0.0926
1078	0.26	0.22	0.3336	0.3162
1081	0.20	0.23	0.6192	0.6376
1090	0.18	0.18	0.2452	0.1106
1143	0.22	0.21	0.0774	0.2230
1173	0.12	0.11	0.3616	0.7016
1179	0.56	1.00	0.2458	1.0000
1200	0.30	0.21	0.2324	0.1198
1210	0.40	0.38	0.2944	0.1356

1215	0.02	0.03	0.0356	0.0278
1222	0.26	1.00	0.5426	0.8714
1225	0.10	0.08	0.0962	0.0318
1229	0.39	0.35	0.1720	0.4664
1232	0.53	0.39	0.1528	0.3922
1233	0.10	0.11	0.1638	0.2808
1234	0.24	0.08	0.3938	0.1682
1236	0.46	0.44	0.4910	0.4634
1237	0.46	0.44	0.4910	0.4634
1238	0.16	0.17	0.3250	0.3366
1242	0.40	0.49	0.1750	0.6990
1243	0.26	0.28	0.4324	0.3800
1279	0.15	0.13	0.2272	0.2058
1282	0.20	0.03	0.1278	0.0412
1283	0.29	0.20	0.1266	0.0342
1289	0.45	0.41	0.4058	0.4580
1300	0.25	0.23	0.5598	0.5596
1302	0.60	0.40	0.2210	0.8714
1330	0.37	0.32	0.0978	0.3242
1335	0.20	0.16	0.1280	0.1514
1336	0.10	0.09	0.2310	0.0564
2498	0.06	0.03	0.1070	0.0222
68				
% < 0.5	87%	90%	87%	81%

Terrain-based landslide model validation test in Qtw terrain

Based on random points

Performance of landslide models at landslides (p-tests for slide locations vs random points)

	using values of model at points				using values in 8m radius			
SLIDE.ID	SHAL	SHALV	PISA	PISAS	SHAL	SHALV	PISA	PISAS
507	1.00	1.00	0.5980	1.0000	0.60	0.57	0.4624	0.4812
510	1.00	1.00	0.8274	1.0000	1.00	1.00	0.9706	1.0000
511	1.00	1.00	0.5176	1.0000	0.60	1.00	0.7124	1.0000
513	0.01	0.00	0.0152	0.0080	0.02	0.01	0.0448	0.0456
514	1.00	1.00	0.7350	1.0000	0.50	1.00	0.6578	0.3852
516	1.00	1.00	0.8610	1.0000	1.00	1.00	0.8828	0.3360
519	1.00	1.00	0.5318	1.0000	0.65	1.00	0.7258	1.0000
521	0.24	1.00	0.3964	1.0000	0.36	0.40	0.5832	1.0000
525	1.00	1.00	0.5260	1.0000	0.02	0.41	0.0088	0.4812
530	1.00	1.00	1.0000	1.0000	0.48	1.00	0.3470	0.1040
532	0.40	1.00	0.2958	1.0000	0.70	1.00	0.5710	1.0000
538	0.06	0.20	0.2318	1.0000	0.22	0.25	0.2756	0.1130
545	0.04	0.06	0.2470	0.1316	0.15	0.13	0.3684	0.2654
550	0.14	0.19	0.0308	1.0000	0.34	0.21	0.0992	1.0000
554	0.14	0.08	0.2992	1.0000	0.10	0.06	0.3078	0.1182
557	0.15	0.13	0.0188	1.0000	0.11	0.01	0.0706	0.0164
560	0.06	1.00	0.0220	1.0000	0.02	0.01	0.0394	0.0494
563	0.20	0.10	0.1072	0.0430	0.29	0.22	0.0640	0.1078
564	1.00	0.09	0.7884	1.0000	0.06	0.11	0.3408	0.4812
567	0.31	0.31	0.1014	1.0000	0.02	0.01	0.0542	0.2854
586	0.36	0.30	0.4010	1.0000	0.55	0.50	0.0914	0.3694
590	0.27	0.30	0.2918	1.0000	0.49	0.50	0.3928	1.0000
591	0.27	0.30	0.2918	1.0000	0.49	0.50	0.3928	1.0000
592	1.00	1.00	0.8172	1.0000	0.44	0.46	0.3650	0.2574
602	0.14	0.15	0.3488	1.0000	0.30	0.29	0.6190	0.4380
608	1.00	1.00	0.9142	1.0000	1.00	1.00	0.9500	1.0000
614	0.06	0.07	0.2754	1.0000	0.09	0.10	0.4724	0.2680
616	1.00	1.00	0.7370	1.0000	0.54	0.51	0.5954	1.0000
617	0.09	0.05	0.0032	0.0260	0.02	0.04	0.0002	0.0118
619	0.10	0.00	0.0016	0.0004	0.02	0.01	0.0014	0.0068
626	0.01	0.02	0.1766	1.0000	0.03	0.06	0.2240	0.3560
633	1.00	1.00	0.5262	1.0000	1.00	0.24	0.8064	1.0000
635	0.14	0.03	0.0638	1.0000	0.02	0.01	0.0536	0.0046
639	1.00	1.00	0.7652	1.0000	1.00	1.00	0.8646	1.0000
640	0.23	0.35	0.0292	1.0000	0.18	0.01	0.0730	1.0000
642	1.00	0.29	0.5536	1.0000	0.55	0.50	0.6642	1.0000
643	0.42	1.00	0.3466	1.0000	0.64	0.53	0.4204	1.0000
644	1.00	1.00	0.5788	1.0000	0.03	0.23	0.1428	1.0000
647	0.29	0.32	0.3544	1.0000	0.55	0.51	0.4298	1.0000
648	1.00	1.00	0.8172	1.0000	0.50	0.35	0.3826	0.2710
653	0.30	1.00	0.2682	1.0000	0.36	0.36	0.1212	0.0856
654	0.38	0.34	0.3962	1.0000	0.50	0.51	0.3010	0.1478
655	0.23	1.00	0.3664	1.0000	0.43	0.45	0.3830	0.4812
659	1.00	1.00	0.4422	1.0000	0.37	0.48	0.2688	0.4812
668	0.00	0.00	0.0100	1.0000	0.02	0.01	0.0474	0.0366
672	1.00	1.00	0.3890	0.0186	1.00	1.00	0.6500	0.0766
674	1.00	0.06	0.7162	1.0000	0.04	0.10	0.0098	0.0066
675	0.13	0.18	0.3458	1.0000	0.23	0.27	0.3784	0.2714
676	1.00	1.00	0.5832	1.0000	1.00	1.00	0.7702	1.0000
679	1.00	1.00	0.5752	1.0000	0.45	0.47	0.5960	1.0000
680	0.23	0.33	0.0290	1.0000	0.53	0.50	0.1250	0.0894
682	1.00	1.00	0.7408	1.0000	1.00	1.00	0.8708	1.0000

683	1.00	1.00	0.8414	1.0000	1.00	1.00	0.9430	1.0000
686	0.17	0.18	0.4572	1.0000	0.37	0.27	0.6514	0.3134
687	0.17	0.18	0.4572	1.0000	0.37	0.27	0.6514	0.3134
688	0.17	0.18	0.4572	1.0000	0.37	0.27	0.6514	0.3134
689	0.41	1.00	0.4308	1.0000	0.46	0.53	0.1688	1.0000
690	0.06	0.00	0.0188	0.0864	0.02	0.01	0.0412	0.0666
692	0.43	1.00	0.4210	1.0000	0.57	0.45	0.1428	1.0000
694	0.18	0.18	0.3492	1.0000	0.31	0.29	0.4552	0.3500
699	0.37	1.00	0.4750	1.0000	0.55	0.53	0.2642	1.0000
700	0.13	0.13	0.0586	0.0618	0.28	0.07	0.1358	0.0356
706	1.00	1.00	0.5178	0.0478	1.00	1.00	0.8510	0.2394
708	1.00	0.17	0.6222	1.0000	0.37	0.18	0.3422	0.1268
709	0.00	0.00	0.0110	0.0002	0.02	0.01	0.0572	0.0030
710	0.13	0.15	0.0908	0.0466	0.31	0.30	0.3116	0.2336
712	0.09	1.00	0.3496	1.0000	0.12	0.12	0.4662	1.0000
713	0.00	0.00	0.0062	0.0004	0.02	0.01	0.0336	0.0056
714	1.00	1.00	1.0000	1.0000	1.00	1.00	0.9254	1.0000
720	0.05	0.05	0.1086	1.0000	0.13	0.09	0.3414	0.4380
722	0.12	0.15	0.0560	0.0454	0.23	0.27	0.1754	0.0596
723	0.09	0.08	0.0376	0.1316	0.02	0.01	0.0538	0.0944
725	1.00	0.11	0.6804	1.0000	0.19	0.17	0.1384	0.0298
728	1.00	0.24	0.6310	1.0000	0.37	0.45	0.4262	0.3560
729	0.00	0.19	0.0000	1.0000	0.02	0.01	0.0002	0.1942
730	1.00	0.10	1.0000	1.0000	0.29	0.18	0.3362	0.2088
736	0.07	0.15	0.4216	1.0000	0.22	0.24	0.5074	1.0000
738	1.00	1.00	0.5290	1.0000	0.49	0.33	0.7608	1.0000
739	1.00	1.00	0.6066	1.0000	0.14	0.23	0.0998	0.4812
740	0.14	0.17	0.1340	1.0000	0.28	0.19	0.1708	1.0000
741	0.14	0.17	0.1340	1.0000	0.28	0.19	0.1708	1.0000
742	1.00	1.00	0.7346	1.0000	0.57	1.00	0.4048	1.0000
743	0.43	1.00	0.0618	1.0000	0.02	0.11	0.0014	0.1718
744	0.36	1.00	0.2348	1.0000	0.50	1.00	0.5674	1.0000
746	0.05	0.02	0.1174	0.0630	0.05	0.05	0.3628	0.1238
747	0.05	0.02	0.1174	0.0630	0.05	0.05	0.3628	0.1238
750	0.40	1.00	0.0588	1.0000	0.56	0.55	0.1354	1.0000
751	1.00	1.00	0.7976	1.0000	1.00	1.00	0.8224	1.0000
752	1.00	1.00	0.5420	1.0000	0.57	0.50	0.6866	1.0000
753	0.03	0.02	0.0558	1.0000	0.06	0.01	0.1428	0.0210
757	0.27	0.28	0.0634	1.0000	0.02	0.01	0.0454	0.1516
758	0.36	0.35	0.1568	1.0000	0.07	0.60	0.3372	1.0000
759	0.36	0.35	0.1568	1.0000	0.07	0.60	0.3372	1.0000
760	1.00	1.00	0.6664	1.0000	0.57	0.33	0.5622	0.3532
761	0.05	0.08	0.2198	0.0872	0.03	0.03	0.4600	0.2836
762	1.00	1.00	0.5786	1.0000	1.00	1.00	0.8532	1.0000
763	0.28	0.29	0.2652	1.0000	0.29	0.34	0.3596	0.2902
764	0.39	1.00	0.1394	1.0000	0.52	0.59	0.1760	1.0000
765	0.39	1.00	0.1394	1.0000	0.52	0.59	0.1760	1.0000
767	0.10	0.15	0.3538	1.0000	0.20	0.27	0.4334	0.4812
769	0.37	0.32	0.0934	1.0000	0.29	0.57	0.0676	1.0000
770	0.26	1.00	0.4258	1.0000	0.41	0.39	0.2482	1.0000
771	0.28	0.33	0.3042	1.0000	0.52	0.58	0.2156	1.0000
772	0.28	0.33	0.3042	1.0000	0.52	0.58	0.2156	1.0000
773	1.00	1.00	0.5694	1.0000	0.39	0.31	0.1602	0.3078
774	1.00	1.00	0.6406	1.0000	0.42	0.45	0.4108	1.0000
775	0.15	0.20	0.2944	0.0872	0.27	0.27	0.3362	0.2848
776	0.07	1.00	0.5190	1.0000	0.23	0.40	0.5844	1.0000
777	1.00	1.00	0.6060	1.0000	1.00	1.00	0.8256	1.0000
778	1.00	1.00	0.5196	1.0000	0.25	0.17	0.6770	1.0000
779	0.40	1.00	0.4448	1.0000	0.64	0.54	0.6898	1.0000

782	0.22	0.13	0.0412	0.1316	0.02	0.13	0.0556	0.3790
783	0.10	0.08	0.0074	1.0000	0.08	0.10	0.0286	0.0152
784	1.00	1.00	1.0000	1.0000	0.21	1.00	0.6866	1.0000
787	0.11	0.10	0.0188	1.0000	0.07	0.06	0.0370	0.0218
788	1.00	1.00	0.5216	1.0000	0.09	0.07	0.7722	0.2600
789	0.01	0.01	0.0380	0.0002	0.06	0.02	0.0142	0.0048
790	0.30	1.00	0.0472	1.0000	0.15	0.23	0.0082	1.0000
791	0.15	0.24	0.0556	1.0000	0.26	0.22	0.0200	1.0000
794	0.00	0.05	0.0002	0.0110	0.02	0.04	0.0026	0.0016
795	0.15	0.19	0.2914	1.0000	0.31	0.35	0.5806	1.0000
797	1.00	1.00	0.7456	1.0000	1.00	1.00	0.8668	1.0000
798	1.00	1.00	0.7456	1.0000	1.00	1.00	0.8668	1.0000
799	0.30	1.00	0.0390	1.0000	0.42	0.40	0.1076	0.4380
800	0.08	1.00	0.3904	1.0000	0.03	0.02	0.2332	0.2476
802	0.39	1.00	0.3318	1.0000	0.69	1.00	0.4308	1.0000
804	0.28	0.25	0.1468	0.1136	0.42	0.45	0.3270	0.3104
805	0.06	0.13	0.0178	0.0622	0.12	0.10	0.0690	0.0142
806	0.06	0.13	0.0178	0.0622	0.12	0.10	0.0690	0.0142
808	0.10	0.07	0.0056	0.0026	0.10	0.09	0.0150	0.0136
809	0.09	0.10	0.2874	1.0000	0.24	0.24	0.1290	0.3078
810	0.15	0.22	0.0116	1.0000	0.12	0.12	0.0088	0.0168
812	0.18	0.12	0.0268	1.0000	0.23	0.09	0.0862	0.0324
814	0.26	0.34	0.0238	1.0000	0.02	0.41	0.0588	0.4812
817	0.00	0.09	0.0000	1.0000	0.02	0.01	0.0010	0.0086
818	0.10	0.12	0.3770	1.0000	0.18	0.20	0.5822	0.3414
825	0.25	0.21	0.1326	1.0000	0.36	0.01	0.1196	0.0876
826	1.00	0.16	0.5504	1.0000	0.27	0.28	0.4766	0.1352
827	1.00	0.02	0.4850	0.1316	0.08	0.06	0.2810	0.0824
830	0.06	0.06	0.0632	0.0120	0.14	0.09	0.2438	0.0774
831	0.12	0.17	0.4226	0.1316	0.32	0.30	0.3392	0.2634
832	1.00	1.00	0.6544	1.0000	0.37	0.24	0.5314	1.0000
834	0.00	0.00	0.0002	0.0014	0.02	0.01	0.0028	0.0006
835	0.22	0.05	0.1654	1.0000	0.22	0.01	0.0780	0.0120
837	0.14	0.15	0.2846	0.0740	0.37	0.25	0.3950	0.0666
838	1.00	1.00	0.5698	1.0000	0.07	1.00	0.3068	1.0000
840	1.00	0.07	0.6586	1.0000	0.11	0.15	0.7394	0.4380
841	0.16	0.20	0.3466	1.0000	0.38	0.42	0.4588	0.3852
842	0.06	0.00	0.0036	0.0010	0.09	0.01	0.0074	0.0086
844	0.42	1.00	0.1936	1.0000	0.63	0.59	0.1376	1.0000
847	1.00	1.00	0.5808	1.0000	0.37	0.46	0.4630	0.4812
849	0.44	1.00	0.3212	1.0000	0.71	1.00	0.1782	0.1986
850	0.44	1.00	0.3212	1.0000	0.71	1.00	0.1782	0.1986
854	1.00	1.00	0.8098	1.0000	1.00	1.00	0.8830	1.0000
855	0.43	1.00	0.1540	1.0000	0.53	0.59	0.0162	1.0000
856	0.06	0.08	0.2154	0.0892	0.09	0.09	0.0298	0.0068
857	1.00	1.00	0.7140	1.0000	1.00	1.00	0.7986	1.0000
858	1.00	1.00	0.4880	1.0000	1.00	1.00	0.8272	1.0000
859	1.00	1.00	0.4880	1.0000	1.00	1.00	0.8272	1.0000
860	1.00	1.00	0.9142	1.0000	1.00	1.00	0.9290	1.0000
861	1.00	1.00	0.6986	1.0000	0.23	0.09	0.6948	1.0000
862	0.04	0.06	0.1008	1.0000	0.15	0.08	0.0106	1.0000
863	1.00	1.00	0.9142	1.0000	0.70	1.00	0.7082	1.0000
864	0.28	0.30	0.0804	1.0000	0.50	0.51	0.1626	1.0000
865	0.12	1.00	0.2620	1.0000	0.19	0.02	0.3950	0.4172
866	1.00	1.00	0.7008	1.0000	0.69	1.00	0.7998	1.0000
867	0.29	0.24	0.2448	0.0872	0.41	0.44	0.0848	0.3740
868	0.01	1.00	0.0406	1.0000	0.02	0.01	0.0350	0.2088
869	1.00	1.00	0.5600	1.0000	0.10	0.10	0.3062	1.0000
871	0.36	0.33	0.2502	1.0000	0.43	0.51	0.1840	1.0000

874	0.19	0.24	0.0868	1.0000	0.03	0.04	0.0552	0.2338
876	1.00	1.00	0.8414	1.0000	1.00	1.00	0.9652	1.0000
877	0.17	1.00	0.3868	1.0000	0.33	0.25	0.1480	1.0000
878	1.00	0.15	0.4678	1.0000	0.23	0.25	0.4118	1.0000
880	1.00	1.00	0.7758	1.0000	0.61	0.52	0.1108	0.1618
881	1.00	1.00	0.7758	1.0000	0.61	0.52	0.1108	0.1618
884	0.05	1.00	0.1392	1.0000	0.13	0.26	0.2240	0.4812
888	0.31	1.00	0.1712	1.0000	0.28	0.15	0.1456	0.1212
889	0.31	1.00	0.1712	1.0000	0.28	0.15	0.1456	0.1212
890	1.00	1.00	0.7838	1.0000	1.00	0.45	0.8230	1.0000
891	0.24	0.21	0.1036	0.0790	0.39	0.35	0.1192	0.1400
893	1.00	1.00	0.8414	1.0000	0.34	0.33	0.0558	0.1124
896	0.12	0.19	0.0358	0.1136	0.35	0.34	0.1606	0.1890
897	1.00	1.00	0.5904	1.0000	0.68	1.00	0.6128	1.0000
899	0.36	1.00	0.4492	1.0000	0.66	0.36	0.4226	1.0000
900	1.00	1.00	0.7674	1.0000	1.00	0.44	0.7972	1.0000
901	1.00	1.00	0.5562	1.0000	0.69	1.00	0.7682	1.0000
903	0.15	1.00	0.1600	1.0000	0.26	0.30	0.1002	1.0000
911	1.00	0.23	0.4824	1.0000	0.42	0.42	0.2370	0.3438
913	0.32	1.00	0.2446	1.0000	0.57	0.54	0.4314	1.0000
923	0.00	1.00	0.2510	1.0000	0.04	0.15	0.3240	1.0000
924	1.00	1.00	0.6404	1.0000	0.10	0.09	0.6066	0.1414
925	1.00	0.22	0.6426	1.0000	0.32	0.19	0.5098	1.0000
927	0.13	0.09	0.3786	1.0000	0.35	0.17	0.4446	1.0000
928	1.00	1.00	0.7174	1.0000	1.00	1.00	0.8400	1.0000
930	0.07	1.00	0.3864	1.0000	0.19	0.21	0.5528	1.0000
931	1.00	1.00	1.0000	1.0000	0.70	1.00	0.7956	1.0000
932	0.25	0.15	0.2430	1.0000	0.26	0.24	0.4690	0.0766
933	1.00	1.00	1.0000	1.0000	1.00	1.00	0.8374	0.1362
935	1.00	0.03	0.5024	1.0000	0.09	0.09	0.4462	0.3040
937	1.00	1.00	0.9142	1.0000	0.45	1.00	0.6174	1.0000
940	0.25	1.00	0.4970	1.0000	0.51	0.49	0.4016	0.4812
945	1.00	1.00	0.6710	1.0000	0.09	0.09	0.5932	1.0000
946	1.00	1.00	0.6710	1.0000	0.09	0.09	0.5932	1.0000
949	0.09	0.07	0.0850	0.0996	0.05	0.07	0.1236	0.0780
950	0.26	0.32	0.0394	1.0000	0.46	0.36	0.1594	0.1202
955	0.34	0.31	0.3560	1.0000	0.37	0.36	0.5010	0.3038
962	0.25	0.31	0.0756	1.0000	0.48	0.42	0.1496	0.2722
963	0.10	0.05	0.2664	1.0000	0.09	0.04	0.3808	0.3280
968	0.18	0.11	0.4426	0.0948	0.43	0.25	0.1978	0.0524
969	0.29	0.15	0.0116	1.0000	0.09	0.06	0.0212	0.0136
974	0.23	0.27	0.3990	1.0000	0.51	0.51	0.5674	0.4812
976	0.32	1.00	0.1884	1.0000	0.02	0.08	0.0502	0.2920
977	1.00	1.00	0.7726	1.0000	0.72	1.00	0.6432	0.2476
978	1.00	1.00	0.8274	1.0000	1.00	1.00	0.9906	1.0000
980	1.00	1.00	0.6270	1.0000	0.19	0.17	0.1536	0.3602
984	0.04	0.02	0.2196	1.0000	0.05	0.05	0.0830	0.2030
985	0.09	0.09	0.3524	1.0000	0.07	0.07	0.6504	0.3310
986	0.05	0.06	0.1036	0.0496	0.14	0.10	0.1422	0.0500
988	0.38	0.35	0.0248	1.0000	0.34	0.29	0.0070	0.2474
995	0.11	0.19	0.2264	0.0256	0.18	0.24	0.2320	0.1574
996	1.00	1.00	1.0000	1.0000	0.18	0.19	0.2320	0.1574
999	1.00	1.00	1.0000	1.0000	0.60	1.00	0.4174	1.0000
1000	0.36	1.00	0.0914	1.0000	0.06	0.49	0.0542	0.2560
1002	0.07	0.16	0.0716	0.1316	0.19	0.23	0.1846	0.0412
1004	1.00	1.00	0.5162	1.0000	1.00	1.00	0.7808	1.0000
1006	1.00	1.00	0.8414	1.0000	0.46	1.00	0.6886	1.0000
1007	1.00	1.00	0.6426	1.0000	0.63	0.57	0.8622	1.0000
1008	1.00	0.15	0.8172	1.0000	0.15	0.21	0.1240	0.0224

1013	0.39	1.00	0.4436	1.0000	0.25	0.53	0.3390	1.0000
1017	1.00	0.01	0.4904	1.0000	0.04	0.03	0.1592	0.1660
1026	1.00	1.00	0.8098	1.0000	0.04	0.10	0.5384	0.3262
1027	1.00	1.00	0.7976	1.0000	0.19	1.00	0.7278	1.0000
1029	0.20	0.22	0.1126	1.0000	0.13	0.13	0.2636	0.3532
1035	1.00	0.06	0.5382	1.0000	0.22	0.17	0.5718	0.4380
1036	0.15	0.11	0.2912	1.0000	0.19	0.15	0.1782	0.1108
1037	1.00	0.11	0.4960	0.1316	0.20	0.17	0.0810	0.0516
1042	1.00	1.00	0.5762	1.0000	0.45	0.43	0.0978	1.0000
1043	1.00	1.00	0.7674	1.0000	0.29	1.00	0.7460	1.0000
1046	0.04	0.06	0.4186	1.0000	0.07	0.10	0.2150	0.0774
1047	1.00	1.00	0.8274	1.0000	1.00	1.00	0.8262	1.0000
1049	1.00	1.00	0.6224	1.0000	0.60	0.42	0.1796	0.4812
1055	1.00	1.00	0.7884	1.0000	1.00	0.37	0.8296	1.0000
1057	0.03	0.03	0.2064	0.0474	0.11	0.10	0.3752	0.1552
1062	0.02	0.02	0.4428	1.0000	0.07	0.06	0.1030	0.0190
1066	0.31	1.00	0.3852	1.0000	0.52	0.29	0.7470	1.0000
1067	1.00	0.02	0.5370	1.0000	0.06	0.05	0.5924	0.2132
1072	0.08	0.06	0.1774	0.0474	0.20	0.03	0.1290	0.0250
1074	0.25	0.24	0.0880	1.0000	0.14	0.07	0.1188	0.0678
1080	0.15	1.00	0.4406	1.0000	0.06	0.06	0.4782	0.3178
1082	0.40	1.00	0.0944	1.0000	0.08	0.06	0.1626	0.1594
1084	0.24	0.26	0.1832	1.0000	0.39	0.36	0.2556	0.1478
1085	1.00	0.33	0.6346	1.0000	0.52	0.51	0.5278	1.0000
1086	0.30	0.27	0.2356	0.0512	0.59	0.42	0.4104	0.2532
1087	0.39	0.35	0.0430	1.0000	0.60	0.57	0.0808	1.0000
1088	0.02	0.03	0.3828	1.0000	0.08	0.07	0.2494	0.1772
1089	0.19	1.00	0.3434	1.0000	0.32	0.32	0.3058	0.4380
1092	0.06	0.02	0.0446	0.0134	0.21	0.04	0.1376	0.0794
1094	1.00	1.00	0.9142	1.0000	0.69	0.11	0.1978	0.4812
1095	1.00	1.00	0.7114	1.0000	1.00	1.00	0.9242	1.0000
1098	0.06	0.06	0.0442	0.1316	0.07	0.05	0.1834	0.0588
1100	0.44	1.00	0.4364	1.0000	0.02	0.58	0.0406	1.0000
1101	0.44	1.00	0.4364	1.0000	0.02	0.58	0.0406	1.0000
1102	1.00	1.00	1.0000	1.0000	1.00	1.00	0.9932	1.0000
1104	1.00	1.00	0.5130	1.0000	0.18	0.27	0.1968	1.0000
1105	1.00	1.00	0.5130	1.0000	0.18	0.27	0.1968	1.0000
1106	1.00	1.00	0.8054	1.0000	1.00	1.00	0.7912	0.4812
1107	0.04	0.06	0.0588	1.0000	0.12	0.09	0.0940	0.0358
1109	0.03	0.00	0.0290	0.0368	0.02	0.01	0.0460	0.0214
1110	0.21	0.24	0.1180	0.0630	0.44	0.42	0.3218	0.2634
1112	0.36	1.00	0.4800	1.0000	0.03	0.02	0.5500	1.0000
1114	1.00	0.14	0.7190	1.0000	0.21	0.23	0.4928	0.3228
1115	0.36	1.00	0.1518	1.0000	0.15	0.33	0.0836	1.0000
1121	0.21	0.31	0.0958	1.0000	0.42	0.38	0.2716	0.3030
1123	1.00	1.00	0.7332	1.0000	1.00	1.00	0.8042	1.0000
1126	0.21	0.23	0.2362	1.0000	0.23	0.11	0.2152	1.0000
1127	0.25	0.14	0.0922	0.0652	0.26	0.14	0.0744	0.0406
1128	0.25	0.14	0.0922	0.0652	0.26	0.14	0.0744	0.0406
1135	0.10	0.04	0.0356	0.0192	0.27	0.01	0.1052	0.0094
1137	1.00	1.00	0.7468	1.0000	0.60	0.58	0.1930	1.0000
1140	0.00	0.00	0.0110	0.0000	0.02	0.01	0.0342	0.0008
1141	0.00	0.00	0.0096	1.0000	0.02	0.01	0.0360	0.0024
1145	0.06	0.20	0.0444	1.0000	0.10	0.01	0.0788	0.0944
1146	1.00	1.00	0.8610	1.0000	1.00	1.00	0.5428	0.2920
1149	0.36	1.00	0.0638	1.0000	0.47	0.49	0.1660	1.0000
1150	0.36	1.00	0.0638	1.0000	0.47	0.49	0.1660	1.0000
1157	0.10	0.12	0.0268	1.0000	0.05	0.01	0.0836	0.0912
1158	0.04	0.05	0.0050	1.0000	0.13	0.10	0.0238	0.1364

1159	0.26	0.07	0.2014	0.0914	0.24	0.17	0.0538	0.3852
1160	0.40	1.00	0.2746	1.0000	0.60	0.57	0.1836	1.0000
1166	0.03	0.05	0.3122	1.0000	0.13	0.09	0.4118	0.1760
1167	0.03	0.05	0.3122	1.0000	0.13	0.09	0.4118	0.1760
1168	0.26	0.26	0.4422	1.0000	0.52	0.44	0.3522	0.3262
1169	0.35	1.00	0.4428	1.0000	0.13	0.09	0.0988	0.0514
1170	1.00	1.00	0.6668	1.0000	0.15	0.12	0.2856	0.0318
1177	0.09	0.05	0.0628	0.0158	0.07	0.01	0.0790	0.0086
1182	1.00	1.00	0.5892	1.0000	0.32	0.27	0.5726	1.0000
1183	1.00	1.00	0.2516	0.0384	1.00	1.00	0.3950	0.1310
1186	1.00	1.00	0.6940	1.0000	1.00	1.00	0.8136	1.0000
1189	0.08	1.00	0.1144	1.0000	0.23	0.22	0.2528	0.2518
1190	1.00	1.00	0.3212	1.0000	0.44	0.47	0.4698	1.0000
1192	0.23	0.21	0.1366	0.1316	0.04	0.14	0.1860	0.1598
1193	1.00	1.00	0.2020	0.1136	1.00	1.00	0.1908	0.1260
1194	0.05	0.02	0.2068	0.0560	0.09	0.07	0.2132	0.0374
1196	0.12	0.08	0.1914	0.0508	0.20	0.20	0.1838	0.1802
1199	0.08	0.10	0.1318	1.0000	0.14	0.08	0.1034	0.3602
1203	1.00	1.00	0.8610	1.0000	0.07	0.10	0.6666	1.0000
1205	1.00	1.00	0.5548	1.0000	0.31	0.27	0.5088	0.2272
1209	1.00	1.00	0.0014	0.0004	1.00	1.00	0.0066	0.0066
1211	0.23	1.00	0.3036	1.0000	0.30	0.35	0.6146	1.0000
1212	0.33	0.26	0.0152	1.0000	0.23	0.15	0.0082	0.0704
1217	1.00	1.00	0.3472	0.0384	1.00	1.00	0.1964	0.0790
1219	1.00	0.02	0.6166	1.0000	0.07	0.06	0.5612	0.1734
1220	1.00	1.00	1.0000	1.0000	1.00	1.00	0.9078	1.0000
1221	0.25	0.29	0.2040	0.1316	0.16	0.46	0.2718	0.3852
1223	0.27	0.16	0.1396	1.0000	0.26	0.01	0.0932	0.0078
1224	0.27	0.16	0.1396	1.0000	0.26	0.01	0.0932	0.0078
1226	0.00	0.30	0.0106	1.0000	0.02	0.01	0.0390	1.0000
1241	1.00	1.00	0.4430	1.0000	1.00	1.00	0.6090	0.4380
1245	1.00	1.00	0.4422	0.0298	1.00	1.00	0.7860	0.1456
1246	0.20	0.19	0.1372	1.0000	0.39	0.21	0.2130	0.1340
1250	0.14	0.19	0.0356	1.0000	0.14	0.01	0.0922	0.0108
1251	0.22	0.20	0.0772	0.0822	0.37	0.33	0.2320	0.0990
1254	0.14	0.06	0.1992	1.0000	0.07	0.05	0.2716	1.0000
1255	0.08	0.16	0.5012	1.0000	0.26	0.34	0.4048	0.3478
1257	0.25	0.23	0.2898	1.0000	0.30	0.36	0.1304	1.0000
1259	0.05	0.05	0.2062	1.0000	0.16	0.10	0.3760	0.2786
1262	0.09	0.08	0.1606	0.0914	0.18	0.17	0.3190	0.3340
1265	0.17	0.21	0.1590	1.0000	0.32	0.36	0.2660	0.2456
1266	0.15	0.11	0.1964	0.1316	0.23	0.20	0.1978	0.2482
1273	0.23	0.18	0.0394	0.1316	0.32	0.21	0.0672	0.1692
1275	0.43	1.00	0.3786	1.0000	0.45	0.31	0.3340	1.0000
1276	0.06	0.04	0.0550	0.0104	0.12	0.05	0.1094	0.0062
1277	1.00	1.00	0.2934	0.1316	1.00	1.00	0.4222	0.4380
1278	0.29	0.30	0.1694	1.0000	0.55	0.44	0.2034	0.1854
1280	0.02	0.04	0.4156	1.0000	0.10	0.10	0.3000	0.2846
1281	0.40	1.00	0.2074	1.0000	0.26	0.16	0.3594	0.2198
1284	0.19	0.20	0.1554	1.0000	0.31	0.31	0.2022	0.2114
1285	1.00	0.22	0.8098	1.0000	0.34	0.25	0.4680	0.2708
1287	0.40	0.34	0.2446	1.0000	0.65	0.49	0.1178	1.0000

1288	0.40	0.34	0.2446	1.0000	0.65	0.49	0.1178	1.0000
1291	0.17	0.19	0.3208	1.0000	0.28	0.30	0.2976	0.1664
1293	0.32	0.33	0.1798	1.0000	0.45	0.40	0.2050	1.0000
1298	0.06	0.12	0.4754	1.0000	0.18	0.24	0.3392	0.4812
1301	0.29	0.29	0.1164	1.0000	0.50	0.44	0.1722	0.3340
1303	0.06	0.10	0.4736	0.1316	0.19	0.20	0.3004	0.1404
1304	1.00	0.19	0.7198	1.0000	0.28	0.35	0.6896	1.0000
1305	0.09	0.11	0.4394	1.0000	0.25	0.24	0.2810	0.2832
1306	0.07	0.08	0.1110	0.0200	0.22	0.20	0.0650	0.1236
1309	0.34	1.00	0.2548	1.0000	0.41	0.38	0.3112	1.0000
1310	0.04	0.04	0.0566	0.0256	0.15	0.12	0.0240	0.0086
1311	1.00	0.09	0.8414	1.0000	0.46	0.12	0.0094	0.0192
1312	0.16	0.14	0.0136	0.0450	0.35	0.22	0.0088	0.0324
1313	1.00	1.00	0.7024	1.0000	0.25	0.21	0.4732	1.0000
1316	0.42	1.00	0.1102	1.0000	0.63	0.57	0.0398	1.0000
1318	0.09	0.11	0.0486	0.0792	0.24	0.20	0.0254	0.0304
1320	0.09	0.09	0.3318	1.0000	0.17	0.15	0.2774	0.1116
1322	0.04	0.07	0.2436	0.0478	0.16	0.18	0.3286	0.2394
1323	0.19	1.00	0.3714	1.0000	0.31	0.33	0.0412	0.4812
1327	0.24	0.31	0.0384	1.0000	0.40	0.01	0.1136	0.2634
1329	0.19	0.20	0.2380	1.0000	0.34	0.35	0.2824	1.0000
1331	0.24	0.15	0.2614	1.0000	0.19	0.13	0.1944	0.2164
1332	0.25	0.25	0.2158	1.0000	0.38	0.33	0.3140	0.3648
1333	0.30	0.33	0.0428	1.0000	0.61	0.54	0.1798	0.4812
1334	0.16	0.24	0.1612	1.0000	0.29	0.31	0.3262	1.0000
1337	0.04	0.00	0.0458	0.0068	0.10	0.01	0.0736	0.0118
1338	0.18	0.20	0.2684	1.0000	0.36	0.33	0.3794	0.2652
1340	0.28	0.21	0.1324	1.0000	0.45	0.11	0.0210	0.1134
1341	1.00	0.22	0.4968	1.0000	0.57	0.14	0.0152	0.1078
1342	1.00	1.00	0.9142	1.0000	0.11	0.11	0.1766	0.0574
1343	0.29	0.29	0.4138	1.0000	0.39	0.40	0.1940	0.4054
1344	0.34	1.00	0.1694	1.0000	0.33	0.36	0.4652	1.0000
1345	0.24	0.27	0.1828	1.0000	0.42	0.45	0.1868	1.0000
1346	0.19	0.18	0.0176	0.0362	0.07	0.29	0.0208	0.1550
1347	0.43	1.00	0.0260	1.0000	0.65	0.53	0.0322	1.0000
1348	0.19	0.09	0.0606	0.0780	0.25	0.12	0.1020	0.1334
1349	0.11	0.08	0.0866	0.0238	0.11	0.09	0.1676	0.0780
1415	0.03	0.02	0.0572	0.0244	0.04	0.05	0.0096	0.0976
1425	0.03	0.06	0.3212	1.0000	0.12	0.14	0.0848	0.2132
1432	0.02	0.03	0.1406	0.0490	0.08	0.09	0.2948	0.1764
1435	0.25	0.26	0.1494	1.0000	0.33	0.35	0.2840	0.3478
1436	0.21	0.13	0.0338	1.0000	0.20	0.01	0.1532	0.0148
1443	0.03	0.02	0.3326	0.0342	0.02	0.01	0.0434	0.0430
1447	0.14	0.10	0.3630	1.0000	0.29	0.11	0.2406	0.0830
1451	1.00	0.29	0.6502	1.0000	0.02	0.31	0.0524	0.3068
1452	0.10	0.10	0.2078	1.0000	0.11	0.13	0.0550	0.2866
1455	0.15	0.13	0.0360	0.0010	0.31	0.31	0.0070	0.0086
1459	1.00	1.00	0.6894	0.0770	0.12	1.00	0.4334	0.3262
1468	0.09	0.05	0.0212	0.0632	0.27	0.03	0.0200	0.0136
1471	0.01	0.01	0.0026	0.0000	0.07	0.03	0.0082	0.0012
1472	0.11	0.04	0.0128	0.0026	0.12	0.05	0.0078	0.0028
1478	0.34	1.00	0.1578	1.0000	0.33	0.59	0.0082	1.0000
1486	0.15	0.18	0.0196	1.0000	0.03	0.04	0.0168	0.1408
2083	1.00	1.00	1.0000	1.0000	1.00	1.00	0.9040	1.0000
2158	0.32	0.32	0.2352	1.0000	0.59	0.54	0.1516	0.3852
2303	0.10	0.05	0.4940	1.0000	0.05	0.07	0.0782	0.0256
2588	1.00	1.00	0.7296	1.0000	1.00	1.00	0.9662	0.4054
397								
% < 0.5	66%	57%	70%	22%	73%	73%	75%	64%

Terrain-based landslide model validation test in Qtw terrain

Based on random points, where p <0.5 for at least one model

Performance of landslide models at landslides (p-tests for slide locations vs random points)

	using values in 8m radius			
SLIDE.ID	SHAL	SHALV	PISA	PISAS
507	0.60	0.57	0.4624	0.4812
513	0.02	0.01	0.0448	0.0456
514	0.50	1.00	0.6578	0.3852
516	1.00	1.00	0.8828	0.3360
521	0.36	0.40	0.5832	1.0000
525	0.02	0.41	0.0088	0.4812
530	0.48	1.00	0.3470	0.1040
538	0.22	0.25	0.2756	0.1130
545	0.15	0.13	0.3684	0.2654
550	0.34	0.21	0.0992	1.0000
554	0.10	0.06	0.3078	0.1182
557	0.11	0.01	0.0706	0.0164
560	0.02	0.01	0.0394	0.0494
563	0.29	0.22	0.0640	0.1078
564	0.06	0.11	0.3408	0.4812
567	0.02	0.01	0.0542	0.2854
586	0.55	0.50	0.0914	0.3694
590	0.49	0.50	0.3928	1.0000
591	0.49	0.50	0.3928	1.0000
592	0.44	0.46	0.3650	0.2574
602	0.30	0.29	0.6190	0.4380
614	0.09	0.10	0.4724	0.2680
617	0.02	0.04	0.0002	0.0118
619	0.02	0.01	0.0014	0.0068
626	0.03	0.06	0.2240	0.3560
633	1.00	0.24	0.8064	1.0000
635	0.02	0.01	0.0536	0.0046
640	0.18	0.01	0.0730	1.0000
643	0.64	0.53	0.4204	1.0000
644	0.03	0.23	0.1428	1.0000
647	0.55	0.51	0.4298	1.0000
648	0.50	0.35	0.3826	0.2710
653	0.36	0.36	0.1212	0.0856
654	0.50	0.51	0.3010	0.1478
655	0.43	0.45	0.3830	0.4812
659	0.37	0.48	0.2688	0.4812
668	0.02	0.01	0.0474	0.0366
672	1.00	1.00	0.6500	0.0766
674	0.04	0.10	0.0098	0.0066
675	0.23	0.27	0.3784	0.2714
679	0.45	0.47	0.5960	1.0000
680	0.53	0.50	0.1250	0.0894

686	0.37	0.27	0.6514	0.3134
687	0.37	0.27	0.6514	0.3134
688	0.37	0.27	0.6514	0.3134
689	0.46	0.53	0.1688	1.0000
690	0.02	0.01	0.0412	0.0666
692	0.57	0.45	0.1428	1.0000
694	0.31	0.29	0.4552	0.3500
699	0.55	0.53	0.2642	1.0000
700	0.28	0.07	0.1358	0.0356
706	1.00	1.00	0.8510	0.2394
708	0.37	0.18	0.3422	0.1268
709	0.02	0.01	0.0572	0.0030
710	0.31	0.30	0.3116	0.2336
712	0.12	0.12	0.4662	1.0000
713	0.02	0.01	0.0336	0.0056
720	0.13	0.09	0.3414	0.4380
722	0.23	0.27	0.1754	0.0596
723	0.02	0.01	0.0538	0.0944
725	0.19	0.17	0.1384	0.0298
728	0.37	0.45	0.4262	0.3560
729	0.02	0.01	0.0002	0.1942
730	0.29	0.18	0.3362	0.2088
736	0.22	0.24	0.5074	1.0000
738	0.49	0.33	0.7608	1.0000
739	0.14	0.23	0.0998	0.4812
740	0.28	0.19	0.1708	1.0000
741	0.28	0.19	0.1708	1.0000
742	0.57	1.00	0.4048	1.0000
743	0.02	0.11	0.0014	0.1718
744	0.50	1.00	0.5674	1.0000
746	0.05	0.05	0.3628	0.1238
747	0.05	0.05	0.3628	0.1238
750	0.56	0.55	0.1354	1.0000
753	0.06	0.01	0.1428	0.0210
757	0.02	0.01	0.0454	0.1516
758	0.07	0.60	0.3372	1.0000
759	0.07	0.60	0.3372	1.0000
760	0.57	0.33	0.5622	0.3532
761	0.03	0.03	0.4600	0.2836
763	0.29	0.34	0.3596	0.2902
764	0.52	0.59	0.1760	1.0000
765	0.52	0.59	0.1760	1.0000
767	0.20	0.27	0.4334	0.4812
769	0.29	0.57	0.0676	1.0000
770	0.41	0.39	0.2482	1.0000
771	0.52	0.58	0.2156	1.0000
772	0.52	0.58	0.2156	1.0000
773	0.39	0.31	0.1602	0.3078
774	0.42	0.45	0.4108	1.0000
775	0.27	0.27	0.3362	0.2848
776	0.23	0.40	0.5844	1.0000
778	0.25	0.17	0.6770	1.0000
782	0.02	0.13	0.0556	0.3790
783	0.08	0.10	0.0286	0.0152
784	0.21	1.00	0.6866	1.0000
787	0.07	0.06	0.0370	0.0218
788	0.09	0.07	0.7722	0.2600
789	0.06	0.02	0.0142	0.0048

790	0.15	0.23	0.0082	1.0000
791	0.26	0.22	0.0200	1.0000
794	0.02	0.04	0.0026	0.0016
795	0.31	0.35	0.5806	1.0000
799	0.42	0.40	0.1076	0.4380
800	0.03	0.02	0.2332	0.2476
802	0.69	1.00	0.4308	1.0000
804	0.42	0.45	0.3270	0.3104
805	0.12	0.10	0.0690	0.0142
806	0.12	0.10	0.0690	0.0142
808	0.10	0.09	0.0150	0.0136
809	0.24	0.24	0.1290	0.3078
810	0.12	0.12	0.0088	0.0168
812	0.23	0.09	0.0862	0.0324
814	0.02	0.41	0.0588	0.4812
817	0.02	0.01	0.0010	0.0086
818	0.18	0.20	0.5822	0.3414
825	0.36	0.01	0.1196	0.0876
826	0.27	0.28	0.4766	0.1352
827	0.08	0.06	0.2810	0.0824
830	0.14	0.09	0.2438	0.0774
831	0.32	0.30	0.3392	0.2634
832	0.37	0.24	0.5314	1.0000
834	0.02	0.01	0.0028	0.0006
835	0.22	0.01	0.0780	0.0120
837	0.37	0.25	0.3950	0.0666
838	0.07	1.00	0.3068	1.0000
840	0.11	0.15	0.7394	0.4380
841	0.38	0.42	0.4588	0.3852
842	0.09	0.01	0.0074	0.0086
844	0.63	0.59	0.1376	1.0000
847	0.37	0.46	0.4630	0.4812
849	0.71	1.00	0.1782	0.1986
850	0.71	1.00	0.1782	0.1986
855	0.53	0.59	0.0162	1.0000
856	0.09	0.09	0.0298	0.0068
861	0.23	0.09	0.6948	1.0000
862	0.15	0.08	0.0106	1.0000
864	0.50	0.51	0.1626	1.0000
865	0.19	0.02	0.3950	0.4172
867	0.41	0.44	0.0848	0.3740
868	0.02	0.01	0.0350	0.2088
869	0.10	0.10	0.3062	1.0000
871	0.43	0.51	0.1840	1.0000
874	0.03	0.04	0.0552	0.2338
877	0.33	0.25	0.1480	1.0000
878	0.23	0.25	0.4118	1.0000
880	0.61	0.52	0.1108	0.1618
881	0.61	0.52	0.1108	0.1618
884	0.13	0.26	0.2240	0.4812
888	0.28	0.15	0.1456	0.1212
889	0.28	0.15	0.1456	0.1212
890	1.00	0.45	0.8230	1.0000
891	0.39	0.35	0.1192	0.1400
893	0.34	0.33	0.0558	0.1124
896	0.35	0.34	0.1606	0.1890
899	0.66	0.36	0.4226	1.0000
900	1.00	0.44	0.7972	1.0000

903	0.26	0.30	0.1002	1.0000
911	0.42	0.42	0.2370	0.3438
913	0.57	0.54	0.4314	1.0000
923	0.04	0.15	0.3240	1.0000
924	0.10	0.09	0.6066	0.1414
925	0.32	0.19	0.5098	1.0000
927	0.35	0.17	0.4446	1.0000
930	0.19	0.21	0.5528	1.0000
932	0.26	0.24	0.4690	0.0766
933	1.00	1.00	0.8374	0.1362
935	0.09	0.09	0.4462	0.3040
937	0.45	1.00	0.6174	1.0000
940	0.51	0.49	0.4016	0.4812
945	0.09	0.09	0.5932	1.0000
946	0.09	0.09	0.5932	1.0000
949	0.05	0.07	0.1236	0.0780
950	0.46	0.36	0.1594	0.1202
955	0.37	0.36	0.5010	0.3038
962	0.48	0.42	0.1496	0.2722
963	0.09	0.04	0.3808	0.3280
968	0.43	0.25	0.1978	0.0524
969	0.09	0.06	0.0212	0.0136
974	0.51	0.51	0.5674	0.4812
976	0.02	0.08	0.0502	0.2920
977	0.72	1.00	0.6432	0.2476
980	0.19	0.17	0.1536	0.3602
984	0.05	0.05	0.0830	0.2030
985	0.07	0.07	0.6504	0.3310
986	0.14	0.10	0.1422	0.0500
988	0.34	0.29	0.0070	0.2474
995	0.18	0.24	0.2320	0.1574
996	0.18	0.19	0.2320	0.1574
999	0.60	1.00	0.4174	1.0000
1000	0.06	0.49	0.0542	0.2560
1002	0.19	0.23	0.1846	0.0412
1006	0.46	1.00	0.6886	1.0000
1008	0.15	0.21	0.1240	0.0224
1013	0.25	0.53	0.3390	1.0000
1017	0.04	0.03	0.1592	0.1660
1026	0.04	0.10	0.5384	0.3262
1027	0.19	1.00	0.7278	1.0000
1029	0.13	0.13	0.2636	0.3532
1035	0.22	0.17	0.5718	0.4380
1036	0.19	0.15	0.1782	0.1108
1037	0.20	0.17	0.0810	0.0516
1042	0.45	0.43	0.0978	1.0000
1043	0.29	1.00	0.7460	1.0000
1046	0.07	0.10	0.2150	0.0774
1049	0.60	0.42	0.1796	0.4812
1055	1.00	0.37	0.8296	1.0000
1057	0.11	0.10	0.3752	0.1552
1062	0.07	0.06	0.1030	0.0190
1066	0.52	0.29	0.7470	1.0000
1067	0.06	0.05	0.5924	0.2132
1072	0.20	0.03	0.1290	0.0250
1074	0.14	0.07	0.1188	0.0678
1080	0.06	0.06	0.4782	0.3178
1082	0.08	0.06	0.1626	0.1594

1084	0.39	0.36	0.2556	0.1478
1086	0.59	0.42	0.4104	0.2532
1087	0.60	0.57	0.0808	1.0000
1088	0.08	0.07	0.2494	0.1772
1089	0.32	0.32	0.3058	0.4380
1092	0.21	0.04	0.1376	0.0794
1094	0.69	0.11	0.1978	0.4812
1098	0.07	0.05	0.1834	0.0588
1100	0.02	0.58	0.0406	1.0000
1101	0.02	0.58	0.0406	1.0000
1104	0.18	0.27	0.1968	1.0000
1105	0.18	0.27	0.1968	1.0000
1106	1.00	1.00	0.7912	0.4812
1107	0.12	0.09	0.0940	0.0358
1109	0.02	0.01	0.0460	0.0214
1110	0.44	0.42	0.3218	0.2634
1112	0.03	0.02	0.5500	1.0000
1114	0.21	0.23	0.4928	0.3228
1115	0.15	0.33	0.0836	1.0000
1121	0.42	0.38	0.2716	0.3030
1126	0.23	0.11	0.2152	1.0000
1127	0.26	0.14	0.0744	0.0406
1128	0.26	0.14	0.0744	0.0406
1135	0.27	0.01	0.1052	0.0094
1137	0.60	0.58	0.1930	1.0000
1140	0.02	0.01	0.0342	0.0008
1141	0.02	0.01	0.0360	0.0024
1145	0.10	0.01	0.0788	0.0944
1146	1.00	1.00	0.5428	0.2920
1149	0.47	0.49	0.1660	1.0000
1150	0.47	0.49	0.1660	1.0000
1157	0.05	0.01	0.0836	0.0912
1158	0.13	0.10	0.0238	0.1364
1159	0.24	0.17	0.0538	0.3852
1160	0.60	0.57	0.1836	1.0000
1166	0.13	0.09	0.4118	0.1760
1167	0.13	0.09	0.4118	0.1760
1168	0.52	0.44	0.3522	0.3262
1169	0.13	0.09	0.0988	0.0514
1170	0.15	0.12	0.2856	0.0318
1177	0.07	0.01	0.0790	0.0086
1182	0.32	0.27	0.5726	1.0000
1183	1.00	1.00	0.3950	0.1310
1189	0.23	0.22	0.2528	0.2518
1190	0.44	0.47	0.4698	1.0000
1192	0.04	0.14	0.1860	0.1598
1193	1.00	1.00	0.1908	0.1260
1194	0.09	0.07	0.2132	0.0374
1196	0.20	0.20	0.1838	0.1802
1199	0.14	0.08	0.1034	0.3602
1203	0.07	0.10	0.6666	1.0000
1205	0.31	0.27	0.5088	0.2272
1209	1.00	1.00	0.0066	0.0066
1211	0.30	0.35	0.6146	1.0000
1212	0.23	0.15	0.0082	0.0704
1217	1.00	1.00	0.1964	0.0790
1219	0.07	0.06	0.5612	0.1734
1221	0.16	0.46	0.2718	0.3852

1223	0.26	0.01	0.0932	0.0078
1224	0.26	0.01	0.0932	0.0078
1226	0.02	0.01	0.0390	1.0000
1241	1.00	1.00	0.6090	0.4380
1245	1.00	1.00	0.7860	0.1456
1246	0.39	0.21	0.2130	0.1340
1250	0.14	0.01	0.0922	0.0108
1251	0.37	0.33	0.2320	0.0990
1254	0.07	0.05	0.2716	1.0000
1255	0.26	0.34	0.4048	0.3478
1257	0.30	0.36	0.1304	1.0000
1259	0.16	0.10	0.3760	0.2786
1262	0.18	0.17	0.3190	0.3340
1265	0.32	0.36	0.2660	0.2456
1266	0.23	0.20	0.1978	0.2482
1273	0.32	0.21	0.0672	0.1692
1275	0.45	0.31	0.3340	1.0000
1276	0.12	0.05	0.1094	0.0062
1277	1.00	1.00	0.4222	0.4380
1278	0.55	0.44	0.2034	0.1854
1280	0.10	0.10	0.3000	0.2846
1281	0.26	0.16	0.3594	0.2198
1284	0.31	0.31	0.2022	0.2114
1285	0.34	0.25	0.4680	0.2708
1287	0.65	0.49	0.1178	1.0000
1288	0.65	0.49	0.1178	1.0000
1291	0.28	0.30	0.2976	0.1664
1293	0.45	0.40	0.2050	1.0000
1298	0.18	0.24	0.3392	0.4812
1301	0.50	0.44	0.1722	0.3340
1303	0.19	0.20	0.3004	0.1404
1304	0.28	0.35	0.6896	1.0000
1305	0.25	0.24	0.2810	0.2832
1306	0.22	0.20	0.0650	0.1236
1309	0.41	0.38	0.3112	1.0000
1310	0.15	0.12	0.0240	0.0086
1311	0.46	0.12	0.0094	0.0192
1312	0.35	0.22	0.0088	0.0324
1313	0.25	0.21	0.4732	1.0000
1316	0.63	0.57	0.0398	1.0000
1318	0.24	0.20	0.0254	0.0304
1320	0.17	0.15	0.2774	0.1116
1322	0.16	0.18	0.3286	0.2394
1323	0.31	0.33	0.0412	0.4812
1327	0.40	0.01	0.1136	0.2634
1329	0.34	0.35	0.2824	1.0000
1331	0.19	0.13	0.1944	0.2164
1332	0.38	0.33	0.3140	0.3648
1333	0.61	0.54	0.1798	0.4812
1334	0.29	0.31	0.3262	1.0000
1337	0.10	0.01	0.0736	0.0118
1338	0.36	0.33	0.3794	0.2652
1340	0.45	0.11	0.0210	0.1134
1341	0.57	0.14	0.0152	0.1078
1342	0.11	0.11	0.1766	0.0574
1343	0.39	0.40	0.1940	0.4054
1344	0.33	0.36	0.4652	1.0000
1345	0.42	0.45	0.1868	1.0000

1346	0.07	0.29	0.0208	0.1550
1347	0.65	0.53	0.0322	1.0000
1348	0.25	0.12	0.1020	0.1334
1349	0.11	0.09	0.1676	0.0780
1415	0.04	0.05	0.0096	0.0976
1425	0.12	0.14	0.0848	0.2132
1432	0.08	0.09	0.2948	0.1764
1435	0.33	0.35	0.2840	0.3478
1436	0.20	0.01	0.1532	0.0148
1443	0.02	0.01	0.0434	0.0430
1447	0.29	0.11	0.2406	0.0830
1451	0.02	0.31	0.0524	0.3068
1452	0.11	0.13	0.0550	0.2866
1455	0.31	0.31	0.0070	0.0086
1459	0.12	1.00	0.4334	0.3262
1468	0.27	0.03	0.0200	0.0136
1471	0.07	0.03	0.0082	0.0012
1472	0.12	0.05	0.0078	0.0028
1478	0.33	0.59	0.0082	1.0000
1486	0.03	0.04	0.0168	0.1408
2158	0.59	0.54	0.1516	0.3852
2303	0.05	0.07	0.0782	0.0256
2588	1.00	1.00	0.9662	0.4054
% < 0.5	82%	82%	84%	72%

Terrain-based landslide model validation test in Ty terrain
Based on random points

Performance of landslide models at landslides (p-tests for slide locations vs random points)

	using values of model at points				using values in 8m radius			
SLIDE.ID	SHAL	SHALV	PISA	PISAS	SHAL	SHALV	PISA	PISAS
494	1.00	1.00	0.5984	1.0000	1.00	1.00	0.7774	0.2750
495	1.00	1.00	0.6746	1.0000	1.00	1.00	0.9168	1.0000
499	1.00	1.00	0.7920	1.0000	1.00	1.00	0.8922	1.0000
500	0.10	0.08	0.0096	0.0076	0.13	0.17	0.0246	0.0064
502	0.32	0.30	0.2146	1.0000	0.38	0.29	0.2580	0.5518
504	0.29	0.25	0.1320	1.0000	0.38	0.34	0.3264	0.4692
508	1.00	1.00	0.5384	1.0000	1.00	1.00	0.8822	1.0000
509	0.30	1.00	0.1500	1.0000	0.38	0.31	0.3506	0.1432
512	0.04	0.01	0.0238	0.0836	0.04	0.04	0.0450	0.0154
520	0.04	0.07	0.1294	1.0000	0.12	0.10	0.2804	0.4758
522	1.00	0.23	0.5716	0.1742	0.50	0.44	0.0318	0.0440
534	0.25	0.30	0.0682	1.0000	0.41	0.42	0.2194	0.2572
536	0.19	1.00	0.3090	1.0000	0.31	0.44	0.5764	1.0000
549	1.00	1.00	0.7048	1.0000	1.00	1.00	0.9476	1.0000
556	0.01	0.01	0.0230	1.0000	0.04	0.04	0.0772	0.1266
570	1.00	1.00	0.4852	1.0000	0.50	0.49	0.6192	0.5352
571	0.35	0.32	0.1800	1.0000	0.55	0.51	0.2056	1.0000
577	1.00	1.00	0.7768	1.0000	0.24	0.43	0.5546	0.4172
580	1.00	1.00	0.5850	1.0000	0.33	0.45	0.0910	0.5080
581	1.00	1.00	0.9264	1.0000	0.61	1.00	0.7844	1.0000
582	1.00	1.00	0.9264	1.0000	0.61	1.00	0.7844	1.0000
583	0.25	0.09	0.1158	0.2424	0.15	0.15	0.2254	0.6066
587	0.37	1.00	0.1634	1.0000	0.04	0.51	0.0762	0.6394
588	0.37	1.00	0.1634	1.0000	0.04	0.51	0.0762	0.6394
589	0.01	0.01	0.0246	1.0000	0.04	0.04	0.0976	0.4482
594	0.10	0.01	0.0822	0.0356	0.04	0.04	0.0872	0.0326
595	1.00	0.11	0.5108	0.2152	0.23	0.19	0.4014	0.1228
596	1.00	1.00	0.4734	1.0000	0.28	0.27	0.2394	0.3470
604	1.00	1.00	0.7276	1.0000	0.61	0.49	0.6266	0.4238
606	0.10	0.14	0.0828	1.0000	0.12	0.04	0.1474	0.2860
611	1.00	1.00	0.4556	1.0000	0.69	0.27	0.5564	0.5480
613	0.01	0.01	0.0022	0.0142	0.04	0.04	0.0070	0.0234
627	1.00	1.00	1.0000	1.0000	1.00	1.00	0.7134	0.3022
628	1.00	1.00	1.0000	1.0000	1.00	1.00	0.7134	0.3022
637	0.12	0.12	0.1100	0.2152	0.24	0.17	0.2288	0.0980
638	0.12	0.12	0.1100	0.2152	0.24	0.17	0.2288	0.0980
651	0.01	0.01	0.0156	0.1454	0.04	0.04	0.0596	0.0602
652	0.06	0.06	0.0324	0.0324	0.04	0.07	0.0898	0.0118
660	0.05	0.03	0.1962	0.0522	0.08	0.06	0.1858	0.0602
661	0.05	0.03	0.1962	0.0522	0.08	0.06	0.1858	0.0602
669	0.09	0.01	0.0544	0.0118	0.06	0.04	0.1042	0.0982
670	0.42	1.00	0.5898	1.0000	0.04	1.00	0.0558	1.0000
684	1.00	1.00	0.7802	1.0000	0.60	1.00	0.6412	1.0000
693	0.27	1.00	0.2398	0.2424	0.51	0.48	0.4952	0.6394
698	1.00	1.00	0.5070	1.0000	0.18	0.22	0.1208	0.2996
701	0.07	0.04	0.0336	0.1318	0.18	0.04	0.1208	0.0326
703	0.04	0.11	0.0002	0.0614	0.09	0.09	0.0002	0.0050
705	1.00	1.00	0.8276	1.0000	1.00	1.00	0.7136	1.0000
718	0.23	1.00	0.1364	1.0000	0.24	0.20	0.2814	0.1456

726	0.14	0.11	0.3256	0.1078	0.14	0.10	0.1212	0.0060
733	0.38	1.00	0.1396	1.0000	0.33	0.55	0.1268	1.0000
734	0.12	0.12	0.0010	0.0096	0.22	0.07	0.0010	0.0144
748	1.00	1.00	0.7812	1.0000	1.00	1.00	0.8740	1.0000
749	1.00	1.00	0.7812	1.0000	1.00	1.00	0.8740	1.0000
756	0.11	0.14	0.0310	1.0000	0.04	0.10	0.0872	0.3914
766	0.13	0.11	0.0760	0.1690	0.25	0.12	0.2430	0.1646
780	0.11	0.15	0.1620	1.0000	0.19	0.22	0.3512	0.3870
781	0.11	0.15	0.1620	1.0000	0.19	0.22	0.3512	0.3870
785	0.21	0.16	0.1230	0.1014	0.43	0.25	0.2636	0.3656
786	1.00	1.00	0.6236	1.0000	0.66	1.00	0.4694	0.5576
792	1.00	1.00	0.4926	0.2040	0.42	1.00	0.6914	0.5678
793	0.09	0.01	0.0702	0.0374	0.04	0.04	0.0754	0.0682
824	0.12	0.05	0.0868	0.1032	0.14	0.04	0.1250	0.1746
853	0.02	0.02	0.0816	1.0000	0.04	0.04	0.0886	0.1844
870	0.03	0.01	0.0070	0.0072	0.09	0.04	0.0174	0.0118
885	0.08	0.17	0.3986	1.0000	0.13	0.15	0.2076	0.0806
895	0.10	0.22	0.1152	1.0000	0.04	0.04	0.0756	0.2384
898	0.15	0.23	0.3712	1.0000	0.11	0.44	0.3466	1.0000
929	0.14	0.16	0.3930	0.1256	0.35	0.33	0.5100	0.3824
941	1.00	1.00	0.5918	1.0000	0.41	0.52	0.1668	1.0000
951	0.02	1.00	0.2876	1.0000	0.05	0.05	0.4036	0.5480
973	0.01	0.01	0.0140	0.0428	0.04	0.04	0.0472	0.0052
979	0.26	0.23	0.0864	1.0000	0.04	0.27	0.0944	0.2678
989	1.00	1.00	0.6640	1.0000	1.00	1.00	0.7792	1.0000
992	0.18	0.14	0.0690	0.0426	0.41	0.15	0.1908	0.0838
993	0.18	0.14	0.0690	0.0426	0.41	0.15	0.1908	0.0838
994	0.18	0.14	0.0690	0.0426	0.41	0.15	0.1908	0.0838
1009	0.01	0.01	0.0212	0.0324	0.04	0.04	0.0524	0.0608
1012	0.11	0.30	0.0336	1.0000	0.04	0.04	0.0730	0.1284
1015	0.08	0.13	0.0318	0.0120	0.24	0.19	0.1186	0.0592
1045	0.19	0.25	0.0450	1.0000	0.04	0.21	0.0762	0.1032
1063	0.28	0.27	0.2444	1.0000	0.32	0.30	0.4648	0.3184
1113	0.20	0.14	0.0566	0.0214	0.09	0.12	0.1738	0.1050
1174	1.00	1.00	0.7894	1.0000	1.00	1.00	0.8466	0.4266
1228	0.24	0.25	0.1478	0.0828	0.45	0.15	0.3816	0.3552
1239	0.37	1.00	0.3452	1.0000	0.48	0.44	0.4254	0.3508
1470	0.08	0.07	0.2314	0.0218	0.04	0.14	0.3204	0.1408
1480	1.00	1.00	0.4826	1.0000	0.50	1.00	0.2218	1.0000
% < 0.5	68%	59%	73%	40%	76%	73%	75%	67%

Terrain-based landslide model validation test in Ty terrain

Based on random points, where p<0.5 for at least one model

Performance of landslide models at landslides (p-tests for slide locations vs random points)

	using values in 8m radius			
SLIDE.ID	SHAL	SHALV	PISA	PISAS
494	1.00	1.00	0.7774	0.2750
500	0.13	0.17	0.0246	0.0064
502	0.38	0.29	0.2580	0.5518
504	0.38	0.34	0.3264	0.4692
509	0.38	0.31	0.3506	0.1432
512	0.04	0.04	0.0450	0.0154
520	0.12	0.10	0.2804	0.4758
522	0.50	0.44	0.0318	0.0440
534	0.41	0.42	0.2194	0.2572
536	0.31	0.44	0.5764	1.0000
556	0.04	0.04	0.0772	0.1266
570	0.50	0.49	0.6192	0.5352
571	0.55	0.51	0.2056	1.0000
577	0.24	0.43	0.5546	0.4172
580	0.33	0.45	0.0910	0.5080
583	0.15	0.15	0.2254	0.6066
587	0.04	0.51	0.0762	0.6394
588	0.04	0.51	0.0762	0.6394
589	0.04	0.04	0.0976	0.4482
594	0.04	0.04	0.0872	0.0326
595	0.23	0.19	0.4014	0.1228
596	0.28	0.27	0.2394	0.3470
604	0.61	0.49	0.6266	0.4238
606	0.12	0.04	0.1474	0.2860
611	0.69	0.27	0.5564	0.5480
613	0.04	0.04	0.0070	0.0234
627	1.00	1.00	0.7134	0.3022
628	1.00	1.00	0.7134	0.3022
637	0.24	0.17	0.2288	0.0980
638	0.24	0.17	0.2288	0.0980
651	0.04	0.04	0.0596	0.0602
652	0.04	0.07	0.0898	0.0118
660	0.08	0.06	0.1858	0.0602
661	0.08	0.06	0.1858	0.0602
669	0.06	0.04	0.1042	0.0982
670	0.04	1.00	0.0558	1.0000
693	0.51	0.48	0.4952	0.6394
698	0.18	0.22	0.1208	0.2996
701	0.18	0.04	0.1208	0.0326
703	0.09	0.09	0.0002	0.0050
718	0.24	0.20	0.2814	0.1456
726	0.14	0.10	0.1212	0.0060
733	0.33	0.55	0.1268	1.0000
734	0.22	0.07	0.0010	0.0144
756	0.04	0.10	0.0872	0.3914

766	0.25	0.12	0.2430	0.1646
780	0.19	0.22	0.3512	0.3870
781	0.19	0.22	0.3512	0.3870
785	0.43	0.25	0.2636	0.3656
786	0.66	1.00	0.4694	0.5576
792	0.42	1.00	0.6914	0.5678
793	0.04	0.04	0.0754	0.0682
824	0.14	0.04	0.1250	0.1746
853	0.04	0.04	0.0886	0.1844
870	0.09	0.04	0.0174	0.0118
885	0.13	0.15	0.2076	0.0806
895	0.04	0.04	0.0756	0.2384
898	0.11	0.44	0.3466	1.0000
929	0.35	0.33	0.5100	0.3824
941	0.41	0.52	0.1668	1.0000
951	0.05	0.05	0.4036	0.5480
973	0.04	0.04	0.0472	0.0052
979	0.04	0.27	0.0944	0.2678
992	0.41	0.15	0.1908	0.0838
993	0.41	0.15	0.1908	0.0838
994	0.41	0.15	0.1908	0.0838
1009	0.04	0.04	0.0524	0.0608
1012	0.04	0.04	0.0730	0.1284
1015	0.24	0.19	0.1186	0.0592
1045	0.04	0.21	0.0762	0.1032
1063	0.32	0.30	0.4648	0.3184
1113	0.09	0.12	0.1738	0.1050
1174	1.00	1.00	0.8466	0.4266
1228	0.45	0.15	0.3816	0.3552
1239	0.48	0.44	0.4254	0.3508
1470	0.04	0.14	0.3204	0.1408
1480	0.50	1.00	0.2218	1.0000
% < 0.5	87%	83%	86%	77%

Appendix D

P-test Results at Landslide Initiation Points Based on Points Randomly Sampled from a Probability Distribution of Unstable Slopes

Terrain-based landslide model validation test in Qh-Qmts-Qrt terrain

Based on points randomly sampled from a probability distribution of potentially unstable slopes defined by hillslope gradient at landslide points

Performance of landslide models at landslides (p-tests for slide locations vs random points)

	using values of model at points				using values in 8m radius			
SLIDE.ID	SHAL	SHALV	PISA	PISAS	SHAL	SHALV	PISA	PISAS
872	0.19	0.13	0.1494	0.0840	0.02	0.02	0.0042	0.0082
873	0.19	0.13	0.1494	0.0840	0.02	0.02	0.0042	0.0082
886	1.00	1.00	1.0000	1.0000	1.00	1.00	0.8896	0.8362
906	1.00	1.00	1.0000	1.0000	1.00	1.00	0.9676	1
907	1.00	1.00	0.5428	1.0000	0.50	0.51	0.709	0.659
908	0.06	0.05	0.2838	0.1456	0.09	0.09	0.1074	0.0556
917	0.10	0.15	0.0176	0.0068	0.11	0.18	0.14	0.0328
918	1.00	0.02	0.7110	1.0000	0.03	0.09	0.175	0.4006
926	0.05	0.03	0.1334	0.0522	0.10	0.09	0.0664	0.03
934	0.46	1.00	0.3368	1.0000	0.51	0.47	0.016	0.157
936	0.27	0.12	0.0152	0.0746	0.06	0.02	0.0072	0.028
938	0.38	1.00	0.2926	1.0000	0.08	0.09	0.2054	0.044
942	1.00	0.13	0.6770	1.0000	0.23	0.15	0.3022	0.4132
943	0.02	0.00	0.0098	0.0002	0.02	0.02	0.0296	0.0016
944	1.00	0.09	0.5870	0.2838	0.27	0.18	0.335	0.084
954	1.00	0.11	0.7232	0.3876	0.40	0.27	0.2462	0.11
957	0.08	0.09	0.0352	0.0516	0.24	0.24	0.0608	0.123
958	0.05	0.00	0.1214	0.0218	0.02	0.02	0.0576	0.0074
959	0.28	0.23	0.0890	0.1184	0.55	0.39	0.0734	0.2546
960	1.00	1.00	0.3366	1.0000	0.67	0.40	0.527	1
964	0.46	1.00	0.0544	1.0000	0.63	0.56	0.0148	0.3674
970	1.00	1.00	0.3930	0.0714	1.00	1.00	0.7426	0.2986
982	0.01	0.02	0.2642	0.0418	0.08	0.08	0.0226	0.0082
983	1.00	1.00	0.9444	1.0000	1.00	1.00	0.7584	0.4146
990	1.00	1.00	0.7650	1.0000	0.47	1.00	0.5066	0.294
991	0.27	0.18	0.0094	0.0270	0.26	0.24	0.0202	0.0174
997	1.00	1.00	0.7356	1.0000	0.09	1.00	0.7802	0.818
998	0.04	0.01	0.0084	0.0018	0.15	0.02	0.0118	0.0144
1001	1.00	1.00	0.9134	1.0000	0.58	0.49	0.7026	0.7538
1003	1.00	1.00	0.4798	0.2102	0.12	0.12	0.5774	0.4028
1011	0.30	0.34	0.0812	0.4100	0.34	0.27	0.1546	0.067
1014	0.07	0.00	0.0160	0.0136	0.16	0.02	0.0708	0.097
1025	0.12	0.17	0.0834	0.3580	0.26	0.14	0.181	0.4948
1030	0.00	0.00	0.0062	1.0000	0.02	0.02	0.0302	0.0136
1031	1.00	1.00	0.8982	1.0000	1.00	1.00	0.9866	0.8908
1032	1.00	1.00	0.8982	1.0000	1.00	1.00	0.9866	0.8908
1033	0.10	0.05	0.0730	0.0122	0.25	0.14	0.1702	0.0688
1040	0.15	0.03	0.0792	0.0740	0.02	0.02	0.0386	0.067
1044	1.00	1.00	0.7016	1.0000	0.72	0.61	0.4906	0.6654
1048	1.00	1.00	0.8458	1.0000	1.00	1.00	0.976	1
1050	0.02	0.04	0.3672	0.1194	0.09	0.13	0.243	0.1916
1061	0.34	1.00	0.1768	1.0000	0.48	0.54	0.1082	0.6744
1068	0.20	0.22	0.3246	0.3344	0.37	0.21	0.1874	0.085
1078	1.00	1.00	0.4038	1.0000	0.29	0.24	0.3712	0.3258
1081	0.14	1.00	0.3920	0.3680	0.24	0.25	0.6996	0.6686
1090	0.06	0.12	0.1718	0.2472	0.20	0.20	0.2702	0.1104
1096	1.00	1.00	0.8252	1.0000	1.00	1.00	0.909	0.8624
1097	1.00	1.00	0.8252	1.0000	1.00	1.00	0.909	0.8624

1143	0.11	1.00	0.0098	1.0000	0.25	0.22	0.0716	0.2404
1173	1.00	1.00	0.6916	1.0000	0.14	0.12	0.399	0.7342
1179	1.00	1.00	0.8930	1.0000	0.64	1.00	0.2708	1
1200	0.20	0.24	0.2102	0.2680	0.33	0.23	0.251	0.1206
1210	0.18	0.22	0.1150	0.0222	0.45	0.44	0.3234	0.1336
1215	0.00	0.00	0.0068	0.0062	0.02	0.02	0.0344	0.0228
1222	1.00	1.00	0.7650	1.0000	0.29	1.00	0.6168	0.8908
1225	0.02	0.02	0.0572	0.0042	0.11	0.09	0.09	0.0262
1229	0.44	1.00	0.0900	1.0000	0.44	0.40	0.178	0.484
1232	0.39	0.35	0.1478	1.0000	0.60	0.47	0.153	0.4026
1233	0.33	0.13	0.3550	0.2976	0.11	0.11	0.169	0.296
1234	1.00	0.10	0.9696	1.0000	0.27	0.08	0.447	0.1696
1236	1.00	1.00	0.6272	1.0000	0.52	0.52	0.5606	0.4814
1237	1.00	1.00	0.6272	1.0000	0.52	0.52	0.5606	0.4814
1238	0.07	1.00	0.1522	1.0000	0.17	0.19	0.364	0.3472
1242	1.00	1.00	0.6430	1.0000	0.46	0.58	0.183	0.7302
1243	0.11	0.18	0.3444	0.1518	0.29	0.31	0.4916	0.3896
1263	1.00	1.00	0.7462	1.0000	0.71	1.00	0.648	1
1272	1.00	1.00	0.9696	1.0000	1.00	1.00	0.9982	1
1279	0.14	0.13	0.0900	0.3140	0.16	0.14	0.248	0.2158
1282	0.07	0.02	0.0448	0.0046	0.23	0.02	0.1244	0.0362
1283	0.25	0.25	0.5004	1.0000	0.33	0.22	0.1228	0.03
1289	0.27	0.30	0.3474	0.3044	0.50	0.48	0.4598	0.4766
1300	1.00	0.21	0.5526	1.0000	0.28	0.26	0.6376	0.5838
1302	1.00	1.00	0.8526	1.0000	0.68	0.48	0.2394	0.8908
1330	0.36	0.31	0.0372	0.4834	0.42	0.37	0.0904	0.3332
1335	0.20	0.20	0.2252	0.2942	0.23	0.18	0.1248	0.1476
1336	0.02	0.03	0.2860	0.0352	0.11	0.10	0.2502	0.0498
1945	1.00	1.00	0.6670	1.0000	1.00	1.00	0.9066	1
2498	0.12	0.08	0.0248	0.1450	0.06	0.02	0.0994	0.0182
% < 0.5	58%	55%	62%	50%	68%	71%	71%	71%

Terrain-based landslide model validation test in Qh-Qmts-Qrt terrain
Based on points randomly sampled from a probability distribution of potentially unstable slopes defined by hillslope gradient at landslide points, where p<0.5 for at least one model

Performance of landslide models at landslides (p-tests for slide locations vs slope-based points)

	using values in 8m radius			
SLIDE.ID	SHAL	SHALV	PISA	PISAS
943	0.02	0.02	0.0296	0.0016
958	0.02	0.02	0.0576	0.0074
872	0.02	0.02	0.0042	0.0082
873	0.02	0.02	0.0042	0.0082
1030	0.02	0.02	0.0302	0.0136
1215	0.02	0.02	0.0344	0.0228
1040	0.02	0.02	0.0386	0.067
918	0.03	0.09	0.175	0.4006
936	0.06	0.02	0.0072	0.028
2498	0.06	0.02	0.0994	0.0182
982	0.08	0.08	0.0226	0.0082
938	0.08	0.09	0.2054	0.044
908	0.09	0.09	0.1074	0.0556
1050	0.09	0.13	0.243	0.1916
997	0.09	1.00	0.7802	0.818
926	0.10	0.09	0.0664	0.03
917	0.11	0.18	0.14	0.0328
1336	0.11	0.10	0.2502	0.0498
1225	0.11	0.09	0.09	0.0262
1233	0.11	0.11	0.169	0.296
1003	0.12	0.12	0.5774	0.4028
1173	0.14	0.12	0.399	0.7342
998	0.15	0.02	0.0118	0.0144
1014	0.16	0.02	0.0708	0.097
1279	0.16	0.14	0.248	0.2158
1238	0.17	0.19	0.364	0.3472
1090	0.20	0.20	0.2702	0.1104
942	0.23	0.15	0.3022	0.4132
1282	0.23	0.02	0.1244	0.0362
1335	0.23	0.18	0.1248	0.1476
1081	0.24	0.25	0.6996	0.6686
957	0.24	0.24	0.0608	0.123
1143	0.25	0.22	0.0716	0.2404
1033	0.25	0.14	0.1702	0.0688
991	0.26	0.24	0.0202	0.0174
1025	0.26	0.14	0.181	0.4948
944	0.27	0.18	0.335	0.084
1234	0.27	0.08	0.447	0.1696
1300	0.28	0.26	0.6376	0.5838
1222	0.29	1.00	0.6168	0.8908
1078	0.29	0.24	0.3712	0.3258
1243	0.29	0.31	0.4916	0.3896
1283	0.33	0.22	0.1228	0.03
1200	0.33	0.23	0.251	0.1206
1011	0.34	0.27	0.1546	0.067
1068	0.37	0.21	0.1874	0.085
954	0.40	0.27	0.2462	0.11
1330	0.42	0.37	0.0904	0.3332
1229	0.44	0.40	0.178	0.484

1210	0.45	0.44	0.3234	0.1336
1242	0.46	0.58	0.183	0.7302
990	0.47	1.00	0.5066	0.294
1061	0.48	0.54	0.1082	0.6744
1289	0.50	0.48	0.4598	0.4766
934	0.51	0.47	0.016	0.157
1236	0.52	0.52	0.5606	0.4814
1237	0.52	0.52	0.5606	0.4814
959	0.55	0.39	0.0734	0.2546
1001	0.58	0.49	0.7026	0.7538
1232	0.60	0.47	0.153	0.4026
964	0.63	0.56	0.0148	0.3674
1179	0.64	1.00	0.2708	1
960	0.67	0.40	0.527	1
1302	0.68	0.48	0.2394	0.8908
1044	0.72	0.61	0.4906	0.6654
970	1.00	1.00	0.7426	0.2986
983	1.00	1.00	0.7584	0.4146
% < 0.5	79%	82%	82%	82%

Terrain-based landslide model validation test in Qtw terrain

Based on points randomly sampled from a probability distribution of potentially unstable slopes defined by hillslope gradient at landslide points

Performance of landslide models at landslides (p-tests for slide locations vs random points)

	using values of model at points				using values in 8m radius			
SLIDE.ID	SHAL	SHALV	PISA	PISAS	SHAL	SHALV	PISA	PISAS
507	1.00	1.00	0.7510	1.0000	0.72	0.68	0.5290	0.4944
510	1.00	1.00	0.9250	1.0000	1.00	1.00	0.9928	1.0000
511	1.00	1.00	0.6616	1.0000	0.71	1.00	0.7986	1.0000
513	0.02	0.00	0.0068	0.0078	0.01	0.01	0.0372	0.0456
514	1.00	1.00	0.8638	1.0000	0.59	1.00	0.7466	0.3956
516	1.00	1.00	0.9420	1.0000	1.00	1.00	0.9372	0.3504
519	1.00	1.00	0.6810	1.0000	0.77	1.00	0.8124	1.0000
521	0.31	1.00	0.4972	1.0000	0.42	0.46	0.6666	1.0000
525	1.00	1.00	0.6716	1.0000	0.01	0.48	0.0062	0.4944
530	1.00	1.00	1.0000	1.0000	0.56	1.00	0.3898	0.1008
532	0.52	1.00	0.3552	1.0000	0.82	1.00	0.6522	1.0000
538	0.08	0.24	0.2640	1.0000	0.25	0.29	0.2898	0.1090
545	0.06	0.05	0.2876	0.1198	0.18	0.14	0.4152	0.2634
550	0.18	0.23	0.0178	1.0000	0.40	0.25	0.0876	1.0000
554	0.17	0.08	0.3600	1.0000	0.11	0.07	0.3282	0.1132
557	0.19	0.14	0.0096	1.0000	0.12	0.01	0.0610	0.0166
560	0.08	1.00	0.0114	1.0000	0.01	0.01	0.0316	0.0482
563	0.26	0.11	0.0948	0.0368	0.33	0.26	0.0528	0.1040
564	1.00	0.09	0.9004	1.0000	0.07	0.13	0.3804	0.4944
567	0.39	0.38	0.0898	1.0000	0.01	0.01	0.0436	0.2882
586	0.47	0.37	0.5014	1.0000	0.64	0.59	0.0794	0.3782
590	0.34	0.37	0.3490	1.0000	0.58	0.58	0.4442	1.0000
591	0.34	0.37	0.3490	1.0000	0.58	0.58	0.4442	1.0000
592	1.00	1.00	0.9192	1.0000	0.52	0.54	0.4116	0.2558
602	0.17	0.18	0.4356	1.0000	0.35	0.34	0.7116	0.4476
608	1.00	1.00	0.9670	1.0000	1.00	1.00	0.9806	1.0000
614	0.07	0.07	0.3232	1.0000	0.11	0.11	0.5410	0.2654
616	1.00	1.00	0.8666	1.0000	0.63	0.60	0.6794	1.0000
617	0.11	0.05	0.0010	0.0230	0.01	0.04	0.0002	0.0100
619	0.13	0.00	0.0002	0.0004	0.01	0.01	0.0006	0.0054
626	0.02	0.02	0.1840	1.0000	0.03	0.07	0.2194	0.3670
633	1.00	1.00	0.6718	1.0000	1.00	0.28	0.8896	1.0000
635	0.18	0.03	0.0460	1.0000	0.01	0.01	0.0426	0.0036
639	1.00	1.00	0.8850	1.0000	1.00	1.00	0.9278	1.0000
640	0.30	0.43	0.0152	1.0000	0.21	0.01	0.0632	1.0000
642	1.00	0.35	0.7050	1.0000	0.65	0.59	0.7522	1.0000
643	0.55	1.00	0.4344	1.0000	0.77	0.62	0.4738	1.0000
644	1.00	1.00	0.7320	1.0000	0.03	0.27	0.1286	1.0000
647	0.37	0.40	0.4422	1.0000	0.64	0.60	0.4902	1.0000
648	1.00	1.00	0.9192	1.0000	0.59	0.41	0.4306	0.2698
653	0.38	1.00	0.3148	1.0000	0.42	0.42	0.1138	0.0812
654	0.49	0.42	0.4968	1.0000	0.59	0.60	0.3204	0.1418
655	0.29	1.00	0.4606	1.0000	0.51	0.52	0.4316	0.4944
659	1.00	1.00	0.5652	1.0000	0.43	0.57	0.2824	0.4944
668	0.00	0.00	0.0048	1.0000	0.01	0.01	0.0384	0.0348
672	1.00	1.00	0.4876	0.0154	1.00	1.00	0.7400	0.0722
674	1.00	0.06	0.8470	1.0000	0.05	0.12	0.0080	0.0052
675	0.17	0.20	0.4330	1.0000	0.26	0.32	0.4258	0.2702
676	1.00	1.00	0.7354	1.0000	1.00	1.00	0.8562	1.0000
679	1.00	1.00	0.7284	1.0000	0.54	0.55	0.6808	1.0000
680	0.30	0.41	0.0150	1.0000	0.62	0.59	0.1172	0.0852
682	1.00	1.00	0.8704	1.0000	1.00	1.00	0.9306	1.0000

683	1.00	1.00	0.9330	1.0000	1.00	1.00	0.9762	1.0000
686	0.22	0.21	0.5858	1.0000	0.43	0.32	0.7408	0.3226
687	0.22	0.21	0.5858	1.0000	0.43	0.32	0.7408	0.3226
688	0.22	0.21	0.5858	1.0000	0.43	0.32	0.7408	0.3226
689	0.53	1.00	0.5484	1.0000	0.54	0.62	0.1548	1.0000
690	0.08	0.00	0.0096	0.0798	0.01	0.01	0.0326	0.0652
692	0.55	1.00	0.5358	1.0000	0.68	0.52	0.1286	1.0000
694	0.23	0.21	0.4358	1.0000	0.37	0.34	0.5214	0.3630
699	0.48	1.00	0.6022	1.0000	0.64	0.63	0.2744	1.0000
700	0.16	0.15	0.0416	0.0532	0.32	0.07	0.1214	0.0340
706	1.00	1.00	0.6624	0.0406	1.00	1.00	0.9204	0.2412
708	1.00	0.19	0.7762	1.0000	0.43	0.20	0.3816	0.1224
709	0.00	0.00	0.0056	0.0000	0.01	0.01	0.0464	0.0032
710	0.16	0.17	0.0778	0.0386	0.36	0.35	0.3366	0.2348
712	0.11	1.00	0.4366	1.0000	0.14	0.13	0.5342	1.0000
713	0.00	0.00	0.0032	0.0002	0.01	0.01	0.0274	0.0040
714	1.00	1.00	1.0000	1.0000	1.00	1.00	0.9648	1.0000
720	0.07	0.05	0.0958	1.0000	0.15	0.11	0.3810	0.4476
722	0.15	0.16	0.0400	0.0384	0.26	0.32	0.1612	0.0566
723	0.12	0.08	0.0246	0.1198	0.01	0.01	0.0428	0.0894
725	1.00	0.12	0.8192	1.0000	0.22	0.19	0.1242	0.0266
728	1.00	0.30	0.7832	1.0000	0.43	0.53	0.4818	0.3670
729	0.00	0.23	0.0000	1.0000	0.01	0.01	0.0002	0.1908
730	1.00	0.11	1.0000	1.0000	0.33	0.21	0.3710	0.2042
736	0.09	0.16	0.5364	1.0000	0.26	0.28	0.5858	1.0000
738	1.00	1.00	0.6762	1.0000	0.58	0.39	0.8466	1.0000
739	1.00	1.00	0.7590	1.0000	0.16	0.27	0.0900	0.4944
740	0.18	0.20	0.1284	1.0000	0.32	0.23	0.1574	1.0000
741	0.18	0.20	0.1284	1.0000	0.32	0.23	0.1574	1.0000
742	1.00	1.00	0.8630	1.0000	0.67	1.00	0.4580	1.0000
743	0.56	1.00	0.0442	1.0000	0.01	0.13	0.0006	0.1664
744	0.47	1.00	0.2662	1.0000	0.58	1.00	0.6500	1.0000
746	0.06	0.02	0.1074	0.0560	0.06	0.05	0.4100	0.1178
747	0.06	0.02	0.1074	0.0560	0.06	0.05	0.4100	0.1178
750	0.52	1.00	0.0418	1.0000	0.65	0.66	0.1212	1.0000
751	1.00	1.00	0.9080	1.0000	1.00	1.00	0.9012	1.0000
752	1.00	1.00	0.6916	1.0000	0.68	0.59	0.7748	1.0000
753	0.04	0.02	0.0394	1.0000	0.07	0.01	0.1290	0.0194
757	0.35	0.34	0.0454	1.0000	0.01	0.01	0.0378	0.1436
758	0.47	0.43	0.1596	1.0000	0.08	0.72	0.3734	1.0000
759	0.47	0.43	0.1596	1.0000	0.08	0.72	0.3734	1.0000
760	1.00	1.00	0.8066	1.0000	0.68	0.38	0.6458	0.3646
761	0.07	0.08	0.2502	0.0804	0.02	0.03	0.5252	0.2846
762	1.00	1.00	0.7310	1.0000	1.00	1.00	0.9208	1.0000
763	0.36	0.35	0.3102	1.0000	0.33	0.40	0.4018	0.2928
764	0.50	1.00	0.1370	1.0000	0.61	0.71	0.1614	1.0000
765	0.50	1.00	0.1370	1.0000	0.61	0.71	0.1614	1.0000
767	0.13	0.17	0.4420	1.0000	0.23	0.32	0.4950	0.4944
769	0.48	0.40	0.0830	1.0000	0.33	0.67	0.0562	1.0000
770	0.33	1.00	0.5408	1.0000	0.49	0.46	0.2516	1.0000
771	0.37	0.41	0.3704	1.0000	0.62	0.69	0.2080	1.0000
772	0.37	0.41	0.3704	1.0000	0.62	0.69	0.2080	1.0000
773	1.00	1.00	0.7214	1.0000	0.46	0.36	0.1480	0.3158
774	1.00	1.00	0.7896	1.0000	0.50	0.53	0.4660	1.0000
775	0.19	0.24	0.3522	0.0804	0.30	0.32	0.3718	0.2876
776	0.09	1.00	0.6628	1.0000	0.27	0.47	0.6684	1.0000
777	1.00	1.00	0.7564	1.0000	1.00	1.00	0.9020	1.0000
778	1.00	1.00	0.6630	1.0000	0.28	0.19	0.7612	1.0000
779	0.52	1.00	0.5696	1.0000	0.76	0.64	0.7784	1.0000
782	0.28	0.15	0.0270	0.1198	0.01	0.15	0.0458	0.3884
783	0.12	0.08	0.0036	1.0000	0.09	0.11	0.0228	0.0140

784	1.00	1.00	1.0000	1.0000	0.25	1.00	0.7748	1.0000
787	0.13	0.11	0.0096	1.0000	0.07	0.07	0.0302	0.0202
788	1.00	1.00	0.6656	1.0000	0.09	0.08	0.8588	0.2578
789	0.01	0.00	0.0248	0.0000	0.06	0.02	0.0110	0.0038
790	0.38	1.00	0.0304	1.0000	0.18	0.27	0.0062	1.0000
791	0.19	0.29	0.0388	1.0000	0.29	0.25	0.0156	1.0000
794	0.00	0.05	0.0000	0.0090	0.01	0.04	0.0014	0.0010
795	0.19	0.23	0.3490	1.0000	0.36	0.41	0.6620	1.0000
797	1.00	1.00	0.8742	1.0000	1.00	1.00	0.9296	1.0000
798	1.00	1.00	0.8742	1.0000	1.00	1.00	0.9296	1.0000
799	0.38	1.00	0.0254	1.0000	0.50	0.48	0.0990	0.4476
800	0.09	1.00	0.4894	1.0000	0.03	0.02	0.2342	0.2488
802	0.51	1.00	0.4112	1.0000	0.81	1.00	0.4910	1.0000
804	0.35	0.30	0.1478	0.1020	0.51	0.53	0.3546	0.3172
805	0.08	0.14	0.0090	0.0550	0.14	0.12	0.0596	0.0124
806	0.08	0.14	0.0090	0.0550	0.14	0.12	0.0596	0.0124
808	0.12	0.07	0.0026	0.0022	0.11	0.10	0.0118	0.0118
809	0.11	0.12	0.3430	1.0000	0.27	0.27	0.1180	0.3158
810	0.19	0.27	0.0058	1.0000	0.14	0.14	0.0062	0.0170
812	0.23	0.14	0.0138	1.0000	0.26	0.10	0.0752	0.0302
814	0.34	0.42	0.0124	1.0000	0.01	0.48	0.0468	0.4944
817	0.00	0.09	0.0000	1.0000	0.01	0.01	0.0006	0.0078
818	0.13	0.13	0.4722	1.0000	0.21	0.24	0.6638	0.3550
825	0.32	0.26	0.1266	1.0000	0.42	0.01	0.1112	0.0822
826	1.00	0.18	0.7010	1.0000	0.30	0.33	0.5444	0.1298
827	1.00	0.02	0.6168	0.1198	0.09	0.06	0.2950	0.0792
830	0.08	0.06	0.0452	0.0100	0.16	0.10	0.2444	0.0736
831	0.15	0.20	0.5370	0.1198	0.37	0.35	0.3774	0.2610
832	1.00	1.00	0.7976	1.0000	0.44	0.28	0.6102	1.0000
834	0.00	0.00	0.0000	0.0014	0.01	0.01	0.0018	0.0000
835	0.27	0.04	0.1700	1.0000	0.25	0.01	0.0660	0.0102
837	0.18	0.16	0.3396	0.0660	0.44	0.30	0.4472	0.0654
838	1.00	1.00	0.7216	1.0000	0.08	1.00	0.3272	1.0000
840	1.00	0.07	0.8004	1.0000	0.13	0.17	0.8230	0.4476
841	0.20	0.24	0.4334	1.0000	0.44	0.49	0.5250	0.3956
842	0.07	0.00	0.0014	0.0008	0.09	0.01	0.0052	0.0078
844	0.55	1.00	0.2110	1.0000	0.75	0.70	0.1234	1.0000
847	1.00	1.00	0.7334	1.0000	0.44	0.54	0.5304	0.4944
849	0.57	1.00	0.3964	1.0000	0.83	1.00	0.1646	0.1940
850	0.57	1.00	0.3964	1.0000	0.83	1.00	0.1646	0.1940
854	1.00	1.00	0.9148	1.0000	1.00	1.00	0.9372	1.0000
855	0.56	1.00	0.1566	1.0000	0.62	0.70	0.0140	1.0000
856	0.07	0.07	0.2438	0.0824	0.10	0.10	0.0242	0.0056
857	1.00	1.00	0.8440	1.0000	1.00	1.00	0.8842	1.0000
858	1.00	1.00	0.6220	1.0000	1.00	1.00	0.9036	1.0000
859	1.00	1.00	0.6220	1.0000	1.00	1.00	0.9036	1.0000
860	1.00	1.00	0.9670	1.0000	1.00	1.00	0.9692	1.0000
861	1.00	1.00	0.8312	1.0000	0.26	0.10	0.7820	1.0000
862	0.05	0.06	0.0892	1.0000	0.18	0.08	0.0088	1.0000
863	1.00	1.00	0.9670	1.0000	0.82	1.00	0.7950	1.0000
864	0.35	0.37	0.0636	1.0000	0.58	0.60	0.1498	1.0000
865	0.15	1.00	0.3054	1.0000	0.23	0.02	0.4476	0.4276
866	1.00	1.00	0.8336	1.0000	0.81	1.00	0.8852	1.0000
867	0.37	0.29	0.2834	0.0804	0.49	0.51	0.0746	0.3836
868	0.02	1.00	0.0262	1.0000	0.01	0.01	0.0294	0.2042
869	1.00	1.00	0.7126	1.0000	0.11	0.12	0.3260	1.0000
871	0.47	0.41	0.2926	1.0000	0.51	0.59	0.1702	1.0000
874	0.24	0.29	0.0738	1.0000	0.03	0.04	0.0454	0.2354
876	1.00	1.00	0.9330	1.0000	1.00	1.00	0.9892	1.0000
877	0.21	1.00	0.4846	1.0000	0.39	0.29	0.1346	1.0000
878	1.00	0.18	0.5946	1.0000	0.26	0.29	0.4668	1.0000

880	1.00	1.00	0.8952	1.0000	0.73	0.61	0.1034	0.1568
881	1.00	1.00	0.8952	1.0000	0.73	0.61	0.1034	0.1568
884	0.07	1.00	0.1368	1.0000	0.16	0.31	0.2192	0.4944
888	0.40	1.00	0.1788	1.0000	0.32	0.17	0.1326	0.1150
889	0.40	1.00	0.1788	1.0000	0.32	0.17	0.1326	0.1150
890	1.00	1.00	0.8984	1.0000	1.00	0.53	0.9018	1.0000
891	0.31	0.25	0.0924	0.0704	0.46	0.41	0.1108	0.1354
893	1.00	1.00	0.9330	1.0000	0.40	0.39	0.0460	0.1088
896	0.15	0.23	0.0236	0.1020	0.41	0.39	0.1480	0.1828
897	1.00	1.00	0.7436	1.0000	0.80	1.00	0.7022	1.0000
899	0.46	1.00	0.5748	1.0000	0.78	0.42	0.4784	1.0000
900	1.00	1.00	0.8864	1.0000	1.00	0.51	0.8822	1.0000
901	1.00	1.00	0.7088	1.0000	0.80	1.00	0.8546	1.0000
903	0.20	1.00	0.1636	1.0000	0.30	0.35	0.0904	1.0000
911	1.00	0.28	0.6140	1.0000	0.50	0.49	0.2382	0.3572
913	0.42	1.00	0.2830	1.0000	0.67	0.65	0.4916	1.0000
923	0.00	1.00	0.2936	1.0000	0.03	0.17	0.3496	1.0000
924	1.00	1.00	0.7892	1.0000	0.12	0.10	0.6956	0.1376
925	1.00	0.27	0.7908	1.0000	0.37	0.23	0.5882	1.0000
927	0.16	0.09	0.4732	1.0000	0.41	0.19	0.5078	1.0000
928	1.00	1.00	0.8476	1.0000	1.00	1.00	0.9126	1.0000
930	0.09	1.00	0.4846	1.0000	0.23	0.25	0.6320	1.0000
931	1.00	1.00	1.0000	1.0000	0.82	1.00	0.8820	1.0000
932	0.33	0.17	0.2804	1.0000	0.29	0.27	0.5392	0.0720
933	1.00	1.00	1.0000	1.0000	1.00	1.00	0.9114	0.1304
935	1.00	0.03	0.6448	1.0000	0.11	0.10	0.5094	0.3100
937	1.00	1.00	0.9670	1.0000	0.53	1.00	0.7100	1.0000
940	0.32	1.00	0.6378	1.0000	0.60	0.57	0.4538	0.4944
945	1.00	1.00	0.8112	1.0000	0.11	0.10	0.6770	1.0000
946	1.00	1.00	0.8112	1.0000	0.11	0.10	0.6770	1.0000
949	0.11	0.07	0.0714	0.0914	0.06	0.07	0.1154	0.0750
950	0.34	0.40	0.0256	1.0000	0.54	0.42	0.1464	0.1144
955	0.43	0.38	0.4462	1.0000	0.43	0.42	0.5774	0.3088
962	0.32	0.39	0.0578	1.0000	0.57	0.49	0.1374	0.2714
963	0.13	0.04	0.3112	1.0000	0.09	0.04	0.4284	0.3444
968	0.23	0.12	0.5656	0.0874	0.51	0.29	0.1914	0.0514
969	0.37	0.18	0.0058	1.0000	0.11	0.07	0.0166	0.0118
974	0.29	0.33	0.4992	1.0000	0.60	0.60	0.6500	0.4944
976	0.41	1.00	0.2026	1.0000	0.01	0.09	0.0400	0.2950
977	1.00	1.00	0.8912	1.0000	0.84	1.00	0.7358	0.2486
978	1.00	1.00	0.9250	1.0000	1.00	1.00	0.9984	1.0000
980	1.00	1.00	0.7800	1.0000	0.22	0.20	0.1410	0.3698
984	0.04	0.01	0.2500	1.0000	0.06	0.05	0.0710	0.1974
985	0.11	0.10	0.4386	1.0000	0.08	0.07	0.7406	0.3452
986	0.06	0.06	0.0924	0.0422	0.16	0.11	0.1280	0.0484
988	0.50	0.43	0.0128	1.0000	0.40	0.34	0.0052	0.2482
995	0.13	0.22	0.2576	0.0228	0.21	0.28	0.2310	0.1506
996	1.00	1.00	1.0000	1.0000	0.21	0.22	0.2310	0.1506
999	1.00	1.00	1.0000	1.0000	0.71	1.00	0.4724	1.0000
1000	0.47	1.00	0.0792	1.0000	0.06	0.58	0.0436	0.2548
1002	0.09	0.19	0.0516	0.1198	0.22	0.26	0.1718	0.0402
1004	1.00	1.00	0.6608	1.0000	1.00	1.00	0.8670	1.0000
1006	1.00	1.00	0.9330	1.0000	0.54	1.00	0.7772	1.0000
1007	1.00	1.00	0.7908	1.0000	0.74	0.68	0.9254	1.0000
1008	1.00	0.16	0.9192	1.0000	0.18	0.25	0.1162	0.0216
1013	0.51	1.00	0.5686	1.0000	0.28	0.62	0.3766	1.0000
1017	1.00	0.01	0.6256	1.0000	0.04	0.03	0.1462	0.1604
1026	1.00	1.00	0.9148	1.0000	0.04	0.12	0.6152	0.3414
1027	1.00	1.00	0.9080	1.0000	0.22	1.00	0.8142	1.0000
1029	0.25	0.27	0.1020	1.0000	0.15	0.15	0.2740	0.3646
1035	1.00	0.06	0.6882	1.0000	0.25	0.19	0.6528	0.4476

1036	0.20	0.12	0.3490	1.0000	0.22	0.17	0.1646	0.1058
1037	1.00	0.12	0.6340	0.1198	0.24	0.20	0.0694	0.0508
1042	1.00	1.00	0.7290	1.0000	0.54	0.50	0.0854	1.0000
1043	1.00	1.00	0.8864	1.0000	0.33	1.00	0.8320	1.0000
1046	0.04	0.05	0.5300	1.0000	0.07	0.11	0.2072	0.0740
1047	1.00	1.00	0.9250	1.0000	1.00	1.00	0.9026	1.0000
1049	1.00	1.00	0.7764	1.0000	0.71	0.48	0.1662	0.4944
1055	1.00	1.00	0.9004	1.0000	1.00	0.43	0.9062	1.0000
1057	0.03	0.03	0.2300	0.0392	0.13	0.11	0.4228	0.1482
1062	0.03	0.01	0.5662	1.0000	0.08	0.07	0.0948	0.0182
1066	0.40	1.00	0.4836	1.0000	0.61	0.34	0.8330	1.0000
1067	1.00	0.02	0.6862	1.0000	0.07	0.06	0.6764	0.2092
1072	0.10	0.06	0.1852	0.0392	0.24	0.03	0.1180	0.0226
1074	0.32	0.30	0.0750	1.0000	0.16	0.07	0.1108	0.0658
1080	0.19	1.00	0.5638	1.0000	0.07	0.07	0.5464	0.3280
1082	0.51	1.00	0.0834	1.0000	0.08	0.07	0.1498	0.1528
1084	0.30	0.32	0.1916	1.0000	0.46	0.42	0.2618	0.1418
1085	1.00	0.42	0.7850	1.0000	0.61	0.60	0.6068	1.0000
1086	0.39	0.33	0.2690	0.0436	0.71	0.49	0.4650	0.2516
1087	0.50	0.43	0.0276	1.0000	0.72	0.68	0.0694	1.0000
1088	0.02	0.03	0.4764	1.0000	0.09	0.08	0.2524	0.1684
1089	0.24	1.00	0.4300	1.0000	0.38	0.37	0.3260	0.4476
1092	0.08	0.01	0.0286	0.0110	0.24	0.04	0.1230	0.0770
1094	1.00	1.00	0.9670	1.0000	0.81	0.13	0.1914	0.4944
1095	1.00	1.00	0.8418	1.0000	1.00	1.00	0.9638	1.0000
1098	0.08	0.06	0.0284	0.1198	0.07	0.04	0.1690	0.0560
1100	0.57	1.00	0.5562	1.0000	0.01	0.69	0.0320	1.0000
1101	0.57	1.00	0.5562	1.0000	0.01	0.69	0.0320	1.0000
1102	1.00	1.00	1.0000	1.0000	1.00	1.00	0.9988	1.0000
1104	1.00	1.00	0.6578	1.0000	0.21	0.32	0.1906	1.0000
1105	1.00	1.00	0.6578	1.0000	0.21	0.32	0.1906	1.0000
1106	1.00	1.00	0.9112	1.0000	1.00	1.00	0.8772	0.4944
1107	0.06	0.06	0.0422	1.0000	0.14	0.11	0.0822	0.0342
1109	0.03	0.00	0.0150	0.0298	0.01	0.01	0.0380	0.0196
1110	0.27	0.29	0.1076	0.0560	0.53	0.49	0.3478	0.2610
1112	0.46	1.00	0.6114	1.0000	0.03	0.02	0.6298	1.0000
1114	1.00	0.16	0.8494	1.0000	0.24	0.27	0.5684	0.3342
1115	0.47	1.00	0.1532	1.0000	0.18	0.39	0.0740	1.0000
1121	0.27	0.38	0.0860	1.0000	0.50	0.45	0.2862	0.3078
1123	1.00	1.00	0.8628	1.0000	1.00	1.00	0.8882	1.0000
1126	0.26	0.28	0.2698	1.0000	0.26	0.13	0.2078	1.0000
1127	0.32	0.16	0.0812	0.0580	0.29	0.16	0.0644	0.0398
1128	0.32	0.16	0.0812	0.0580	0.29	0.16	0.0644	0.0398
1135	0.12	0.04	0.0236	0.0158	0.31	0.01	0.0970	0.0080
1137	1.00	1.00	0.8752	1.0000	0.71	0.70	0.1836	1.0000
1140	0.00	0.00	0.0054	0.0000	0.01	0.01	0.0280	0.0004
1141	0.00	0.00	0.0048	1.0000	0.01	0.01	0.0298	0.0024
1145	0.08	0.24	0.0284	1.0000	0.11	0.01	0.0676	0.0900
1146	1.00	1.00	0.9420	1.0000	1.00	1.00	0.6216	0.2950
1149	0.47	1.00	0.0456	1.0000	0.56	0.57	0.1514	1.0000
1150	0.47	1.00	0.0456	1.0000	0.56	0.57	0.1514	1.0000
1157	0.12	0.13	0.0138	1.0000	0.05	0.01	0.0740	0.0866
1158	0.04	0.04	0.0024	1.0000	0.16	0.11	0.0174	0.1308
1159	0.33	0.07	0.2224	0.0850	0.27	0.20	0.0432	0.3956
1160	0.52	1.00	0.3230	1.0000	0.71	0.67	0.1690	1.0000
1166	0.03	0.04	0.3820	1.0000	0.15	0.10	0.4668	0.1682
1167	0.03	0.04	0.3820	1.0000	0.15	0.10	0.4668	0.1682
1168	0.33	0.32	0.5652	1.0000	0.61	0.51	0.3950	0.3414
1169	0.45	1.00	0.5662	1.0000	0.15	0.10	0.0870	0.0500
1170	1.00	1.00	0.8076	1.0000	0.17	0.13	0.3008	0.0296
1177	0.11	0.05	0.0448	0.0122	0.08	0.01	0.0678	0.0074

1182	1.00	1.00	0.7410	1.0000	0.37	0.32	0.6540	1.0000
1183	1.00	1.00	0.2944	0.0326	1.00	1.00	0.4476	0.1262
1186	1.00	1.00	0.8274	1.0000	1.00	1.00	0.8952	1.0000
1189	0.10	1.00	0.1036	1.0000	0.26	0.26	0.2586	0.2512
1190	1.00	1.00	0.3962	1.0000	0.53	0.55	0.5398	1.0000
1192	0.30	0.25	0.1318	0.1198	0.03	0.16	0.1746	0.1538
1193	1.00	1.00	0.2224	0.1020	1.00	1.00	0.1816	0.1198
1194	0.06	0.02	0.2302	0.0486	0.09	0.08	0.2064	0.0360
1196	0.15	0.08	0.2078	0.0436	0.23	0.23	0.1696	0.1726
1199	0.10	0.12	0.1258	1.0000	0.16	0.09	0.0950	0.3698
1203	1.00	1.00	0.9420	1.0000	0.08	0.11	0.7532	1.0000
1205	1.00	1.00	0.7062	1.0000	0.36	0.32	0.5866	0.2242
1209	1.00	1.00	0.0002	0.0004	1.00	1.00	0.0048	0.0052
1211	0.29	1.00	0.3694	1.0000	0.35	0.42	0.7070	1.0000
1212	0.43	0.32	0.0072	1.0000	0.26	0.17	0.0062	0.0676
1217	1.00	1.00	0.4346	0.0326	1.00	1.00	0.1890	0.0770
1219	1.00	0.02	0.7688	1.0000	0.08	0.07	0.6444	0.1668
1220	1.00	1.00	1.0000	1.0000	1.00	1.00	0.9552	1.0000
1221	0.32	0.35	0.2254	0.1198	0.19	0.54	0.2872	0.3956
1223	0.35	0.18	0.1370	1.0000	0.30	0.01	0.0818	0.0068
1224	0.35	0.18	0.1370	1.0000	0.30	0.01	0.0818	0.0068
1226	0.00	0.37	0.0050	1.0000	0.01	0.01	0.0316	1.0000
1241	1.00	1.00	0.5670	1.0000	1.00	1.00	0.6984	0.4476
1245	1.00	1.00	0.5652	0.0258	1.00	1.00	0.8708	0.1406
1246	0.26	0.22	0.1342	1.0000	0.45	0.25	0.2058	0.1292
1250	0.18	0.23	0.0236	1.0000	0.16	0.01	0.0812	0.0094
1251	0.28	0.24	0.0598	0.0758	0.43	0.39	0.2320	0.0950
1254	0.17	0.06	0.2210	1.0000	0.08	0.05	0.2864	1.0000
1255	0.09	0.18	0.6416	1.0000	0.29	0.41	0.4586	0.3604
1257	0.32	0.28	0.3470	1.0000	0.35	0.43	0.1188	1.0000
1259	0.06	0.04	0.2284	1.0000	0.19	0.11	0.4240	0.2792
1262	0.11	0.08	0.1644	0.0850	0.21	0.20	0.3448	0.3472
1265	0.22	0.26	0.1616	1.0000	0.37	0.42	0.2762	0.2476
1266	0.19	0.12	0.2146	0.1198	0.27	0.23	0.1914	0.2496
1273	0.29	0.20	0.0256	0.1198	0.37	0.25	0.0560	0.1640
1275	0.56	1.00	0.4732	1.0000	0.53	0.36	0.3672	1.0000
1276	0.08	0.04	0.0384	0.0090	0.13	0.05	0.1006	0.0046
1277	1.00	1.00	0.3512	0.1198	1.00	1.00	0.4774	0.4476
1278	0.37	0.36	0.1764	1.0000	0.64	0.51	0.1946	0.1788
1280	0.02	0.04	0.5260	1.0000	0.11	0.11	0.3186	0.2872
1281	0.51	1.00	0.2312	1.0000	0.29	0.19	0.4014	0.2162
1284	0.25	0.24	0.1590	1.0000	0.35	0.36	0.1934	0.2060
1285	1.00	0.27	0.9148	1.0000	0.40	0.29	0.5380	0.2692

1287	0.52	0.42	0.2830	1.0000	0.77	0.57	0.1100	1.0000
1288	0.52	0.42	0.2830	1.0000	0.77	0.57	0.1100	1.0000
1291	0.22	0.23	0.3948	1.0000	0.33	0.35	0.3150	0.1612
1293	0.41	0.41	0.1862	1.0000	0.54	0.47	0.1948	1.0000
1298	0.08	0.14	0.6026	1.0000	0.21	0.27	0.3776	0.4944
1301	0.37	0.35	0.1052	1.0000	0.59	0.51	0.1600	0.3472
1303	0.07	0.11	0.6012	0.1198	0.22	0.23	0.3190	0.1364
1304	1.00	0.23	0.8506	1.0000	0.33	0.41	0.7776	1.0000
1305	0.11	0.12	0.5610	1.0000	0.28	0.28	0.2950	0.2836
1306	0.09	0.08	0.0998	0.0164	0.26	0.24	0.0542	0.1178
1309	0.45	1.00	0.2978	1.0000	0.49	0.44	0.3352	1.0000
1310	0.05	0.04	0.0402	0.0226	0.18	0.14	0.0178	0.0078
1311	1.00	0.09	0.9330	1.0000	0.55	0.14	0.0078	0.0182
1312	0.21	0.15	0.0066	0.0382	0.41	0.26	0.0068	0.0304
1313	1.00	1.00	0.8358	1.0000	0.29	0.25	0.5420	1.0000
1316	0.54	1.00	0.0976	1.0000	0.75	0.68	0.0318	1.0000
1318	0.11	0.12	0.0312	0.0714	0.28	0.24	0.0194	0.0278
1320	0.11	0.09	0.4106	1.0000	0.20	0.17	0.2916	0.1080
1322	0.05	0.07	0.2816	0.0406	0.19	0.21	0.3562	0.2412
1323	0.24	1.00	0.4664	1.0000	0.36	0.39	0.0328	0.4944
1327	0.31	0.38	0.0248	1.0000	0.47	0.01	0.1058	0.2604
1329	0.24	0.24	0.2740	1.0000	0.40	0.41	0.2962	1.0000
1331	0.31	0.17	0.3040	1.0000	0.22	0.15	0.1862	0.2132
1332	0.32	0.30	0.2444	1.0000	0.45	0.38	0.3398	0.3738
1333	0.38	0.41	0.0276	1.0000	0.72	0.65	0.1664	0.4944
1334	0.21	0.29	0.1654	1.0000	0.33	0.36	0.3528	1.0000
1337	0.04	0.00	0.0304	0.0058	0.12	0.01	0.0634	0.0100
1338	0.23	0.24	0.3150	1.0000	0.42	0.39	0.4262	0.2630
1340	0.36	0.26	0.1264	1.0000	0.53	0.13	0.0162	0.1096
1341	1.00	0.27	0.6372	1.0000	0.68	0.17	0.0126	0.1048
1342	1.00	1.00	0.9670	1.0000	0.13	0.12	0.1622	0.0544
1343	0.38	0.35	0.5236	1.0000	0.45	0.47	0.1856	0.4160
1344	0.43	1.00	0.1764	1.0000	0.39	0.42	0.5326	1.0000
1345	0.30	0.33	0.1904	1.0000	0.50	0.52	0.1754	1.0000
1346	0.24	0.21	0.0090	0.0288	0.08	0.34	0.0160	0.1482
1347	0.56	1.00	0.0134	1.0000	0.77	0.63	0.0264	1.0000
1348	0.24	0.09	0.0440	0.0700	0.29	0.13	0.0928	0.1290
1349	0.14	0.08	0.0734	0.0198	0.13	0.11	0.1542	0.0762
1415	0.03	0.02	0.0404	0.0202	0.05	0.04	0.0080	0.0932
1425	0.03	0.05	0.3954	1.0000	0.13	0.16	0.0746	0.2092
1432	0.02	0.03	0.1372	0.0408	0.09	0.11	0.3124	0.1682
1435	0.33	0.31	0.1500	1.0000	0.39	0.41	0.2982	0.3604
1436	0.26	0.14	0.0224	1.0000	0.23	0.01	0.1408	0.0132
1443	0.04	0.02	0.4130	0.0282	0.01	0.01	0.0348	0.0430
1447	0.17	0.11	0.4548	1.0000	0.33	0.13	0.2400	0.0794
1451	1.00	0.36	0.7956	1.0000	0.01	0.36	0.0416	0.3132
1452	0.13	0.12	0.2316	1.0000	0.12	0.15	0.0448	0.2890
1455	0.19	0.15	0.0238	0.0008	0.37	0.36	0.0052	0.0076
1459	1.00	1.00	0.8248	0.0686	0.14	1.00	0.4950	0.3414
1468	0.12	0.04	0.0112	0.0560	0.31	0.03	0.0156	0.0120
1471	0.02	0.01	0.0004	0.0000	0.07	0.03	0.0062	0.0006
1472	0.13	0.04	0.0058	0.0022	0.14	0.06	0.0052	0.0028
1478	0.44	1.00	0.1600	1.0000	0.39	0.70	0.0058	1.0000
1486	0.18	0.21	0.0102	1.0000	0.03	0.04	0.0140	0.1366
2083	1.00	1.00	1.0000	1.0000	1.00	1.00	0.9522	1.0000
2158	0.42	0.40	0.2670	1.0000	0.70	0.65	0.1398	0.3956
2303	0.13	0.04	0.6284	1.0000	0.05	0.07	0.0674	0.0228
2588	1.00	1.00	0.8598	1.0000	1.00	1.00	0.9892	0.4160
% < 0.5	60%	57%	60%	22%	66%	66%	71%	64%

Terrain-based landslide model validation test in Qtw terrain

Based on points randomly sampled from a probability distribution of potentially unstable slopes defined by hillslope gradient at landslide points, where p<0.5 for at least one model

Performance of landslide models at landslides (p-tests for slide locations vs slope-based points)

	using values in 8m radius			
SLIDE.ID	SHAL	SHALV	PISA	PISAS
834	0.01	0.01	0.0018	0.0000
1140	0.01	0.01	0.0280	0.0004
794	0.01	0.04	0.0014	0.0010
1141	0.01	0.01	0.0298	0.0024
709	0.01	0.01	0.0464	0.0032
635	0.01	0.01	0.0426	0.0036
713	0.01	0.01	0.0274	0.0040
619	0.01	0.01	0.0006	0.0054
817	0.01	0.01	0.0006	0.0078
617	0.01	0.04	0.0002	0.0100
1109	0.01	0.01	0.0380	0.0196
668	0.01	0.01	0.0384	0.0348
1443	0.01	0.01	0.0348	0.0430
513	0.01	0.01	0.0372	0.0456
560	0.01	0.01	0.0316	0.0482
690	0.01	0.01	0.0326	0.0652
723	0.01	0.01	0.0428	0.0894
757	0.01	0.01	0.0378	0.1436
743	0.01	0.13	0.0006	0.1664
729	0.01	0.01	0.0002	0.1908
868	0.01	0.01	0.0294	0.2042
567	0.01	0.01	0.0436	0.2882
976	0.01	0.09	0.0400	0.2950
1451	0.01	0.36	0.0416	0.3132
782	0.01	0.15	0.0458	0.3884
814	0.01	0.48	0.0468	0.4944
1100	0.01	0.69	0.0320	1.0000
1101	0.01	0.69	0.0320	1.0000
1226	0.01	0.01	0.0316	1.0000
525	0.01	0.48	0.0062	0.4944
761	0.02	0.03	0.5252	0.2846
800	0.03	0.02	0.2342	0.2488
644	0.03	0.27	0.1286	1.0000
1112	0.03	0.02	0.6298	1.0000
874	0.03	0.04	0.0454	0.2354
626	0.03	0.07	0.2194	0.3670
1486	0.03	0.04	0.0140	0.1366
923	0.03	0.17	0.3496	1.0000
1192	0.03	0.16	0.1746	0.1538
1026	0.04	0.12	0.6152	0.3414
1017	0.04	0.03	0.1462	0.1604
674	0.05	0.12	0.0080	0.0052
1415	0.05	0.04	0.0080	0.0932
1157	0.05	0.01	0.0740	0.0866
2303	0.05	0.07	0.0674	0.0228
984	0.06	0.05	0.0710	0.1974
949	0.06	0.07	0.1154	0.0750
746	0.06	0.05	0.4100	0.1178
747	0.06	0.05	0.4100	0.1178
1000	0.06	0.58	0.0436	0.2548
789	0.06	0.02	0.0110	0.0038
564	0.07	0.13	0.3804	0.4944
753	0.07	0.01	0.1290	0.0194
1080	0.07	0.07	0.5464	0.3280

1067	0.07	0.06	0.6764	0.2092
1098	0.07	0.04	0.1690	0.0560
787	0.07	0.07	0.0302	0.0202
1471	0.07	0.03	0.0062	0.0006
1046	0.07	0.11	0.2072	0.0740
985	0.08	0.07	0.7406	0.3452
1254	0.08	0.05	0.2864	1.0000
758	0.08	0.72	0.3734	1.0000
759	0.08	0.72	0.3734	1.0000
1062	0.08	0.07	0.0948	0.0182
1219	0.08	0.07	0.6444	0.1668
1177	0.08	0.01	0.0678	0.0074
838	0.08	1.00	0.3272	1.0000
1346	0.08	0.34	0.0160	0.1482
1203	0.08	0.11	0.7532	1.0000
1082	0.08	0.07	0.1498	0.1528
783	0.09	0.11	0.0228	0.0140
1088	0.09	0.08	0.2524	0.1684
1432	0.09	0.11	0.3124	0.1682
827	0.09	0.06	0.2950	0.0792
842	0.09	0.01	0.0052	0.0078
788	0.09	0.08	0.8588	0.2578
1194	0.09	0.08	0.2064	0.0360
963	0.09	0.04	0.4284	0.3444
856	0.10	0.10	0.0242	0.0056
935	0.11	0.10	0.5094	0.3100
945	0.11	0.10	0.6770	1.0000
946	0.11	0.10	0.6770	1.0000
969	0.11	0.07	0.0166	0.0118
614	0.11	0.11	0.5410	0.2654
1145	0.11	0.01	0.0676	0.0900
1280	0.11	0.11	0.3186	0.2872
808	0.11	0.10	0.0118	0.0118
869	0.11	0.12	0.3260	1.0000
554	0.11	0.07	0.3282	0.1132
924	0.12	0.10	0.6956	0.1376
1337	0.12	0.01	0.0634	0.0100
1452	0.12	0.15	0.0448	0.2890
557	0.12	0.01	0.0610	0.0166
840	0.13	0.17	0.8230	0.4476
1342	0.13	0.12	0.1622	0.0544
1349	0.13	0.11	0.1542	0.0762
1057	0.13	0.11	0.4228	0.1482
1425	0.13	0.16	0.0746	0.2092
1276	0.13	0.05	0.1006	0.0046
1107	0.14	0.11	0.0822	0.0342
1459	0.14	1.00	0.4950	0.3414
805	0.14	0.12	0.0596	0.0124
806	0.14	0.12	0.0596	0.0124
712	0.14	0.13	0.5342	1.0000
810	0.14	0.14	0.0062	0.0170
1472	0.14	0.06	0.0052	0.0028
1029	0.15	0.15	0.2740	0.3646
1166	0.15	0.10	0.4668	0.1682
1167	0.15	0.10	0.4668	0.1682
720	0.15	0.11	0.3810	0.4476
1169	0.15	0.10	0.0870	0.0500
884	0.16	0.31	0.2192	0.4944
1158	0.16	0.11	0.0174	0.1308
1250	0.16	0.01	0.0812	0.0094
986	0.16	0.11	0.1280	0.0484
1074	0.16	0.07	0.1108	0.0658
739	0.16	0.27	0.0900	0.4944
1199	0.16	0.09	0.0950	0.3698
830	0.16	0.10	0.2444	0.0736

1170	0.17	0.13	0.3008	0.0296
862	0.18	0.08	0.0088	1.0000
790	0.18	0.27	0.0062	1.0000
545	0.18	0.14	0.4152	0.2634
1115	0.18	0.39	0.0740	1.0000
1008	0.18	0.25	0.1162	0.0216
1310	0.18	0.14	0.0178	0.0078
1259	0.19	0.11	0.4240	0.2792
1221	0.19	0.54	0.2872	0.3956
1322	0.19	0.21	0.3562	0.2412
1320	0.20	0.17	0.2916	0.1080
1104	0.21	0.32	0.1906	1.0000
1105	0.21	0.32	0.1906	1.0000
640	0.21	0.01	0.0632	1.0000
1262	0.21	0.20	0.3448	0.3472
1298	0.21	0.27	0.3776	0.4944
995	0.21	0.28	0.2310	0.1506
996	0.21	0.22	0.2310	0.1506
818	0.21	0.24	0.6638	0.3550
1303	0.22	0.23	0.3190	0.1364
980	0.22	0.20	0.1410	0.3698
1027	0.22	1.00	0.8142	1.0000
725	0.22	0.19	0.1242	0.0266
1331	0.22	0.15	0.1862	0.2132
1002	0.22	0.26	0.1718	0.0402
1036	0.22	0.17	0.1646	0.1058
865	0.23	0.02	0.4476	0.4276
930	0.23	0.25	0.6320	1.0000
1436	0.23	0.01	0.1408	0.0132
767	0.23	0.32	0.4950	0.4944
1196	0.23	0.23	0.1696	0.1726
1072	0.24	0.03	0.1180	0.0226
1037	0.24	0.20	0.0694	0.0508
1114	0.24	0.27	0.5684	0.3342
1092	0.24	0.04	0.1230	0.0770
784	0.25	1.00	0.7748	1.0000
538	0.25	0.29	0.2898	0.1090
1035	0.25	0.19	0.6528	0.4476
835	0.25	0.01	0.0660	0.0102
1306	0.26	0.24	0.0542	0.1178
736	0.26	0.28	0.5858	1.0000
861	0.26	0.10	0.7820	1.0000
675	0.26	0.32	0.4258	0.2702
722	0.26	0.32	0.1612	0.0566
1126	0.26	0.13	0.2078	1.0000
1212	0.26	0.17	0.0062	0.0676
812	0.26	0.10	0.0752	0.0302
1189	0.26	0.26	0.2586	0.2512
878	0.26	0.29	0.4668	1.0000
1266	0.27	0.23	0.1914	0.2496
776	0.27	0.47	0.6684	1.0000
1159	0.27	0.20	0.0432	0.3956
809	0.27	0.27	0.1180	0.3158
1318	0.28	0.24	0.0194	0.0278
778	0.28	0.19	0.7612	1.0000
1305	0.28	0.28	0.2950	0.2836
1013	0.28	0.62	0.3766	1.0000
1313	0.29	0.25	0.5420	1.0000
1348	0.29	0.13	0.0928	0.1290
1255	0.29	0.41	0.4586	0.3604
791	0.29	0.25	0.0156	1.0000
932	0.29	0.27	0.5392	0.0720
1281	0.29	0.19	0.4014	0.2162
1127	0.29	0.16	0.0644	0.0398
1128	0.29	0.16	0.0644	0.0398

903	0.30	0.35	0.0904	1.0000
1223	0.30	0.01	0.0818	0.0068
1224	0.30	0.01	0.0818	0.0068
775	0.30	0.32	0.3718	0.2876
826	0.30	0.33	0.5444	0.1298
1135	0.31	0.01	0.0970	0.0080
1468	0.31	0.03	0.0156	0.0120
700	0.32	0.07	0.1214	0.0340
888	0.32	0.17	0.1326	0.1150
889	0.32	0.17	0.1326	0.1150
740	0.32	0.23	0.1574	1.0000
741	0.32	0.23	0.1574	1.0000
1304	0.33	0.41	0.7776	1.0000
1291	0.33	0.35	0.3150	0.1612
563	0.33	0.26	0.0528	0.1040
730	0.33	0.21	0.3710	0.2042
1334	0.33	0.36	0.3528	1.0000
763	0.33	0.40	0.4018	0.2928
769	0.33	0.67	0.0562	1.0000
1447	0.33	0.13	0.2400	0.0794
1043	0.33	1.00	0.8320	1.0000
602	0.35	0.34	0.7116	0.4476
1211	0.35	0.42	0.7070	1.0000
1257	0.35	0.43	0.1188	1.0000
1284	0.35	0.36	0.1934	0.2060
795	0.36	0.41	0.6620	1.0000
710	0.36	0.35	0.3366	0.2348
1323	0.36	0.39	0.0328	0.4944
1205	0.36	0.32	0.5866	0.2242
1455	0.37	0.36	0.0052	0.0076
694	0.37	0.34	0.5214	0.3630
831	0.37	0.35	0.3774	0.2610
1182	0.37	0.32	0.6540	1.0000
925	0.37	0.23	0.5882	1.0000
1265	0.37	0.42	0.2762	0.2476
1273	0.37	0.25	0.0560	0.1640
1089	0.38	0.37	0.3260	0.4476
877	0.39	0.29	0.1346	1.0000
1435	0.39	0.41	0.2982	0.3604
1344	0.39	0.42	0.5326	1.0000
1478	0.39	0.70	0.0058	1.0000
550	0.40	0.25	0.0876	1.0000
893	0.40	0.39	0.0460	0.1088
1285	0.40	0.29	0.5380	0.2692
1329	0.40	0.41	0.2962	1.0000
988	0.40	0.34	0.0052	0.2482
896	0.41	0.39	0.1480	0.1828
1312	0.41	0.26	0.0068	0.0304
927	0.41	0.19	0.5078	1.0000
1338	0.42	0.39	0.4262	0.2630
653	0.42	0.42	0.1138	0.0812
521	0.42	0.46	0.6666	1.0000
825	0.42	0.01	0.1112	0.0822
708	0.43	0.20	0.3816	0.1224
955	0.43	0.42	0.5774	0.3088
1251	0.43	0.39	0.2320	0.0950
659	0.43	0.57	0.2824	0.4944
686	0.43	0.32	0.7408	0.3226
687	0.43	0.32	0.7408	0.3226
688	0.43	0.32	0.7408	0.3226
728	0.43	0.53	0.4818	0.3670
837	0.44	0.30	0.4472	0.0654
847	0.44	0.54	0.5304	0.4944
832	0.44	0.28	0.6102	1.0000
841	0.44	0.49	0.5250	0.3956

1332	0.45	0.38	0.3398	0.3738
1343	0.45	0.47	0.1856	0.4160
1246	0.45	0.25	0.2058	0.1292
891	0.46	0.41	0.1108	0.1354
1084	0.46	0.42	0.2618	0.1418
773	0.46	0.36	0.1480	0.3158
1327	0.47	0.01	0.1058	0.2604
770	0.49	0.46	0.2516	1.0000
1309	0.49	0.44	0.3352	1.0000
867	0.49	0.51	0.0746	0.3836
1345	0.50	0.52	0.1754	1.0000
911	0.50	0.49	0.2382	0.3572
1121	0.50	0.45	0.2862	0.3078
774	0.50	0.53	0.4660	1.0000
799	0.50	0.48	0.0990	0.4476
804	0.51	0.53	0.3546	0.3172
968	0.51	0.29	0.1914	0.0514
871	0.51	0.59	0.1702	1.0000
655	0.51	0.52	0.4316	0.4944
592	0.52	0.54	0.4116	0.2558
1190	0.53	0.55	0.5398	1.0000
1110	0.53	0.49	0.3478	0.2610
1340	0.53	0.13	0.0162	0.1096
1275	0.53	0.36	0.3672	1.0000
1042	0.54	0.50	0.0854	1.0000
1293	0.54	0.47	0.1948	1.0000
689	0.54	0.62	0.1548	1.0000
950	0.54	0.42	0.1464	0.1144
1311	0.55	0.14	0.0078	0.0182
1149	0.56	0.57	0.1514	1.0000
1150	0.56	0.57	0.1514	1.0000
530	0.56	1.00	0.3898	0.1008
962	0.57	0.49	0.1374	0.2714
738	0.58	0.39	0.8466	1.0000
590	0.58	0.58	0.4442	1.0000
591	0.58	0.58	0.4442	1.0000
864	0.58	0.60	0.1498	1.0000
648	0.59	0.41	0.4306	0.2698
654	0.59	0.60	0.3204	0.1418
514	0.59	1.00	0.7466	0.3956

1301	0.59	0.51	0.1600	0.3472
940	0.60	0.57	0.4538	0.4944
974	0.60	0.60	0.6500	0.4944
1066	0.61	0.34	0.8330	1.0000
764	0.61	0.71	0.1614	1.0000
765	0.61	0.71	0.1614	1.0000
1168	0.61	0.51	0.3950	0.3414
771	0.62	0.69	0.2080	1.0000
772	0.62	0.69	0.2080	1.0000
855	0.62	0.70	0.0140	1.0000
680	0.62	0.59	0.1172	0.0852
1278	0.64	0.51	0.1946	0.1788
586	0.64	0.59	0.0794	0.3782
647	0.64	0.60	0.4902	1.0000
699	0.64	0.63	0.2744	1.0000
750	0.65	0.66	0.1212	1.0000
742	0.67	1.00	0.4580	1.0000
913	0.67	0.65	0.4916	1.0000
760	0.68	0.38	0.6458	0.3646
692	0.68	0.52	0.1286	1.0000
1341	0.68	0.17	0.0126	0.1048
2158	0.70	0.65	0.1398	0.3956
1086	0.71	0.49	0.4650	0.2516
1160	0.71	0.67	0.1690	1.0000
999	0.71	1.00	0.4724	1.0000
1049	0.71	0.48	0.1662	0.4944
1137	0.71	0.70	0.1836	1.0000
507	0.72	0.68	0.5290	0.4944
1087	0.72	0.68	0.0694	1.0000
1333	0.72	0.65	0.1664	0.4944
880	0.73	0.61	0.1034	0.1568
881	0.73	0.61	0.1034	0.1568
844	0.75	0.70	0.1234	1.0000
1316	0.75	0.68	0.0318	1.0000
643	0.77	0.62	0.4738	1.0000
1347	0.77	0.63	0.0264	1.0000
1287	0.77	0.57	0.1100	1.0000
1288	0.77	0.57	0.1100	1.0000
899	0.78	0.42	0.4784	1.0000
1094	0.81	0.13	0.1914	0.4944
802	0.81	1.00	0.4910	1.0000
849	0.83	1.00	0.1646	0.1940
850	0.83	1.00	0.1646	0.1940
977	0.84	1.00	0.7358	0.2486
1209	1.00	1.00	0.0048	0.0052
672	1.00	1.00	0.7400	0.0722
1217	1.00	1.00	0.1890	0.0770
1193	1.00	1.00	0.1816	0.1198
1183	1.00	1.00	0.4476	0.1262
933	1.00	1.00	0.9114	0.1304
1245	1.00	1.00	0.8708	0.1406
706	1.00	1.00	0.9204	0.2412
1146	1.00	1.00	0.6216	0.2950
516	1.00	1.00	0.9372	0.3504
2588	1.00	1.00	0.9892	0.4160
1241	1.00	1.00	0.6984	0.4476
1277	1.00	1.00	0.4774	0.4476
1106	1.00	1.00	0.8772	0.4944
633	1.00	0.28	0.8896	1.0000
1055	1.00	0.43	0.9062	1.0000

% < 0.5	75%	76%	81%	73%

Terrain-based landslide model validation test in Ty terrain

Based on points randomly sampled from a probability distribution of potentially unstable slopes defined by hillslope gradient at landslide points

Performance of landslide models at landslides (p-tests for slide locations vs random points)

	using values of model at points				using values in 8m radius			
SLIDE.ID	SHAL	SHALV	PISA	PISAS	SHAL	SHALV	PISA	PISAS
494	1.00	1.00	0.7596	1.0000	1.00	1.00	0.8604	0.3066
495	1.00	1.00	0.8204	1.0000	1.00	1.00	0.9570	1.0000
499	1.00	1.00	0.9024	1.0000	1.00	1.00	0.9450	1.0000
500	0.12	0.10	0.0100	0.0128	0.14	0.21	0.0228	0.0068
502	0.42	0.38	0.2786	1.0000	0.45	0.35	0.2950	0.6044
504	0.37	0.32	0.1500	1.0000	0.45	0.40	0.3906	0.5156
508	1.00	1.00	0.7042	1.0000	1.00	1.00	0.9346	1.0000
509	0.38	1.00	0.1748	1.0000	0.45	0.37	0.4226	0.1514
512	0.04	0.01	0.0228	0.1014	0.04	0.05	0.0474	0.0144
520	0.04	0.09	0.1448	1.0000	0.12	0.11	0.3274	0.5240
522	1.00	0.29	0.7368	0.2170	0.59	0.52	0.0312	0.0404
534	0.31	0.38	0.0638	1.0000	0.49	0.49	0.2414	0.2862
536	0.24	1.00	0.4250	1.0000	0.37	0.52	0.6912	1.0000
549	1.00	1.00	0.8410	1.0000	1.00	1.00	0.9724	1.0000
556	0.00	0.01	0.0228	1.0000	0.04	0.05	0.0778	0.1318
570	1.00	1.00	0.6442	1.0000	0.59	0.57	0.7312	0.5842
571	0.46	0.41	0.2236	1.0000	0.65	0.61	0.2256	1.0000
577	1.00	1.00	0.8930	1.0000	0.27	0.50	0.6704	0.4598
580	1.00	1.00	0.7478	1.0000	0.39	0.53	0.0894	0.5558
581	1.00	1.00	0.9646	1.0000	0.72	1.00	0.8646	1.0000
582	1.00	1.00	0.9646	1.0000	0.72	1.00	0.8646	1.0000
583	0.31	0.11	0.1260	0.3000	0.17	0.18	0.2494	0.6620
587	0.49	1.00	0.1994	1.0000	0.04	0.61	0.0770	0.6962
588	0.49	1.00	0.1994	1.0000	0.04	0.61	0.0770	0.6962
589	0.00	0.01	0.0230	1.0000	0.04	0.05	0.0988	0.4948
594	0.11	0.01	0.0802	0.0488	0.04	0.05	0.0848	0.0298
595	1.00	0.13	0.6742	0.2676	0.26	0.23	0.4820	0.1250
596	1.00	1.00	0.6304	1.0000	0.33	0.32	0.2680	0.3748
604	1.00	1.00	0.8584	1.0000	0.72	0.57	0.7416	0.4674
606	0.12	0.17	0.0824	1.0000	0.13	0.05	0.1548	0.3172
611	1.00	1.00	0.6110	1.0000	0.80	0.32	0.6718	0.5974
613	0.00	0.01	0.0016	0.0240	0.04	0.05	0.0066	0.0210
627	1.00	1.00	1.0000	1.0000	1.00	1.00	0.8140	0.3342
628	1.00	1.00	1.0000	1.0000	1.00	1.00	0.8140	0.3342
637	0.14	0.14	0.1168	0.2676	0.28	0.20	0.2542	0.0992
638	0.14	0.14	0.1168	0.2676	0.28	0.20	0.2542	0.0992
651	0.00	0.01	0.0160	0.1854	0.04	0.05	0.0612	0.0560
652	0.07	0.08	0.0286	0.0456	0.04	0.09	0.0880	0.0114
660	0.06	0.03	0.2512	0.0672	0.08	0.07	0.1982	0.0560
661	0.06	0.03	0.2512	0.0672	0.08	0.07	0.1982	0.0560
669	0.11	0.01	0.0526	0.0204	0.06	0.05	0.1070	0.0992
670	0.56	1.00	0.7506	1.0000	0.04	1.00	0.0572	1.0000
684	1.00	1.00	0.8950	1.0000	0.70	1.00	0.7542	1.0000
693	0.34	1.00	0.3222	0.3000	0.60	0.56	0.6056	0.6962
698	1.00	1.00	0.6708	1.0000	0.21	0.26	0.1256	0.3318
701	0.07	0.04	0.0290	0.1632	0.20	0.05	0.1252	0.0298
703	0.04	0.13	0.0000	0.0758	0.09	0.11	0.0000	0.0054
705	1.00	1.00	0.9178	1.0000	1.00	1.00	0.8146	1.0000
718	0.29	1.00	0.1558	1.0000	0.27	0.24	0.3290	0.1562

726	0.17	0.13	0.4472	0.1304	0.15	0.11	0.1260	0.0062
733	0.51	1.00	0.1612	1.0000	0.39	0.66	0.1332	1.0000
734	0.14	0.14	0.0004	0.0184	0.26	0.09	0.0006	0.0128
748	1.00	1.00	0.8956	1.0000	1.00	1.00	0.9298	1.0000
749	1.00	1.00	0.8956	1.0000	1.00	1.00	0.9298	1.0000
756	0.13	0.18	0.0274	1.0000	0.04	0.12	0.0842	0.4330
766	0.16	0.13	0.0724	0.2094	0.29	0.13	0.2726	0.1814
780	0.14	0.19	0.1954	1.0000	0.21	0.26	0.4234	0.4260
781	0.14	0.19	0.1954	1.0000	0.21	0.26	0.4234	0.4260
785	0.25	0.19	0.1382	0.1212	0.52	0.30	0.3046	0.3958
786	1.00	1.00	0.7800	1.0000	0.78	1.00	0.5738	0.6126
792	1.00	1.00	0.6518	0.2528	0.50	1.00	0.7934	0.6194
793	0.10	0.01	0.0650	0.0530	0.04	0.05	0.0764	0.0646
824	0.15	0.07	0.0914	0.1240	0.16	0.05	0.1308	0.1936
853	0.01	0.02	0.0792	1.0000	0.04	0.05	0.0850	0.2018
870	0.03	0.01	0.0072	0.0106	0.09	0.05	0.0156	0.0110
885	0.09	0.21	0.5466	1.0000	0.15	0.17	0.2270	0.0744
895	0.12	0.28	0.1252	1.0000	0.04	0.05	0.0768	0.2628
898	0.19	0.29	0.5052	1.0000	0.11	0.52	0.4142	1.0000
929	0.17	0.19	0.5380	0.1528	0.41	0.39	0.6236	0.4224
941	1.00	1.00	0.7524	1.0000	0.48	0.61	0.1768	1.0000
951	0.01	1.00	0.3990	1.0000	0.05	0.06	0.4872	0.5974
973	0.00	0.01	0.0144	0.0582	0.04	0.05	0.0482	0.0054
979	0.33	0.29	0.0894	1.0000	0.04	0.32	0.0940	0.2982
989	1.00	1.00	0.8106	1.0000	1.00	1.00	0.8606	1.0000
992	0.23	0.18	0.0648	0.0580	0.49	0.18	0.2042	0.0760
993	0.23	0.18	0.0648	0.0580	0.49	0.18	0.2042	0.0760
994	0.23	0.18	0.0648	0.0580	0.49	0.18	0.2042	0.0760
1009	0.00	0.01	0.0204	0.0444	0.04	0.05	0.0534	0.0568
1012	0.13	0.39	0.0292	1.0000	0.04	0.05	0.0748	0.1330
1015	0.10	0.17	0.0286	0.0206	0.27	0.22	0.1232	0.0554
1045	0.23	0.31	0.0402	1.0000	0.04	0.25	0.0770	0.1024
1063	0.37	0.34	0.3296	1.0000	0.38	0.36	0.5708	0.3512
1113	0.24	0.18	0.0544	0.0312	0.10	0.15	0.1850	0.1046
1174	1.00	1.00	0.9010	1.0000	1.00	1.00	0.9098	0.4720
1228	0.30	0.31	0.1698	0.1004	0.53	0.18	0.4586	0.3836
1239	0.48	1.00	0.4716	1.0000	0.57	0.51	0.5178	0.3778
1470	0.10	0.09	0.3056	0.0320	0.04	0.17	0.3814	0.1494
1480	1.00	1.00	0.6412	1.0000	0.59	1.00	0.2430	1.0000
% < 0.5	66%	59%	64%	40%	69%	64%	70%	65%

Terrain-based landslide model validation test in Ty terrain

Based on points randomly sampled from a probability distribution of potentially unstable slopes defined by hillslope gradient at landslide points, where p<0.5 for at least one model

Performance of landslide models at landslides (p-tests for slide locations vs slope-based points)

	using values in 8m radius			
SLIDE.ID	SHAL	SHALV	PISA	PISAS
973	0.04	0.05	0.0482	0.0054
652	0.04	0.09	0.0880	0.0114
512	0.04	0.05	0.0474	0.0144
613	0.04	0.05	0.0066	0.0210
594	0.04	0.05	0.0848	0.0298
651	0.04	0.05	0.0612	0.0560
1009	0.04	0.05	0.0534	0.0568
793	0.04	0.05	0.0764	0.0646
1045	0.04	0.25	0.0770	0.1024
556	0.04	0.05	0.0778	0.1318
1012	0.04	0.05	0.0748	0.1330
895	0.04	0.05	0.0768	0.2628
979	0.04	0.32	0.0940	0.2982
756	0.04	0.12	0.0842	0.4330
589	0.04	0.05	0.0988	0.4948
587	0.04	0.61	0.0770	0.6962
588	0.04	0.61	0.0770	0.6962
670	0.04	1.00	0.0572	1.0000
1470	0.04	0.17	0.3814	0.1494
853	0.04	0.05	0.0850	0.2018
951	0.05	0.06	0.4872	0.5974
669	0.06	0.05	0.1070	0.0992
660	0.08	0.07	0.1982	0.0560
661	0.08	0.07	0.1982	0.0560
703	0.09	0.11	0.0000	0.0054
870	0.09	0.05	0.0156	0.0110
1113	0.10	0.15	0.1850	0.1046
898	0.11	0.52	0.4142	1.0000
520	0.12	0.11	0.3274	0.5240
606	0.13	0.05	0.1548	0.3172
500	0.14	0.21	0.0228	0.0068
885	0.15	0.17	0.2270	0.0744
726	0.15	0.11	0.1260	0.0062
824	0.16	0.05	0.1308	0.1936
583	0.17	0.18	0.2494	0.6620
701	0.20	0.05	0.1252	0.0298
698	0.21	0.26	0.1256	0.3318
780	0.21	0.26	0.4234	0.4260
781	0.21	0.26	0.4234	0.4260
734	0.26	0.09	0.0006	0.0128
595	0.26	0.23	0.4820	0.1250
1015	0.27	0.22	0.1232	0.0554
577	0.27	0.50	0.6704	0.4598
718	0.27	0.24	0.3290	0.1562
637	0.28	0.20	0.2542	0.0992
638	0.28	0.20	0.2542	0.0992

766	0.29	0.13	0.2726	0.1814
596	0.33	0.32	0.2680	0.3748
536	0.37	0.52	0.6912	1.0000
1063	0.38	0.36	0.5708	0.3512
580	0.39	0.53	0.0894	0.5558
733	0.39	0.66	0.1332	1.0000
929	0.41	0.39	0.6236	0.4224
502	0.45	0.35	0.2950	0.6044
509	0.45	0.37	0.4226	0.1514
504	0.45	0.40	0.3906	0.5156
941	0.48	0.61	0.1768	1.0000
534	0.49	0.49	0.2414	0.2862
992	0.49	0.18	0.2042	0.0760
993	0.49	0.18	0.2042	0.0760
994	0.49	0.18	0.2042	0.0760
785	0.52	0.30	0.3046	0.3958
1228	0.53	0.18	0.4586	0.3836
1239	0.57	0.51	0.5178	0.3778
522	0.59	0.52	0.0312	0.0404
1480	0.59	1.00	0.2430	1.0000
571	0.65	0.61	0.2256	1.0000
604	0.72	0.57	0.7416	0.4674
611	0.80	0.32	0.6718	0.5974
494	1.00	1.00	0.8604	0.3066
627	1.00	1.00	0.8140	0.3342
628	1.00	1.00	0.8140	0.3342
1174	1.00	1.00	0.9098	0.4720
% < 0.5	84%	77%	85%	78%

Appendix E

Results from sampling approach to determining landslide hazard threshold based on model values at landslides and random points

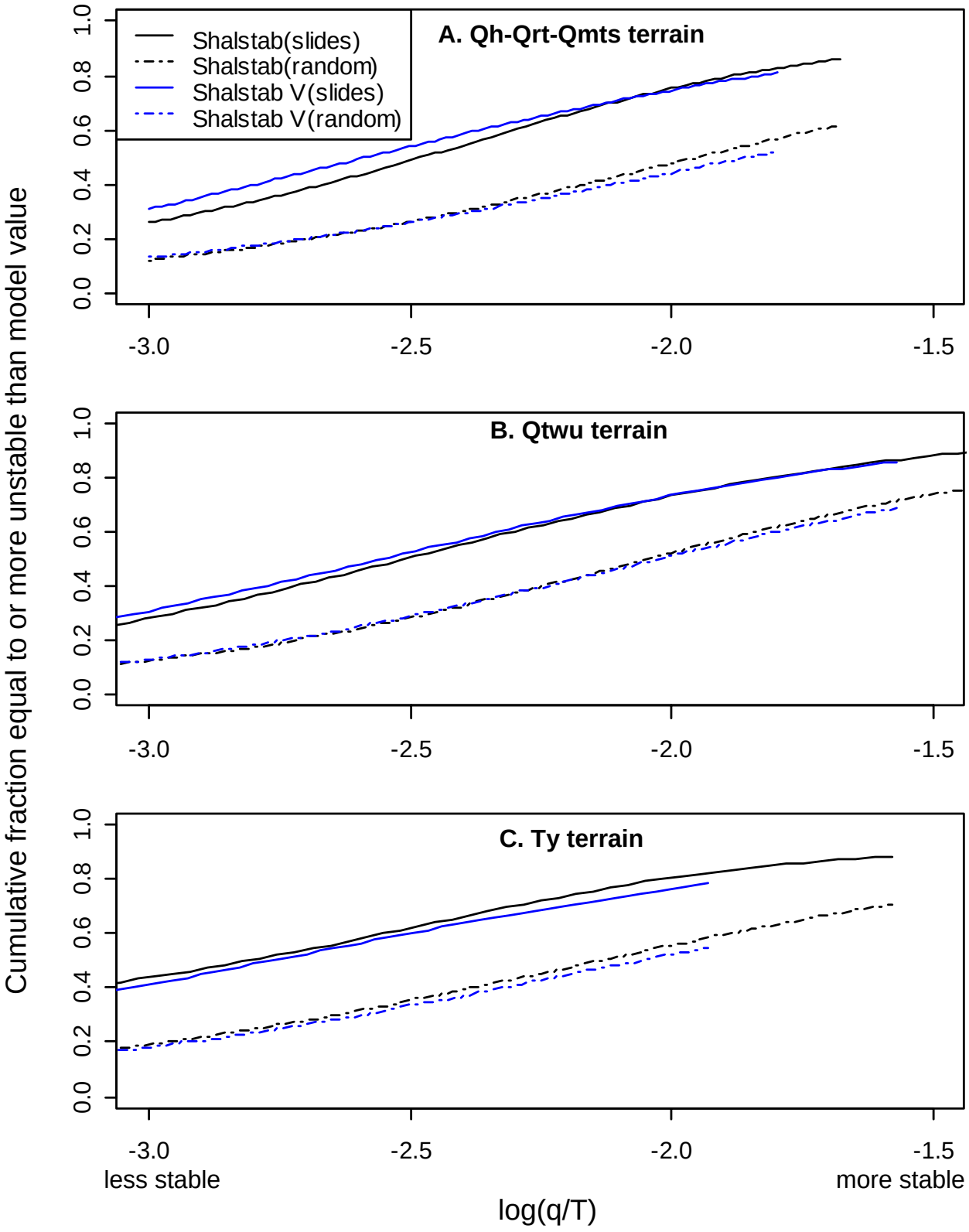

Figure E-1. Cumulative fraction of slides and random points located within areas equal to or more unstable than a specified log (q/T) value from SHALSTAB and SHALSTAB.V.

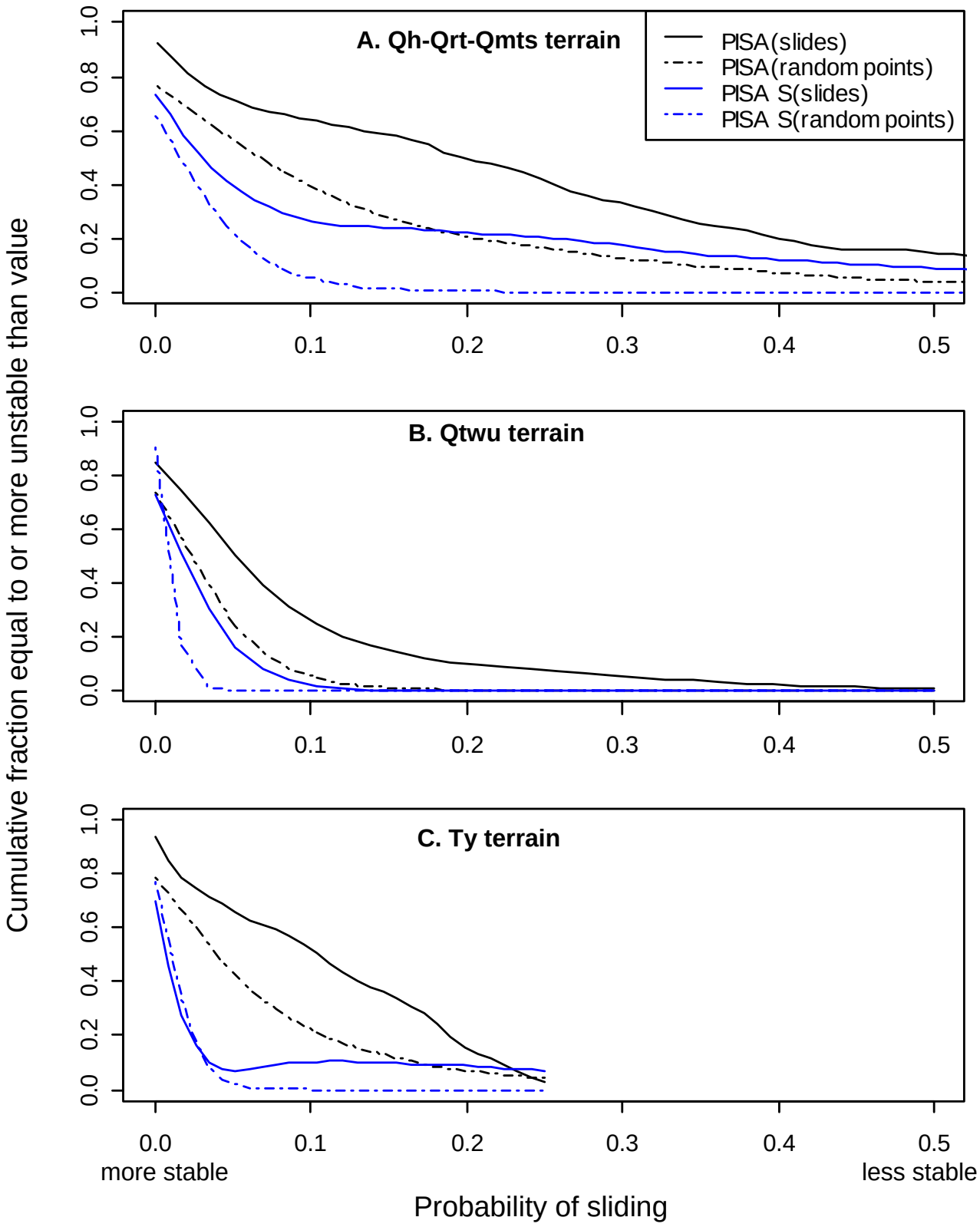

Figure E-2. Cumulative fraction of slides and random points located within areas equal to or more unstable than a specified probability of sliding value form PISA and PISA.V.

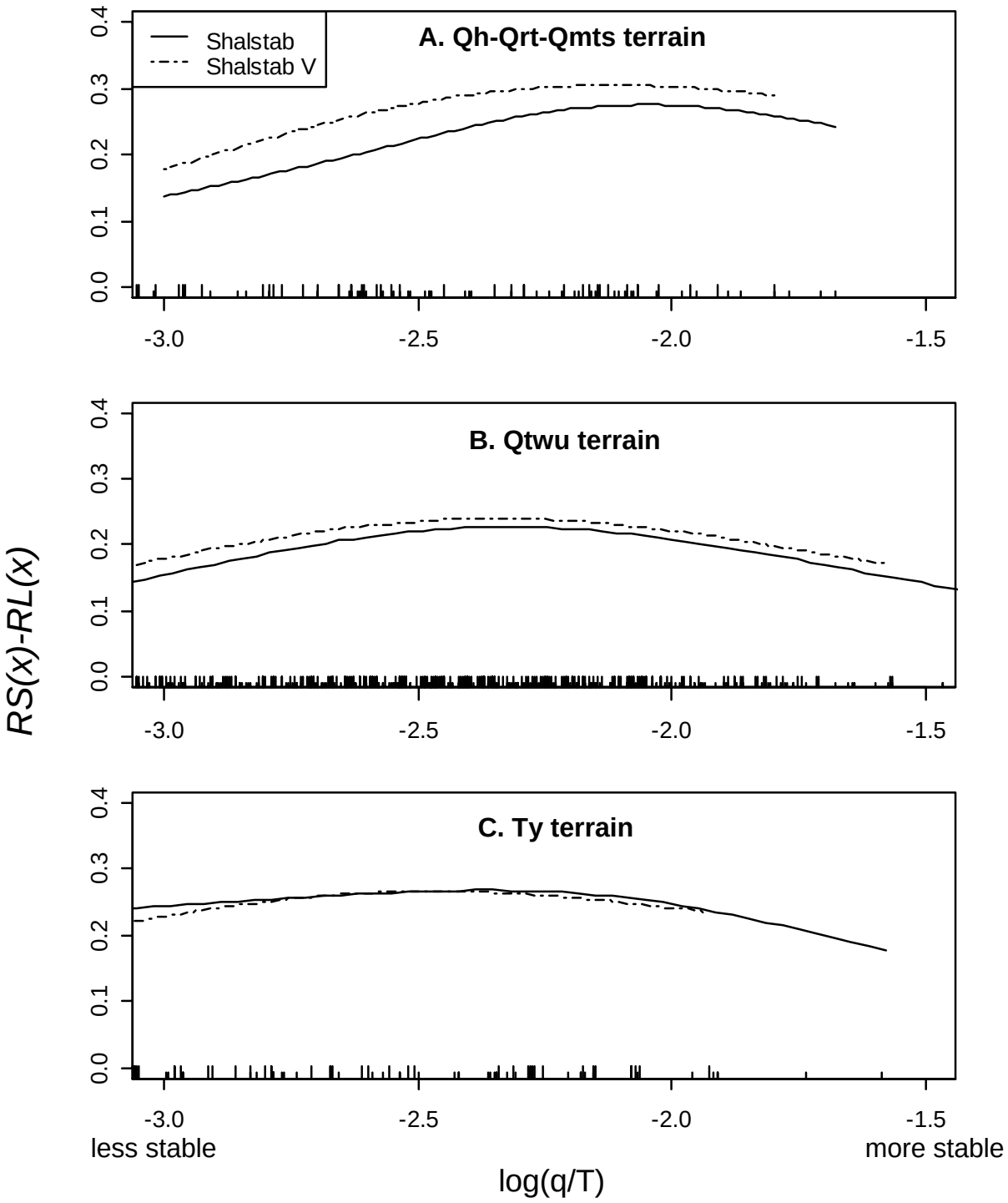

Figure E-3. Difference between the fraction of the Project Area and the fraction of slides for which log (q/T) is equal to or more unstable than a specified value. Rug plots indicate model values at landslides points (short ticks for SHALSTAB, longer ticks for SHALSTAB V).

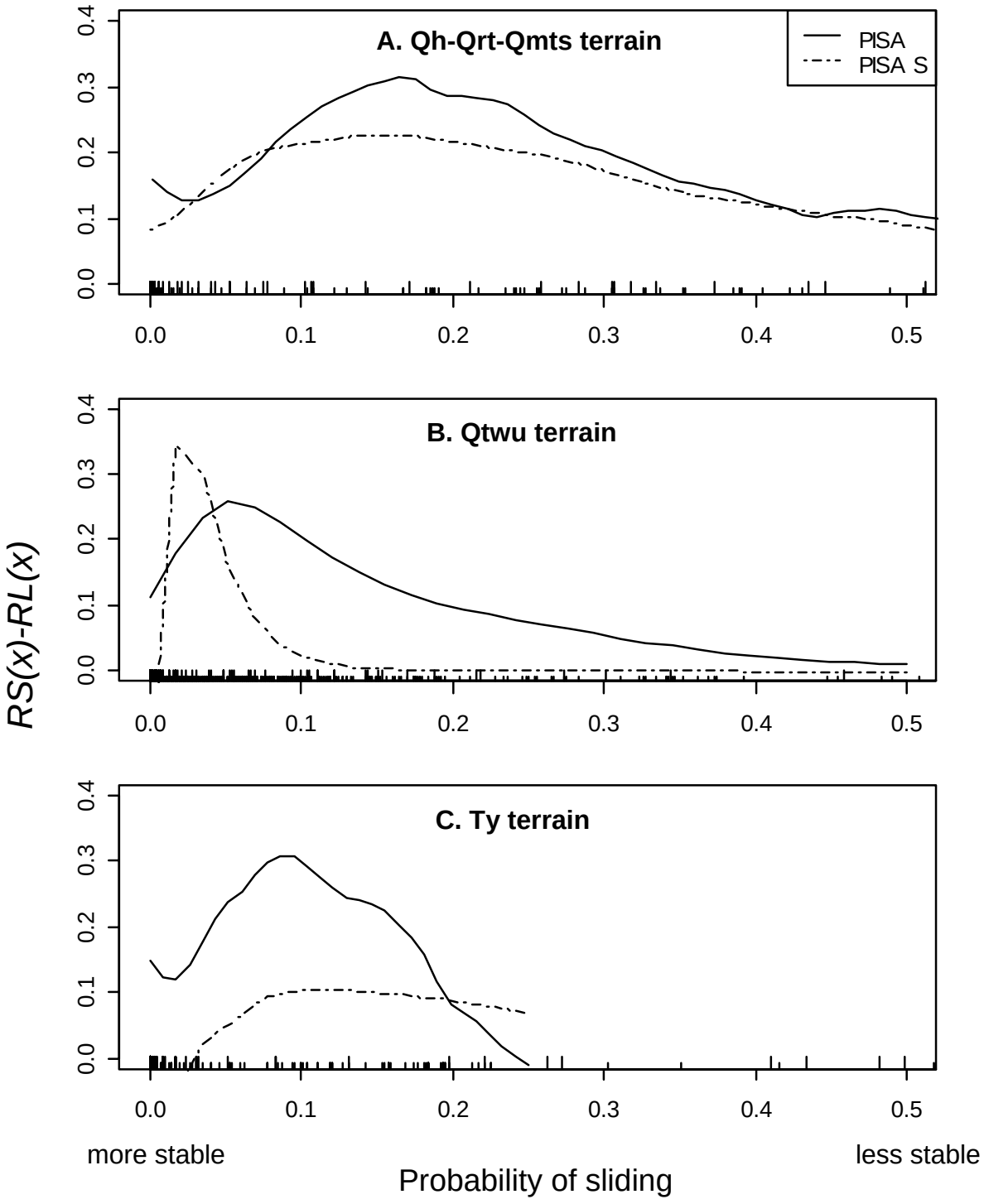

Figure E-4. Difference between the fraction of the Project Area and the fraction of slides for which probability of sliding is equal to or more unstable than a specified value. Rug plots indicate model values at landslides points (short ticks for PISA.V, longer ticks for PISA).